



UNIVERSITAT<sub>DE</sub>  
BARCELONA

# Polypurine Reverse Hoogsteen hairpins: stability, lack of immunogenicity and gene silencing in cancer therapy

Xenia Villalobos Alberú



Aquesta tesi doctoral està subjecta a la llicència Reconeixement- NoComercial – Compartir Igual 4.0. Espanya de Creative Commons.

Esta tesis doctoral está sujeta a la licencia Reconocimiento - NoComercial – Compartir Igual 4.0. España de Creative Commons.

This doctoral thesis is licensed under the Creative Commons Attribution-NonCommercial-ShareAlike 4.0. Spain License.







UNIVERSITAT DE BARCELONA

FACULTAT DE FARMÀCIA  
DEPARTAMENT DE BIOQUÍMICA I BIOLOGIA MOLECULAR  
Programa de doctorado en Biomedicina

**Polypurine Reverse Hoogsteen hairpins: stability, lack of immunogenicity and gene silencing in cancer therapy**

XENIA VILLALOBOS ALBERÚ  
Barcelona, 2015







UNIVERSITAT DE BARCELONA

FACULTAT DE FARMÀCIA  
DEPARTAMENT DE BIOQUÍMICA I BIOLOGIA MOLECULAR  
Programa de doctorado en Biomedicina

**Polypurine Reverse Hoogsteen hairpins: stability, lack of immunogenicity and gene silencing in cancer therapy**

Memoria presentada por Xenia Villalobos Alberú para optar al título de doctor por la  
Universitat de Barcelona

Dr. Carlos J. Ciudad Gómez  
Director

Dra. Verónica Noé Mata  
Directora

Xenia Villalobos Alberú

Barcelona, 2015







Creo que en un par de páginas no podré agradecer a todas las personas que me han ayudado durante estos años ¡pero lo intentaré! Todos me han enseñado algo durante esta etapa de mi vida:

En primer lugar quisiera agradecer a Carlos y Vero, mis directores, por apoyarme desde la primera vez que puse pie en su despacho y por integrarme en un grupo de investigación único, donde tuve la suerte de conocer a gente maravillosa. Gracias por exigirme cuando fue necesario y por enseñarme a creer en mis resultados.

Carlos, siempre recordaré la clase del master de la Pompeu cuando nos conocimos, tanto por el entusiasmo con que compartías tu trabajo, como por tu vestimenta. Gracias por intentar enseñarme todo lo que sabes, no solo sobre biología molecular sino también sobre otras cosas: las galgas y la mecánica; los coys, las cocas y las divisas de la Armada; los efectos bradicárdicos de la canela; la Bremsstrahlung... Gracias por las manzanas del mediodía y media tarde de los viernes. Aunque a veces quisieras matarme (y yo a ti), ¡hacemos un buen equipo! Vero, gracias por siempre saber qué decir, a nivel profesional y personal, y por ser un referente en el laboratorio. ¡Gracias por las *ladies nights* y los congresos! Nunca olvidaré la RANN de Sevilla, con el recorrido apocalíptico por los bares, el tequila fatídico y la huida del hotel.

A las mejores compañeras de laboratorio que pude tener, todas son un ejemplo a seguir: Carlota, gracias por todas las horas que pasamos juntas, no solo en el laboratorio, sino también en los viajes y salidas por Barcelona. ¡Te echo mucho de menos! Núria, fuiste mi primera mentora cuando llegué al lab: gracias por tu paciencia e ilusión. ¡Eres lo máximo! Laura, la mejor compañera en esta aventura; nuestros momentos “oferta” en el bar pasarán a la historia. Gracias por las palabras de ánimo cuando éste me faltaba. Claudia, gracias a ti recuperaré un poco de mi mexicanidad. Tenerte al lado fue una gran motivación “*Go big or go home*”! Annacleta, m’encanten el teu pragmatisme i objectivitat, m’has ensenyat moltíssim. Només et puc dir: GRÀCIES... i ja saps que t’estimo! To Gizem, for being a genuine good person, thank you for trying to teach us Turkish! A Cris, por tomar con tanto entusiasmo el proyecto de *delivery* ¡Estoy segura de que lo conseguirás!

Malu: ¡Gracias por las conversaciones durante los trayectos a nuestras casas!

Albert y Xana, gracias por la compañía a la hora de comer. Y Albert, aunque seas adoptado ¡te queremos igualmente! Si és que ho tens tot! ¡Gracias por todos los planes que nos organizas!

A todos los integrantes del departamento de Bioquímica y Biología Molecular, por los encuentros en los pasillos, los bailoteos y los karaokes; las risas y las locuras espontáneas. ¡Gracias! También quiero agradecer a Andrés y Quim, los técnicos del departamento, que nunca dudaron en ayudarme cuando tenía problemas y preguntas.

Y porque durante estos años también he implicado a mis amigos en este proyecto que fue el doctorado: Alba, gracias por ayudarme a relativizar las “desgracias” del laboratorio y por siempre animarme. He aprendido mucho de ti durante los años que nos conocemos y me enorgullezco de ser tu amiga. Sara, gracias por la alegría y serenidad que me transmites siempre. Eres la persona más cuidadosa y sensata que he conocido, no dudes de ti ¡Te queda el último empujón! Anna, gracias por escuchar mis rollos siempre que nos vemos, ¡y por estar al pendiente de mi! Marta, ¡gracias por las escapadas a Londres!

También me gustaría agradecer a mis compañeros de Pint of Science: el mejor proyecto en el que podría estar involucrada. Especialmente a Laurent: Merci pour toutes les soirées que nous avons partagé en discutant de science, bière et films.

A mis amigos de México, por seguir ahí a pesar del tiempo y la distancia: Bárbara, ¡que vinieras a Barcelona fue lo mejor que me pudo pasar! Gracias Pablo por hacer que se quedara. Fernando: Nos conocemos desde los 6 años y se que siempre podré contar contigo ¡¡Gracias por la portada!!

A mi familia: gracias por ayudarme a ser la persona que soy hoy. Mamá y Papá, me han apoyado siempre en todas las formas en que se puede ser apoyado. Gracias por ser mis padres. A mi hermano Diego, gracias por ser el ejemplo de equilibrio. Marivés, tus consejos me han ayudado mucho, ¡ya sabes que te hago caso! Abuelita, gracias por interesarte siempre por mi trabajo, aunque no sea fácil de entender, y por cuidarme siempre que vienes a Barcelona. A la familia Alberú ¡Los quiero mucho! Gracias por estar ahí siempre.

## ABBREVIATIONS





## ABBREVIATIONS

A	<i>Adenine</i>
AIM2	<i>Absent in melanoma 2</i>
aODN	<i>Antisense oligodeoxynucleotides</i>
BAN	<i>Biological association network</i>
BCL2	<i>B-cell CLL/lymphoma 2</i>
BSA	<i>Bovine serum albumin</i>
C	<i>Cytosine</i>
Ci	<i>Curie</i>
CPT	<i>Camptothecin</i>
CSC	<i>Cancer stem cells</i>
CTC	<i>Circulating tumor cell</i>
DC	<i>Dendritic cell</i>
DC-Chol	<i>3<math>\beta</math>-(N-(N',N'-dimethylaminoethane)-carbamoyl)cholesterol</i>
DHF	<i>Dihydrofolate</i>
DHFR	<i>Dihydrofolate Reductase</i>
DNA	<i>Deoxyribonucleic acid</i>
DOPE	<i>Dioleoyl phosphatidylethanolamine</i>
DOTAP	<i>N-(2,3-dioleyloxy)propyl)-N,N,N-trimethylammonium methyl-sulfate</i>
dsDNA	<i>Double stranded DNA</i>
EMSA	<i>Electrophoretic mobility shift assay</i>
EPR	<i>Enhanced permeability and retention</i>
H	<i>Hypoxanthine</i>
G	<i>Guanine</i>
HER2	<i>Human epidermal growth factor receptor 2</i>
IFI16	<i>IFN inducible protein 16</i>
IFN	<i>Interferon</i>

IFP	<i>Interstitial fluid pressure</i>
IL	<i>Interleukin</i>
IRF	<i>Interferon regulatory factors</i>
IV	<i>Intravenous</i>
LGP2	<i>Laboratory of genetics and physiology 2</i>
LNA	<i>Locked nucleic acid</i>
MDA5	<i>Melanoma differentiation-associated gene 5</i>
miRNA	<i>MicroRNA</i>
mRNA	<i>Messenger RNA</i>
NF- $\kappa$ B	<i>Nuclear factor <math>\kappa</math>B</i>
NLR	<i>NOD-like receptor</i>
PAMP	<i>Pathogen associated molecular patterns</i>
PBMCs	<i>Peripheral blood mononuclear cells</i>
PD	<i>Pharmacodynamics</i>
PEG	<i>Polyethylene glycol</i>
PK	<i>Pharmacokinetics</i>
PNA	<i>Peptide nucleic acid</i>
PPRH, Hp	<i>Polypurine reverse Hoogsteen hairpin</i>
PRR	<i>Pattern recognition receptors</i>
PYHIM	<i>Pyrin and HIN200 domain-containing</i>
RES	<i>Reticuloendothelial system</i>
RIG-1	<i>Retinoic acid inducible gene</i>
RISC	<i>RNAi induced silencing complex</i>
RLR	<i>RIG-1-like receptor</i>
RLU	<i>Relative light units</i>
RNA	<i>Ribonucleic acid</i>
RNAi	<i>RNA interference</i>
SC	<i>Subcutaneous</i>
SELEX	<i>Systematic evolution of ligands by exponential enrichment</i>

siRNA	<i>Small-interfering RNA</i>
ssDNA	<i>Single stranded DNA</i>
SSO	<i>Splice-switching oligonucleotide</i>
STING	<i>Stimulator of type I IFN gene</i>
T	<i>Thymidine</i>
TBK1	<i>TANK-binding kinase-1</i>
TF	<i>Transcription factor</i>
THF	<i>Tetrahydrofolate</i>
TLR	<i>Toll-like-receptors</i>
TNF $\alpha$	<i>Tumor necrosis factor alpha</i>
TOP1	<i>Topoisomerase-1</i>
TTS	<i>Triple-helix target sites</i>
VEGF	<i>Vascular endothelial growth factor</i>



## INDEX



## INDEX

<b>Presentation</b>	1
<b>1. Introduction</b>	5
1.1 Use of oligonucleotides in therapy	7
1.1.1 Gene silencing oligonucleotides	8
1.1.1.1 TFOs	9
1.1.1.2 Antisense oligodeoxynucleotides	10
1.1.1.3 siRNAs	11
1.1.1.4 Ribozymes	12
1.1.2 Other therapeutic oligonucleotides	14
1.1.2.1 Aptamers	14
1.1.2.2 Decoys and circular oligonucleotides	15
1.1.3 PPRHs	17
1.2 Advantages and disadvantages of using oligonucleotides in therapy	19
1.2.1 Delivery and stability	19
1.2.2 Immunogenicity	21
1.2.3 Chemical modifications	24
1.3 Cancer and relevant targets	25
1.3.1 Target genes with therapeutic applications	26
1.3.1.1 <i>BCL2</i>	26
1.3.1.2 <i>TOP1</i>	27
1.3.1.3 <i>MTOR</i>	28
1.3.1.4 <i>MDM2</i>	28
1.3.1.5 <i>MYC</i>	28
1.3.1.6 <i>DHFR</i>	29
<b>2. Objectives</b>	31
<b>3. Materials and methods</b>	35
3.1 Materials	37
3.1.1 Cell lines	37
3.1.2 Culture media	37
3.1.3 PPRHs	38
3.1.4 siRNAs	43



3.1.5 Aptamers	43
3.1.6 Primers	44
3.1.7 Other sequences	44
3.1.8 Plasmid vectors	44
3.2 Methods	46
3.2.1 Design of PPRHs	46
3.2.2 Stability in Fetal Calf Serum, Mouse Serum, and Human Serum	47
3.2.3 PPRHs and siRNA Half-Life in Cells.	48
3.2.4 Determination of the immune response	48
3.2.4.1 Determination of mRNA levels	48
3.2.4.2 Western blot	49
3.2.4.3 Caspase-1 proteolytic activity	50
3.2.5 <i>In silico</i> studies	50
3.2.6 Confocal microscopy	50
3.2.7 Luciferase experiments	51
<b>4. Results</b>	53
4.1 Article I	55
4.1.1 Additional results to article I	69
4.1.1.1 Binding of an RNA-PPRH to its target duplex	69
4.1.1.2 Effect of an RNA-PPRH on cell viability	70
4.2 Article II	71
4.2.1 Additional results to article II	85
4.2.1.1 Effect of PPRHs designed against transcription factor Sp1	85
4.3 Article III	87
<b>5. Discussion</b>	119
5.1 Delivery and stability	121
5.2 Immunogenicity	124
5.3 Improving the structure of PPRHs	126
5.4 RNA-PPRHs	128
5.5 Validation of PPRHs	128
5.6 Use of aptamers	131
5.7 Concluding remarks	132

<b>6. Conclusions</b>	135
<b>Bibliography</b>	139
<b>Appendix</b>	151
Article IV	153
Article V	169



# PRESENTATION



This work is focused on the study of the stability and immunogenic properties of the Polypurine Reverse Hoogsteen hairpins (PPRHs), and on their use as a gene-silencing tool.

Our group has studied different types of gene silencing molecules, such as antisense oligonucleotides (aODNs) and small-interfering RNA (siRNAs), in functional validation experiments (Peñuelas *et al.* 2005; Selga *et al.* 2008; Mencía *et al.* 2010) and also as potential anticancer therapeutics (Rodríguez *et al.* 2002; Coma *et al.* 2004). However, these molecules present several drawbacks that difficult their use in human therapy, including: low stability, unintended side effects –specifically immunotoxicity– and elevated cost of synthesis. PPRHs were developed to overcome these problems taking advantage of the capacity of nucleic acids to form Watson-Crick and reverse Hoogsteen bonds at the same time.

PPRHs are non-modified DNA molecules formed by two antiparallel polypurine strands linked by a pentathymidine loop that allows the formation of intramolecular reverse Hoogsteen bonds between both strands. Previously in our laboratory it was demonstrated that these hairpins bind to their polypyrimidine target in a dsDNA via Watson-Crick bonds, displacing the polypurine strand of the target duplex (Coma *et al.* 2005). The effect of PPRHs in cells and their mechanism of action were first described using PPRHs designed against the template (de Almagro *et al.* 2009) and coding (de Almagro *et al.* 2011) strands of the *DHFR* gene. A PPRH against *survivin* was further validated in a xenograft tumor model, establishing the proof of principle for the use of PPRHs as a therapeutic tool (Rodríguez *et al.* 2013). Finally, to improve the PPRHs effect and to decrease the possible off-target effects, it was determined that PPRHs of 30bp had greater effect than shorter PPRHs of 20bp, and that when a purine interruption is found in the pyrimidine target, the PPRH sequence should contain the complementary base in front of the interruption (Rodríguez *et al.* 2015).

In this work we increased the knowledge we have about PPRHs. We were able to establish that PPRHs, unlike siRNAs, are very stable molecules and lack immunogenic potential, two features that have lagged the development of siRNAs as therapeutic oligonucleotides. Another element that we studied was the modification of the PPRH structure, since it has been shown that circular structures can provide advantages over linear structures. Therefore, we analyzed the efficacy of two other

types of PPRH: i) nicked-circle-PPRHs, a new structure in which a second loop was introduced to form a nearly circular sequence, and ii) PPRHs made out of RNA (RNA-PPRHs). Additionally, to broaden the applicability of PPRHs in cancer therapy, we evaluated their capacity to silence genes involved in a variety of biological functions linked to cancer hallmarks. Finally, we also present an approach to increase the specificity of PPRHs that involves the use of a DNA aptamer that has been shown to have an effect in HER2 positive cells (Mahlknecht *et al.* 2013).

# ONE | INTRODUCTION

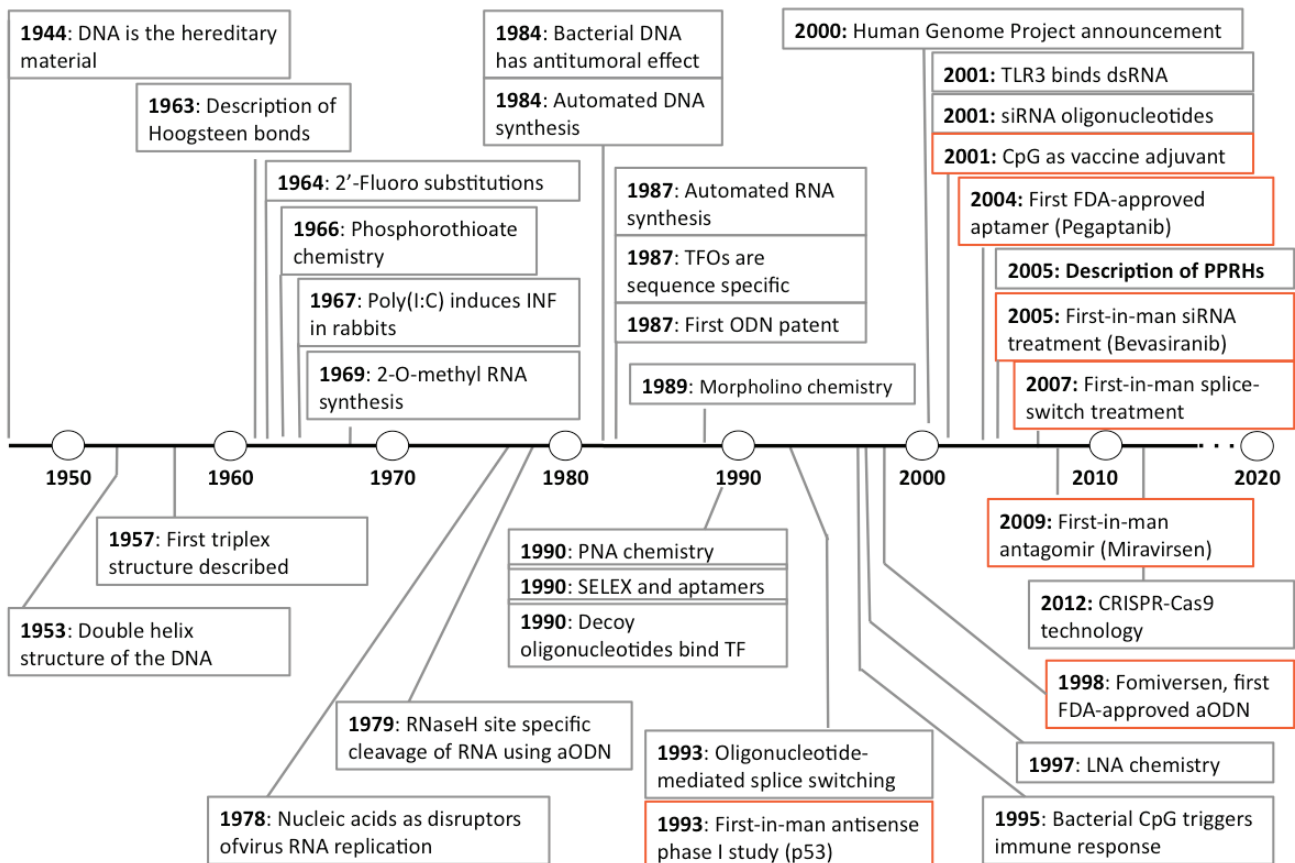




## 1.1 USE OF OLIGONUCLEOTIDES IN THERAPY

The discovery of DNA double-helix structure in 1953 (Watson & Crick 1953) set a landmark in molecular biology. It implied that DNA replication is possible through the complementary nature of the two strands, corroborating that the DNA is the carrier of the genetic information, as stated earlier by Avery in 1944 (Avery *et al.* 1944). Ten years later Karst Hoogsteen proposed an additional model (Hoogsteen 1963) that explained the existence of a triple stranded structure described by Felsenfeld and Rich in 1957 (Felsenfeld *et al.* 1957). These discoveries established the bases for the use of nucleic acids as therapeutic tools since they allowed rationalizing the design of molecules following a set of pairing rules. The use of nucleic acids as disruptors of genetic flow was first described in 1978, when Zamecnik and Stephenson reported that a 13 nucleotide-long oligodeoxynucleotide complementary to a target sequence in Rous sarcoma virus RNA inhibited its viral replication and protein translation *in vitro* (Zamecnik & Stephenson 1978). In their report, they foresaw the profound implication of this discovery, and even proposed the term “hybridon” to designate an oligonucleotide of specific sequence that acts by competitive hybridization. Today we refer to these molecules as antisense oligonucleotides (aODN).

Significant advances in organic chemistry occurred in parallel, which made possible the synthesis of relatively short fragments of oligonucleotides. Since the late 70s several other discoveries, such as the chemical modifications on internucleotide linkages, the automated DNA-synthesis, the description of the RNA interference pathway, or the discovery of aptamers, have remarkably amplified and pushed forward the field of antisense and antigene therapy. Finally, in the year 2001 the Human Project presented its preliminary results of the human genome sequence (International Human Genome Sequencing Consortium. Lander *et al.* 2001). This opened the possibility to rationally design DNA and RNA molecules able to specifically target sequences within the genome. The full genomic sequence was completed and published in April 2003. Figure 1 depicts the evolution of therapeutic oligonucleotides.



**Figure 1.** History of oligonucleotide therapeutics. Basic biology and chemistry discoveries are in black boxes and clinical applications are in orange boxes. Adapted from Lundin *et al.* 2015.

### 1.1.1 GENE SILENCING OLIGONUCLEOTIDES

Nowadays, several types of oligonucleotides can be used to inhibit the expression of a given gene. They act at different levels on the flow of genetic information, allowing for the following classification:

- Oligonucleotides inhibiting the transcription process: directed against the DNA, are also named antigene oligonucleotides. In this category we find the Triplex Forming Oligonucleotides (TFOs).
- Oligonucleotides inhibiting the translation process: directed against the mRNA. These include antisense oligonucleotides (aODN), small interfering RNAs (siRNAs), microRNAs (miRNAs) and ribozymes.

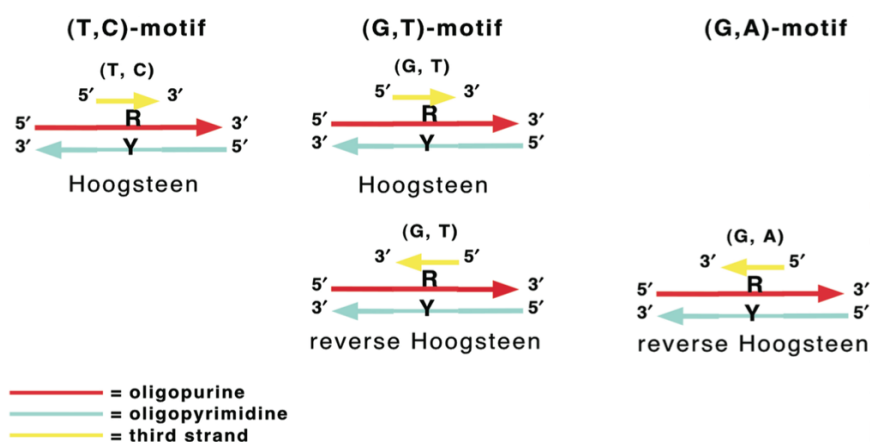
- Oligonucleotides acting at the protein level: are able to bind to the proteins and block their activity. Aptamers are included in this category, as well as decoy oligonucleotides for transcription factors (TFs) (Hosoya 1999)

Other oligonucleotides called antagomirs are used to silence endogenous microRNAs, therefore although they modulate gene expression, they are not silencing oligonucleotides.

### 1.1.1.1 TFOs

TFOs are single stranded DNA molecules that bind to the major groove of the double-stranded DNA, forming a triplex structure. They bind in a sequence specific manner to polypurine stretches by Hoogsteen or reverse Hoogsteen hydrogen bonds. There are three types of TFOs that vary in their composition and orientation relative to the target strand (figure 2):

- Pyrimidine TFOs (T,C-TFOs): parallel to the purine target sequence and form Hoogsteen bonds. Triplets obtained are T·A\* $T^+$  and C·G\* $C^+$ .
- Purine TFOs (G,A-TFOs): antiparallel relative to the purine target sequence and form reverse Hoogsteen bonds. Triplexes obtained are T·A\*A and C·G\*G.
- Mix TFOs (G,T-TFOs): can be parallel, forming Hoogsteen bonds, or antiparallel, forming reverse Hoogsteen bonds, creating the triplets T·A\* $T^+$  and C·G\*G.



**Figure 2.** Orientation of the triple helix motifs. Obtained from Duca *et al.* 2008.

TFOs are capable of inhibiting gene transcription either by blocking the binding of TFs or by distorting the normal double helical structure (Hartman *et al.* 1992), and thus inhibiting the activity of the RNA polymerase. The dissociation constants for TFOs are comparable to those of the TFs (Praseuth *et al.* 1999), and they can compete with them for the binding to the dsDNA. It has also been reported that the binding of the TFOs can trigger the DNA repair mechanisms, which can be exploited for site-directed correction of point mutations (Culver *et al.* 1999; Faruqi *et al.* 2000; Kalish *et al.* 2005).

It is reasonable to think that the presence of polypurine-polypyrimidine sequences in the target DNA would be a limitation. However, triple-helix target sites (TTS) are over-represented in the human genome, especially at regulatory regions such as promoters. It is suggested that even if TTS are not directly targeted by TFs, they may be important for gene functionality by acting as spacing fragment to help the correct positioning of transcription factors (Goni 2004; Goñi *et al.* 2006). It has been reported that an intramolecular triplex modulates transcription in the human *c-MYC* promoter (Belotserkovskii *et al.* 2007). Nevertheless, the use of TFOs is limited by the low stability of the triple-helical structure.

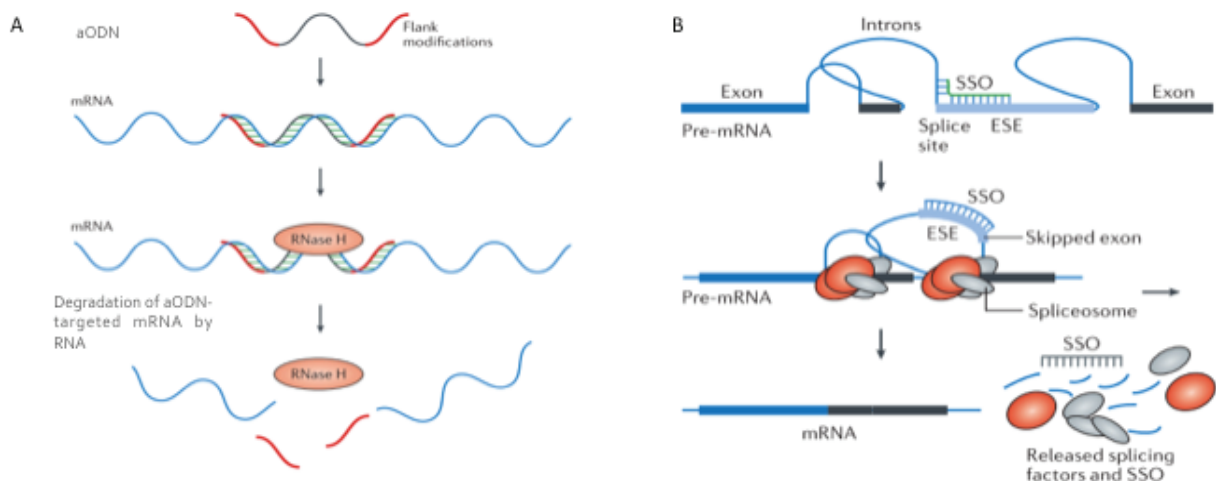
#### 1.1.1.2 Antisense oligodeoxynucleotides

Antisense oligonucleotides are ssDNA molecules, typically of 20 nucleotides in length. They are designed to bind a target mRNA sequence through Watson-Crick bonds to modulate protein translation. aODNs can be separated into two broad classes depending on their mechanism of action:

- RNase H-dependent oligonucleotides (also called gapmers): have a phosphorothioate backbone with flanks that are modified in the 2'-position of the residues (highlighted in red in figure 3A). The unmodified 'gap' in the aODN-mRNA duplex is recognized by ribonuclease H (RNase H), which degrades the mRNA. Since RNase H has to recognize the duplex, nucleotides can be chemically modified to a limited degree.

- Steric-blocking oligonucleotides: physically prevent or inhibit the progression of splicing (splice-switching oligonucleotide; SSO) or the translational machinery (figure 3B). The SSO approach is being investigated to restore the normal reading frame of dystrophin in Duchenne muscular dystrophy, a change that results in the production of a shorter but functional protein.

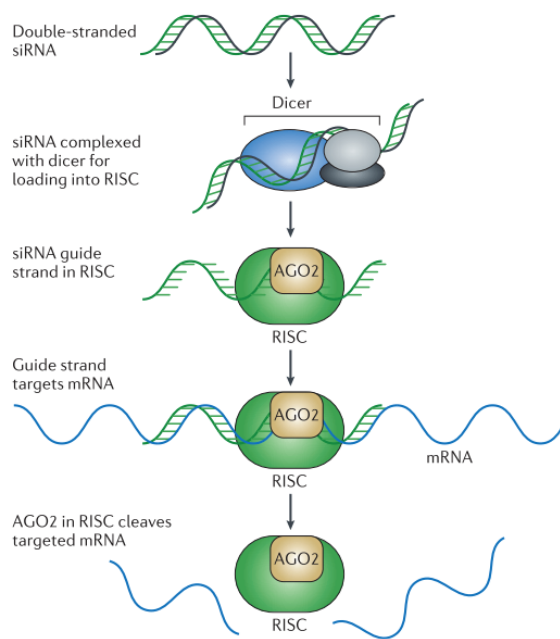
According to the desired application of the aODN, and to favor its effect, several modifications can be introduced in the sequence. These are directed to increase the resistance of aODN to nucleases or to improve the uptake of the aODN by the cells. In 1998 the first aODN drug, fomiverson, was registered as a treatment for cytomegalovirus-induced retinitis in immunocompromised patients with AIDS and more recently, in 2013, the cholesterol-reducing antisense oligonucleotide mipomersen was approved.



**Figure 3** Mechanisms of action of the aODNs. **A.** RNase H-dependant oligonucleotides **B.** Steric blocking oligonucleotides include exon skipping and SSOs. A chemically modified, RNA-blocking oligonucleotide targeted to a splice site in pre-mRNA prevents the proper assembly of the spliceosome or translational machinery. Adapted from (Kole *et al.* 2012).

### 1.1.1.3 siRNAs

siRNAs are double-stranded RNA oligonucleotides of 21-22 bases in length with a 3' overhang of two bases. One of the strands is called the antisense (or guide) strand, while the other one is the sense (or passenger) strand. siRNAs are the substrate of the natural intracellular protein complex called RNAi induced silencing complex (RISC). Within the



**Figure 4** Synthetic double-stranded siRNA is complexed with components of the RNA interference pathway, dicer, AGO2, and other proteins, to form RISC. RISC binds to a targeted mRNA via the unwound guide strand of siRNA, allowing AGO2 to degrade the RNA. Obtained from Kole *et al.* 2012.

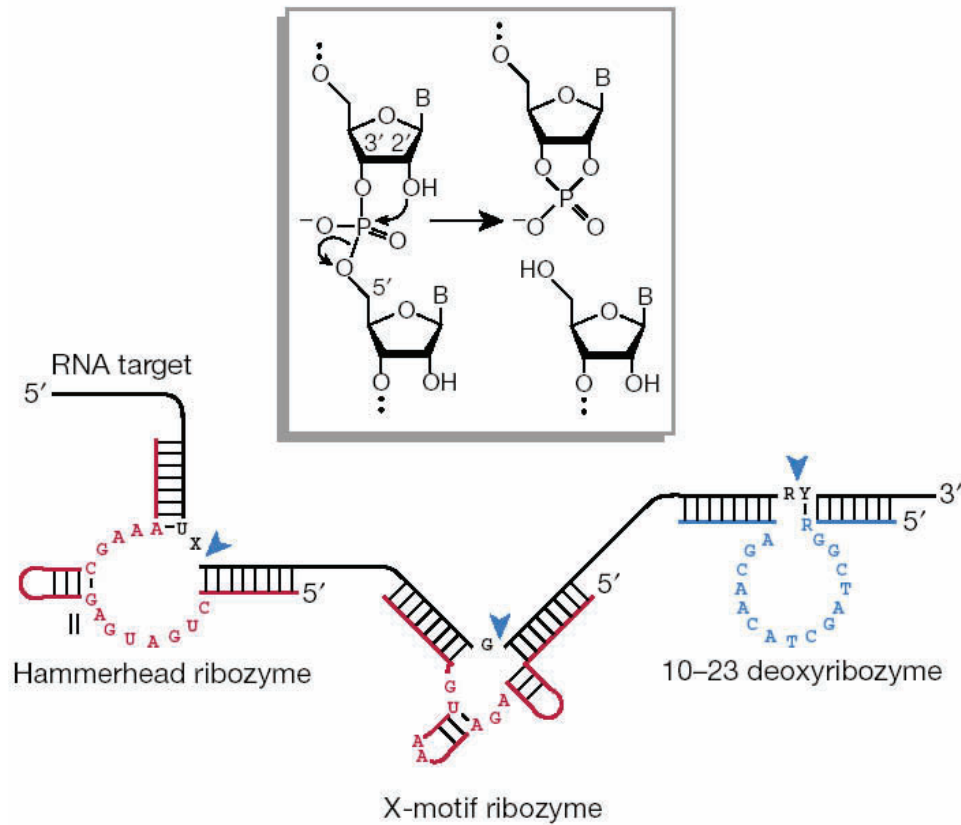
RISC, the siRNA is unwound and the sense strand is discarded. The antisense or guide strand binds to mRNA and when it is fully complementary to its target, the endonuclease argonaute 2 (AGO2) — a component of RISC — cleaves the mRNA 10 nucleotides downstream from the 5' end of the antisense strand (figure 4). In animals, this mechanism was first demonstrated in the nematode *C. elegans* (Fire *et al.* 1998), when the delivery of exogenous double-stranded RNA (dsRNA) effectively decreased the mRNA levels of the target gene (*unc22*, an abundant but nonessential myofilament protein). The RNA interference (RNAi) process is a gene silencing mechanism that is conserved in eukaryotes. Its primary functions are the

regulation of gene expression and the defense against virus and other exogenous genetic elements. Since the RISC complex is located in the cytoplasm, siRNAs only target mature RNA.

#### 1.1.1.4 Ribozymes

Ribozymes derive from catalytic RNAs found in virus, bacteria and some eukaryotes. They are ssRNA molecules that catalyze the cleavage and formation of covalent bonds in RNA strands at specific sites. These sites can be located in an external RNA (trans-cleavage) or in an RNA linked to the ribozyme (cis- or self-cleavage). The catalytic domains of the different ribozymes are highly conserved and they hydrolyze the target RNA upon recognition of their specific target sequence. Cleavage occurs by nucleophilic attack of the 2'-OH group onto the neighboring phosphorus (Müller 2015). The "hammerhead" ribozyme motif has been deeply studied in gene therapy to treat cancer and viral infections, such as HIV, hepatitis B and C. Other synthetic ribozymes have been

developed, such as the X-motif ribozyme or the DNA-based 10-23 deoxyribozyme (figure 5).



**Figure 5.** The natural hammerhead ribozyme as well as the engineered X-motif ribozyme and 10–23 deoxyribozyme motifs catalyze RNA cleavage. Base pairing between the RNA target and the substrate-binding arms of ribozymes can be designed to target different RNA sequences. Target RNA (black), the ribozymes (red) and deoxyribozyme (blue). Obtained from (Breaker 2004)

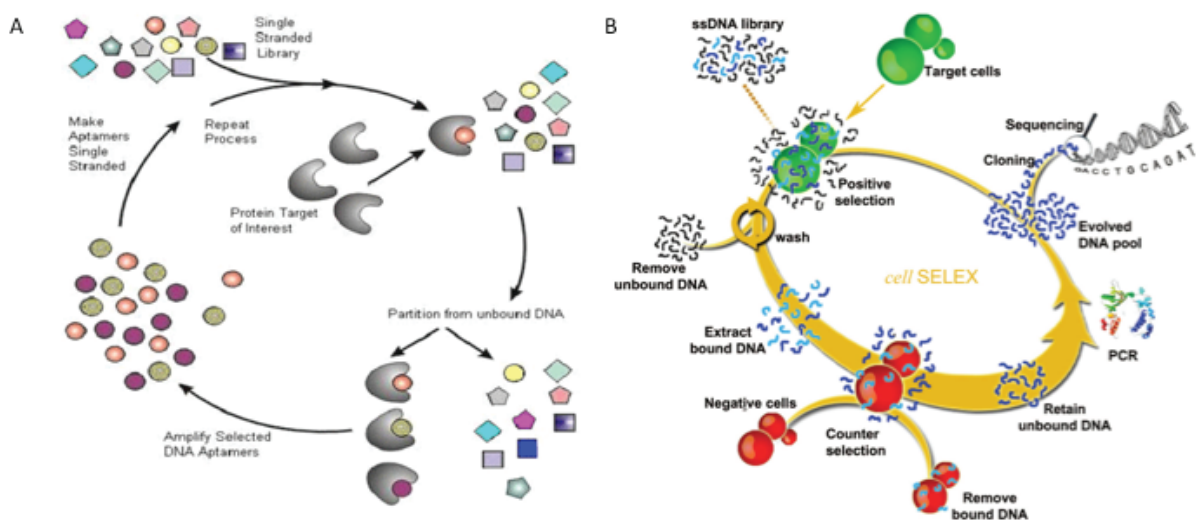


## 1.1.2 OTHER THERAPEUTIC OLIGONUCLEOTIDES

Oligonucleotides are capable of interacting with other macromolecules in the cell. A clear example of these interactions are TFs, which bind to promoter sequences in genes. Additionally, ssDNA sequences fold within themselves and acquire specific tertiary structures that enable the DNA to interact with various molecular targets. These characteristics can be exploited to design other therapeutic oligonucleotides that do not act by Watson-Crick or Hoogsteen binding.

### 1.1.2.1 Aptamers

Aptamers are DNA or RNA sequences that have been evolved *in vitro* to bind to a desired target –protein or small molecule– after an iterative process called “Systematic evolution of ligands by exponential enrichment” (SELEX), shown in figure 6A. The Gold and Szostak laboratories described this process simultaneously in 1990 (Tuerk & Gold 1990; Ellington & Szostak 1990). Aptamers are a class of nucleic acid-based molecules with therapeutic potential. Indeed, in 2004 the aptamer pegaptanib (Macugen), a selective vascular endothelial growth factor (VEGF) antagonist, was accepted for the treatment of age-related macular degeneration.

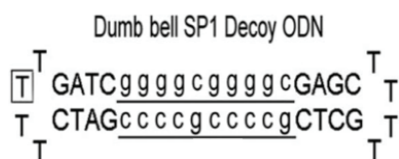


**Figure 6.** Obtaining aptamers. **A.** The SELEX process begins by confronting the target to a library of ssDNA or ssRNA. The unbound sequences are removed while the bound sequences are amplified by PCR. The process is repeated until one sequence is selected. **B.** Cell SELEX follows the same process, but the oligonucleotides library is confronted to the target cell, and a counter selection step is added to reduce unspecificities.

Like antibodies, the action of aptamers depends on their tertiary structure. Therefore changes in the sequence or chemical modifications may alter their activity so any modifications should be introduced during the SELEX procedure. This restricts chemical modifications of the starting nucleotides to those accepted by the polymerase used in the PCR step. Because of their capacity to bind efficiently to specific targets, several aptamers have been developed for their use in cancer research taking advantage of the particularities of cancer cells, such as the overexpression of some membrane proteins. Whole living cells are also employable as selection targets. This technology is called Cell-SELEX (figure 6B), and it has the advantage that the aptamers recognize the native conformation of the target molecule on living cells. In this way, cell surface proteins would be targets even when their purification in native conformation is difficult. In addition, cell-specific aptamers can be obtained without any knowledge about cell surface molecules on the target cells. Aptamers have been conjugated to drugs (Ray *et al.* 2012; Thiel *et al.* 2012), photosensitizers (Ferreira *et al.* 2008) and liposomes (Song *et al.* 2015), and can also be used for diagnostic purpose (Shigdar *et al.* 2013).

### 1.1.2.2 Decoys and circular oligonucleotides

Proteins such as TFs recognize and bind to certain sequences in DNA. Therefore, they are able to bind to the same sequence in a double-stranded decoy oligonucleotide. Decoy oligonucleotides are used to lure TFs away from their binding sites in DNA and a variety of therapeutic applications have been suggested, ranging from cancer (Ahn *et al.* 2003), graft rejection after a transplant (Suzuki *et al.* 2012), to viral replication inhibition (Nakaya *et al.* 1997). Any modifications introduced to improve nuclease resistance must not prevent recognition by the protein. Partial protection against exonucleases may be achieved by modifying the ends of the decoy or by using circular oligonucleotides (figure 7) with self-complementary sequences giving a dumb-bell configuration (Deng *et al.* 2013).

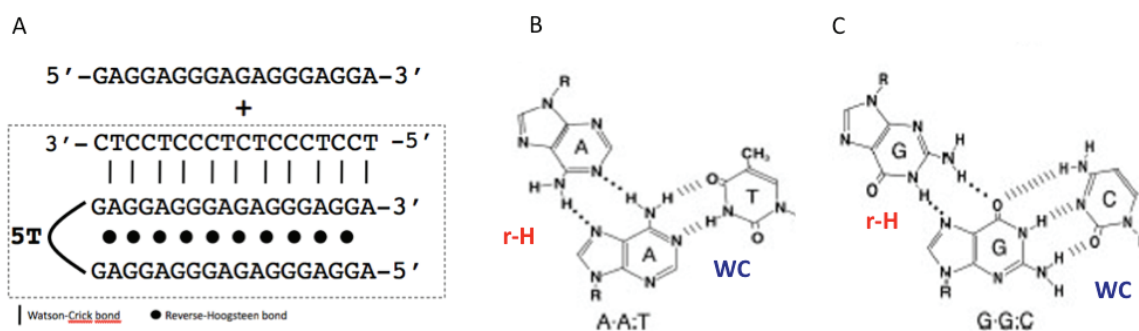


**Figure 7.** Example of a DNA decoy against the SP1 factor. The underlined sequences correspond to the binding site of the TF SP1. Obtained from Deng *et al.* 2013.

DNA decoys are not the only circular oligonucleotides that have been described. It has been described that circular oligonucleotides can also be designed to form triple helical structures (Kool, 1991). In his report, Kool designed a circular oligonucleotide that was formed by parallel pyrimidine sequences. In that case, the internal hydrogen bonds corresponded to Hoogsteen bonds. The target sequence was a polypurine stretch that was able to bind to the circular oligonucleotide by Watson-Crick bonds, obtaining T·A\*<sup>+</sup>T and C·G\*<sup>+</sup>C<sup>+</sup> triplets. It was also shown that the circular oligonucleotide had an increased resistance to nucleases, and a higher binding selectivity to its DNA target.

### 1.1.3 PPRHs

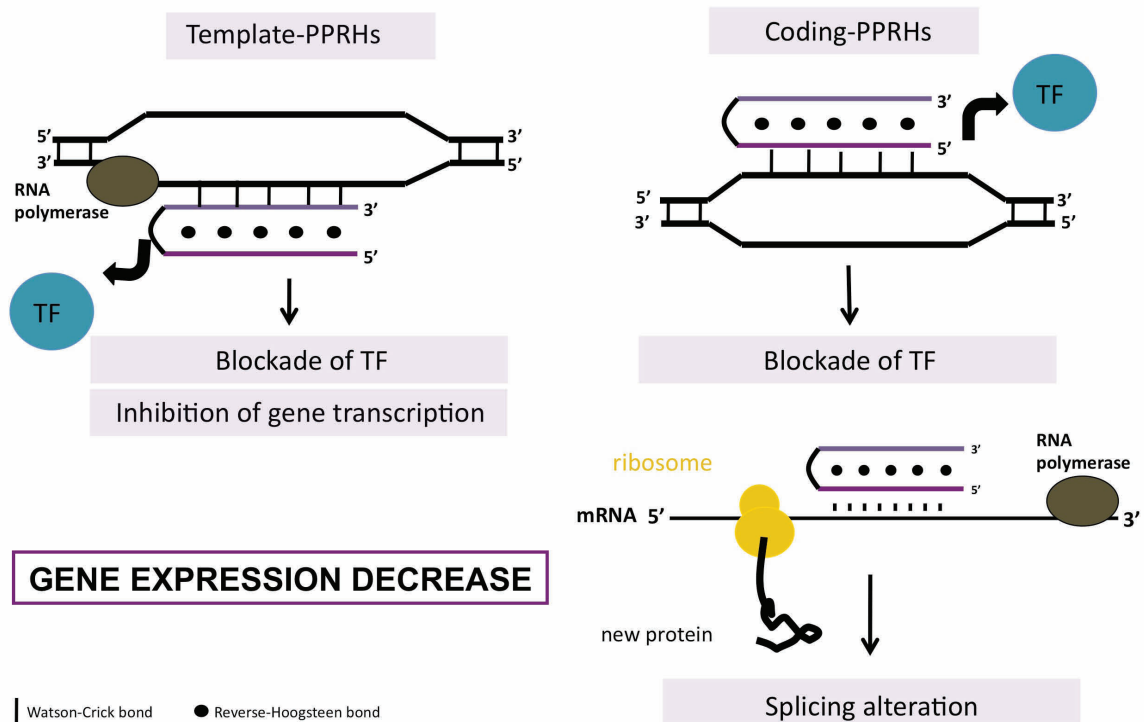
PPRHs are non-modified DNA molecules formed by two antiparallel polypurine strands linked by a pentathymidine loop that allows the formation of intramolecular reverse-Hoogsteen bonds between both strands. These hairpins bind to polypyrimidine stretches in the DNA via Watson-Crick bonds, while maintaining the hairpin structure (fig. 8). It was demonstrated that upon binding their polypyrimidine target in a dsDNA, PPRHs were able to displace the polypurine strand of the target duplex (Coma *et al.* 2005).



**Figure 8.** Schematic representation of the triplex formed upon PPRH binding to the target sequence (A). Formation of the Watson-Crick (WC) and reverse Hoogsteen bonds (r-H) between two adenines (B) and two guanines (C).

Because the polypyrimidine domains are located in both strands of the DNA PPRHs can be designed to target both strands of genomic DNA. PPRHs directed against the template strand of the DNA are called template-PPRHs, while the ones targeting the coding strand of the DNA are called coding-PPRHs, which are also able to bind transcribed mRNA, since it has the same sequence and orientation than the coding strand of the DNA. Therefore, PPRHs can act as antigene and antisense oligonucleotides depending on the strand they target. The mechanism of action of PPRHs, shown in figure 9, depends on the location of their target. Previous works in the laboratory demonstrated that template-PPRHs inhibit transcription (de Almagro *et al.* 2009) whereas a coding-PPRH directed against a polypyrimidine region in intron 3 of DHFR pre-mRNA produced a splicing alteration by preventing the binding of the splicing factor U2AF65 (de Almagro *et al.* 2011). This produced the accumulation of the immature mRNA, leading to a decrease in DHFR protein levels. Subsequently, we demonstrated that two PPRHs directed against the template or coding strand of the *survivin* promoter sequence decreased the binding of transcription factors Sp1 and GATA-3, respectively. Moreover, the *in vivo* administration

of the coding-PPRH against the promoter region of *survivin* was able to delay tumor growth in a prostate xenograft mouse model, establishing the proof of principle for their use as a therapeutic tool (Rodríguez *et al.* 2013). To improve the use of the PPRHs and decrease their possible off-target effects, we studied two main points conferring specificity to the PPRHs: their length and purine interruptions found in the target sequence. We compared the effect of three PPRHs that differed in length (20, 25 and 30 bp) and that were directed against the same sequence of the *telomerase* gene, and determined that increasing the PPRH length, produced a greater effect. It has been calculated that a sequence of 17 nucleotides is long enough to be unique in the genome. Indeed, the PPRHs that are normally designed in our laboratory are at least 20 bp in length, which ensures good target specificity. The second issue to consider is that we normally find 1-3 purine interruptions within the polypyrimidine target. When the PPRHs were first developed it was found that adenines could be used as wild cards to place in front of the interruptions, and indeed this strategy was useful. However, we recently determined that by placing in the PPRH the complementary base in front of the purine interruption, the binding capacity as well as its cytotoxic activity were increased (Rodríguez *et al.* 2015).



**Figure 9.** Mechanism of action of the template-PPRHs and the coding-PPRHs. While acting at different levels, both types of PPRHs are capable of decreasing the expression of the target genes.

## 1.2 ADVANTAGES AND DISADVANTAGES OF USING OLIGONUCLEOTIDES IN THERAPY

The continuous interest on nucleic acids as antigene or antisense therapeutic agents comes from the fact that the same rational design principle can be used to treat many diseases. If only three nucleic acid-based molecules have been cleared for therapeutic use it is because there are two major impediments that have not been totally solved: i) achieving a high-enough concentration of drug near the target, this is dependent on the stability of the oligonucleotides and on their pharmacokinetics (PK), and ii) averting the unintended effects caused by the activation of the immune response.

### 1.2.1 Delivery and stability

The *in vivo* administration of silencing molecules is substantially complex. To be efficacious, the gene silencing molecules must reach the target cells within a specific organ: they have to escape blood exonucleases, endonucleases, and ribonucleases. To avoid this degradation and enhance the stability of oligonucleotides chemical modifications in the 2' position of the pentose sugar are introduced. Once in the blood stream oligonucleotides must go across the blood vessel, the interstitial space, and extracellular matrix. Then they have to enter the cell membrane, which presents limited permeability to negatively charged molecules, and escape from the endosome to find their target sequences, either mRNA or DNA.

Different types of vectors have been developed to facilitate the systemic administration of gene silencing molecules and their subsequent uptake by the cells. These vectors can be divided into viral and non-viral vectors. Despite the advantages of viral vectors, like great transfection efficiency and the broad types of cells that can be transduced, they present important drawbacks in terms of immune response activation and possible unintended gene integration in the host's genome, causing insertional mutagenesis. Non viral vectors constitute a valid alternative in gene therapy, even if they are less efficient in delivering the oligonucleotides into the cells, they are safer and easier to synthesize than viral vectors. There are several non-viral systems to introduce oligonucleotides into the cells, like electroporation, injections of naked DNA or

biobalistics. However, cationic liposomes and polymers are the most used and studied vehicles.

- Cationic liposomes: lipids that have an amphipathic structure that allows electrostatic interactions to be formed between the negative charges of the oligonucleotide and the positive charges of the lipids, this complex is called lipoplex. To this end, several lipids have been tested, including among many others: mixture of dioleoyl phosphatidylethanolamine (DOPE); N-(2,3-dioleoyloxy)propyl)-N,N,N-trimethylammonium chloride (DOTAP); and 3 $\beta$ -(N-(N',N'-dimethylaminoethane)-carbamoyl)cholesterol (DC-Chol). (Omid *et al.* 2013). The advantages of this approach are i) the simplicity to formulate the lipoplex, ii) the stability of the formulation and protection against nucleases, and iii) the applicability of the method for delivery to different types of solid tumors.
- Cationic polymers: they have the capacity to condense the oligonucleotides forming polyplexes. There are different cationic polymers that have been studied, among these polyethyleneimine (PEI), polylysines, and poly(lactic-co-glycolic acid) (PLGA) have been widely studied. Perhaps of these, PEI is the most widely used polymer. The ratio between negative phosphate charges of the DNA and the positive nitrogen charges (N/P ratio) is very important for optimal condensation and transfection, and also to avoid unintended toxic effects. Indeed, in our laboratory we have successfully used a linear PEI (jetPEI®) in a subcutaneous prostate xenograft model in mice (Rodríguez *et al.* 2013).

These non-viral vectors can be functionalized with imaging molecules (fluorescent dyes, quantum dots) or targeting molecules such as antibodies or aptamers, to form nanoparticles (NP), and can be conjugated to other polymers like, polyethylene glycol (PEG), to improve their pharmacokinetic properties. In this sense, NP with sizes ranging 100-250 nm (Li *et al.* 2012) are big enough to avoid being cleared by the kidneys, where the glomerulus have pores sizes of 40-60 nm, or by the liver where the sinusoidal endothelium has pores ranging 70-150 nm (Seymour 1992), and small enough to



extravasate from the tumor microvasculature (100-1000 nm) (Adisheshaiah *et al.* 2009; Hobbs *et al.* 1998). This, together with a poor lymphatic drainage, produces an enhanced permeability and retention effect (EPR), which is responsible for the accumulation of macromolecules or nanoparticles in the tumors.

### 1.2.2 Immunogenicity

The second drawback for using oligonucleotides as therapeutic agents is the unintended activation of the immune response. One strategy in which mammalian host cells respond to infectious agents is by recognizing the foreign nucleic acids, which is achieved by the Pattern Recognition Receptors (PRRs). These receptors detect highly conserved microbial products named pathogen associated molecular patterns (PAMPs) and upon activation trigger the innate immune response, which leads to increased levels of proinflammatory cytokines (type I interferon's (IFN), TNF- $\alpha$ , IL-6, pro-IL-1 $\beta$  and pro-IL-18). PRRs are localized in compartments within certain cellular niches, such as the cell membrane, endosomes or cytoplasm. Three types of PRRs have been identified as nucleic acid-sensing PRRs: endosomal TLRs, cytoplasmic retinoic acid inducible gene (RIG-I)-like receptors (RLRs) and cytoplasmic DNA sensors, which activate the inflammasome.

The first and best-documented group of PRRs is the family of Toll-like-receptors (TLRs), which detects a variety of PAMPs, such as lipids, proteins, lipoproteins, and nucleic acids (Brown *et al.* 2011; Yoneyama & Fujita 2010). To date, 10 human TLRs have been identified, and each TLR has a specific set of ligands that it can detect. The TLRs responsible for detecting nucleic acids are: i) TLR3 that detects dsRNA sequences, expressed predominantly in the intracellular compartments of dendritic cells (DCs) and macrophages ii) TLR7 and TLR8 that recognize ssRNA, located in DCs and, in the case of TLR8, in macrophages and iii) TLR9 implicated in the detection of CpG-containing DNA, and predominantly expressed in the endosomal compartment of DCs and B cells. TLR signaling is dependent upon the recruitment of adaptor molecules to activate downstream kinases and transcription factors, such as interferon regulatory factors 3 and 7 (IRF3/7) and NF- $\kappa$ B, that regulate the production of type I IFNs and inflammatory cytokines, respectively.



In addition to TLR3, host cells can detect dsRNA of actively replicating viruses via RLRs, which are cytosolic RNA helicases that activate interferon regulatory factor 3 and 7 (IRF3/7), and nuclear factor- $\kappa$ B (NF- $\kappa$ B) (Yoneyama & Fujita 2010). The RLR family is comprised of RIG-I, melanoma differentiation-associated gene 5, (MDA5), and laboratory of genetics and physiology 2 (LGP2). RLRs are ubiquitously expressed in most cell types.

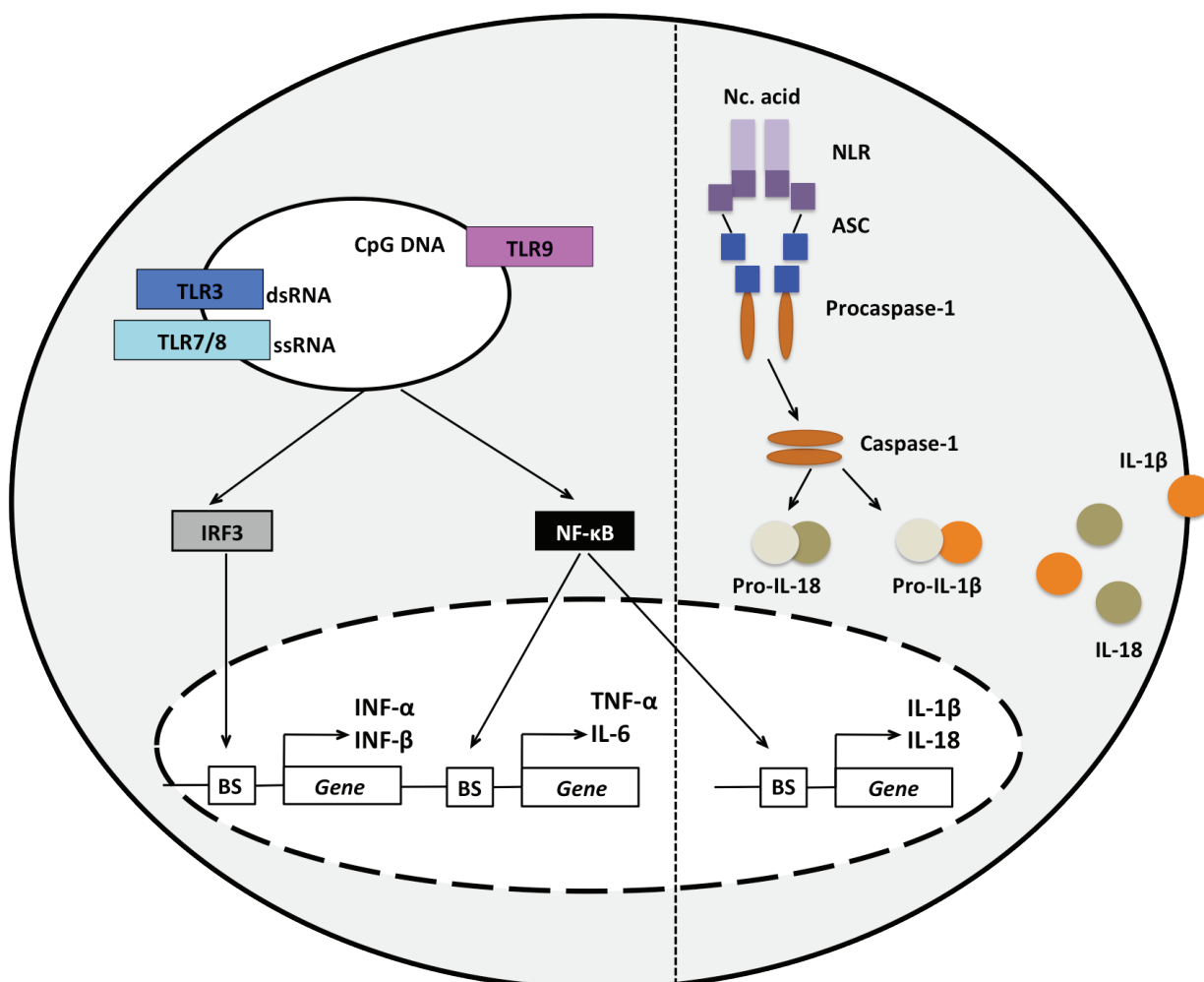
The counterpart of RLRs, which sense exogenous RNA, are the cytosolic sensors that detect microbial DNA. Two distinct pathways are activated upon recognition by cytosolic DNA detectors. The first involves the inflammasome-dependant activation of caspase-1. The second pathway leads to the transcription of type I IFN and proinflammatory genes via a Tank-binding kinase 1 (TBK1)/IRF3-dependent pathway (Ishii *et al.* 2006; Stetson & Medzhitov 2006).

The inflammasome is a multiprotein complex formed by a cytosolic DNA sensor, an adaptor protein called ASC, and pro-caspase-1. The cytosolic sensors can be of two different families of proteins: i) NOD-like receptors (NLR), from which NLRP3 and NLRP4 are the best-studied sensors, and ii) pyrin and HIN200 domain-containing (PYHIN) receptors, which include absent in melanoma 2 (AIM2), and IFN inducible protein 16 (IFI16). Interestingly, some of these sensors detect the DNA in an indirect way, sensing changes in the cellular milieu or membrane perturbations associated with viral entry. This has been suggested that for the NLRP3 inflammasome (Barlan *et al.* 2011). On the contrary, AIM2 and IFI16 act as direct sensors for cytoplasmic DNA.

Upon activation of these sensors, the other components of the inflammasome are recruited to provoke the proteolysis of pro-caspase-1 into caspase-1, which ultimately leads to the processing of pro-IL-1 $\beta$  and pro-IL-18 into their active forms. This cascade culminates in cell death by pyroptosis, in the secretion of IFN- $\gamma$  and natural killer cells activation.

Type I IFN production is another consequence of cytosolic DNA sensing, although the molecular bases of this response are less clear. It has been established that a signaling pathway consisting of stimulator of type I IFN gene (STING)–TBK1–IRF3 is essential for

type I IFN responses to DNA. The involvement of TBK1 is not surprising since it was originally characterized as the kinase activating IRF3 in TLR and RLR pathways (Fitzgerald *et al.* 2003; McWhirter *et al.* 2004). This means that IRF3 phosphorylation is a key element in the transcription of type I IFN (Atianand & Fitzgerald 2013).

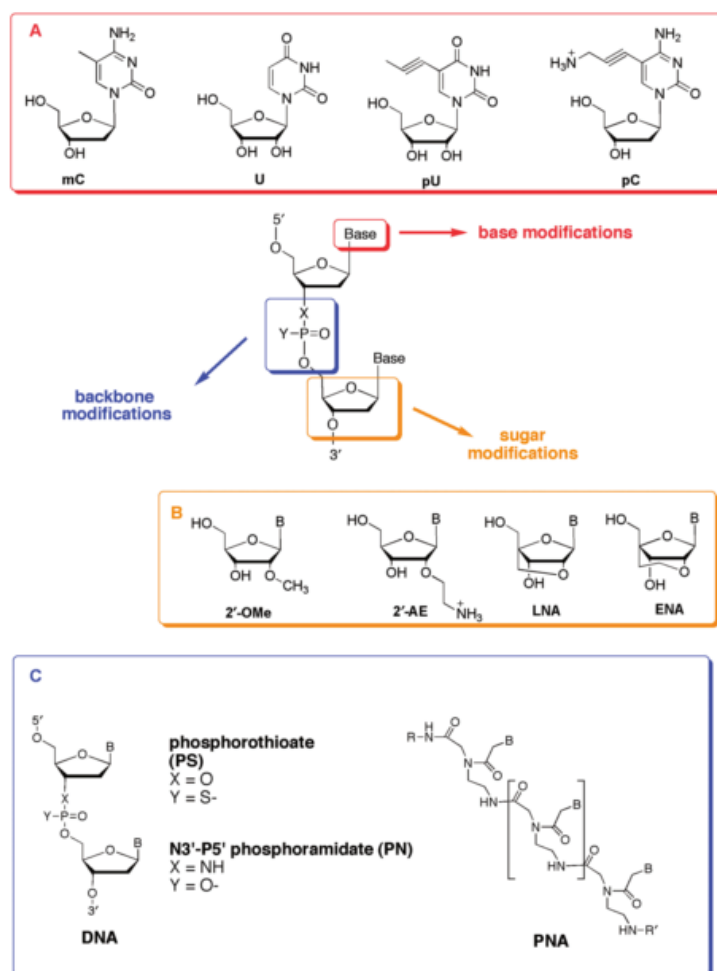


**Figure 10.** Schematic representation of the pathways studied in this thesis. The left side of the panel represents the TLR pathway, while the right side represents the inflammasome activation.

Therefore, the activation of the innate immune system by nucleic acids converges in the activation of transcription factors, such as IRF3/7 and NF-κB, that will produce a generalized increase in transcription of type I IFN and several other proinflammatory cytokines: IL-6, TNF $\alpha$ , pro-IL-1 $\beta$  and pro-IL-18, as well as triggering the formation of the inflammasome (figure 10).

### 1.2.3 Chemical modifications

Chemical modifications can improve the pharmacokinetic (PK) and pharmacodynamic (PD) properties of therapeutic oligonucleotides, and to decrease their unintended immunogenic effects. These modifications include changes in the sugar, base or backbone (figure 11). Common modifications to sugar moieties include replacing of the 2'-position hydrogen by 2'-O-methyl, 2'-fluoro, 2'-amine, or the introduction of locked nucleic acids (LNA). Base modifications aim to substitute the positions that are exposed to solvents in the major groove (i.e., the 4-position and 5-position of pyrimidines and the 6-position and 7-position of purines) (Herdewijn 2000). Among well-known base modifications, 5-methylcytosine (mC) ameliorates the pH restrictions on TFOs in the pyrimidine motif.

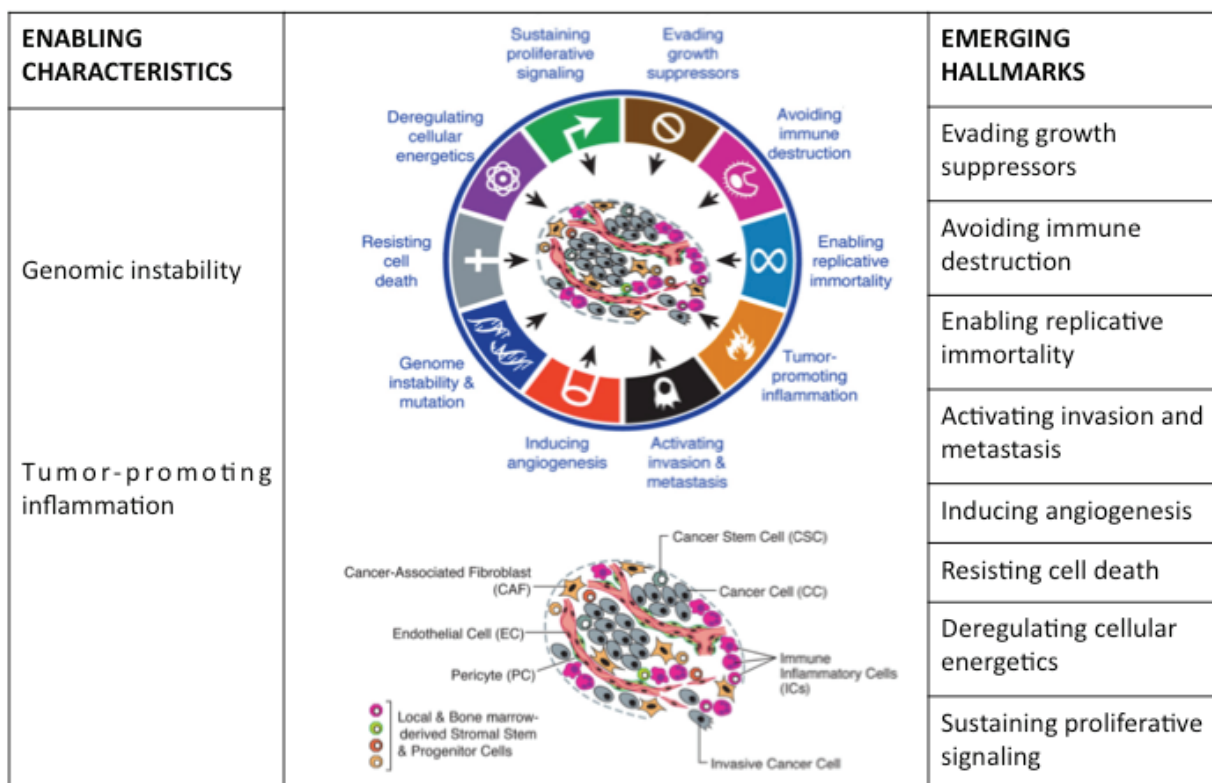


Backbone modifications include introducing phosphorothioate bonds, which have increased nuclease resistance and are capable of activating RNase H activity, or replacing the phosphate-ribose backbone by a polyamide one (PNA). A common denominator in therapeutic oligonucleotides is the use of phosphorothioate backbones and 2'-modifications.

**Figure 11.** Some chemical modifications. (A) Base modifications. (B) sugar modifications and (C) backbone modifications. mC: methylcytosine; pU: 5-propynyl-uridine; pC: propynyl-cytosine; 2'-OMe: 2'-O-methyl; 2'-AE: 2'-aminoethyl; LNA: locked nucleic acid; ENA: O2',O4'-ethylene-linked nucleic acid; PNA: peptide nucleic acid. Obtained from Duca *et al.* 2008.

### 1.3 CANCER AND RELEVANT TARGETS

Cancer is a disease characterized by an uncontrolled and aberrant proliferation of cells. It is the result of an acquired self-sufficiency that allows the cells to ignore the normal division, differentiation or death signals. Cancer development is a multistep process that requires genetic alterations to transform normal cells into malignant cells, acquiring during this transition a succession of hallmark capabilities that enables them to survive, proliferate and disseminate (Hanahan & Weinberg 2000). These hallmarks are common in most and perhaps all types of cancers and are listed in figure 12. Cells also require enabling characteristics, such as genome instability and an inflammatory state present in pre-malignant states that contribute and facilitate the succession of alterations that may start tumorigenesis (Hanahan & Weinberg 2011).



**Figure 12.** Illustration encompassing the enabling characteristics and the eight acquired capabilities of cancer cells, as well as the representation of the different cell types constituting solid tumors, all of which contribute to the tumorigenic process. Adapted from Hanahan and Weinberg, 2011.

The cells forming a tumor are heterogeneous and have an important genetic diversity. This was evidenced by sequencing the genomes of cancer cells from different

sectors of the same tumor (Yachida *et al.* 2010). These subpopulations have different degrees of differentiation, vascularization, proliferation and invasive capacity. This is of high clinical importance because almost all current therapeutic regimens predominantly target the rapidly proliferating cells. The cell types that contribute differently to the biology of the tumors are: cancer stem cells (CSC), which can self-renew and drive tumorigenesis, endothelial cells, pericytes, immune inflammatory cells and cancer-associated fibroblasts. These cells create a microenvironment that is propitious for tumor growth. An additional layer of complexity to cancer is metastasis, and the fact that mutations found in a primary tumor may vary from the mutations found in the corresponding metastatic disease, as evidenced by analyzing the PIK3CA mutations of primary breast cancer tumors and the metastatic lesions (Dupont Jensen *et al.* 2011). Circulating tumor cells (CTCs) also show a high heterogeneity, and cell-to-cell variations have been reported even within a single blood draw (Powell *et al.* 2012).

The understanding of signaling pathways that are altered in cancer cells, together with the possibility of building biological association networks (BANs), allows to comprehend the operative network within these cells, and to pinpoint important genes in cancer development, progression or drug-resistance (Selga *et al.* 2009), ultimately leading to a more rationalized understanding of cancer, and therefore, of its treatment.

### **1.3.1 Target genes with therapeutic applications**

The target genes chosen in this work encompass a variety of biological functions: antiapoptotic genes, topoisomerases, protein kinases, and transcription factors. They are essential for cell viability or are involved in anti-apoptotic activity. Therefore, inhibiting these genes results in cell death, opening the possibility to use them to eliminate cancer cells.

#### **1.3.1.1 BCL2**

B-cell CLL/lymphoma 2 (BCL2) is an integral outer mitochondrial membrane protein, member of a family of proteins that control apoptosis. This control depends on the balance between pro-apoptotic proteins –BAX, BAK and BOK– and anti-apoptotic

proteins –BCL2, BCL-X<sub>L</sub>, BCL<sub>W</sub> and MCL-1. BCL2 blocks apoptosis by regulating the mitochondrial permeability since it prevents the formation of pores in the mitochondria, by inhibiting BAX. This allows the release of cytochrome-c, ultimately activating the cascade of caspases that lead to apoptosis.

The translocation of this gene is involved in the appearance of cancer, such as follicular lymphoma, breast cancer and melanoma. The overexpression of BCL2 contributes to cancer progression and it is also related to the appearance of the multi-drug resistance phenotype (Azmi *et al.* 2011; Miyashita & Reed 1993). Regarding solid tumors, BCL2 is overexpressed in 30%–60% of prostate cancers at diagnosis and in nearly 100% of castration-resistant prostate cancer (Hall *et al.* 2013) and its content has been related to increased resistance to gemcitabine (Bold *et al.* 1999). Antisense oligonucleotides (oblimersen), antibodies, peptides, and small molecules against BCL2 are under development. Even though partially successful, none of these approaches has been proven to be useful in the clinic because they present problems of specificity, side effects, short half-life, and delivery.

### 1.3.1.2 *TOP1*

Topoisomerase-1 (TOP1) is an enzyme that controls DNA topology. During transcription or DNA replication, the dsDNA needs to unwind, producing additional torsions in the regions flanking the DNA. To avoid these tensions, topoisomerase-1 catalyzes the transient breaking and rejoining of a single strand of DNA, which allows the strands to pass through one another. Topoisomerase-1 is a clinically validated target; TOP1 inhibitors, such as camptothecin (CPT) and its derivatives (irinotecan and topotecan), have been used as anticancer therapy since the late 90s. The rationale of these drugs is based on the stabilization of TOP1–DNA cleavage complexes, leading to persisting single-stranded DNA breaks that convert into cytotoxic DNA double-strand breaks during DNA synthesis. The cytotoxicity of these drugs is dependent on the expression of TOPI, which is overexpressed in tumors, relative to the corresponding normal tissue (Giovanello *et al.* 1989) and during DNA replication (Goldwasser *et al.* 1996; Mross *et al.* 2004).

### **1.3.1.3 *MTOR***

Mammalian target of rapamycin (mTOR) is a 289 kDa serine/threonine protein kinase that belongs to the phosphatidylinositol 3-kinase-related kinase (PIKK) family. PIKK family members regulate cell cycle progression and cell cycle checkpoints that govern cellular responses to DNA damage and DNA recombination (Mita *et al.* 2003). mTOR is a central modulator of cell growth and plays a critical role in transducing proliferative signals mediated by the PI3K/AKT/mTOR signaling pathway in response to nutrient availability and growth factor stimuli (Tokunaga *et al.* 2008; Wullschleger *et al.* 2006). The PI3K/AKT/mTOR pathway is a prosurvival pathway that is constitutively activated in many types of cancer. It plays an important role in cancer development, progression, and therapeutic resistance.

### **1.3.1.4 *MDM2***

Murine double minute 2 (MDM2) is a negative regulator of the tumor suppressor protein p53, which is the most frequently mutated gene in human cancer (Vogelstein *et al.* 2000). Releasing p53 from MDM2 has been suggested as a mechanism for cancer therapy (Lane *et al.* 2010), especially in cancer types with wild-type p53 and overexpressed MDM2. In 2004, Nutlins, MDM2 inhibitors, were identified and studies with these compounds have strengthened the idea that p53 activation might represent an alternative to chemotherapy (Vassilev 2004). It has been shown that Nutlins, especially Nutlin-3, are able to induce cell cycle arrest, apoptosis, and growth inhibition of human tumor xenografts in mice models (Vassilev *et al.* 2004) and to produce a synergistic effect when used in combination with the chemotherapeutic drugs used for the treatment of hematological malignancies (Gu *et al.* 2008) and pancreatic cancer (Conradt *et al.* 2013).

### **1.3.1.5 *MYC***

MYC is a transcription factor involved in many biological processes, including cell growth, cell cycle progression, metabolism, and survival. MYC alteration is observed in a wide range of tissue types including breast, lung, and prostate cancer and it is one of the most frequently amplified oncogene in human cancers: up to 30% of all cancers present overexpression of MYC, which also correlates with poor prognosis. It has been established

that MYC overexpression is essential for tumor initiation and maintenance (Li *et al.* 2014) and its overactivation frequently results in the dependence of tumor survival on high levels of MYC, also called MYC addiction. The direct inhibition of MYC through small molecules has not been accomplished: as a transcription factor, MYC represents a challenging target since it functions via protein-protein interactions and lacks enzymatic activity. Therefore, MYC is considered the prototype of an undruggable target.

#### **1.3.1.6 DHFR**

The dihydrofolate reductase (DHFR) enzyme converts dihydrofolate (DHF) into tetrahydrofolate (THF). THF acts as a methyl group transporter, which is required for the *de novo* synthesis of purines, thymidylate, and glycine. Therefore, DHFR enzyme is involved in DNA replication during cell division. During the last 65 years the use of antifolates have been very important for the treatment of infectious and inflammatory diseases, as well as for cancer. Methotrexate is one of such antifolates, and it has been used for the treatment of osteosarcoma, Non-Hodgkin lymphoma and breast, head and neck, and bladder cancer (Assaraf 2007). Combination therapies of methotrexate, oxiplatinum and 5-fluoruracil have been tested in colon cancer (Guglielmi *et al.* 2004; Zampino *et al.* 2006).





## TWO | OBJECTIVES



The main objectives of this thesis were to study the properties of the PPRHs and to validate their use as gene silencing molecules in several cancer cell lines. To do so we established the following goals:

1. To determine the stability and immunogenic potential of PPRHs. This objective is subdivided as follows:
  - To study the stability of PPRHs and siRNAs in different types of serum, as well as in cells.
  - To study the activation of the TLR and inflammasome pathways upon incubation with PPRHs and siRNAs.
2. To evaluate the activity of other structures of PPRHs, specifically nicked-circular-PPRHs and RNA-PPRHs
3. To validate the use of PPRHs as silencing tools for a set of cancer-relevant genes, such as *BCL2*, *MTOR*, *TOP1*, *MDM2* or *MYC*, in different cell types.
4. To study the applicability of DNA aptamers as targeting and enhancing molecules for PPRHs.



## THREE | MATERIALS AND METHODS



Methods are described within the articles presented in the “Results” section of this thesis. However, methods that are considered innovative are described in more detail, as well as the biologic material used in this work.

### 3.1 Materials

#### 3.1.1 Cell lines

All cell lines used were derived from human solid tumors, except for the THP-1 cell line, which is of hematopoietic origin. They were obtained from the ATCC repository, and are specified in Table 1.

CELL LINE	CELL TYPE
HCT-116	Colorectal carcinoma
MCF7	Breast adenocarcinoma
MDA-MB-231	Breast adenocarcinoma
MDA-MB-468	Breast adenocarcinoma
MiaPaCa-2	Pancreas carcinoma
PC3	Prostate adenocarcinoma
SKBR3	Breast adenocarcinoma
THP-1	Acute monocytic leukemia
THP-1 iGLuc	Acute monocytic leukemia stably transduced with iGLuc reporter vector.

**Table 1** Cell lines used in the experiments including information about cell type.

#### 3.1.2 Culture media

All cell lines were grown in Ham’s F-12 medium supplemented with sodium bicarbonate (14mM, Applichem), Penicillin G sodium salt (100U/mL, Sigma-Aldrich), streptomycin (100mg/L, Sigma-Aldrich) and 7% fetal bovine serum (FBS, GIBCO, Invitrogen). Cells were incubated at 37°C and 5% of CO<sub>2</sub>. Trypsinization to expand



cells was performed using 0.05% Trypsin (Sigma-Aldrich) in PBS 1X (154mM NaCl, 3.88mM H<sub>2</sub>NaPO<sub>4</sub>, 6.1mM HNaPO<sub>4</sub>, pH 7.4).

The experiments in which *dhfr* was targeted a selective Ham's F-12, lacking the final products of the DHFR enzymatic activity glycine, hypoxanthine (H) and thymidine (T) medium was used (-GHT medium, Gibco). As selective medium it can also be used MEM or RPMI from Gibco, since they do not contain either H or T. Those media are supplemented with serum that has been dialyzed against PBS to eliminate small molecular compounds such as H and T that could be present in the serum.

### 3.1.3 PPRHs

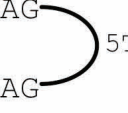
The nomenclature of PPRHs is as follows:

- Hp: PPRH hairpin
- Target gene: d for *dhfr*; Bcl for *bcl2*; Tor for *mtor*; Top for *top1*; Mdm for *mdm2*; Myc for *c-myc*; LacZ for *lacZ* (*E. coli*); s for *survivin*;
- Target region within the gene: I for intron; E for exon; Pr for promoter. The number after these letters represent the position of the exon or intron within the gene (E1: exon one; I7: intron seven)
- Type of PPRH: B for blunted; T for template; C for coding.
- Negative controls: Sc for scrambled PPRHs that do not have targets in the genome; WC for PPRHs that form intramolecular Watson-Crick bonds.
- Nc: nicked-circle.

PPRHs targeting specific genes	
Name	PPRHs against <i>dhfr</i>
<b>HpdI3-B</b>	5' - GGAGGAGGGAGAGGGAGGAG 5T 3' - GGAGGAGGGAGAGGGAGGAG
<b>ncPPRH-in</b>	5T ( GGAGGAGGGAGAGGGAGGAG ) 5T 3'   5' GGAGGAGGGAGAGGGAGGAG GGAGGAGGGAGAGGGAGGAG
<b>ncPPRH-out</b>	5T ( GGAGGAGGGAGAGGGAGGAG ) 5T GGAGGAGGGAGAGGGAGGAG 5'   3' GGAGGAGGGAGAGGGAGGAG
<b>RNA-HpdI3-B</b>	5' - GGAGGAGGGAGAGGGAGGAG 5U 3' - GGAGGAGGGAGAGGGAGGAG

The structure of the PPRHs is shown; the 5' and 3' ends are indicated. In the case of ncPPRH-in and ncPPRH-out the black bar corresponds to the nick present in the sequences.

Name	PPRHs against <i>bcl2</i>
<b>HpBcl2Pr-C</b>	5' - GG <b>A</b> GAGGGG <b>A</b> GGGGAGAAGGAGG 5T 3' - GG <b>A</b> GAGGGG <b>A</b> GGGGAGAAGGAGG
<b>HpBcl2E1-C</b>	5' - <b>G</b> AGGGGAGAGGGAG <b>A</b> AAAAA 5T 3' - <b>G</b> AGGGGAGAGGGAG <b>A</b> AAAAA
<b>HpBcl2I2-T</b>	5' - GAAGGGGG <b>A</b> AG <b>A</b> AGAGAGAGAAG <b>A</b> GAGAGA 5T 3' - GAAGGGGG <b>A</b> AG <b>A</b> AGAGAGAGAAG <b>A</b> GAGAGA
<b>HpBcl2I2-C</b>	5' - GGGGAGGAGGAAAAGAAGGAAGGAAGAGG 5T 3' - GGGGAGGAGGAAAAGAAGGAAGGAAGAGG

Name	PPRHs against <i>mtor</i>
<b>HpTorPr-C</b>	5' - GGGAG <b>C</b> GAGGGAAGGAGGG  3' - GGGAG <b>C</b> GAGGGAAGGAGGG
<b>HpTorE5-C</b>	5' - GGAAGAAGAAGGAAGGGAAG  3' - GGAAGAAGAAGGAAGGGAAG
<b>HpTor-T</b>	5' - GA <b>TGGT</b> GGAGAAAGGAAGAGAGGG  3' - GA <b>TGGT</b> GGAGAAAGGAAGAGAGGG
<b>HpTorI17-C</b>	5' - GGGAAAGGGGAGGGAAAAAGA  3' - GGGAAAGGGGAGGGAAAAAGA

---

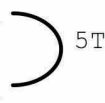

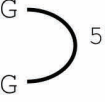
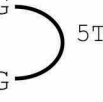
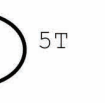
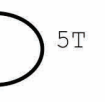
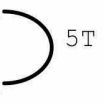
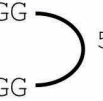
Name	PPRHs against <i>top1</i>
<b>HpTop12-T</b>	5' - GGAG <b>A</b> GGAGGAGGGAGAAAA  3' - GGAG <b>A</b> GGAGGAGGGAGAAAA

---

PPRHs against <i>mdm2</i>	
<b>HpMdm17-T</b>	5' - GGGAAGGA <b>A</b> AGAAGA <b>A</b> GGG <b>A</b> G  3' - GGGAAGGA <b>A</b> AGAAGA <b>A</b> GGG <b>A</b> G

---

PPRHs against <i>c-myc</i>	
<b>HpMyc11-T</b>	5' - GGG <b>A</b> AAAAGGGAGA <b>A</b> GGAAAGAGGAGAGGG <b>A</b> AGAA  3' - GGG <b>A</b> AAAAGGGAGA <b>A</b> GGAAAGAGGAGAGGG <b>A</b> AGAA

PPRHs against <i>sp1</i>	
<b>HpSP1Pr-C</b>	5' -GAGGGAGGGGGAAAGGAGGGA 3' -GAGGGAGGGGGAAAGGAGGGA 
<b>HpSP1E2I2-T</b>	5' -GGAGGAGGAGGG <b>CAGGTAAGTGA</b> 3' -GGAGGAGGAGGG <b>CAGGTAAGTGA</b> 
<b>HpSP1I3-T</b>	5' -AGGAAGGGAGAAGGAAAGGGAG 3' -AGGAAGGGAGAAGGAAAGGGAG 
PPRHs used as negative controls	
Name	Scrambled PPRHs
<b>Hp-Sc1 (HpsPr-Sc)</b>	5' - AAGAGAAAAAGAGAAAGAAGAGAGGG 3' - AAGAGAAAAAGAGAAAGAAGAGAGGG 
<b>Hp-Sc2</b>	5' - AGAGGAGAGAAGGAAGGAGG 3' - AGAGGAGAGAAGGAAGGAGG 
<b>Hp-Sc3</b>	5' - GAGAAGAGGAAGAGAGGAAGG 3' - GAGAAGAGGAAGAGAGGAAGG 
<b>Hp-Sc4</b>	5' - AGAGAAGAGGAAGAGAGGAAAGAGAGGAAGAGGA 3' - AGAGAAGAGGAAGAGAGGAAAGAGAGGAAGAGGA 
<b>HptI8-Sc</b>	5' - AAAAGAAGAAGAAGAAGAAGAAGG 3' - AAAAGAAGAAGAAGAAGAAGAAGG 

Watson-Crick PPRHs	
<b>HpBcl2E1-WC</b>	5' - <b>C</b> TCCCCTCTCCCTCTTTTTT 3' - <b>G</b> AGGGGAGAGGGAGAAAAA
<b>HpTorPr-WC</b>	5' - CCCTCCTTCCCTCCCTCCC 3' - GGGAGGAAGGGAG <b>C</b> GAGGG
<b>HpTopI2-WC</b>	5' - CCT <b>C</b> TCTCCTCCCTCTTTT 3' - GGAG <b>A</b> GGAGGAGGGAGAAAA
<b>HpMdm17-WC</b>	5' - CCCTCCTGTCTTCTGCCCGC 3' - GGGAAGGAAAGAAGAAGGGAG
<b>HpMyc11-WC</b>	5' - CCCTTTTTCCCTCTTCCTTCTCCTCTCCCTTCTT 3' - GGGAAAAAGGGAGAAGGAAGAGGAGAGGGGAAGAA
<b>PPRHs targeting bacterial genes</b>	
<b>HpLacZ</b>	5' - GGAGAAAGGGGGAAGAG 3' - GGAGAAAGGGGGAAGAG
Fluorescent PPRHs	
Name	PPRHs against <i>dhfr</i>
<b>F-PPRH-D (HpdI3-BF)</b>	5' - <b>F</b> -GGAGGAGGGAGAGGGAGGAG 3' - GGAGGAGGGAGAGGGAGGAG
<b>F-PPRH-S (HpsPr-CF)</b>	5' - <b>F</b> -AGGGGAGGGAAGGAGAGAAG 3' - AGGGGAGGGAAGGAGAGAAG
<b>ncPPRH-in-F</b>	5T ( ) 5T GGAGGAGGGAGAGGGAGGAG 3'   5' <b>F</b> GGAGGAGGGAGAGGGAGGAG
<b>ncPPRH-out-F</b>	5T ( ) 5T GGAGGAGGGAGAGGGAGGAG 5'   3' <b>F</b> GGAGGAGGGAGAGGGAGGAG

### 3.1.4 siRNAs

Both the sense and antisense strand are indicated. For sequences obtained commercially, the reference is provided. The orientation for all sequences is 5' → 3'.

siRNAs used in immunogenicity studies	
<b>siLUC</b>	Anti UAAGGCUAUGAAGAGAUACTT Sense GUAUCUCUUCAUAGCCUUATT
<b>siRNA-A</b>	Santa Cruz Biotechnology. Ref: sc-37003
<b>siRNA-B</b>	Santa Cruz Biotechnology. Ref: sc-44230

Fluorescence-labeled siRNA used in uptake and/or stability experiments	
<b>F-siRNA</b>	Anti GCGCAACCGGACGAAUGCUTT Sense F-AGCAUUCGUCCGGUUGCGCTT

### 3.1.5 Aptamers

Sequence orientation is 5' → 3'. Bold letters represent the linker between the aptamer and the PPRH. Underscored letters represent the scrambled oligonucleotides from the original ApHER2(t) aptamer.

Aptamers	
ApHER2(t)	GCAGCGGTGTGGGGGCAGCGGTGTGGGGGCAGC GGTGTGGGG
ApHER2(t)-5T-HpdI3-B	GCAGCGGTGTGGGGGCAGCGGTGTGGGGGCAGC GGTGTGGGG <b>TTTTT</b> GGAGGAGGGAGAGGGAGG AGTTTTT <b>G</b> AGGAGGGAGAGGGAGGAGG
ApHER2(t)Sc-5T-HpdI3-B	<u>GACGGCGGT</u> TGGGGG <u>CCGAG</u> GTGTGGGGGCAGC GGTGTGGGG <b>TTTTT</b> GGAGGAGGGAGAGGGAGG AGTTTTT <b>G</b> AGGAGGGAGAGGGAGGAGG

### 3.1.6 Primers

Primer sequences (5' → 3' forward, reverse) used for the RT-real time PCR

Primers sequences	
INF- $\alpha$	TTATCCAGGCTGTGGGTCT, GCAAGCCCAGAAGTATCTGC
INF- $\beta$	TGGAGAAGCACAAACAGGAG, AACCTTTCGAAGCCTTTGCT;
IL-6	CATTTGTGGTTGGGTCAGG, AGTGAGGAACAAGCCAGAGC;
TNF- $\alpha$	GCCAGAGGGCTGATTAGAG, TCAGCCTCTTCTCCTTCCTG;
IL-1 $\beta$	GTGGCAATGAGGATGACTTGTTTC, TAGTGGTGGTCGGAGATTCGTA
IL-18	CCTCAGACCTTCCAGATCGC, TTCCAGGTTTTTCATCATCTTCAGC
APRT	GCAGCTGGTTGAGCAGCGGAT, AGAGTGGGGCCTGGCAGCTTC.

### 3.1.7 Other sequences

Sequences used in EMSA. The underlined letters correspond to the target sequence of HpdI3-B

Sequences used as probes in EMSA	
Target seq fwd strand	CATTCTCTTGATTG <u>CCTCCTCCCTCTCCCTCCTC</u>
Target seq rev strand	<u>GAGGAGGGAGAGGGAGGAGGCAATCAAGAGAATG</u>

### 3.1.8 Plasmid vectors

Vectors carrying the LUC gene allow studying the eukaryotic transcription by determining the enzymatic activity of the luciferase oxidative enzyme.

- pGL3-Basic (Promega): it is a vector that lacks promoter and enhancer sequences. It allows studying different promoters by placing them upstream the translation site of the luciferase gene. This vector contains the ampicillin resistance gene.

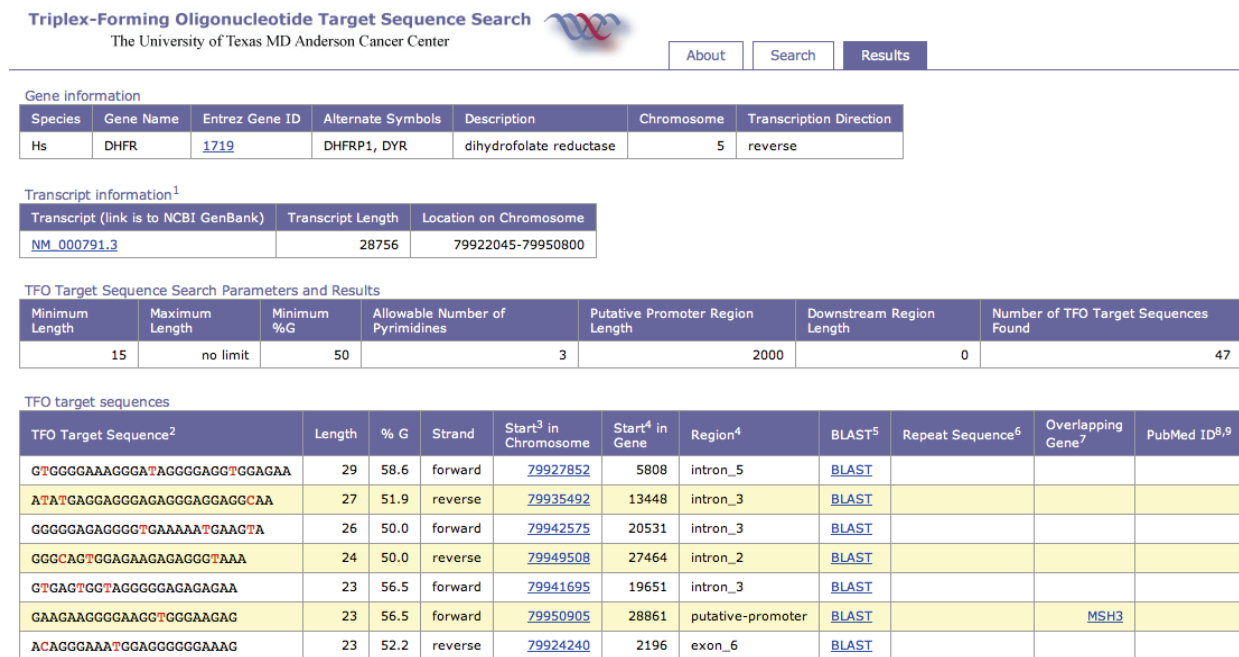
- pGL3-for5: construct obtained by cloning 1593 bp of the *SP1* promoter into pGL3-Basic vector, between the position -1612 and -20 of the translation start site. Fragments were obtained by digesting with the restriction enzymes XhoI and NheI (Nicolas *et al.* 2001).
- pSilencer 2.1-U6 Neo-NR / pSilencer-NR (Thermo Fisher Scientific): this vector is generally used for the expression of siRNA, but was used here as the starting empty vector to generate a construct to express PPRHs intracellularly. It contains the antibiotic resistance gene (neomycin) to enable selection of transfected cells, and also the ampicillin resistance gene. It features the human RNA polymerase III promoter (U6). The DNA sequences that will produce a hairpin siRNA after transcription are cloned downstream the U6 promoter. In this case a non-related control sequence was used; the sequence contains an internal XhoI restriction site.
- pSilencer-HpdI3-B: This construct was obtained by cloning the dsDNA sequence encoding for HpdI3-B into the pSilencer-NR vector described above. It contains an internal restriction site for XhoI enzyme.



## 3.2 Methods

### 3.2.1 Design of PPRHs

PPRHs were designed using the Triplex-Forming Oligonucleotide Target Sequence Search tool, available at <http://spi.mdanderson.org/tfo/>. This software finds the polypurine tracks present in a gene, allowing us to determine the sequence of the polypyrimidine targets. The search of the targets began by introducing the name of the gene of interest, together with other parameters that can be selected by the user, such as maximum number of interruption or the %G. The software provides a list of polypurine sequences within the gene, and the strand (forward or reverse), genic (promoter, exon or intron) and genomic locations. An example of this tool output is shown in figure 13. This sequence allowed us to design the PPRHs following the WC and reverse Hoogsteen base pairing rules.



**Figure 13.** Results obtained in the Triplex-Forming Oligonucleotide Target Sequence Search tool when looking for polypurine stretches within the human *dhfr* gene.

Sequences of at least 20nt were chosen to design the PPRHs. If purine interruptions (up to 3) were present in the pyrimidine target sequence, when designing the PPRHs those positions were substituted by either an adenine or the complementary

pyrimidine. The specificity of the chosen polypurine tracks was evaluated by BLAST analyses.

PPRHs were synthesized as non-modified oligodeoxynucleotides by Sigma-Aldrich (Madrid, Spain), including desalted purification. They were dissolved at 1 mM (stock solution) in sterile RNase-free Tris-EDTA buffer (1 mM EDTA and 10 mM Tris, pH 8.0) and stored at -20°C until use.

### **3.2.2 Stability in Fetal Calf Serum, Mouse Serum, and Human Serum.**

Fluorescence-labeled oligonucleotides, were used to assess the half-lives of both PPRHs and siRNA in FCS, mouse and human serum. To do so, a determined amount of the specific oligonucleotide was incubated with 100% serum at 37 °C in a water-bath. At different periods of time (0, 5, 15, 30, 60, 120, 180, 240, 300, and 360 min) aliquots of 150 ng of oligonucleotide were withdrawn, and serum was inactivated by the addition of 1 µL of 0.5 M EDTA (pH 8.01). Then, samples were treated with proteinase K (0.5 µg/µL, Gibco) and 1% SDS and incubated for 2 h at 60 °C at 400 rpm in a Thermo-mixer Compact (Eppendorf, Hamburg, Germany) to remove serum proteins. The samples were resolved by gel electrophoresis, and the fluorescence associated with each band was quantified using the ImageQuant software.

For stability experiments of the different types of PPRHs bound to their target, a determined amount of the different F-PPRHs, F-PPRH-D, F-nicked-circle-PPRH-in, and F-nicked- circle-PPRH-out (150 ng/point) was incubated with a 5-fold mass excess of the target sequence in binding buffer (10 mM MgCl<sub>2</sub>, 100 mM NaCl and 50 mM HEPES, pH 7.2) in 20 µL reactions for 30 min at 37 °C. An equal volume of FCS was then added to the binding reaction, and the different mixes were incubated in a water-bath at 37 °C for up to 120 min. At different periods of time (0, 60, and 120) aliquots of 150 ng of the labeled PPRHs were withdrawn and serum was inactivated by the addition of 1 µL of 0.5 M EDTA (pH 8.01). Samples were treated with proteinase K (0.5 µg/µL) and 1% SDS and incubated for 30 min in a Thermo-mixer Compact at 60 °C at 400 rpm. The samples were resolved by gel electrophoresis, and the fluorescence associated to each band was quantified using the ImageQuant software.

### 3.2.3 PPRHs and siRNA Half-Life in Cells.

PC3 cells (150 000) were plated in 35-mm dishes in 2 mL of Ham's F-12 medium and transfected with 30 nM of either F-PPRH or F-siRNA. Twenty-four hours after transfection, cells were washed once with PBS and incubated for different periods of time, ranging from 6 to 72 h, in Ham's F-12 medium. Then cells were collected in 2 mL Eppendorf tubes and centrifuged at 800g at 4 °C in a micro-centrifuge. The supernatant was removed and the pellet was washed in 1 mL of ice-cold PBS, centrifugation was repeated, and the cells resuspended in 500 µL of PBS and propidium iodide (5 µg/mL). The fluorescence of the cells was analyzed in a cytometer XL-Coulter.

### 3.2.4 Determination of the immune response

To determine the immune response of THP-1 cells to PPRHs we studied the mRNA levels of several proinflammatory cytokines, including INF- $\alpha$ , INF- $\beta$ , TNF- $\alpha$ , IL-6, IL-1 $\beta$  and IL-18. In the case of IL-1 $\beta$ , Western blot was also performed to analyze the protein levels. The levels of TFs NF- $\kappa$ B and IRF3, as well as the phosphorylation of the latter, were determined by western blot. Finally, the levels and activity of the proteolytic enzyme caspase-1 were determined by Western blot, and by a novel luciferase-based reporter system (Bartok *et al.* 2013), respectively. These determinations allowed us to study the TLR pathway and the inflammasome activation

#### 3.2.4.1 mRNA determination

mRNA levels of the proinflammatory cytokines were determined by RT-real time PCR. Reverse transcription was performed using 1µg of RNA obtained from THP-1 cells extracted by the Trizol method (Invitrogen, Madrid, Spain). Complementary DNA was synthesized in a total volume of 20 µl by mixing the RNA, 125 ng of random hexamers (Roche), in the presence of 75 mM KCl, 3 mM MgCl<sub>2</sub>, 10 mM dithiothreitol, 20 units of RNasin (Promega), 0.5 mM dNTPs (AppliChem), 200 units of M-MLV reverse transcriptase (Invitrogen) and 50 mM Tris-HCl buffer, pH 8.3. The reaction mixture was incubated at 37°C for 60 min. The cDNA product was used for subsequent Real-time PCR amplification using the OneStep Plus TM Real-Time PCR System

(Applied Biosystems). mRNA levels were determined with SYBR-Green (Applied Biosystems, Life Technologies SA, Madrid, Spain) and specific designed primers. APRT was used as endogenous control. The primer sequences have been described in section 3.1.7 of this thesis. Results were analyzed following the  $\Delta\Delta C_t$  method.

#### 3.2.4.2 Western blot

THP-1 cells ( $10^6$ ) were plated in a 6-well dish (800  $\mu$ L) and transfected with 30 nM and 100 nM of either nonspecific PPRHs (HptI8-sc, HpsPr-sc and HpLacZ) or nonspecific siRNAs (siLUC, siRNA-A and siRNA-B). After 4 or 9 h of transfection, cells were collected and centrifuged for 5 min at 800g at 4 °C. Cells were resuspended in 30  $\mu$ L of RIPA buffer (150 mM NaCl, 5 mM EDTA, 50 mM Tris-HCl pH 7.4 (all from AppliChem, Barcelona, Spain), 1% Igepal CA-630, 0.5 mM PMSF, Protease inhibitor cocktail, 1 mM NaF (all from Sigma-Aldrich). Cell lysate was kept on ice for 30 min with vortexing every 10 min. Cell debris was removed by centrifugation at 15000g at 4 °C for 10 min. Five microliters of the extract was used to determine the protein concentration using the Bradford assay (Bio-Rad). Vehicles and the immunogenic cocktail LPS-ATP (0.1  $\mu$ g/mL and 2 mM, respectively) were also analyzed. Activation with LPS-ATP was used as catalyzer 2, 4, or 7 h before harvesting cells as indicated in the figure legends. Whole cell extracts (100  $\mu$ g) were resolved in 15% SDS-polyacrylamide gels and transferred to PVDF membranes (Immobilon P, Millipore) using a semidry electro- blotter. The blocking solution was 5% Blotto and when detecting phosphorylated IRF3, 5% BSA was used. Membranes were probed overnight at 4 °C with primary antibodies against IRF3 (1:200 dilution; sc-33641), NF- $\kappa$ B (1:200 dilution; sc-109), interleukine-1 $\beta$  (1:50 dilution; sc-7884), caspase-1 (1:200 dilution; sc-515), tubulin (1:200 dilution; sc-487) (all from Santa-Cruz Biotechnology Inc.), and p-IRF3 (1:1000 dilution; Cell Signaling, 4961S). Signals were detected by secondary horseradish peroxidase-conjugated antibody, either antirabbit (1:5000; Dako, Denmark) or antimouse (1:2500 dilution, sc-2005 Santa Cruz Biotechnology Inc.) and enhanced chemiluminescence using the ECL method, as recommended by the manufacturer (GE Healthcare). Chemiluminescence was detected with ImageQuant LAS 4000 mini technology (GE Healthcare).

### 3.2.4.3 Caspase-1 proteolytic activity determination

THP-1 iGLuc cells ( $2 \times 10^5$ ) were plated in 96-well dishes in 200  $\mu$ L of culture medium. Cells were allowed to attach and then transfected with 30 nM and 100 nM of either nonspecific PPRHs (HptI8-sc, HpsPr-sc, and HpLacZ) or nonspecific siRNAs (siLUC, siRNA-A and siRNA-B), as described in the Oligonucleotides Transfection section, in a final volume of 50  $\mu$ L. The supernatants (SN) were recovered 16 h after treatment. Equal volumes (15  $\mu$ L) of the supernatants were mixed with distilled water containing 4.4  $\mu$ M Coelenterazine (P.j.k. GmbH, Kleinblittersdorf, Germany) and light production (RLU) was determined in a Glomax<sup>TM</sup> 20/20 Luminometer (Promega). Each condition was analyzed in three different experiments. Vehicles and the positive controls LPS-ATP (0.1  $\mu$ g/mL and 2 mM, respectively) and dsDNA > 100 bp (250 bp) were also assessed for proteolytic activity. RLUs were corrected by total protein concentration, which was determined using the Bio-Rad protein assay reagent Bradford according to the manufacturer's protocol.

### **3.2.5 *In silico* studies**

The secondary structure of the aptamers was predicted using the mfold server (the RNA Institute, College of Arts and Sciences University of Albany; <http://mfold.rna.albany.edu/?q=mfold/DNA-Folding-Form>) (Zuker 2003) which predicts minimum free energy structures and base pair probabilities from single RNA or DNA sequences. The DNA Folding Form was chosen and the parameters of the ionic conditions were changed to 140 mM Na<sup>+</sup> and 10 mM Mg<sup>2+</sup> for the structural prediction.

### **3.2.6 Confocal microscopy**

Cells (300,000) were plated on cover-slips placed inside 35 mm dishes 24 h before the transfection with ApHER2(t)-F. After 24 h of the transfection cells were washed once with fresh F12 medium and incubated with Wheat Germ Agglutinin, Alexa Fluor® 555 Conjugate (Life Technologies, Madrid, Spain) at 4°C for 30 min. Cells were washed twice with PBS 1X for 5 min at RT and fixed with paraformaldehyde 4% for 10 min, two more washes with PBS 1X were performed. Cover-slips were mounted on slides using mowiol (Calbiochem, Madrid, Spain) and were kept protected from light at RT overnight. Confocal laser scanning microscopy was performed using a Leica TCS-SP2.

### 3.2.7 Luciferase experiments

Luciferase assays were performed to study the transcriptional activity of the transcription factor Sp1. We designed three PPRHs against Sp1, specifically against the coding strand of the promoter sequence (HpSP1Pr-C), the template strand of the exon2-intron2 boundary (HpSP1E2I2-T), and the template strand of intron three (HpSP1I3-T). SKBR3 cells (250,000) were plated in 6-well dishes, in a final volume of 800  $\mu$ L. After 24 h, the three PPRHs and the negative control were transfected using DOTAP. This consisted in mixing the appropriate amount of PPRH and DOTAP (Biontexas, München, Germany), considering a 1:100 molar ratio (PPRH:DOTAP), for 20 minutes in a volume of 200  $\mu$ l of medium at room temperature, followed by the addition of the mixture to the cells in a total volume of 1 mL. The final concentration of the PPRHs was 100 nM. After 48 h the medium was removed and 1 mL of fresh medium was added to each well to transfect 1  $\mu$ g of the plasmids pGL3-Basic and pGL3-for5. This transfection was performed with Fugene 6 (Promega, Madrid, Spain). For each experimental point, Fugene 6 was incubated for 5 min with serum and antibiotic-free medium, followed by the addition of plasmid DNA and incubated for 20 minutes. The volume for each reaction was 100  $\mu$ l. The ratio transfection reagent:plasmid was of 3:1 ( $\mu$ L of transfection reagent: $\mu$ g of plasmid). Luciferase activity was determined 30 h after plasmid transfection. Cell extracts were prepared by lysing the cells with 200  $\mu$ L of luciferase Lysis Buffer (2 mM DTT, 2 mM EDTA, 10% glycerol, 1% Triton X100, 25 mM Tris-Phosphate pH 7.8), which was prepared immediately before use. The lysate was centrifuged at 12,000 g for 2 min (4 °C) to pellet the cell debris, and the supernatants were transferred to a new eppendorf. The extract (25  $\mu$ L) was added to 25  $\mu$ L of the luciferase assay substrate (Promega, Madrid, Spain) at room temperature. Luminescence of the samples was measured immediately after mixture in the Glomax<sup>TM</sup> (Promega, Madrid, Spain) 20/20 Luminometer, in which the light production (relative luminescence units; RLU) was measured with 5 s integration during 10 s. Three different experiments were performed for each transfection. Luciferase results were corrected by total protein concentration, which was determined with the Bio-Rad protein assay reagent Bradford (Bio-Rad, Barcelona, Spain) according to the manufacturer's protocol.



## FOUR | RESULTS





## 4.1 ARTICLE I:

### **Stability and Immunogenicity Properties of the Gene-Silencing Polypurine Reverse Hoogsteen Hairpins**

Xenia Villalobos, Laura Rodríguez, Jeanne Prévot, Carlota Oleaga, Carlos J. Ciudad, and Véronique Noé

Mol. Pharmaceutics 2014, 11, 254–264 (Impact factor: 4.384)

#### *Background*

PPRHs are DNA-based silencing molecules, formed by two polypurine domains that are linked by a five-thymidine loop. PPRHs form intramolecular reverse Hoogsteen bonds and are capable of binding to a polypyrimidine target sequence by Watson-Crick bonds. PPRHs are designed against pyrimidine stretches present mainly in regulatory regions of genes, and upon binding cause a decrease in gene expression. There are two types of PPRHs depending on the location of their target sequence: template or coding PPRHs. Additionally, PPRHs can be designed to bind polypyrimidine stretches in different gene regions –promoter, intron or exon. Previously in our group, both types of PPRHs against *DHFR* were proved to decrease viability of breast cancer cells by means of decreasing *DHFR* levels (de Almagro *et al.* 2009; de Almagro *et al.* 2011). More recently we performed *in vivo* studies in a subcutaneous xenograft tumor model of PC3 prostate cancer cells and established the proof of concept of PPRHs as gene silencing tools in cancer therapy (Rodríguez *et al.* 2013).

#### *Objectives*

The aim of this work was to compare the stability and immunogenic properties between PPRHs and siRNAs, and to test other structures (*i.e.* nicked-circular PPRHs) to improve the over-all performance of PPRHs.

#### *Results*

To perform the stability experiments we used two different fluorescent PPRH sequences and one fluorescent siRNA sequence. The experiments were performed by incubating the different oligonucleotides for different periods of time in mouse, human,

and fetal calf serum, and in PC3 cells. This revealed that the half-life of PPRHs is much longer than that of siRNAs in all cases.

To determine if the binding affinity and efficacy of the PPRHs could be improved, we designed PPRHs with a circular structure, containing two pentathymidine loops, which we named nicked-circle-PPRHs (ncPPRHs). These PPRHs have a nick in one of the strands: ncPPRH-out has the nick in the strand of the hairpin that does not bind the dsDNA target sequence, while in the ncPPRH-in the nick is located in the strand of the hairpin that binds the target. By means of binding assays, we determined that the usage of PPRHs with a nicked-circular structure increased the binding affinity to their target sequence and their half-life in FCS when bound to the target.

To compare the possible inherent immunogenic activity of regular PPRHs (DNA polymer molecules) with that of siRNAs (ribonucleic acid polymer molecules), a monocytic cell line (THP-1 cells) was transfected with either nonspecific PPRHs (HptI8-sc, HpsPr-sc, and HpLacZ) or a siRNAs (siLUC, siRNA-A, and siRNA-B). Two pathways involved in innate immune response were studied: the toll-like receptor pathway and the inflammasome activation. We determined that the levels of the transcription factors IRF3 and its phosphorylated form, as well as NF- $\kappa$ B were increased by siRNAs but not by PPRHs; that the expression levels of several proinflammatory cytokines including IL-6, TNF- $\alpha$ , IFN- $\alpha$ , IFN- $\beta$ , IL-1 $\beta$ , and IL-18 were not significantly increased by PPRHs; and that the cleavage and activation of the proteolytic enzyme caspase-1 was not triggered by PPRHs. These determinations indicated that PPRHs, unlike siRNAs, do not activate the innate inflammatory response.

#### *Conclusions:*

In summary, PPRHs as DNA molecules present substantial advantages over siRNAs such as high stability, low immunogenicity, and versatility of design since they can be directed against different gene regions such as promoter, introns, and exons. In addition, it is not necessary to introduce chemical modifications in the DNA synthesis, making PPRHs 10 times less expensive than siRNAs.

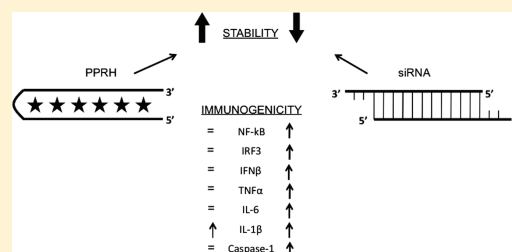
## Stability and Immunogenicity Properties of the Gene-Silencing Polypurine Reverse Hoogsteen Hairpins

Xenia Villalobos, Laura Rodríguez, Jeanne Prévot, Carlota Oleaga, Carlos J. Ciudad, and Véronique Noé\*

Department of Biochemistry and Molecular Biology, School of Pharmacy, University of Barcelona, Av. Diagonal 643, E-08028 Barcelona, Spain

**ABSTRACT:** Gene silencing by either small-interference RNAs (siRNA) or antisense oligodeoxynucleotides (aODN) is widely used in biomedical research. However, their use as therapeutic agents is hindered by two important limitations: their low stability and the activation of the innate immune response. Recently, we developed a new type of molecule to decrease gene expression named polypurine reverse Hoogsteen hairpins (PPRHs) that bind to polypyrimidine targets in the DNA. Herein, stability experiments performed in mouse, human, and fetal calf serum and in PC3 cells revealed that the half-life of PPRHs is much longer than that of siRNAs in all cases. Usage of PPRHs with a nicked-circular structure increased the binding affinity to their target sequence and their half-life in FCS when bound to the target. Regarding the innate immune response, we determined that the levels of the transcription factors IRF3 and its phosphorylated form, as well as NF- $\kappa$ B were increased by siRNAs and not by PPRHs; that the expression levels of several proinflammatory cytokines including IL-6, TNF- $\alpha$ , IFN- $\alpha$ , IFN- $\beta$ , IL-1 $\beta$ , and IL-18 were not significantly increased by PPRHs; and that the cleavage and activation of the proteolytic enzyme caspase-1 was not triggered by PPRHs. These determinations indicated that PPRHs, unlike siRNAs, do not activate the innate inflammatory response.

**KEYWORDS:** gene silencing, PPRH, stability, immunogenicity, TLR, inflammasome, nucleic acid



### INTRODUCTION

The silencing of gene expression by nucleic acids has become a common and useful tool for laboratory research. There are different molecules used *in vitro* as gene modulating tools, such as antisense oligodeoxynucleotides (aODN) or the prevailing small-interference RNAs (siRNA). However, the use of these molecules as therapeutic agents must overcome two major hurdles: (i) a low stability, which implies a short half-life<sup>1</sup> and (ii) the activation of the immune response, especially by siRNAs.<sup>2,3</sup> In order to be efficacious, the molecules must reach their target organ after passing several physiological barriers. This is particularly difficult since they are easily degraded by nucleases present in the serum. Moreover, upon recognition by the pattern recognition receptors (PRR), nucleic acids trigger the innate immune response: they activate the toll-like receptor-dependent pathway, leading to increased levels of proinflammatory cytokines (type I interferons, TNF- $\alpha$ , IL-6, pro-IL-1 $\beta$ , and pro-IL-18).<sup>4</sup> On the other hand, nucleic acids are capable of activating the inflammasome, a multiprotein complex that cleaves procaspase-1 to its active form, which is needed for the posttranslational activation of IL-1 $\beta$  and IL-18.<sup>5</sup>

Recently, we developed a new type of silencing molecule called polypurine reverse Hoogsteen hairpins (PPRHs). PPRHs are nonmodified DNA molecules formed by two antiparallel polypurine strands linked by a pentathymidine loop that allows the formation of intramolecular reverse-Hoogsteen bonds between both strands. These hairpins bind to polypyrimidine stretches in the DNA via Watson–Crick bonds while maintaining

the hairpin structure. We described the ability of PPRHs to bind both the template<sup>6</sup> and coding<sup>7</sup> strands of the dsDNA, forming a triplex structure that knocks down the expression of genes. Template PPRHs bind to the template strand of the DNA and inhibit transcription. On the other hand, coding PPRHs bind to the coding sequence of the DNA and can also bind to transcribed RNA. We demonstrated that a coding PPRH directed against a polypyrimidine region in intron 3 of the *dhfr* mRNA produced a splicing alteration by preventing the binding of the splicing factor U2AF65.<sup>7</sup>

Therefore, the aim of this study was to compare the properties between PPRHs and siRNAs in terms of stability, determining their half-life in three different types of serum and in PC3 cells, and in terms of immunogenicity by analyzing the activation of the toll-like receptor and the inflammasome pathways. Also, we explored the characteristics of nicked-circle-PPRHs (ncPPRH), which increase both their binding and stability properties. We conclude that PPRHs outdo siRNAs in terms of stability and immunogenicity.

### MATERIALS AND METHODS

**Oligonucleotides.** PPRHs and primers were synthesized as nonmodified oligodeoxynucleotides by Sigma-Aldrich

**Received:** July 25, 2013

**Revised:** October 21, 2013

**Accepted:** November 19, 2013

**Published:** November 19, 2013

(Madrid, Spain). They were dissolved at 100  $\mu$ M (stock solution) in sterile RNase-free Tris-EDTA buffer (1 mM EDTA and 10 mM Tris, pH 8.0) and stored at  $-20$  °C until use. F-siRNA was synthesized by Sigma-Aldrich (Madrid, Spain) and siLUC by Thermo (Barcelona, Spain). Control siRNA-A (ref sc-37007) and siRNA-B (ref sc-44230) were acquired from Santa-Cruz Biotechnology Inc. (Heidelberg, Germany). The Triplex-Forming Oligonucleotide Target Sequence Search tool was used as starting point for the design of PPRHs (<http://spi.mdanderson.org/tfo/>). The specificity of the chosen polypurine tracks was checked by BLAST analyses.<sup>8</sup> The template-PPRH against *dhfr* intron 3 was designed as described.<sup>6</sup> The nicked-circle-PPRH-in and the nicked-circle-PPRH-out were designed so that the nick in the PPRH is placed in front of the middle of the target sequence, and upon binding they acquire a circular shape. Table 2 describes all oligonucleotides names and sequences used in this work.

**Cell Culture.** Human acute monocytic leukemia THP-1, prostate cancer PC-3, and breast cancer SKBR3 cell lines were used throughout the study. The cell line THP-1, iGLuc C1, stably transduced with the reporter iGLuc (pro-IL-1b-GLuc-Flag) used to determine the proteolytic activity of caspase-1 was kindly provided by Dr. Hornung.<sup>9</sup> Cell lines were routinely grown in Ham's F-12 medium supplemented with 7% fetal calf serum (FCS, both from Gibco) at 37 °C in a 5% CO<sub>2</sub> controlled humidified atmosphere.

**Stability in Fetal Calf Serum, Mouse Serum, and Human Serum.** Two PPRHs, F-PPRH-D against the *dhfr* gene and F-PPRH-S against the *survivin* gene, as well as F-siRNA against *survivin* gene, all labeled with fluorescein were used to assess their half-lives in FCS, mouse and human serum. A determined amount of the specific oligonucleotide was incubated with 100% serum at 37 °C in a water-bath. At different periods of time (0, 5, 15, 30, 60, 120, 180, 240, 300, and 360 min) aliquots of 150 ng of oligonucleotide were withdrawn, and serum was inactivated by the addition of 1  $\mu$ L of 0.5 M EDTA (pH = 8.01). Then, samples were treated with proteinase K (0.5  $\mu$ g/ $\mu$ L, Gibco) and 1% SDS and incubated for 2 h at 60 °C at 400 rpm in a Thermo-mixer Compact (Eppendorf, Hamburg, Germany). The samples were resolved by gel electrophoresis, and the fluorescence associated with each band was quantified using the ImageQuant software.

For stability experiments of the different types of PPRHs bound to their target, a determined amount of the different F-PPRHs, F-PPRH-D, F-nicked-circle-PPRH-in, and F-nicked-circle-PPRH-out (150 ng/point) was incubated with a 5-fold mass excess of the target sequence in binding buffer (10 mM MgCl<sub>2</sub>, 100 mM NaCl and 50 mM HEPES, pH 7.2) in 20  $\mu$ L reactions for 30 min at 37 °C. An equal volume of FCS was then added to the binding reaction, and the different mixes were incubated in a water-bath at 37 °C for up to 120 min. At different periods of time (0, 60, and 120) aliquots of 150 ng of the labeled PPRHs were withdrawn and serum was inactivated by the addition of 1  $\mu$ L of 0.5 M EDTA (pH = 8.01). Samples were treated with proteinase K (0.5  $\mu$ g/ $\mu$ L) and 1% SDS and incubated for 30 min in a Thermo-mixer Compact at 60 °C at 400 rpm. The samples were resolved by gel electrophoresis, and the fluorescence associated to each band was quantified using the ImageQuant software.

**Oligonucleotides Transfection.** In all cases, PPRHs were lipofected using DOTAP (Roche, Mannheim, Germany) in a molar ratio of 1:100 (PPRH/DOTAP). siRNAs were transfected

using MetafectenePRO (Biontix, Martinsried/Planegg, Germany) following the specifications of the manufacturer.

**PPRHs and siRNA Half-Life in Cells.** PC3 cells (150 000) were plated in 35-mm dishes in 2 mL of HAM's F-12 medium and transfected with 30 nM of either F-PPRH or F-siRNA as described in the Oligonucleotides Transfection section. Twenty-four hours after transfection, cells were washed once with PBS and incubated for different periods of time, ranging from 6 to 72 h, in Ham's F-12 medium. Then cells were collected in 2 mL Eppendorf tubes and centrifuged at 800g at 4 °C in a micro-centrifuge. The supernatant was removed and the pellet was washed in 1 mL of ice-cold PBS 1X, centrifugation was repeated, and the cells resuspended in 500  $\mu$ L of PBS and propidium iodide (5  $\mu$ g/mL). The fluorescence of the cells was analyzed in a cytometer XL-Coulter.

**RT Real-Time PCR.** Reverse transcription was performed using 1  $\mu$ g of RNA obtained from THP-1 cells extracted by the Trizol method (Invitrogen, Madrid, Spain). This was followed by real-time PCR performed according to Oleaga et al.<sup>10</sup> except for the use of the OneStep Plus Real-Time PCR System (Applied Biosystems) and of APRT mRNA as endogenous control. The primer sequences (5'-3' forward, reverse) used were

INF- $\alpha$ : TTATCCAGGCTGTGGGTCT, GCAAGC-  
CCAGAAGTATCTGC;

INF- $\beta$ : TGGAGAAGCACAAACAGGAG, AACCTT-  
TCGAAGCCTTTGCT;

IL-6: CATTGTGGTTGGGTCAGG, AGTGAG-  
GAACAAGCCAGAGC;

TNF- $\alpha$ : GCCAGAGGGCTGATTAGAG, TCAGCCT-  
CTTCTCCTTCCTG;

IL-1 $\beta$ : GTGGCAATGAGGATGACTTGTTTC,  
TAGTGGTGGTCCGAGATTCGTA;

IL-18: CCTCAGACCTTCCAGATCGC, TTCCAGG-  
TTTTTCATCATCTTCAGC and

APRT: GCAGCTGGTTGAGCAGCGGAT,  
AGAGTGGGGCCTGGCAGCTTC.

Results were analyzed following the  $\Delta\Delta$ Ct method.

**Western Blot.** THP-1 cells (10<sup>6</sup>) were plated in a 6-well dish (800  $\mu$ L) and transfected with 30 nM and 100 nM of either nonspecific PPRHs (Hpt18-sc, HpsPr-sc and HpLacZ) or nonspecific siRNAs (siLUC, siRNA-A and siRNA-B) as described in the Oligonucleotides Transfection section. After 4 or 9 h of transfection, cells were collected and centrifuged for 5 min at 800g at 4 °C. Cells were resuspended in 30  $\mu$ L of RIPA buffer (150 mM NaCl, 5 mM EDTA, 50 mM Tris-HCl pH 7.4 (all from Applichem, Barcelona, Spain), 1% Igepal CA-630, 0.5 mM PMSF, Protease inhibitor cocktail, 1 mM NaF (all from Sigma-Aldrich). Cell lysate was kept on ice for 30 min with vortexing every 10 min. Cell debris was removed by centrifugation at 15000g at 4 °C for 10 min. Five microliters of the extract was used to determine the protein concentration using the Bradford assay (Bio-Rad). Vehicles and the immunogenic cocktail LPS-ATP (0.1  $\mu$ g/mL and 2 mM, respectively) were also analyzed. Activation with LPS-ATP was used as catalyzer 2, 4, or 7 h before harvesting cells as indicated in the figure legends. Whole cell extracts (100  $\mu$ g) were resolved in 15% SDS-polyacrylamide gels and transferred to PVDF membranes (Immobilon P, Millipore) using a semidry electro-blotter. The blocking solution was 5% Blotto and when detecting phosphorylated IRF3, 5% BSA was used. Membranes were probed overnight at 4 °C with primary antibodies against IRF3 (1:200 dilution; sc-33641), NF- $\kappa$ B (1:200 dilution; sc-109),



interleukine-1 $\beta$  (1:50 dilution; sc-7884), caspase-1 (1:200 dilution; sc-515), tubulin (1:200 dilution; sc-487) (all from Santa-Cruz Biotechnology Inc.), and p-IRF3 (1:1000 dilution; Cell Signaling, 4961S). Signals were detected by secondary horseradish peroxidase-conjugated antibody, either antirabbit (1:5000; Dako, Denmark) or antimouse (1:2500 dilution, sc-2005 Santa Cruz Biotechnology Inc.) and enhanced chemiluminescence using the ECL method, as recommended by the manufacturer (Amersham). Chemiluminescence was detected with ImageQuant LAS 4000 mini technology (GE Healthcare).

**Table 1. F-PPRH and F-siRNA Half-Life (h) in Different Sera and in PC3 Cells<sup>a</sup>**

	$t_{1/2}$ (h)			
	FCS	mouse serum	human serum	cell
F-PPRH-D	11.6	19.3	28.9	69
F-PPRH-S	9.1	24.8	11.6	ND
F-siRNA	1.1	2.9	3.9	30

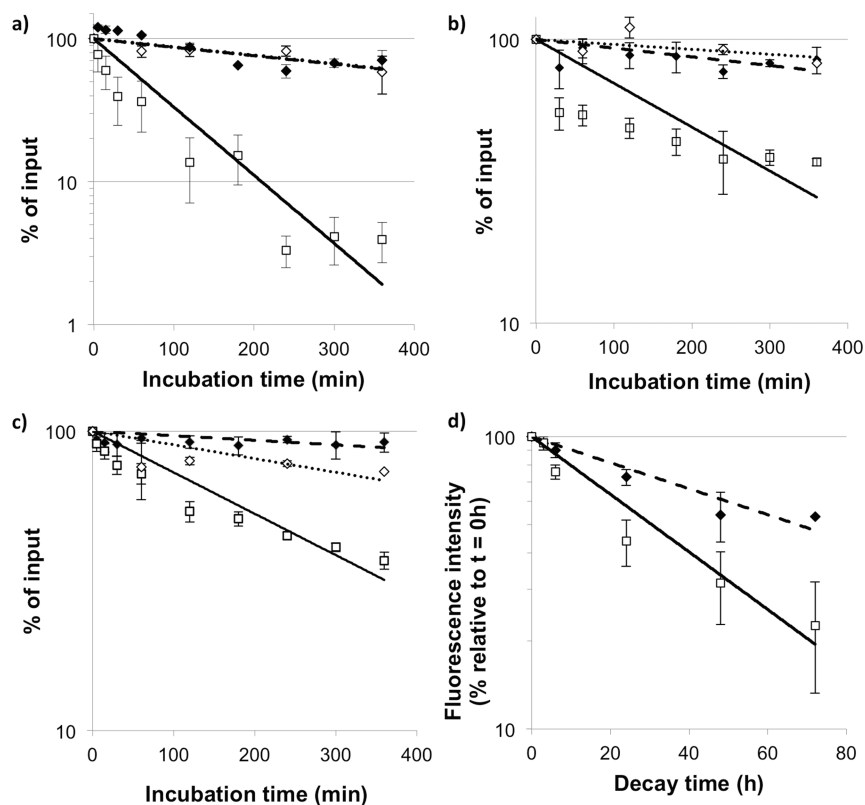
<sup>a</sup>Comparison between PPRHs and siRNA stability in FCS, mouse and human serum, as well as in cultured PC3 cells. Results represent the half-life ( $t_{1/2}$ ) of the nucleic acid molecule in hours.

**Caspase-1 Proteolytic Activity Determination.** THP-1 iGLuc cells ( $2 \times 10^5$ ) were plated in 96-well dishes in 200  $\mu$ L of culture medium. The cells were allowed to attach and then transfected with 30 nM and 100 nM of either nonspecific PPRHs (HptI8-sc, HpsPr-sc, and HpLacZ) or nonspecific siRNAs (siLUC, siRNA-A and siRNA-B), as described in the Oligonucleotides Transfection section, in a final volume of 50  $\mu$ L. The supernatants (SN) were recovered 16 h after treatment. Equal volumes (15  $\mu$ L) of the supernatants were mixed with distilled water containing 4.4  $\mu$ M Coelenterazine (P.j.k. GmbH, Kleinblittersdorf, Germany) and light production (RLU) was determined in a Glomax<sup>TM</sup> 20/20 Luminometer (Promega). Each condition was analyzed in three different experiments. Vehicles and the positive controls LPS-ATP (0.1  $\mu$ g/mL and 2 mM, respectively) and dsDNA > 100 bp (250 bp) were also assessed for proteolytic activity. RLU were corrected by total protein concentration using the Bio-Rad protein assay reagent Bradford according to the manufacturer's protocol.

**Binding Experiments. Preparation of Polypurine/Polypyrimidine Duplexes.** The polypurine/polypyrimidine duplexes to be targeted by the PPRHs were formed by mixing 25  $\mu$ g of each single-stranded oligodeoxynucleotide (Target seq fwd strand and Target seq rev strand) in 150 mM NaCl.

**Table 2. Oligonucleotides Used in This Study**

Oligonucleotide name	Sequence (5'-3')
PPRH-D	GGAGGAGGGAGAGGGAGGAGTTTTGAGGAGGGAGAGGGAGGAGG
F-PPRH-D	F-GGAGGAGGGAGAGGGAGGAGTTTTGAGGAGGGAGAGGGAGGAGG
F-PPRH-S	F-AGGGGAGGGAAGGAGAGAAGTTTTGAAGAGAGGAAGGGAGGGGA
HptI8-Sc	AAAAGAAGAAGAAGAAGAAGAAGAAGAAGTTTTTGAAGAAGAAGAAGAAG AAGAAGAAG AAGAAGAAGAAA
HpsPr-Sc	AAGAGAAAAAGAGAAAAGAAGAGAGGGTTTTTGGGAGAGAGAAGAAAGAGAAAAAGAGAA
HpLacZ	GGAGAAAGGGGGAAGAGTTTTTGAAGGGGGAAAGAGG
F-siRNA	Anti GCGCAACCGGACGAAUGCUTT Sense F-AGCAUUCGUCCGUUGCGCTT
siLUC	Anti UAAGGCUAUGAAGAGAUACTT Sense GUAUCUCUUAUAGCCUUATT
siRNA-A	Santa Cruz Biotechnology. Ref: sc-37003
siRNA-B	Santa Cruz Biotechnology. Ref: sc-44230
ncPPRH-in	AGGGAGGAGTTTTTGGAGGAGGGAGAGGGAGGAGTTTTTGAGGAGGGAG
ncPPRH-out	GAGGGAGGAGTTTTTGGAGGAGGGAGAGGGAGGAGTTTTTGAGGAGGGAG
Target seq. rev strand	CATTCTCTTGATTGCCTCCTCCCTCTCCCTCCTC
Target seq. fwd strand	GAGGAGGGAGAGGGAGGAGGCAATCAAGAGAATG



**Figure 1.** Half-life of siRNAs and PPRHs in fetal calf serum, mouse and human serum and prostate cancer PC3 cells. Fluorescein-labeled PPRHs (F-PPRH-D,  $\blacklozenge$  and F-PPRH-S,  $\diamond$ ) or siRNA (F-siRNA:  $\square$ ) (1650 ng) were incubated with different sera: FCS (a), mouse serum (b), and human serum (c) in a final volume of 71.5  $\mu\text{L}$ . At the different times shown in the graphs, aliquots of 6.5  $\mu\text{L}$ /point corresponding to 150 ng of oligonucleotide were withdrawn. The decay was determined by quantifying the remaining fluorescence using the Image Quant 5.2 software after gel electrophoresis. In (d), the labeled oligonucleotides were transfected into PC3 cells for 24 h ( $t = 0$ ) when the medium was renewed, and then the fluorescence intensity was determined at different times in a flow cytometer. Values represent the mean  $\pm$  SE of at least three independent experiments.  $t_{1/2}$  was calculated from the regression line from the semilogarithmic plot when  $y = 50$ .

After incubation at 90  $^{\circ}\text{C}$  for 5 min, samples were allowed to cool down slowly to room temperature. Duplexes were purified in nondenaturing 20% polyacrylamide gels and quantified by their absorbance at 260 nm.

**Oligodeoxynucleotide Labeling.** One hundred nanograms of double-stranded oligodeoxynucleotide was 5'-end labeled with [ $\gamma$ - $^{32}\text{P}$ ]ATP by T4 polynucleotide kinase (New England Bio-Laboratories) in a 10- $\mu\text{L}$  reaction mixture, according to the manufacturer's protocol. After incubation at 37  $^{\circ}\text{C}$  for 1 h, 90  $\mu\text{L}$  of TE buffer (1 mM EDTA, 10 mM Tris, pH 8.0) were added to the reaction mixture, which was filtered through a Sephadex G-25 spin column to eliminate the unincorporated [ $\gamma$ - $^{32}\text{P}$ ]ATP.

**Electrophoretic Mobility Shift Assay.** Triplex formation was analyzed by incubating radiolabeled double-stranded DNA targets in the presence or absence of unlabeled PPRHs (10 nM, 30 nM, and 100 nM) in a buffer containing 10 mM  $\text{MgCl}_2$ , 100 mM NaCl and 50 mM HEPES, pH 7.2. Binding reactions (20  $\mu\text{L}$ ) were incubated 30 min at 37  $^{\circ}\text{C}$  before the electrophoresis, which was performed on nondenaturing 12% polyacrylamide gels containing 10 mM  $\text{MgCl}_2$ , 5% glycerol, and 50 mM HEPES, pH 7.2. Gels were run for 3–4 h at 180 V at 4  $^{\circ}\text{C}$ , dried, and analyzed on a Storm 840 PhosphorImager (Molecular Dynamics). Quantification was performed using the ImageQuant 5.2 software (GE Healthcare).

**Cell Survival Experiments (MTT).** SKBR3 cells (10 000) were plated in 35-mm dishes in -GHT medium. Seven days

after PPRHs transfection, 0.63 mM 3-(4,5-dimethylthiazol-2-yl)-2,5-diphenyltetrazolium bromide and 100  $\mu\text{M}$  sodium succinate (both from Sigma-Aldrich; final concentration) were added to the culture medium and allowed to react for 3 h at 37  $^{\circ}\text{C}$  before the addition of the solubilization reagent (0.57% acetic acid and 10% SDS in DMSO). Cell viability was measured at 570 nm in a WPA S2100 diode array spectrophotometer. The results were expressed as the percentage of cell survival relative to the control (untreated cells).

**Statistical Methods.** Values are expressed as the mean  $\pm$  SE. Data were evaluated by unpaired Student's  $t$  test when analyzing the difference between two conditions, control and treated. The analyses were performed using the software PASW Statistics v18.0.0. Differences with  $p$ -values  $< 0.05$  were taken as statistically significant.

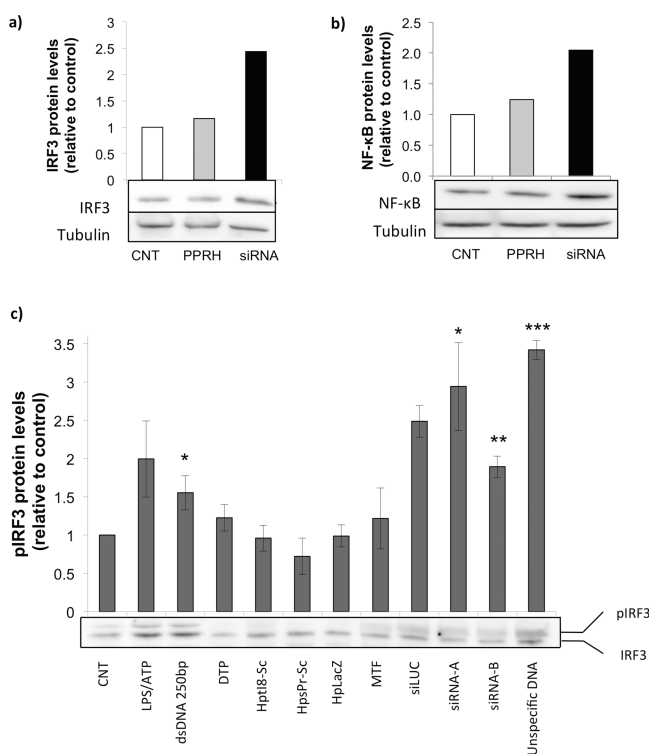
## RESULTS

**Stability of PPRHs vs siRNA in Serum and in Cultured Cells.** Fluorescein-labeled PPRHs (F-PPRH-D and F-PPRH-S) or fluorescein-labeled siRNA (F-siRNA) were used to assess their stability in different types of serum. At different times after the incubation with the fluorescent molecules, samples were withdrawn and analyzed for integrity by electrophoresis and subsequently quantified. The half-lives of the PPRHs and siRNA in the different sera or in cells are shown in Table 1. In all cases, F-PPRHs half-lives were longer than that of F-siRNA (Figure 1a–c). To determine if a difference in stability was

maintained in a cellular environment, we transfected F-PPRH-D and F-siRNA into PC3 cells, and, after an incubation period of 24 h, the oligonucleotides were allowed to decay for up to 72 h. Under these conditions, the half-life of F-PPRH-D was 2.3 times higher than that of F-siRNA (Figure 1d).

**Innate Immune Response Evaluation upon Nucleic Acid Molecules Incubation.** To compare the possible inherent immunogenic activity of PPRHs (DNA polymer molecules) with that of siRNAs (ribonucleic acid polymer molecules), a monocytic cell line (THP-1 cells) was transfected with either nonspecific PPRHs (HptI8-sc, HpsPr-sc, and HpLacZ) or a siRNAs (siLUC, siRNA-A, and siRNA-B). Two pathways involved in innate immune response were studied: the toll-like receptor pathway and the inflammasome activation.

**Toll-Like Receptor Pathway.** We analyzed the TLR pathway effectors IRF3 and NF- $\kappa$ B 4 h after transfection of HptI8-sc and siLUC, which was the optimal time to detect their expression. The PPRH molecule did not induce the protein levels of IRF3 nor NF- $\kappa$ B as opposed to siRNA transfection that induced 2.5 times the levels of IRF3 (Figure 2a) and 2 times the levels of NF- $\kappa$ B (Figure 2b). Phosphorylation of IRF-3 was also



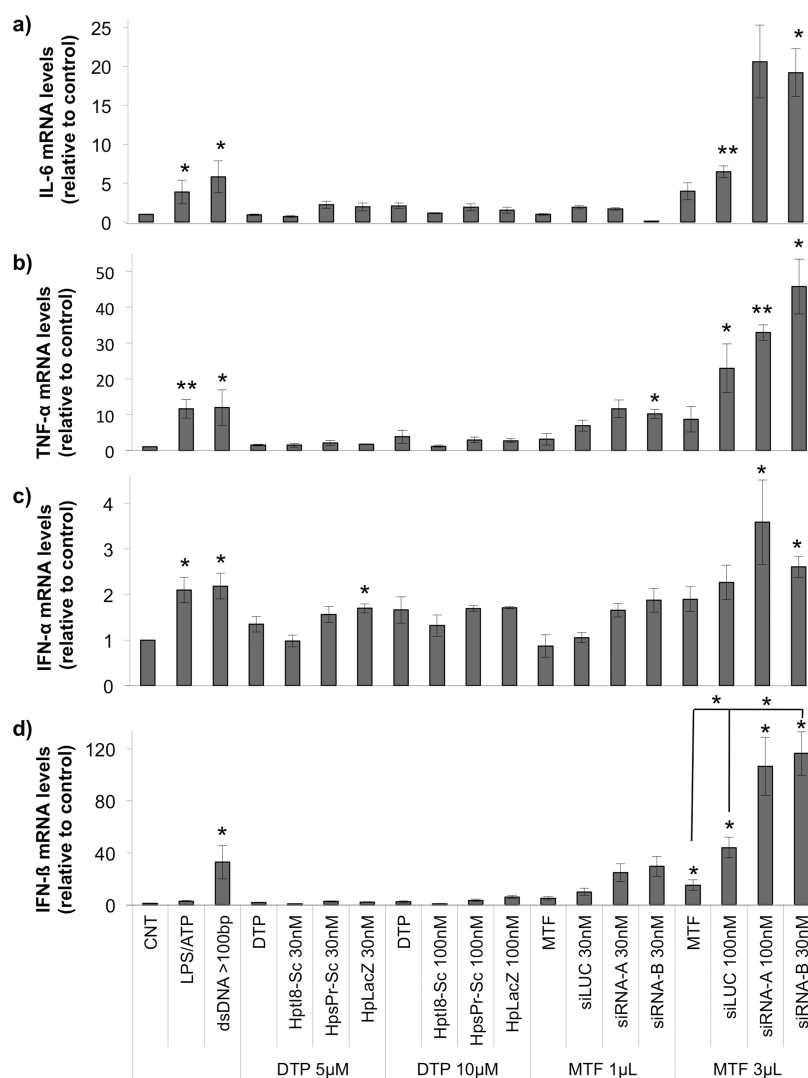
**Figure 2.** Effectors of the toll-like receptor pathway. PPRH (HptI8-Sc; gray bars) or siRNA (siLUC; black bars) (100 nM) were transfected into THP-1 cells. Cells were collected 4 h after transfection for quantification of IRF3 (a) or NF- $\kappa$ B (b). When determining NF- $\kappa$ B, LPS-ATP (0.1  $\mu$ g/mL and 2 mM, respectively) was added 2 h before harvesting the cells. In (c) 100 nM of three PPRHs (HptI8-sc, HpsPr-sc, and HpLacZ) and three siRNAs (siLUC, siRNA-A, and siRNA-B) were transfected into THP-1 cells. Cells were collected 4 h after transfection for quantification of phospho-IRF3. LPS-ATP (0.1  $\mu$ g/mL and 2 mM, respectively), a dsDNA > 100 bp (250 bp) (100 nM) and unspecific DNA (salmon sperm DNA; 100 nM) were used as positive controls. Western blots were performed with 100  $\mu$ g of total extracts and were normalized to tubulin levels, or total protein loading. Values are expressed relative to the control. A representative image of the Western analyses is shown. \* $p$  < 0.05, \*\* $p$  < 0.01, \*\*\* $p$  < 0.001 compared with the corresponding control.

determined upon transfection of three different siRNAs and three PPRHs. An increase of the phosphorylated protein was observed when siRNAs were transfected (Figure 2c). Moreover, upon siRNAs transfection a substantial increase in mRNA expression levels of IL-6 (Figure 3a), TNF- $\alpha$  (Figure 3b), and IFN- $\beta$  (Figure 3d) were observed at 100 nM, in contrast with the slight increases measured after PPRHs incubation. The difference in the stimulation of IFN- $\alpha$  after the PPRHs or siRNAs transfection was lower (Figure 3c). As expected, treatment with LPS-ATP (Sigma-Aldrich, Madrid, Spain), used as positive control, caused a significant increase in IL-1 $\beta$  (Figure 4a) and TNF- $\alpha$  (Figure 3b).<sup>11,12</sup> Likewise, transfection of a dsDNA longer than 100 bp (250bp) caused an increase in IL-6 of 6.2 fold, TNF- $\alpha$  of 5.4 fold, and IFN- $\beta$  of 12.1 fold.<sup>13</sup> The immune response produced by the transfecting reagents themselves was also analyzed. Cationic liposomes, such as DOTAP, can cause some degree of toxicity, and the surface charge may play a role in this toxicity<sup>14</sup>). Therefore, when the transfecting agent is complexed with the nucleic acid (PPRH) the surface charge is changed, which could explain the observed decrease in inflammatory response. MetafectenePro (MTF) was the transfecting agent used for siRNA. In fact, MTF always caused a higher immune response than DTP, and that is the reason by which we always compared the effect of the nucleic acids with their respective transfecting reagent.

**Inflammasome Activation.** The mRNA levels of IL-1 $\beta$  and IL18 were determined by RT-qPCR 24 h after transfecting three different PPRHs and three siRNAs. All siRNAs provoked an increase in IL-1 $\beta$ , ranging between 5- and 8-fold, whereas only one PPRH molecule increased it by 2-fold (Figure 4a). None of them induced the expression of IL-18 (Figure 4b). Moreover, we determined the protein levels of pro-IL-1 $\beta$  and procaspase-1 by Western blot after transfection of HptI8-sc and siLUC. The siRNA molecule caused a 2.5 increase in pro-IL-1 $\beta$  levels, whereas the PPRH induced a slight 1.5 increase in this cytokine levels (Figure 4c). Under these conditions, neither the siRNA nor the PPRH caused a significant increase in procaspase-1 levels. Nevertheless, the cleavage of procaspase-1 to caspase-1, which is mediated by the inflammasome, was clearly induced upon transfection of the siRNA, but not upon PPRH transfection (Figure 5a). Since active IL-1 $\beta$  is secreted to the medium once it has been cleaved by caspase-1, we analyzed caspase-1 proteolytic activity through a novel pro-interleukin (IL)-1 $\beta$ -Gaussia luciferase (iGLuc) reporter system developed by Bartok et al, 2013,<sup>9</sup> in which the formation of pro-IL-1 $\beta$ -GLuc protein aggregates renders GLuc enzyme inactive. Cleavage of pro-IL-1 $\beta$  by caspase-1 releases GLuc, which can then be secreted to the medium, resulting in a strong gain in luciferase activity (Figure 5b). We transfected THP-1 iGLuc cells with 30 nM and 100 nM of either three different siRNAs or three PPRHs and analyzed the luciferase activity in cells supernatants. As shown in Figure 5c, the proteolytic activity of caspase-1 of cells transfected with 100 nM of the siRNAs was induced on average 2.3 times, whereas the PPRHs did not induce caspase-1 proteolytic activity.

**Nicked-circle-PPRHs.** To determine if the binding affinity and efficacy of the PPRHs could be improved, we designed PPRHs with a circular structure, containing two pentathymidine loops, which we named nicked-circle-PPRHs (ncPPRHs). These PPRHs have a nick in one of the strands: ncPPRH-out has the nick in the strand of the hairpin that does not bind the dsDNA target sequence, while in the ncPPRH-in the nick is located in the strand of the hairpin that binds the target





**Figure 3.** Targets of the toll-like receptor pathway. Three different PPRHs (HptI8-Sc, HpsPr-sc, and HpLacZ) and three different siRNAs (siLUC, siRNA-A, and siRNA-B) (30 nM and 100 nM) were transfected into THP-1 cells, and the expression levels of the pro-inflammatory cytokines IL-6 (a), TNF- $\alpha$  (b), IFN- $\alpha$  (c), and IFN- $\beta$  (d) were determined by RT-qPCR. LPS-ATP (0.1  $\mu$ g/mL and 2 mM, respectively) and a dsDNA of 250 bp (100 nM) were used as positive controls. The effect on cytokine expression of the transfection agents DTP (DOTAP) and MTF (MetafectenePRO) was also assessed. mRNA levels were normalized to APRT. Values represent the mean  $\pm$  SE of three independent experiments and are expressed relative to the control. \* $p$  < 0.05, \*\* $p$  < 0.01 compared with the corresponding control.

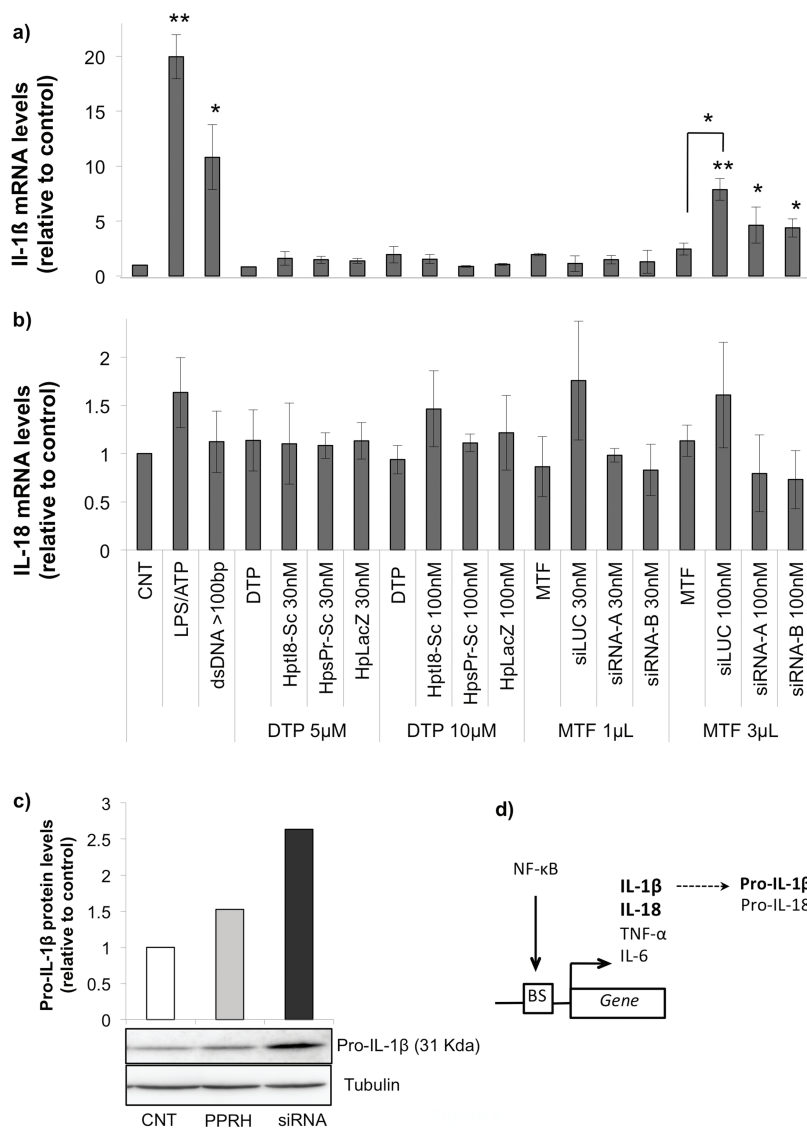
sequence in the dsDNA (Figure 6a). We compared the binding capacity of a regular PPRH with both ncPPRHs by EMSA. We quantified the formation of the triplex after incubation of the radiolabeled dsDNA target with increasing amounts (10, 30, and 100 nM strand concentration) of unlabeled ncPPRH-in, ncPPRH-out or regular PPRH. As shown in Figure 6b, the binding capacity of all PPRHs increased in a dose-dependent manner. However, the bands corresponding to both ncPPRHs were better defined than those corresponding to the regular PPRH. When using 100 nM of PPRHs, the binding capacity of both ncPPRHs is increased by a 50% relative to the regular PPRH (Figure 6c).

The efficacy of the ncPPRHs compared with the regular PPRH was determined by MTT assays in human breast cancer SKBR3 cells using the *dihydrofolate reductase* (*dhfr*) gene as the target. All PPRHs were designed to bind to *dhfr* intron 3, so binding of the PPRHs to that DNA region should result in a decreased cell growth when cells are incubated in selective -GHT medium, which lacks the final products of DHFR

activity: glycine, hypoxanthine, and thymidine. The PPRHs were transfected at a 100nM concentration into the cells and cell survival was determined 7 days later. All three PPRHs had a similar cytotoxic activity (Figure 7a), inhibiting cell viability by 60–70%. It has to be noted, though, that when bound to their target sequence, the stability to degradation of the nicked-circle-PPRHs was higher than the regular PPRH given their structure. Specifically, ncPPRH-in half-life was increased by a 10% and that of the ncPPRH-out was increased by a 50% (Figure 7b). The stability to degradation in serum between regular and ncPPRH-out in the absence of target was similar: 693 min for ncPPRHout vs 696 min for PPRH (Figure 7c). Therefore, the higher stability of the ncPPRH takes place only when bound to the target due to their almost circular structure, as compared with the open structure of the regular PPRH.

## DISCUSSION

In this work, we studied the properties of PPRHs in terms of stability and immunogenicity and compared them with those

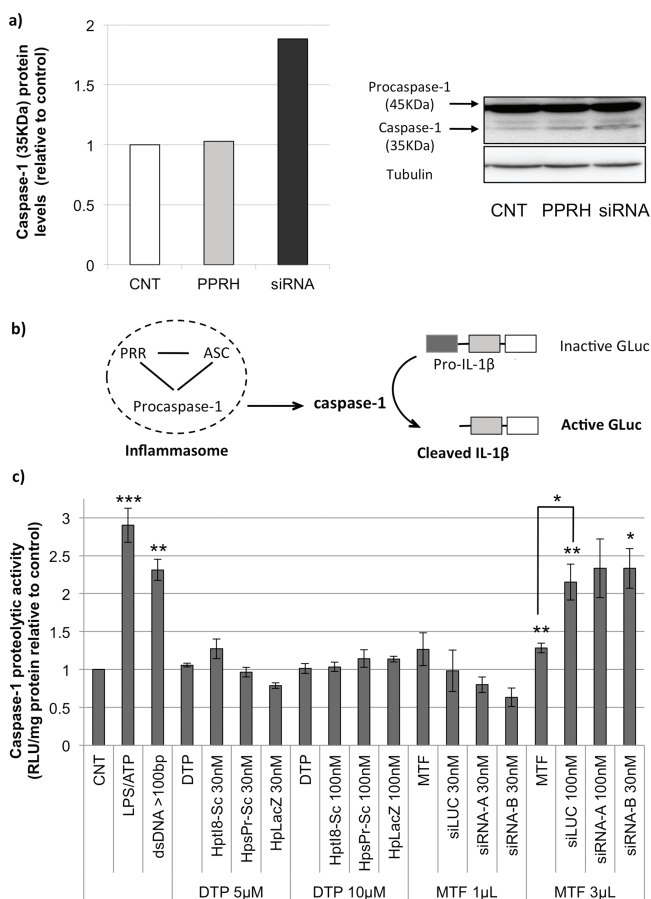


**Figure 4.** IL-1 $\beta$  and IL-18 expression upon incubation with oligonucleotides. Three different PPRHs (HptI8-Sc, HpsPr-sc, and HpLacZ) and three different siRNAs (siLUC, siRNA-A, and siRNA-B) (30 nM and 100 nM) were transfected into THP-1 cells. The expression levels of IL-1 $\beta$  (a) and IL-18 (b) were determined by RT-qPCR after 24 h of transfection following the same procedure as in Figure 3. For protein quantification of pro-IL-1 $\beta$  levels, cells were harvested 9 h after HptI8-sc and siLUC transfection (c). Western blots were performed with 100  $\mu$ g of total extracts and were normalized to tubulin levels. (d) Target genes for the NF- $\kappa$ B transcription factors. Values represent the mean  $\pm$  SE of three different experiments and are expressed relative to the control (white bars). \* $p$  < 0.05 and \*\* $p$  < 0.01 compared with the corresponding control.

shown by siRNAs. The relevance of comparing the stability of these two silencing molecules is that regardless their different mechanisms of action, an increased stability of the PPRHs will extend their biological effects. The first environment to which silencing oligonucleotides are exposed is blood, where several nucleases exert their action: DNase I<sup>15</sup> and RNase A families<sup>16</sup> are the predominant enzymes to degrade circulating oligonucleotides; therefore, nuclease-resistant oligonucleotides are necessary to enable their systemic distribution. Particular attention has been paid to the stability of siRNAs since their rapid degradation is a serious drawback to their use as therapeutic agents. The reported half-life for unmodified siRNAs in serum ranges from several minutes to 1 h,<sup>17–19</sup> depending on the experimental conditions. Notably, the siRNAs sequence can impact on their own stability: regions rich in UpA clusters, which have low thermal stability, are most susceptible toward RNase A degradation,<sup>16</sup> especially when they are located toward

the end of the strands.<sup>20</sup> Phosphate modifications at the 3'-end and the inclusion of 2'-protected nucleosides at internal sites are necessary to provide protection against exonucleases and endonucleases, respectively.

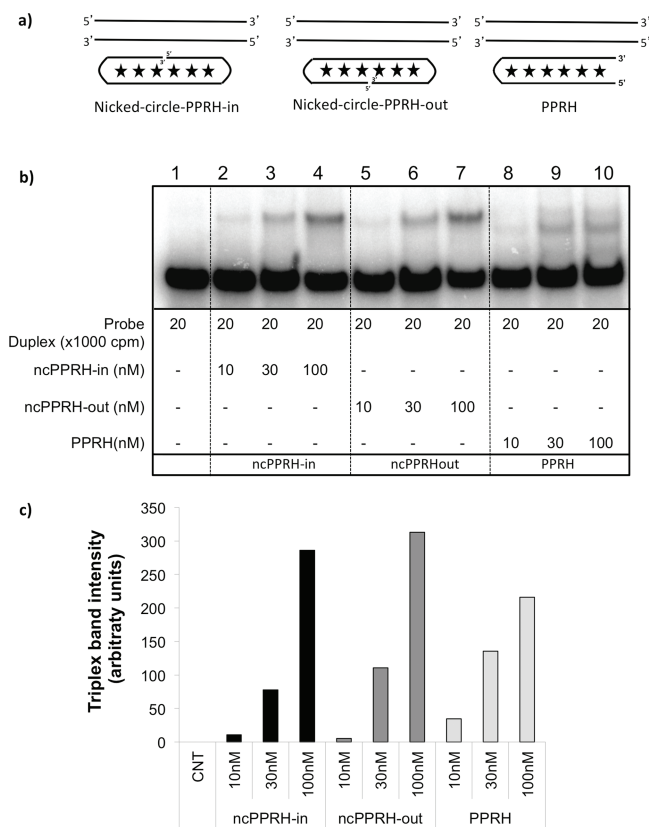
DNase I recognizes the B form of dsDNA and degrades it by single-stranded nicking mechanisms in the presence of Mg<sup>2+</sup>, or by double-stranded cutting, in the presence of Mn<sup>2+</sup> or Mg<sup>2+</sup> and Ca<sup>2+</sup>.<sup>15,21</sup> The rate of hydrolysis of this enzyme depends strongly on the oligonucleotide conformation and sequence: extended A–T or G–G sites are quite resistant to degradation,<sup>22</sup> as seen in G-rich anti-HIV oligonucleotides<sup>23</sup> and in aptamers against nucleolin.<sup>24</sup> The longer half-life of the PPRHs, around 10 h, could be explained by the nature of its structure since they are double-stranded DNA molecules, protected by the pentathymidine loop on one side and intramolecularly linked by reverse Hoogsteen bonds. We studied two different PPRHs and determined that their half-lives are much longer compared



**Figure 5.** Inflammasome-dependent caspase-1 activation and caspase-1-mediated IL-1 $\beta$  cleavage. PPRH (HptI8-Sc; gray bars) or siRNA (siLUC; black bars) (100 nM) were transfected into THP-1 cells. Cells were collected 9 h after transfection for protein cleavage detection of caspase-1 (a); a representative Western blot, performed with 100  $\mu$ g of total extracts and normalized to tubulin, is shown at the top of the figure. (b) Schematic representation of the iGLuc reporter system. (c) caspase-1 proteolytic activity was determined in cells supernatants 16 h after transfection with three PPRHs (HptI8-sc, HpsPr-sc, and HpLacZ) or three siRNAs (siLUC, siRNA-A, and siRNA-B) (30 nM and 100 nM) into THP-1 iGLuc C1 cells. Values represent the mean  $\pm$  SE of three different experiments and are expressed relative to control. \* $p$  < 0.05 and \*\* $p$  < 0.01 compared with the corresponding control.

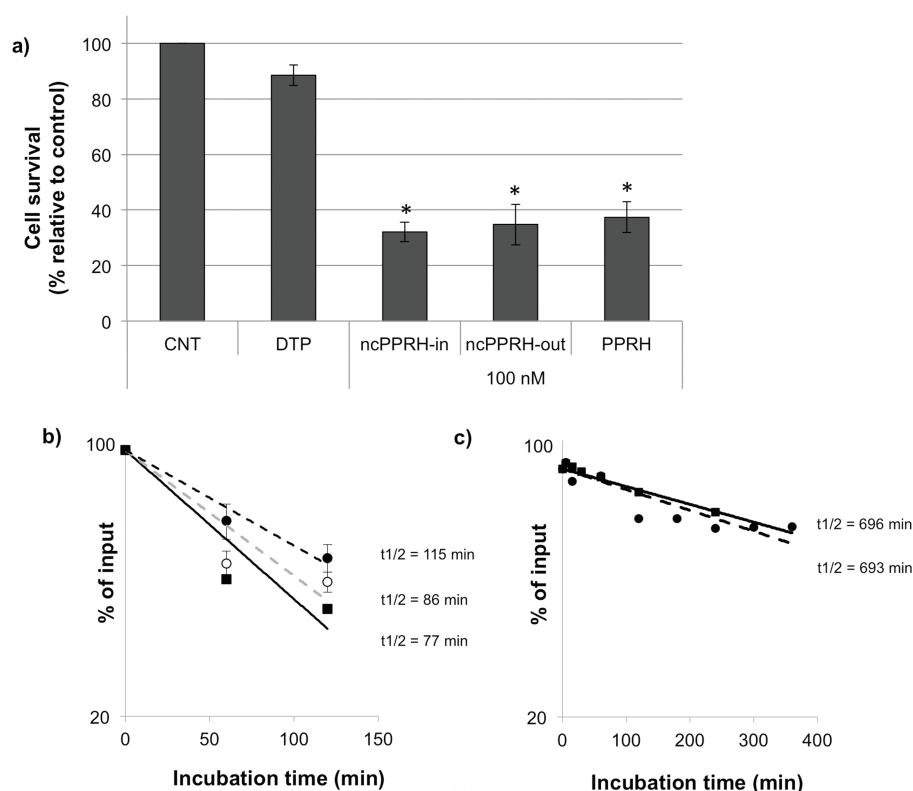
to the siRNA. It is known that bound TFOs by Hoogsteen bonds to dsDNA confer protection against DNase I.<sup>25</sup> We have demonstrated that PPRHs half-life inside the cell is also superior to that of siRNAs.

A major concern about the use of siRNAs is the unintended activation of the immune response. The innate immune system can sense microbial pathogens through the presence of their genomes. This recognition, mediated by the PRRs, is based in two key aspects: (i) recognition of patterns that are not naturally occurring in the human cell, such as dsRNA or unmethylated cytosine-phosphate-guanosine (CpG)-rich DNA and (ii) sensing of nucleic acids in cellular compartments that are normally free of these molecules (i.e., the cytoplasm). Several PRRs participate in the recognition of nucleic acids patterns; from them the toll-like receptor family has been best characterized. TLR3, TLR7/TLR8, and TLR9 are located in the endolysosomes of dendritic cells and macrophages and are



**Figure 6.** Binding of ncPPRH-in, ncPPRH-out, and PPRH to the dsDNA target sequence. (a) Schematic representation of the design of the different types of PPRHs. Reverse Hoogsteen bonds are represented by stars. (b) Binding assays were performed incubating increasing concentrations (10, 30, and 100 nM) of ncPPRH-in, ncPPRH-out, and PPRH with 20 000 cpm of [ $\gamma$ -<sup>32</sup>P]-target duplex. The image was obtained using a Storm 840 PhosphorImager (Molecular Dynamics). (c) The intensity of the bindings was quantified using the Image Quant 5.2 software. ncPPRH-in (black bars), ncPPRH-out (gray bars), and PPRH (white bars).

responsible for the recognition of dsRNA, ssRNA, and CpG-rich DNA, respectively. Upon detection and binding of nonself genetic material, these TLRs trigger the phosphorylation and nuclear translocation of transcription factors, such as IRF3, which controls the expression of type 1 interferons, and NF- $\kappa$ B, which controls the expression of the proinflammatory cytokines IL-6, TNF $\alpha$ , IL-1 $\beta$ , and IL-18. Data suggest that siRNAs are recognized in a sequence-independent and sequence-dependent manner,<sup>25–27</sup> with immunostimulatory sequences appearing very frequently in conventionally designed siRNAs.<sup>26</sup> Our results on the immunostimulatory effect of siRNAs are in agreement with previous results,<sup>26–28</sup> in which siRNAs activate the innate immune response through the TLR pathway, as shown by the increase of IL-6, TNF- $\alpha$ , and IFN $\beta$  expression levels. PPRHs on the other hand did not have an immunostimulatory effect, probably because they are relatively short DNA molecules, less than 100 bases in length, and usually around 50 nucleotides. It is well established that TLR9 recognizes unmethylated CpG-rich DNA, which is characteristic of bacterial DNA and a potent inducer of innate immune response.<sup>29</sup> PPRHs are unmethylated oligonucleotides rich in adenines and guanines, and thus cannot possess the unmethylated CpG sequences. This may allow them to escape from TLR9 recognition and avert the innate immune activation. Other families of



**Figure 7.** Effects and stability of PPRH-D, ncPPRH-in, and ncPPRH-out. (a) Comparison of the effect of PPRH-D, ncPPRH-in, and ncPPRH-out on cell viability at a concentration of 100 nM. SKBR3 cells (10 000) were transfected in 35-mm well plates with the different PPRHs using 10  $\mu$ M DOTAP. One week after treatment, the MTT assays were performed. (b) 150 ng/point of either fluorescein-labeled PPRH (F-PPRH: ■), ncPPRH-in (F-ncPPRH-in: ○), or ncPPRH-out (F-ncPPRH-out: ●) were bound to their target sequence in 20  $\mu$ L binding reactions for 30 min at 37 °C. After this time 20  $\mu$ L of FCS was added to the different PPRHs binding reactions. At the different times shown in the graphs, aliquots were withdrawn and serum was inactivated. In (c) F-PPRH-D and F-ncPPRH-out were incubated in FCS following the procedure described in Figure 1. The decay was determined by quantifying the remaining fluorescence using the Image Quant software after gel electrophoresis. Values represent the mean  $\pm$  SE of three different experiments and are expressed relative to control. \* $p$  < 0.05 compared with the corresponding control.

receptors recognize nucleic acids in the cytoplasm: NLR-family proteins recognize many ligands, including nucleic acids. The dsRNA is sensed specifically by RIG-1 and PKR, while DAI and AIM2 recognize dsDNA. These receptors trigger a series of pathways that also culminate in the expression and activation of proinflammatory cytokines. The inflammasome is a multiprotein complex that, upon binding of its ligand, mediates the proteolysis of procaspase-1 to the active caspase-1, which leads to the post-transcriptional activation of IL-1 $\beta$  and IL-18, and to pyroptosis. Some of these receptors such as AIM2 do not discriminate between self and nonself DNA, so the fact that PPRHs do not induce the inflammasome response is an interesting finding. Moreover, pro-IL-1 $\beta$  and -IL-18 are limiting factors in this pathway,<sup>30</sup> and their transcription depends on NF- $\kappa$ B. In this regard, PPRHs have a double advantage over siRNAs: (i) they do not induce the levels of NF- $\kappa$ B and hence the levels of pro-IL-1 $\beta$  nor -IL-18, and (ii) they most likely do not promote the assembly of the inflammasome since they do not activate the proteolytic activity of caspase-1.

We also demonstrate that slight modifications to the core design of the PPRHs can improve their properties. Circular structures, not exclusively nucleic acids, can have advantages over noncyclic molecules of similar structure.<sup>31</sup> Among these advantages are a tighter binding affinity, a greater specificity for binding a particular intended target and, in the case of oligonucleotides, resistance to degradation by nucleases,<sup>32</sup> all of which are interesting properties for our purposes. By designing

the nicked-circle-PPRHs, we aimed to preorganize the PPRHs into their functional conformation to increase the binding affinity to their dsDNA target sequence and to protect the PPRHs against nucleases, specifically once the PPRHs were bound to their targets. It has to be noted that the binding between the PPRHs and the dsDNA target sequence requires Mg<sup>2+</sup>, which increases DNase I activity. Therefore, the stability to degradation of the PPRHs in this condition is shorter than when no binding is required. As expected, the half-life of both ncPPRHs, when bound to their target, was longer than the regular PPRH, even when the stability to degradation of the regular PPRH and the ncPPRH-out by themselves was similar. Therefore, the higher stability of the ncPPRH takes place only when it is bound to the target due to their almost circular structure, as compared with the open structure of the regular PPRH. Interestingly, ncPPRH-in half-life when bound to the target is shorter than that of ncPPRH-out. It is worth noting that PPRHs bind to their target sequence through WC bonds; once the ncPPRH-in is bound to its target, the strand that is forming WC bonds has a nick, and this could render the ncPPRH-in more vulnerable to the attack of endonucleases present in the serum. On the other hand, ncPPRH-out is forming a perfectly matched triplex, and since serum contains very active endonucleases but less rapidly acting exonucleases,<sup>33</sup> the stability of the ncPPRH-out is enhanced.

In summary, PPRHs as DNA molecules present substantial advantages as a new silencing tool such as high stability, low



immunogenicity, and versatility of design since they can be directed against different gene regions such as promoter, introns, and exons, providing various mechanisms to knock down gene expression. In fact, we have incorporated the use of PPRHs as a silencing tool on a regular basis.<sup>10,34,35</sup> In addition, it is not necessary to introduce chemical modifications in the DNA synthesis, making PPRHs 10 times less expensive than siRNAs. Thus, we wish to put forward the use of PPRHs as a new silencing tool. We believe that developing new approaches, and not only modifying the existent molecules, could broaden the therapeutic scope of gene silencing.

## AUTHOR INFORMATION

### Corresponding Author

\*Phone: +34934034455. Fax: +34934024520. E-mail: vnoe@ub.edu.

### Notes

The authors declare no competing financial interest.

## ACKNOWLEDGMENTS

Work was supported by Grant SAF2011-23582 from “Plan Nacional de Investigación Científica” (Spain). Our group holds the Quality Mention from the “Generalitat de Catalunya” SGR2009-118. L.R. is the recipient of a fellowship (FI) from the “Generalitat de Catalunya”.

## ABBREVIATIONS

siRNA, short interfering RNA; aODN, antisense oligonucleotide; PPRH, polypurine reverse Hoogsteen hairpin; TLR, toll-like receptor; PRR, pattern recognition receptors; DOTAP, N-[1-(2,3-dioleoyloxy)propyl]-N,N,N-trimethylammonium methylsulfate; EMSA, electrophoretic mobility shift assay; MTT, (3-(4,5-dimethylthiazol-2-yl)-2,5-diphenyltetrazolium bromide

## REFERENCES

- (1) Whitehead, K. A.; Langer, R.; Anderson, D. G. Knocking down barriers: advances in siRNA delivery. *Nat. Rev. Drug Discovery* **2009**, *8* (2), 129–138.
- (2) Kole, R.; Krainer, A. R.; Altman, S. RNA therapeutics: beyond RNA interference and antisense oligonucleotides. *Nat. Rev. Drug Discovery* **2012**, *11* (2), 125–140.
- (3) Whitehead, K. A.; Dahlman, J. E.; Langer, R. S.; Anderson, D. G. Silencing or stimulation? siRNA delivery and the immune system. *Annu. Rev. Chem. Biomol. Eng.* **2011**, *2*, 77–96.
- (4) Brown, J.; Wang, H.; Hajishengallis, G. N.; Martin, M. TLR-signaling networks: an integration of adaptor molecules, kinases, and cross-talk. *J. Dent. Res.* **2011**, *90* (4), 417–427.
- (5) Roberts, T. L.; Idris, A.; Dunn, J. A.; Kelly, G. M.; Burnton, C. M.; Hodgson, S.; Hardy, L. L.; Garceau, V.; Sweet, M. J.; Ross, I. L.; Hume, D. A.; Stacey, K. J. HIN-200 proteins regulate caspase activation in response to foreign cytoplasmic DNA. *Science* **2009**, *323* (5917), 1057–1060.
- (6) de Almagro, M. C.; Coma, S.; Noe, V.; Ciudad, C. J. Polypurine hairpins directed against the template strand of DNA knock down the expression of mammalian genes. *J. Biol. Chem.* **2009**, *284* (17), 11579–11589.
- (7) de Almagro, M. C.; Mencia, N.; Noe, V.; Ciudad, C. J. Coding polypurine hairpins cause target-induced cell death in breast cancer cells. *Hum. Gene Ther.* **2011**, *22* (4), 451–463.
- (8) Altschul, S. F.; Gish, W.; Miller, W.; Myers, E. W.; Lipman, D. J. Basic local alignment search tool. *J. Mol. Biol.* **1990**, *215* (3), 403–410.
- (9) Bartok, E.; Bauernfeind, F.; Khaminets, M. G.; Jakobs, C.; Monks, B.; Fitzgerald, K. A.; Latz, E.; Hornung, V. iGLuc: a luciferase-based inflammasome and protease activity reporter. *Nat. Methods* **2013**, *10* (2), 147–154.

- (10) Oleaga, C.; Welten, S.; Belloc, A.; Sole, A.; Rodriguez, L.; Mencia, N.; Selga, E.; Tapias, A.; Noe, V.; Ciudad, C. J. Identification of novel Sp1 targets involved in proliferation and cancer by functional genomics. *Biochem. Pharmacol.* **2012**, *84* (12), 1581–1591.

- (11) Judge, A.; MacLachlan, I. Overcoming the innate immune response to small interfering RNA. *Hum. Gene Ther.* **2008**, *19* (2), 111–124.

- (12) Schlee, M.; Hornung, V.; Hartmann, G. siRNA and isRNA: two edges of one sword. *Mol. Ther.* **2006**, *14* (4), 463–470.

- (13) Atianand, M. K.; Fitzgerald, K. A. Molecular basis of DNA recognition in the immune system. *J. Immunol.* **2013**, *190* (5), 1911–1918.

- (14) Omid, Y.; Hollins, A. J.; Benboubetra, M.; Drayton, R.; Benter, I. F.; Akhtar, S. Toxicogenomics of non-viral vectors for gene therapy: a microarray study of lipofectin- and oligofectamine-induced gene expression changes in human epithelial cells. *J. Drug Target.* **2003**, *11* (6), 311–323.

- (15) Pan, C. Q.; Ulmer, J. S.; Herzka, A.; Lazarus, R. A. Mutational analysis of human DNase I at the DNA binding interface: implications for DNA recognition, catalysis, and metal ion dependence. *Protein Sci.* **1998**, *7* (3), 628–636.

- (16) Hauptenthal, J.; Baehr, C.; Kiermayer, S.; Zeuzem, S.; Piiper, A. Inhibition of RNase A family enzymes prevents degradation and loss of silencing activity of siRNAs in serum. *Biochem. Pharmacol.* **2006**, *71* (5), 702–710.

- (17) Bartlett, D. W.; Davis, M. E. Effect of siRNA nuclease stability on the in vitro and in vivo kinetics of siRNA-mediated gene silencing. *Biotechnol. Bioeng.* **2007**, *97* (4), 909–921.

- (18) Layzer, J. M.; McCaffrey, A. P.; Tanner, A. K.; Huang, Z.; Kay, M. A.; Sullenger, B. A. In vivo activity of nuclease-resistant siRNAs. *RNA* **2004**, *10* (5), 766–771.

- (19) Dykxhoorn, D. M.; Palliser, D.; Lieberman, J. The silent treatment: siRNAs as small molecule drugs. *Gene Ther.* **2006**, *13* (6), 541–552.

- (20) Turner, J. J.; Jones, S. W.; Moschos, S. A.; Lindsay, M. A.; Gait, M. J. MALDI-TOF mass spectral analysis of siRNA degradation in serum confirms an RNase A-like activity. *Mol. Biosyst.* **2007**, *3* (1), 43–50.

- (21) Jones, S. J.; Worrall, A. F.; Connolly, B. A. Site-directed mutagenesis of the catalytic residues of bovine pancreatic deoxyribonuclease I. *J. Mol. Biol.* **1996**, *264* (5), 1154–1163.

- (22) Fujihara, J.; Yasuda, T.; Ueki, M.; Iida, R.; Takeshita, H. Comparative biochemical properties of vertebrate deoxyribonuclease I. *Comp. Biochem. Physiol. B Biochem. Mol. Biol.* **2012**, *163* (3–4), 263–273.

- (23) Bishop, J. S.; Guy-Caffey, J. K.; Ojwang, J. O.; Smith, S. R.; Hogan, M. E.; Cossum, P. A.; Rando, R. F.; Chaudhary, N. Intramolecular G-quartet motifs confer nuclease resistance to a potent anti-HIV oligonucleotide. *J. Biol. Chem.* **1996**, *271* (10), 5698–5703.

- (24) Bates, P. J.; Choi, E. W.; Nayak, L. V. G-rich oligonucleotides for cancer treatment. *Methods Mol. Biol.* **2009**, *542*, 379–392.

- (25) Blume, S. W.; Lebowitz, J.; Zacharias, W.; Guarcello, V.; Mayfield, C. A.; Ebbinghaus, S. W.; Bates, P.; Jones, D. E., Jr.; Trent, J.; Vigneswaran, N.; Miller, D. M. The integral divalent cation within the intermolecular purine\*purine. pyrimidine structure: a variable determinant of the potential for and characteristics of the triple helical association. *Nucleic Acids Res.* **1999**, *27* (2), 695–702.

- (26) Judge, A. D.; Sood, V.; Shaw, J. R.; Fang, D.; McClintock, K.; MacLachlan, I. Sequence-dependent stimulation of the mammalian innate immune response by synthetic siRNA. *Nat. Biotechnol.* **2005**, *23* (4), 457–462.

- (27) Sioud, M. Induction of inflammatory cytokines and interferon responses by double-stranded and single-stranded siRNAs is sequence-dependent and requires endosomal localization. *J. Mol. Biol.* **2005**, *348* (5), 1079–1090.

- (28) Hornung, V.; Guenther-Biller, M.; Bourquin, C.; Ablasser, A.; Schlee, M.; Uematsu, S.; Noronha, A.; Manoharan, M.; Akira, S.; de Fougerolles, A.; Endres, S.; Hartmann, G. Sequence-specific potent

induction of IFN- $\alpha$  by short interfering RNA in plasmacytoid dendritic cells through TLR7. *Nat. Med.* **2005**, *11* (3), 263–270.

(29) Hanagata, N. Structure-dependent immunostimulatory effect of CpG oligodeoxynucleotides and their delivery system. *Int. J. Nanomed.* **2012**, *7*, 2181–2195.

(30) Davis, B. K.; Wen, H.; Ting, J. P. The inflammasome NLRs in immunity, inflammation, and associated diseases. *Annu. Rev. Immunol.* **2001**, *29*, 707–735.

(31) Kool, E. T. Recognition of DNA, RNA, and Proteins by Circular Oligonucleotides. *Acc. Chem. Res.* **1998**, *31* (8), 502–510.

(32) Rubin, E.; Rumney, S. t.; Wang, S.; Kool, E. T. Convergent DNA synthesis: a non-enzymatic dimerization approach to circular oligodeoxynucleotides. *Nucleic Acids Res.* **1995**, *23* (17), 3547–3553.

(33) Chu, B. C.; Orgel, L. E. The stability of different forms of double-stranded decoy DNA in serum and nuclear extracts. *Nucleic Acids Res.* **1992**, *20* (21), 5857–5858.

(34) Mencia, N.; Selga, E.; Noe, V.; Ciudad, C. J. Underexpression of miR-224 in methotrexate resistant human colon cancer cells. *Biochem. Pharmacol.* **2011**, *82* (11), 1572–1582.

(35) Barros, S.; Mencia, N.; Rodriguez, L.; Oleaga, C.; Santos, C.; Noe, V.; Ciudad, C. J. The redox state of cytochrome c modulates resistance to methotrexate in human MCF7 breast cancer cells. *PLoS One* **2013**, *8* (5), e63276.

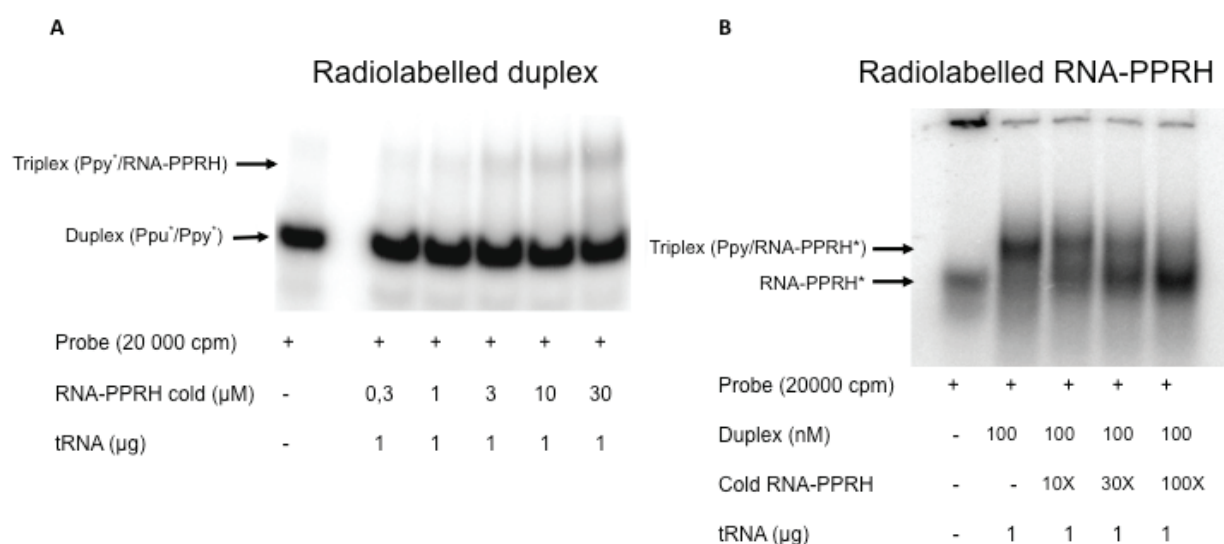


#### 4.1.1 Additional results to article I.

Reverse Hoogsteen bonds can be formed between purines of desoxyribonucleic acid and of ribonucleic acid. Therefore, we analyzed the capacity of a PPRH made out of RNA (RNA-PPRH) to form triple-helix structures and to decrease cell survival.

##### 4.1.1.1 Binding of a RNA-PPRH to its target duplex

We performed binding experiments to determine if an RNA-PPRH targeting the *dhfr* gene was able to bind to its dsDNA target. To do so, we radiolabelled the target duplex with [<sup>32</sup>P] and incubated it with growing concentrations of the RNA-PPRH. It can be seen that upon incubation with the RNA-PPRH a shifted band appears, and that its intensity increases with the concentration of RNA-PPRH used (figure 14A).



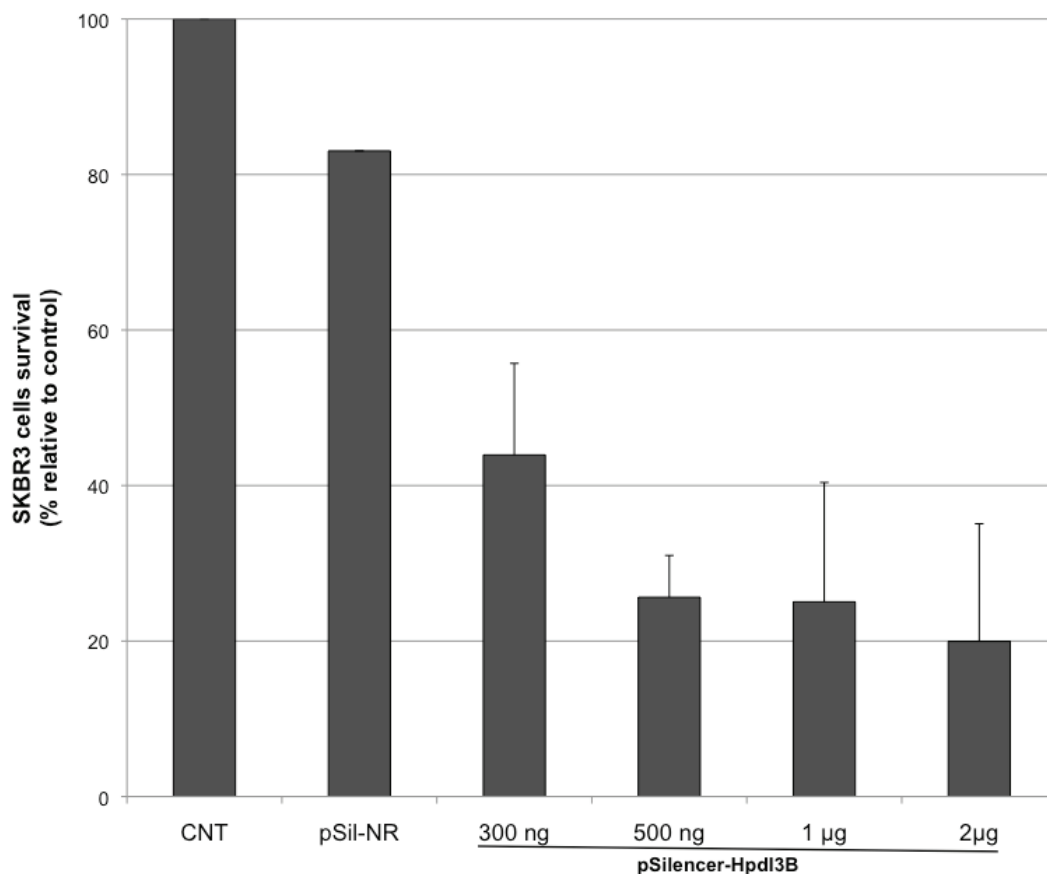
**Figure 14.** Binding assays showing the triplex formation of an RNA-PPRH with its target DNA. **A.** The RNA-PPRH was incubated with the radiolabelled target to determine its binding capacity. The formation of the triples between the RNA-PPRH and the polypyrimidine (Ppy) sequence is marked by an arrow. **B.** The radiolabelled RNA-PPRH was incubated with the target duplex. Then, competition with cold RNA-PPRH was performed, observing a reversal of the shifted band.

The specificity of this binding was confirmed performing competition experiments, in which a radiolabelled RNA-PPRH was incubated with a fixed concentration (100 nM) of target duplex and with growing concentrations of cold RNA-PPRH. In this case, it can be seen that the shifted band corresponding to the RNA-PPRH/polypyrimidine strand triplex disappears as the concentration of cold RNA-PPRH increases (figure 14B).



#### 4.1.1.2 Effect of an RNA-PPRH on cell viability

After determining that an RNA-PPRH was able to bind to a dsDNA target, we performed cell survival experiments with an RNA-PPRH directed against the *dhfr* gene. To do this, we used a vector that contains the dsDNA sequence encoding for the HpdI3-B (which targets intron 3 of the *dhfr* gene) into the pSilencer vector. Upon transfection the sequence corresponding to the PPRH is transcribed, producing the RNA-PPRH intracellularly. We transfected the plasmid into SKBR3 cells and determined the cell survival after 7 days. The transient transfection of 300 ng or 500 ng of this plasmid induced a decrease in cell viability in SKBR3 cells of 50% and 80%, respectively. A plasmid containing a non-related sequence was used as a negative control, and in this case upon transfection the cell viability only decreased a 20% (figure 15).



**Figure 15.** SKBR3 cells survival upon pSilencer-HpdI3-B transfection. SKBR3 cells (10 000) were plated and increasing amounts of the pSilencer-HpdI3-B vector were transfected using Fugene® 6. MTT assay were performed 6 days after transfection to determine cell viability.

## 4.2 ARTICLE II:

### **Effect of Polypurine Reverse Hoogsteen Hairpins on Relevant Cancer Target Genes in Different Human Cell Lines**

Xenia Villalobos, Laura Rodríguez, Anna Solé, Carolina Lliberós, Núria Mencia, Carlos J. Ciudad, and Véronique Noé

Nucleic Acid Therapeutics 2015 Aug;25(4):198-208. (Impact factor: 2.929)

#### *Background:*

In previous studies we demonstrated that PPRHs are capable of silencing cancer-related target genes, such as *DHFR* (de Almagro *et al.* 2009; de Almagro *et al.* 2011) *survivin* (Rodríguez *et al.* 2013) and *telomerase (TERT)* (Rodríguez *et al.* 2015). Several genes have been described as relevant for cancer. These include the antiapoptotic protein *BCL2*, the enzyme *Topoisomerase-1 (TOP1)*, which is a clinically validated target, the protein kinase mTOR, the protooncogene *MDM2*, and the transcription factor *MYC*. These targets are usually overexpressed either by gene amplification or by over-activation in tumors. Therefore, we designed PPRHs against the above-mentioned genes: *BCL2*, *TOP1*, *MTOR*, *MDM2* and *MYC*, and tested them for mRNA levels, cytotoxicity, and apoptosis in prostate, pancreas, colon, and breast cancer cell lines.

#### *Objectives:*

The aim of this study was to demonstrate the general applicability of PPRHs as silencing tools in cancer therapy. Therefore, we tested several PPRHs directed against an array of relevant genes in different cancer cell lines.

#### *Results:*

All PPRHs were effective, yet the most remarkable results in decreasing cell survival and mRNA levels and in increasing apoptosis were obtained with those against *BCL2* in prostate, colon, and pancreatic cancer cells. Additionally, we cotransfected two PPRHs directed against two different *BCL2* regions, exon 1 (HpBcl2E1-C) and promoter (HpBcl2Pr-C) to evaluate possible additive or synergistic effects. When cotransfecting at low concentrations (12.5 nM each, 25nM in total) a greater effect was

## Results

observed than when cotransfecting 25 nM of each PPRH separately. For higher concentrations we did not observe any improvement since the PPRHs by themselves were very effective, especially HpBcl2E1-C. Also, 3 out of 4 PPRHs designed against *MTOR* were highly effective in HCT 116 cells. Additionally, in this case we performed time-course experiments in which we observed that short incubations of 8 h after transfection already produced a 50% decrease in HCT 116 cells survival. In the case of *TOP1*, *MDM2*, and *MYC*, their corresponding PPRHs produced a strong effect in decreasing cell viability and mRNA levels and increasing apoptosis in the three breast cancer cell lines used. The negative controls used did not have a significant effect on survival, apoptosis or target mRNA expression in any case.

### *Conclusions:*

The results presented in this article confirm that the PPRH technology is broadly useful to silence the expression of genes related in cancer. Regardless of the gene or cell line tested, PPRHs were able to decrease cell survival and mRNA expression levels, and to increase apoptosis, to a greater or lesser extent.

# Effect of Polypurine Reverse Hoogsteen Hairpins on Relevant Cancer Target Genes in Different Human Cell Lines

Xenia Villalobos, Laura Rodríguez, Anna Solé, Carolina Lliberós,  
Núria Mencia, Carlos J. Ciudad, and Véronique Noé

We studied the ability of polypurine reverse Hoogsteen hairpins (PPRHs) to silence a variety of relevant cancer-related genes in several human cell lines. PPRHs are hairpins formed by two antiparallel polypurine strands bound by intramolecular Hoogsteen bonds linked by a pentathymidine loop. These hairpins are able to bind to their target DNA sequence through Watson–Crick bonds producing specific silencing of gene expression. We designed PPRHs against the following genes: *BCL2*, *TOP1*, *mTOR*, *MDM2*, and *MYC* and tested them for mRNA levels, cytotoxicity, and apoptosis in prostate, pancreas, colon, and breast cancer cell lines. Even though all PPRHs were effective, the most remarkable results were obtained with those against *BCL2* and mammalian target of rapamycin (*mTOR*) in decreasing cell survival and mRNA levels and increasing apoptosis in prostate, colon, and pancreatic cancer cells. In the case of *TOP1*, *MDM2*, and *MYC*, their corresponding PPRHs produced a strong effect in decreasing cell viability and mRNA levels and increasing apoptosis in breast cancer cells. Thus, we confirm that the PPRH technology is broadly useful to silence the expression of cancer-related genes as demonstrated using target genes involved in metabolism (*DHFR*), proliferation (*mTOR*), DNA topology (*TOP1*), lifespan and senescence (*telomerase*), apoptosis (*survivin*, *BCL2*), transcription factors (*MYC*), and proto-oncogenes (*MDM2*).

## Introduction

**G**ENE SILENCING HAS BECOME an essential technique for molecular biology validation and therapeutics. Up until now, RNA-targeting approaches such as antisense oligodeoxynucleotides (aODNs) and small interfering RNAs (siRNAs) have been used, and recently, protein-based approaches [zinc-finger nucleases (ZFN), TALENs, and CRISPR/Cas9] have emerged [1,2,3–5]. As an additional tool, we developed a new type of silencing molecules called polypurine reverse Hoogsteen hairpins (PPRHs). These molecules have the advantages of increased stability and low immunogenicity compared to siRNAs [6].

PPRHs are nonmodified DNA molecules formed by two antiparallel polypurine strands linked by a pentathymidine loop that allows the formation of intramolecular reverse-Hoogsteen bonds between both strands, acquiring a hairpin structure. The hairpins bind by Watson–Crick bonds to polypyrimidine stretches in the DNA, which can be located in the promoter, exonic, and intronic regions. We described the ability of PPRHs to bind both the template [7] and coding [8] strands of the dsDNA, forming a triplex structure that knocks down the expression of the target genes. Template-PPRHs bind to the template strand of the DNA, whereas coding-PPRHs bind to the coding sequence of the DNA and can also

bind to transcribed RNA. The mechanism of action of PPRHs depends on the location of their target; we demonstrated that a coding-PPRH directed against a polypyrimidine region in intron 3 of *DHFR* pre-mRNA produced a splicing alteration by preventing the binding of the splicing factor U2AF65. On the other hand, two PPRHs directed against the template or coding strand of the *survivin* promoter sequence decreased the binding of transcription factors Sp1 and GATA-3, respectively. The *in vivo* administration of the coding-PPRH against the promoter region of the *survivin* gene was able to delay tumor growth in a prostate xenograft mouse model [9].

Several genes have been described as relevant for cancer. These include the antiapoptotic protein *BCL2*, the proto-oncogene *MDM2*, the transcription factor *MYC*, the enzyme Topoisomerase-1 (*TOP1*), which is a clinically validated target, and the protein kinase *mTOR*. These targets are usually overexpressed either by gene amplification or by overactivation in tumors [10–16].

The aim of this study was to demonstrate the general applicability of PPRHs as silencing tools in cancer therapy. Therefore, we tested several PPRHs directed against an array of relevant genes in different cancer cell lines, including pancreatic cancer MIA PaCa-2 cells, colon cancer HCT 116 cells, prostate cancer PC-3 cells, and breast cancer cell lines

MCF7, MDA-MB-468, and SKBR3. The ability of the designed PPRHs to decrease cell survival of the different cell lines by causing apoptosis and their effect on the mRNA levels of the targets were evaluated.

## Materials and Methods

### Oligonucleotides

PPRHs and primers were synthesized as nonmodified oligodeoxynucleotides by Sigma-Aldrich. They were dissolved at 1 mM (stock solution) in a sterile RNase-free Tris-EDTA buffer (1 mM EDTA and 10 mM Tris, pH 8.0) and stored at  $-20^{\circ}\text{C}$  until use. PPRHs were designed using the Triplex-Forming Oligonucleotide Target Sequence Search tool available at <http://spi.mdanderson.org/tfo/> to find the polypurine tracks present in a gene and, thus, the polypyrimidine targets. If purine interruptions (up to three) were present in the pyrimidine target sequence, when designing the PPRHs those positions were substituted by either an adenine or the complementary pyrimidine. The specificity of the chosen polypurine tracks was evaluated by BLAST analyses.

Two types of negative controls were used for every targeted gene: (1) sequences that form intramolecular Watson-Crick bonds (Hp-WC), instead of reverse Hoogsteen bonds, thus preventing the formation of an additional W:C bond to the target DNA, and consequently triplex formation [7,8] and (2) scrambled sequences that do not bind to the target (Hp-Sc). For the initial screening of the study, we used several PPRHs for either BCL2 or mTOR. Then, we used the same scrambled PPRH to corroborate that an oligonucleotide with a hairpin conformation did not affect cellular viability. For the rest of the genes, Topoisomerase, MDM2, and Myc, we decided to use specific scrambled PPRHs for each gene containing a similar G/A polypurine content. Therefore, globally we used a collection of different negative controls. Table 1 describes all oligonucleotide names and sequences used in this work.

### Cell culture

Pancreatic cancer MIA PaCa-2, prostate cancer PC-3, colon cancer HCT 116, and breast cancer SKBR3, MCF7, and MDA-MB-468 cell lines were used throughout the study. Cell lines were routinely grown in Ham's F-12 medium supplemented with 7% fetal calf serum (both from Gibco) at  $37^{\circ}\text{C}$  in a 5%  $\text{CO}_2$ -controlled humidified atmosphere.

### Transfection of PPRHs

Cells were plated the day before transfection, which consisted in mixing the appropriate amount of PPRH and N-[1-(2,3-dioleoyloxy)propyl]-N,N,N-trimethylammonium methylsulfate (DOTAP; Roche or Biontex) for 20 min in a volume of 200  $\mu\text{L}$  of medium at room temperature, followed by the addition of the mixture to the cells in a total volume of 1 mL. When transfecting the PPRHs at 100 nM (final concentration), DOTAP was used at 10  $\mu\text{M}$ ; for lower concentrations of PPRH, DOTAP was used at 5  $\mu\text{M}$ .

### Cellular uptake of PPRHs

One hundred fifty thousand cells were plated in 50-mm dishes with 2 mL complete F-12 medium and transfected with

100 nM of a fluorescent-labeled PPRH and DOTAP (10  $\mu\text{M}$ ). Twenty-four hours after transfection, cells were collected, centrifuged at 800g at  $4^{\circ}\text{C}$  for 5 min, and washed once in phosphate-buffered saline (PBS). The pellet was resuspended in 500  $\mu\text{L}$  PBS plus propidium iodide (PI, final concentration 5  $\mu\text{g}/\text{mL}$ ; Sigma-Aldrich). Cells were kept on ice for no longer than 30 min before flow cytometry analysis was performed in a Coulter XL cytometer (Beckman Coulter, Inc.).

### RNA extraction

At the end of the experiments, total RNA was extracted from cells using either Ultraspec (Biotecx) or TRIzol (Life Technologies) following the manufacturer's specifications. Quantification of RNA was conducted measuring its absorbance at 260 nm using a NanoDrop ND-1000 spectrophotometer (Thermo Scientific).

### RNA determination

cDNA was synthesized by reverse transcription in a 20  $\mu\text{L}$  reaction mixture containing 1  $\mu\text{g}$  of total RNA, 125 ng of random hexamers (Roche), 10 mM dithiothreitol, 20 U of RNasin (Promega), 0.5 mM of each dNTP (AppliChem), 4  $\mu\text{L}$  of buffer (5 $\times$ ), and 200 U of Moloney murine leukemia virus reverse transcriptase (Invitrogen). The reaction was incubated at  $37^{\circ}\text{C}$  for 1 h. Three microliters of the cDNA mixture was used for real-time PCR amplification using StepOnePlus<sup>TM</sup> Real-Time PCR Systems (Applied Biosystems, Life-Technologies) with specific primers for each gene to be determined.

In the case of BCL2 and mammalian target of rapamycin (mTOR), RNA levels were determined using the assays-on-demand (HS00608023\_M1) and (HS00234508\_M1), respectively, and HS00975725\_M1 for adenine phosphoribosyltransferase (APRT) as the endogenous control (all from Applied Biosystems). The reaction was performed following the manufacturer's recommendations. For MDM2, MYC, and TOP1, mRNA levels were determined by SYBR-Green reverse transcription quantitative-PCR and the pair of primers listed in Table 2, using APRT as an endogenous control. Fold changes in gene expression were calculated using the standard  $\Delta\Delta\text{Ct}$  method.

### Cell survival experiments (MTT)

Cells were plated in six-well dishes in the Ham's F-12 medium. Six days after PPRH transfection, 0.63 mM of 3-(4,5-dimethylthiazol-2-yl)-2,5-diphenyltetrazolium bromide and 100  $\mu\text{M}$  of sodium succinate (both from Sigma-Aldrich) were added to the culture medium and allowed to react for 3 h at  $37^{\circ}\text{C}$  before the addition of the solubilization reagent (0.57% acetic acid and 10% SDS in DMSO). Cell viability was measured at 570 nm in a WPA S2100 Diode Array Spectrophotometer. The results were expressed as the percentage of cell survival relative to the control (untreated cells).

### Apoptosis

Apoptosis was determined by measuring the activity of caspase-3 and caspase-7 with the Caspase-Glo<sup>®</sup> 3/7 Assay (Promega). Cells (5,000) were plated in 96-well plates in the F12 medium. After 24 h, 100 nM of each PPRH was

TABLE 1. POLYPURINE REVERSE HOOGSTEEN HAIRPINS USED IN THIS STUDY

Name	Sequence (5' → 3')	Location	Type
HpBcl2Pr-C	GGAGAGGGGAGGGGAGAAGGAGGTTTTTTGGAGGAAGAGGGGAGGGGA GAGG	Promoter - 378	+
HpBcl2E1-C	GAGGGGAGAGGGGAGAAAAATTTTTAAAAAAGAGGGAGAGGGGAG	Exon 1 + 65	+
HpBcl2I2-T	GAAGGGGGAAGAAGAGAGAGAAGAGAGAGATTTTTAGAGAGAGAAGA GAGAGAAGAAGGGGGAAG	Intron 2 + 32279	+
HpBcl2I2-C	GGGGAGGAGGAAAAGAAGGAAGGAAGAGGTTTTTGGAGAAGGAAG GAAGAAAAGGAGGAGGGG	Intron 2 + 112542	+
HpBcl2E1-WC	CTCCCTCTCCCTCTTTTTTTTTTTAAAAAAGAGGGAGAGGGGAG	-	-
HpTorPr-C	GGGAGCGAGGGAAGGAGGGTTTTTGGGAGGAAGGGAGCGAGGG	Promoter - 3137	+
HpTorE5-C	GGAAGAAGAAGGAAGGGAAGTTTTTGAAGGAAGGAAGAAGAAGG	Exon 5 149614	+
HpTor-T	GATGGTGGAGAAAGGAAGAGAGGGTTTTTGGGAGAGAAGGAAA GAGGTGGTAG	Intron 15 126405	+
HpTorI17-C	GGGAAAGGGGAGGGAAAAAAGATTTTTAGAAAAAAGGGAGGG GAAAGGG	Intron 17 124527	+
HpTorPr-WC	CCCTCCTTCCCTCGCTCCCTTTTTTGGGAGGAAGGGAGCGAGGG	Promoter - 3137	-
Hp-Sc1	AAGAGAAAAAGAGAAAAGAAGAGAGGGTTTTTGGGAGAGAAGAAAGA GAAAAAGAGAA	-	-
HpTopI2-T	GGAGAGGAGGAGGGAGAAAATTTTTAAAAGAGGGAGGAGGAGAGG	Intron 2 + 2363	+
HpTopI2-WC	CCTCACCTCCTCCCTCTTTTTTTTTTAAAAGAGGGAGGAGGAGAGG	Intron 2 + 2363	-
Hp-Sc2	AGAGGAGAGAAGGAAGGAGGTTTTTGGAGGAAGGAAGAGAGGAGA	-	-
HpMdmI7-T	GGGAAGGAAAGAAGAAGGGAGTTTTT GAGGGAAGAAGAAAGGAAGGG	Intron 7 + 17644	+
HpMdmI7-WC	CCCTCCTGTCTTCTGCCCGCTTTTT GAGGGAAGAAGAAAGGAAGGG	Intron 7 + 17644	-
Hp-Sc3	GAGAAGAGGAAGAGAGGAAGGTTTTTGGAAAGGAGAGAAGGAGAAGAG	-	-
HpMycI1-T	GGGAAAAAGGGAGAAAGGAAGAGGAGGGGAAGAATTTTTAAGAAGG GAGAGGAGAAGGAAGAGGGAAAAAGGG	Intron 1 + 745	+
HpMycI1-WC	CCCTTTTCCCTCTTCTTCTCCTCTCCTCTTTTTTTAAGAAGGGAGAG GAGAAGGAAGAGGGAAAAAGGG	Intron 1 + 745	-
Hp-Sc4	AGAGAAGAGGAAGAGAGGAAAAGAGAGGAAGAGGATTTTTAGGAGAAG GAGAGAAAGGAGAGAAGGAGAAGAGA	-	-

Name, sequence, gene location, and type: specific (+) or negative control (-) of the PPRHs used in this study. Letters in *bold* indicate the bases placed opposite the purine interruptions present in the pyrimidine target, either adenine substitutions or the complementary pyrimidine.

transfected using 10 μM of DOTAP (final concentration) in a volume of 50 μL, and 24 h after transfection, 50 μL of the Caspase-Glo 3/7 reagent was added. Luminescence was measured after 1 h using a Modulus™ Microplate luminometer (Turner Biosystems; Promega). The F12 medium was considered the blank control and untreated cells the background. In the case of SKBR3, MCF7, and MDA-MB-

468 cells, apoptosis was also determined by the rhodamine method: cells (120,000) were plated in 50-mm dishes with 2 mL of complete F-12 medium and transfected with 100 nM of each PPRH. Twenty-four hours after treatment, rhodamine (final concentration 5 μg/mL) (Sigma-Aldrich) was added for 30 min, the cells were collected, centrifuged at 800g at 4°C for 5 min, and washed once in PBS. The pellet

TABLE 2. PRIMERS USED FOR REVERSE TRANSCRIPTION QUANTITATIVE-PCR

	FWD primer (5'-3')	REV primers (5'-3')	Amplicon (bp)
MDM2	CAGCTTCGGAACAAGAGACC	GTCCGATGATTCCTGCTGAT	293
MYC	TTCGGGTAGTGAAAACCAG	CCTCCTCGTCGCAGTAGAAA	120
TOP1	GAGAAGGACCGGAAAAGTC	TATTTTTGCATCCCCAGAGG	186
APRT	GCAGCTGGTTGAGCAGCGGAT	AGAGTGGGGCCTGGCAGCTTC	272

Sequence of the primers used for determining MDM2, MYC, and TOP1 RNA levels and amplicon length.



TABLE 3. TRANSFECTION EFFICIENCY OF THE DIFFERENT CELL LINES

Cell line	% Positive cells	Mean fluorescence
MIA PaCa2	85.05 ± 6.3	57 ± 24.8
PC3	90.2 ± 2.9	555.3 ± 166.7
HCT 116	90.8 ± 8.2	241 ± 81
SKBR3	89.8 ± 4.5	434.5 ± 49.5
MCF7	81.95 ± 16.1	762.5 ± 117
MDA-MB-468	95.8 ± 3.6	498.4 ± 103.5

Percentage of fluorescent cells and the raw mean fluorescence 24 h after transfection. Cells were incubated with 100 nM fluorescent PPRHs for 24 h. Fluorescence was determined by flow cytometry.

was resuspended in 500  $\mu$ L of PBS with PI (final concentration 5  $\mu$ g/mL; (Sigma-Aldrich). Flow cytometry analyses were performed in a Coulter XL cytometer, and data were analyzed using the software Summit v4.3. The percentage of Rho-negative and IP-negative cells corresponded to the apoptotic population.

#### Statistical methods

Values are expressed as the mean  $\pm$  SE. Data were evaluated by unpaired Student's *t*-test when analyzing the difference between two conditions, control and treated. The analyses were performed using the software IBM SPSS Statistics v20. Differences with *P* values < 0.05 were taken as statistically significant.

### Results and Discussion

The goal of this work was to evaluate whether PPRHs could be used as silencing agents against different targets in cell lines corresponding to several cancer types to expand the usage of PPRHs in cancer therapy and prove their general applicability. For this purpose, we chose an array of therapeutically interesting genes to act as reporter genes for the silencing activity of the PPRHs. The chosen target genes encompass a variety of biological functions: antiapoptotic genes, topoisomerases, protein kinases, and transcription factors. We were able to design PPRHs directed against polypyrimidine stretches of every gene to be targeted; three of these stretches were located in introns (*MYC*, *MDM2*, *TOP1*), one in a promoter region (*mTOR*), and one in an

exonic sequence (*BCL2*), which were tested in a variety of cell lines (HCT 116, PC-3, MIA PaCa-2, SKBR3, MCF7, and MDA-MB-468).

The transfection efficiency was determined through uptake experiments performed by transfecting 100 nM of fluorescent PPRHs with 10  $\mu$ M DOTAP in the different cell lines. In Table 3 it can be seen that the percentage of fluorescent cells in all cell lines was very high, although the mean intensity varied among them.

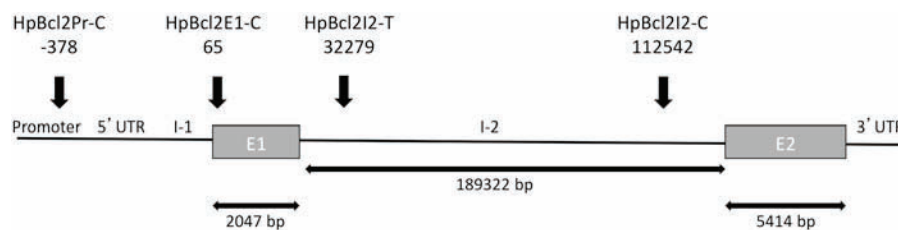
The results obtained for each PPRH are presented and discussed below.

#### *BCL2* protein

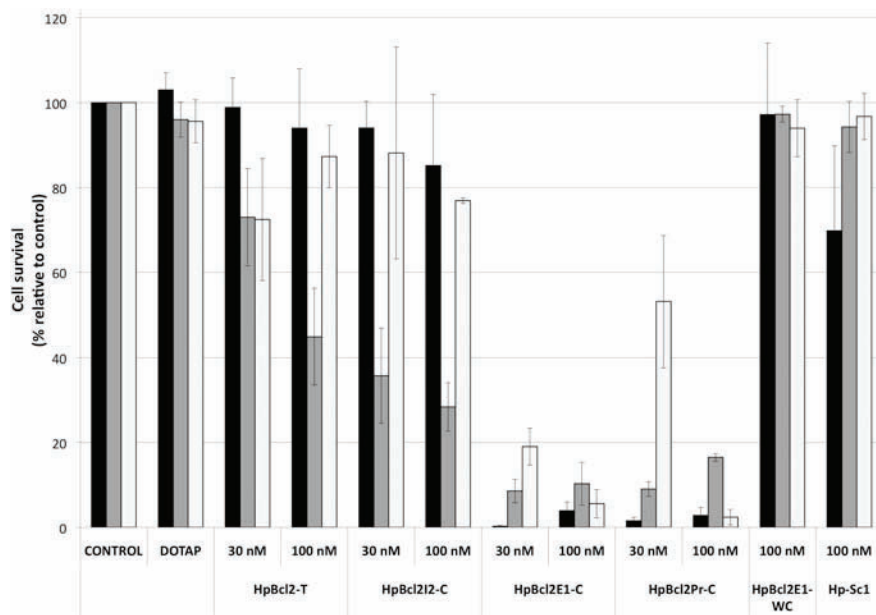
*BCL2* is an antiapoptotic protein, the overexpression of which in multiple cell lines contributes to cancer progression and it is also related to resistance to chemotherapy [17]. Regarding solid tumors, *BCL2* is overexpressed in 30%–60% of prostate cancers at diagnosis and in nearly 100% of castration-resistant prostate cancer [12] and its content has been related to increased resistance to gemcitabine [18]. Antisense oligonucleotides (oblimersen), antibodies, peptides, and small molecules against *BCL2* are under development. Even though partially successful, none of these approaches has been proven to be useful in the clinic because they present problems of specificity, side effects, short half-life, and delivery [17].

We performed an initial screening of four PPRHs against different target sequences within the *BCL2* gene (Fig. 1); the screening consisted in determining the cell survival of three different cell lines (MIA PaCa-2, PC-3, and HCT 116) after transfecting the PPRHs at different concentrations (30 and 100 nM). In Fig. 2, it can be observed that not all PPRHs were equally effective and, in this case, the most effective PPRH was HpBcl2E1-C, directed against the coding strand of exon 1, which was able to decrease survival by 90%–95% in all cell lines at a concentration of 100 nM. As negative controls, HpBcl2E1-WC and Hp-Sc1 were used; these did not cause a significant decrease of survival in any cell line.

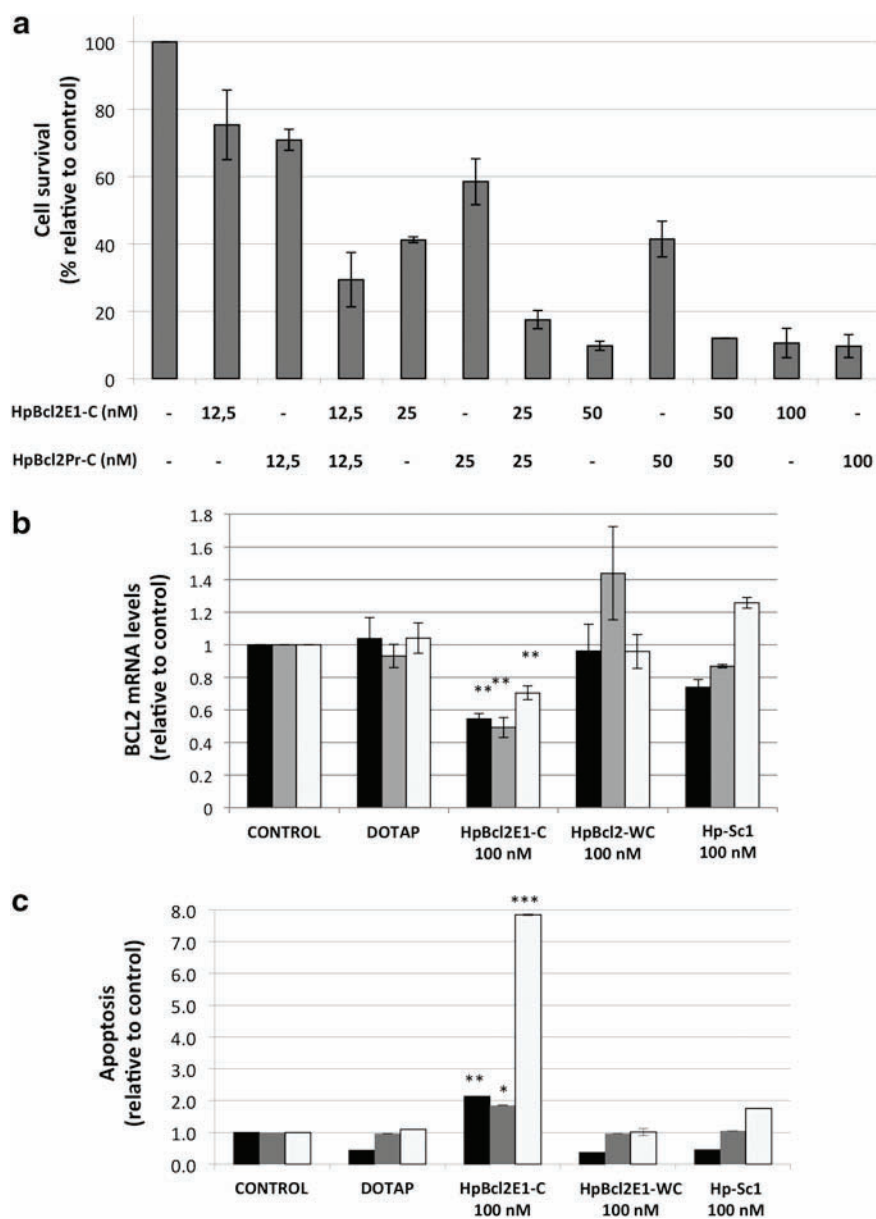
We explored whether a combination of two different PPRHs was able to increase their efficiency. As seen in Fig. 3a, when cotransfecting HpBcl2E1-C and HpBcl2Pr-C at low concentrations (12.5 nM each, 25 nM in total), their effect was greater than when transfecting 25 nM of each PPRH separately. For higher concentrations, we did not observe any improvement since the PPRHs by themselves, especially



**FIG. 1.** Scheme representing the target sequences of the polypurine reverse Hoogsteen hairpins (PPRHs) against the *BCL2* gene. Four PPRHs were designed for the *BCL2* gene directed against the promoter (HpBcl2Pr-C), exon 1 within the 5'UTR (HpBcl2E1-C) and two other PPRHs against intron 2, one template (HpBcl2I2-T) and one coding (HpBcl2I2-C). The nomenclature used was Hp (Hairpin), Bcl2 (*BCL2*), Pr (promoter), I (intron), and E (exon). The numbering below the PPRHs corresponds to the target sequence start referred to the transcriptional start site of the gene. The arrows indicate the length of each gene element.



**FIG. 2.** Initial screening of PPRHs against *BCL2*. Ten thousand MIA PaCa-2 (■, black bars), PC-3 (■, gray), and HCT 116 (□, white) cells were plated and transfected the following day with either 30 or 100 nM of the different PPRHs. MTT assays to determine cell survival were performed 6 days after transfection. Data are the mean  $\pm$  SE values of at least three experiments. As negative controls HpBcl2-WC and Hp-Sc1 at 100 nM were used.



**FIG. 3.** Effect of HpBcl2E1-C on cell viability, BCL2 mRNA levels, and apoptosis. **(a)** MTT assays to determine survival of PC-3 (■, gray) cells were performed 6 days after transfecting different concentrations of HpBcl2E1-C and HpBcl2Pr-C. **(b)** Total RNA was extracted from MIA PaCa-2 (■, black bars), PC-3, and HCT 116 (□, white) cells (60,000) 24 h after the transfection with the different PPRHs at a concentration of 100 nM. **(c)** MIA PaCa-2, PC-3, and HCT 116 cells were transfected with 100 nM of either HpBcl2E1-C or the negative controls HpBcl2-WC and Hp-Sc1. Apoptosis was determined by the activity of caspase-3 and caspase-7 after 24 h of transfection. All results are expressed as change in relative light units (RLU) relative to control. Data are the mean  $\pm$  SE values of at least three experiments. \* $P < 0.05$ , \*\* $P < 0.01$ , \*\*\* $P < 0.005$  compared with control.



HpBcl2E1-C, are very efficient. The subsequent mRNA determinations were performed for HpBcl2E1-C. This reduction in cell survival was accompanied by a twofold decrease in BCL2 mRNA levels in MIA PaCa-2 and PC3 cells and by a 1.4-fold decrease in HCT 116 cells (Fig. 3b) when HpBcl2E1-C was transfected, but not when the negative controls were used. It has been reported [19] that a twofold decrease in BCL2 caused a decrease in tumor growth. Since BCL2 acts as an antiapoptotic protein, we studied whether the decrease in cell survival was due to an increase in apoptosis. We transfected HpBcl2E1-C into the different cell lines, and after a 24-h incubation, we determined the activity of caspase-3 and caspase-7 with the Caspase-Glo 3/7 Assay. Apoptosis was increased 2.2-, 2-, and 7.8-fold in MIA PaCa-2, PC-3, and HCT 116 cells, respectively (Fig. 3c).

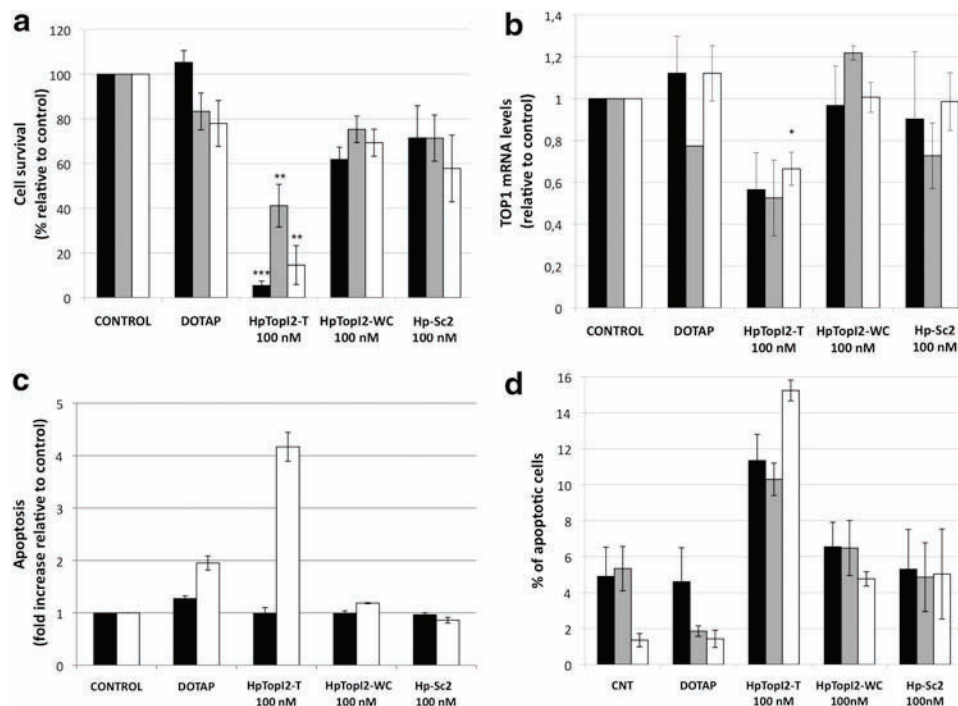
### Topoisomerase-1

Topoisomerase-1 is a clinically validated target; TOP1 inhibitors, such as camptothecin (CPT) and its derivatives (irinotecan and topotecan), have been used as anticancer therapy since the late 90s. The cytotoxicity of these drugs is dependent on the expression of topoisomerase I, which is overexpressed in tumors, relative to the corresponding normal tissue [20] and during DNA replication [21,22]. We examined if silencing the expression of this gene using a

specific PPRH led to decreased survival as well. The target sequence for the PPRH against *TOP1* (HpTopI2-T) is located in the template strand of intron 2. Our results showed that inhibition of TOP1 produced a decrease in cell survival of 95%, 60%, and 85% in SKBR3, MCF7, and MDA-MB-468 cell lines, respectively (Fig. 4a). The negative controls HpTopI2-WC and Hp-Sc2 produced a slight decrease in cell survival, between 20% and 40% depending on the cell line, but this decrease did not reach significance. The decrease in cell survival when the specific PPRH was transfected was paralleled by a decrease in TOP1 mRNA levels of 1.8-, 2-, and 1.4-fold in SKBR3, MCF7, and MDA-MB-468 cells, respectively (Fig. 4b). HpTopI2-T at 100 nM caused a 4.2-fold increase in apoptosis measured by the caspase 3/7 method in MDA-MB-468 cells, while in SKBR3 cells, apoptosis was not detected (Fig. 4c). Since MCF7 cells do not express caspase-3, the apoptosis produced by HpTopI2-T was measured by the rhodamine method in the three cell lines, observing an increase of apoptotic cells in all these cell lines (Fig. 4d).

### Mammalian target of rapamycin

mTOR is a 289 kDa serine/threonine protein kinase. mTOR is a central modulator of cell growth and plays a critical role in transducing proliferative signals mediated by the PI3K/AKT/



**FIG. 4.** Effect of HpTopI2-T on cell viability, TOP1 mRNA levels, and apoptosis. **(a)** SKBR3 (■, black bars), MCF7 (■, gray), and MDA-MB-468 (□, white) cells (30,000) were plated in six-well dishes and transfected with HpTopI2-T and the negative controls HpTopI2-WC and Hp-Sc2 at 100 nM. MTT assays to determine the cell survival were performed 6 days after transfection. **(b)** RNA was extracted from SKBR3, MCF7, and MDA-MB-468 cells (30,000) 48 h after the transfection with HpTopI2-T, HpTopI2-WC, and Hp-Sc2 at 100 nM. **(c)** Apoptosis in SKBR3 and MDA-MB-468 cells was measured with the Caspase-Glo<sup>®</sup> 3/7 Assay. All results are expressed as change in RLU relative to the control. **(d)** Apoptosis in SKBR3, MCF7, and MDA-MB-468 cells (120,000) determined by the rhodamine method. Rho123-negative and IP-negative cells were considered as apoptotic cells. Data are the mean ± SE values of at least three experiments. \**P* < 0.05, \*\**P* < 0.01, \*\*\**P* < 0.005, compared with control.

## EFFECT OF PPRHs ON CANCER TARGETS

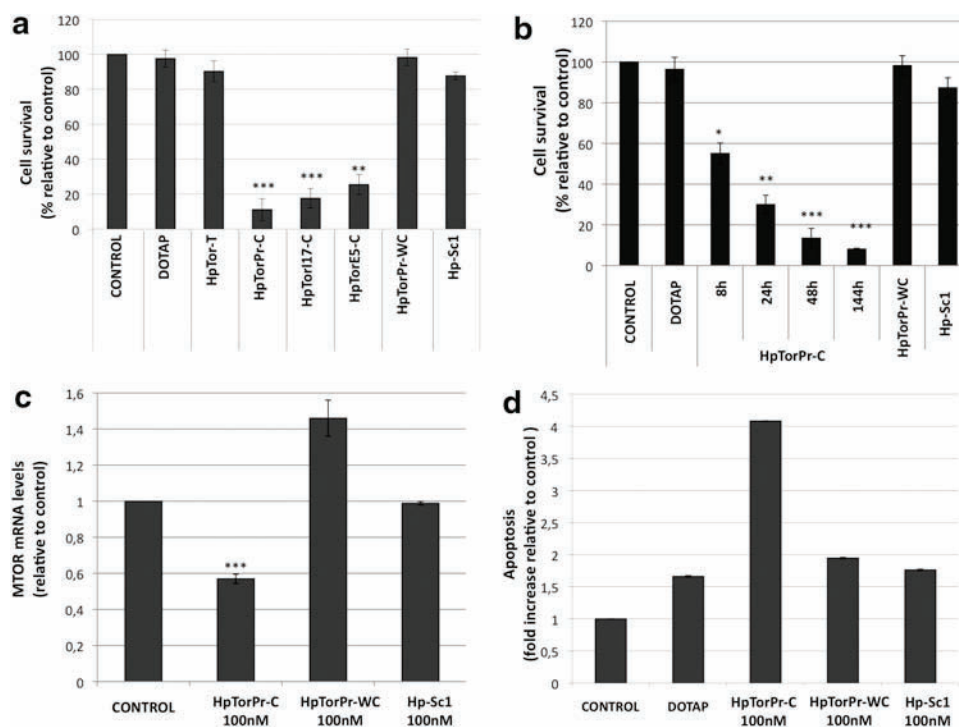
mTOR signaling pathway in response to nutrient availability and growth factor stimuli [23,24]. The PI3K/AKT/mTOR pathway is a prosurvival pathway that is constitutively activated in many types of cancer. It plays an important role in cancer development, progression, and therapeutic resistance.

We designed four PPRHs against the *mTOR* gene, one against a polypyrimidine stretch in the template strand of intron 15 and three against different regions of the coding strand: promoter, exon 5, and intron 17. After the initial screening in HCT 116 cells (Fig. 5a), we determined that the PPRH against the promoter region (HpTorPr-C) was the most effective, causing a decrease on cell survival higher than 90%. We incubated cells for different periods of time before renewing the culture medium to determine the time dependency, observing that short incubations already had a strong effect on cell survival. Figure 5b shows that incubations as short as 24 h with 100 nM of HpTorPr-C produced a 70% decrease in cell survival; cell survival further decreased as the incubation time with the PPRH increased. We corroborated the effect of HpTorPr-C by determining mTOR mRNA levels, which decreased 1.6-fold (Fig. 5c) 48 h after transfecting the specific PPRH. The negative controls, HpTorPr-WC and Hp-Sc1, did not produce a sig-

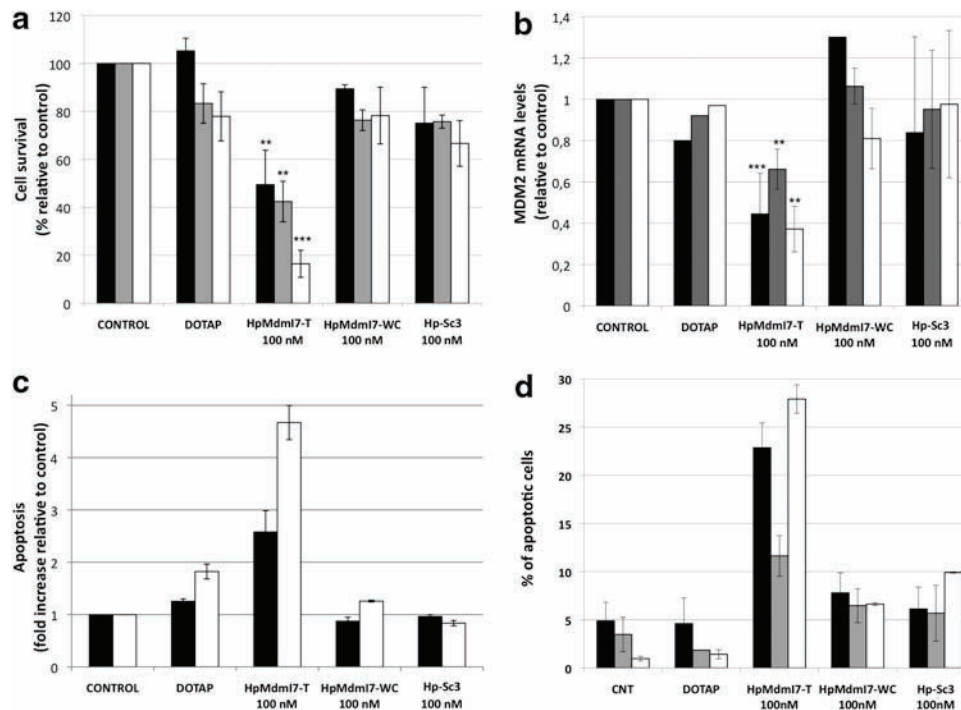
nificant decrease in cell survival or in mRNA levels. Apoptosis measured by the caspase 3/7 method increased fourfold after 24 h of treatment with HpTorPr-C (Fig. 5d) compared with the slight effect observed by the transfection agent DOTAP or the negative controls. These results confirm the efficacy of HpTorPr-C in disrupting the PI3K/AKT/mTOR pathway in HCT 116 cells.

*MDM2 regulator*

MDM2 is a negative regulator of the tumor suppressor protein p53, which is the most frequently mutated gene in human cancer [25]. Releasing p53 from MDM2 has been suggested as a mechanism for cancer therapy [26], especially in cancer types with wild-type p53 and overexpressed MDM2. In 2004, Nutlins, MDM2 inhibitors, were identified and studies with these compounds have strengthened the idea that p53 activation might represent an alternative to chemotherapy [27]. A way of mimicking the activation of p53 through inhibition of MDM2 is by silencing the expression of MDM2. We designed a template-PPRH that targets intron 7 of the *MDM2* gene. Transfection of this PPRH led to a decrease in cell survival of 50%, 60%, and 85% in SKBR3,



**FIG. 5.** Screening of PPRHs against mammalian target of rapamycin (mTOR), time course, and effect of HpTorPr-C on mTOR mRNA levels, and apoptosis. **(a)** HCT 116 cells (5,000) were plated in six-well dishes and transfected with 100 nM of four different PPRHs (HpTor-B, HpTorPr-C, HpTorI17-C, HpTorE5-C). MTT assays to determine cell survival were performed 6 days after transfection. **(b)** Time course of HpTorPr-C on cell viability was performed by renewing the medium after 8, 24, 48, or 144 h of the transfection. The negative controls HpTorPr-WC and Hp-Sc1 were transfected at 100 nM for 144 h. MTT assays of all time points were performed 6 days after the initial transfection. **(c)** Total RNA was extracted from HCT 116 cells (60,000) 48 h after the transfection with either HpTorPr-C or the negative controls HpTorPr-WC and Hp-Sc1 at a concentration of 100 nM. **(d)** HCT 116 cells (5,000) were plated in 96-well dishes and transfected with 100 nM of either HpTorPr-C or the negative controls HpTorPr-WC and Hp-Sc1. Apoptosis was measured by the activity of caspase-3 and -7 after 24 h of transfection. All results are expressed as change in RLU relative to control. Data are the mean  $\pm$  SE values of at least three experiments. \* $P < 0.05$ , \*\* $P < 0.01$ , \*\*\* $P < 0.005$ , compared with control.



**FIG. 6.** Effect of HpMdmI7-T on cell viability, MDM2 mRNA levels, and apoptosis. (a) SKBR3 (■, black bars), MCF7 (■, gray), and MDA-MB-468 (□, white) cells (30,000) were plated in six-well dishes and transfected with HpMdmI7-T and the negative controls HpMdmI7-WC and Hp-Sc3 at 100 nM. MTT assays to determine the cell survival were performed 6 days after transfection. (b) Total RNA was extracted from SKBR3, MCF7, and MDA-MB-468 cells (30,000) 48 h after the transfection with either HpMdmI7-T or the negative controls HpMdmI7-WC and Hp-Sc3 100 nM. (c) Apoptosis in SKBR3 and MDA-MB-468 cells was measured with the Caspase-Glo 3/7 Assay. All results are expressed as change in RLU relative to the control. (d) Apoptosis in SKBR3, MCF7, and MDA-MB-468 cells (120,000) determined by the rhodamine method. Rho123-negative and IP-negative cells were considered as apoptotic cells. Data are the mean  $\pm$  SE values of at least three experiments. \*\* $P < 0.01$ , \*\*\* $P < 0.005$ , compared with control.

MCF7, and MDA-MB-468 cells, respectively (Fig. 6a); the negative controls HpMdmI7-WC and Hp-Sc3 did not cause any relevant effect on cell survival. A decrease in MDM2 mRNA levels was also evident achieving a 2.3-, 1.5-, and 2.7-fold decrease depending on the cell line (Fig. 6b). Regarding apoptosis, it increased 2.6-fold in SKBR3 cells and 4.7-fold in MDA-MB-468 cells (Fig. 6c) as measured by the caspase 3/7 method, whereas the negative controls did not have any significant effect. Rhodamine determination showed that the percentage of apoptotic cells greatly increased in the three cell lines (Fig. 6d).

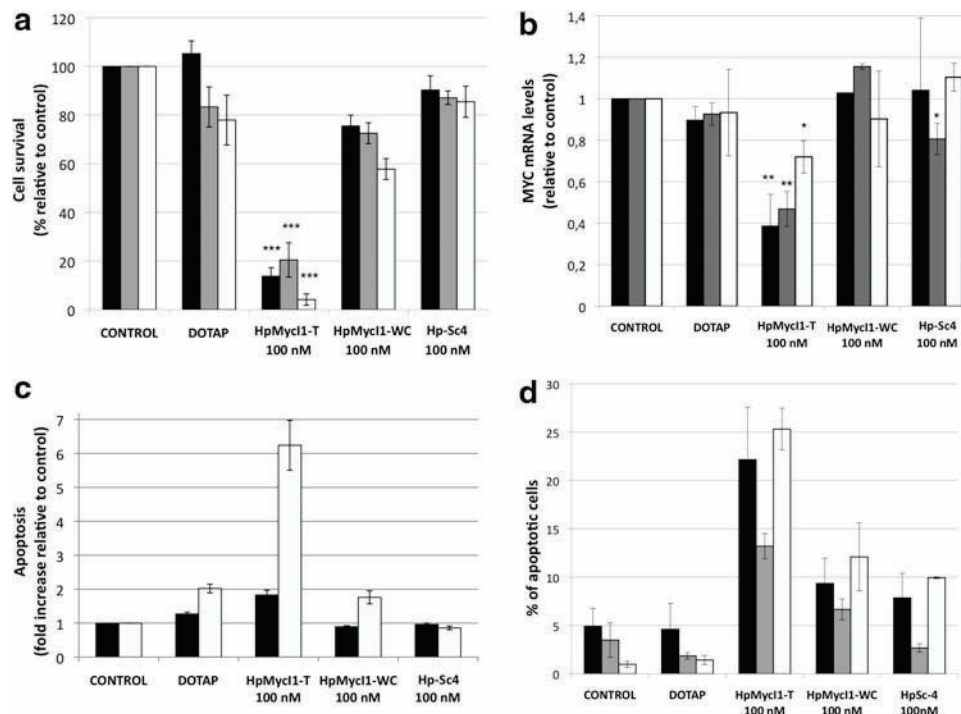
Interestingly, our results show that releasing p53 from MDM2 significantly reduces survival of the three cell lines, regardless of their p53 status; SKBR3 cells and MDA-MB-468 cells contain a mutated version of p53, while MCF7 cells contain wild-type p53. In this sense, our results are in agreement with Wang and collaborators [28] who described that silencing of MDM2, using antisense oligonucleotides, in MCF7 and MDA-MB-468 cell lines had significant antitumor activity, both *in vitro* and *in vivo*. It is possible that silencing MDM2 using the PPRH technology is an alternative way to cause cell death through p53-dependent and p53-independent mechanisms.

#### MYC transcription factor

MYC is a transcription factor involved in many biological processes, including cell growth, cell cycle progression, me-

tabolism, and survival. It has been established that MYC overexpression is essential for tumor initiation and maintenance [29] and its overactivation frequently results in the dependence of tumor survival on high levels of MYC, also called MYC addiction. The direct inhibition of MYC through small molecules has not been accomplished; as a transcription factor, MYC represents a challenging target since it functions through protein-protein interactions and lacks enzymatic activity. Therefore, MYC is considered the prototype of an undruggable target. The template-PPRH HpMycI1-T targets intron 1 of the *MYC* gene.

Our results showed that silencing of MYC using HpMycI1-T produced a decrease in cell viability in all the breast cancer cell lines used: 85% in SKBR3 cells, 80% in MCF7 cells, and 95% in MDA-MB-468 cells (Fig. 7a). The negative control HpMycI1-WC had a slight effect on cell survival that can be due to the binding of the negative control to the target, because it shares the target-binding sequence with the specific PPRH (HpMycI1-T). The decrease in cell viability was accompanied by a decrease in the levels of mRNA of 2.5-, 2.1-, and 1.4-fold in SKBR3, MCF7, and MDA-MB-468 cells, respectively (Fig. 7b). Apoptosis by the caspase 3/7 method was increased after transfection with HpMycI1-T in MDA-MB-468 cells (6.2-fold) and in SKBR3 cells (2-fold) (Fig. 7c). Rhodamine determination showed that the percentage of apoptotic cells greatly increased in the three cell lines. The negative controls did not produce an important



**FIG. 7.** Effect of HpMycI1-T on cell viability, MYC mRNA levels, and apoptosis. **(a)** SKBR3 (■, black bars), MCF7 (■, gray), and MDA-MB-468 (□, white) cells (30,000) were plated in six-well dishes and transfected with HpMycI1-T or the negative controls HpMycI1-WC and Hp-Sc4 at 100 nM. MTT assays to determine the cell survival were performed 6 days after transfection. **(b)** Total RNA was extracted from SKBR3, MCF7, and MDA-MB-468 cells (30,000) 48 h after the transfection with 100 nM of either HpMycI1-T or the negative controls HpMycI1-WC and Hp-Sc4. **(c)** Apoptosis in SKBR3 and MDA-MB-468 cells was measured with the Caspase-Glo 3/7 Assay. All results are expressed as change in RLU relative to the control. **(d)** Apoptosis in SKBR3, MCF7, and MDA-MB-468 cells (120,000) determined by the rhodamine method. Rho123-negative and IP-negative cells were considered as apoptotic cells. Data are the mean  $\pm$  SE values of at least three experiments. \* $P < 0.05$ , \*\* $P < 0.01$ , \*\*\* $P < 0.005$ , compared with control.

increase in apoptosis. It is interesting to note that the triple-negative cell line MDA-MB-468 was affected in greater measure by the inhibition of MYC, despite maintaining relatively high MYC mRNA levels, compared to the other cell lines. On the other hand, HER2<sup>+</sup> cells (SKBR3) showed a substantial decrease in cell survival, in line with the observed decrease on mRNA levels and increase in apoptosis. These results are in agreement with Kang and collaborators [30], who found that HER2<sup>+</sup> cell proliferation is dependent on MYC function. Finally, MCF7 cells also showed decreased survival and decreased MYC mRNA levels. It is possible that for each cell line, there is a specific threshold level of MYC required to maintain cell proliferation [29,31]. These results show that PPRHs could represent a valid alternative for nondruggable targets.

Taking these results into account, PPRHs could be included in the group of oligonucleotides with therapeutic potential, together with the triplex forming oligonucleotides (TFOs), aODNs, and siRNAs. All of them have in common the silencing of gene expression. It is important to note that although PPRHs share with TFOs the formation of triplex structures, there are differences in their binding properties; while the TFOs bind to the double-stranded DNA by Hoogsteen bonds, PPRHs bind intramolecularly by reverse Hoogsteen bonds and to the double-stranded DNA by Watson and Crick bonds. Previously, we studied the differences of both

PPRHs and TFOs [32] and determined two important features: (1) PPRHs have a higher binding affinity to the dsDNA target and (2) PPRHs have a higher biological activity than TFOs. Therefore, for the purpose of inhibiting gene expression, we showed that PPRHs offer advantages over TFOs. Moreover, previous results [6] indicate that PPRHs, while working at a similar range of concentrations [7], have advantages over siRNAs in terms of stability, lack of immunogenicity, and economy and no off-target effects were found for PPRHs [8,9]. Another silencing approach is based on pyrrole-imidazole polyamides, oligomers that bind to the minor groove of the DNA targeting short sequences of DNA of around 6bp [33,34]. In comparison, PPRHs cover a 19–25 nucleotide region, which would confer a greater specificity.

Regarding the potential target sites for PPRHs, triplex target sites are generally found in regulatory regions, specifically in promoters, introns, and to a lesser extent in exons. It has been described that these regions are overrepresented in promoters, although they are not necessarily the binding sites for transcription factors [35], PPRHs not only bind to transcription factors binding sites but also other regions in the promoter and within both intronic and exonic sequences. Moreover, PPRHs have the ability to bind to transcribed mRNA.

Other approaches are protein based with different degrees of complexity; these include ZFN, TALENs, and CRISPR-Cas9, and their initial goal was the editing of the genome. Their



mechanism of action is based on the introduction of double-strand breaks and its subsequent repair through homology-directed repair or nonhomologous end joining, where the latter can cause unwanted insertions or deletions [36]. Even if these methods are considered very robust platforms for genome editing, they present several drawbacks, including potential off-target DNA cleavage and unwanted cytotoxic activity [37], which are labor- and time-consuming [38,39], and they face the additional complications linked to viral gene therapy [40].

Another concern for these strategies could be the immune response triggered by the peptides from editing nucleases or by the large amounts of virus necessary for the *in vivo* delivery. In contrast, PPRHs are easy to design and to synthesize, since they are just like a regular unmodified oligonucleotide of about 50 bases and can be directly used without further manipulation, avoiding engineering issues. PPRHs can be labeled in their primary synthesis with fluorophores or biotin and can also be fused to targeting or delivering agents, such as aptamers and antibodies. Moreover, several PPRH-binding sites can be found per targeted gene allowing for combination therapy. Finally, PPRHs can bind not only to DNA but also to RNA.

We have previously studied the *in vivo* efficiency of the PPRHs [9] using a subcutaneous xenograft tumor model of prostate cancer. Using two different types of administration, intratumoral and intravenous, a PPRH against survivin promoter (HpsPr-C) was able to delay the tumor growth, without affecting mice weight. We determined the decrease in the levels of survivin and a lower degree of blood vessel formation. Altogether, PPRHs constitute an innovative and promising technology in the area of gene silencing.

## Conclusions

The results presented in this work confirm that the PPRH technology is broadly useful to silence the expression of genes with a special emphasis in genes related to cancer. Regardless of the gene or cell line tested, PPRHs were able to decrease cell survival, mRNA expression levels, and apoptosis to a greater or lesser extent. Thus, we have extended the number of PPRHs used in cancer therapy, now spanning metabolism (DHFR [7]), proliferation (mTOR), DNA-topology (TOP1), lifespan and senescence (Telomerase [7]), apoptosis (Survivin [9], BCL2), transcription factors (MYC), and proto-oncogenes (MDM2).

## Acknowledgments

This work was supported by grant SAF2011-23582 and SAF2014-51843 from Plan Nacional de Investigación Científica (Spain). Our group holds the Quality Mention from the Generalitat de Catalunya 2014SGR96. X.V. is the recipient of an APIF fellowship from the University of Barcelona. L.R. and A.S. are the recipients of a fellowship Formació d'Investigadors (FI) from the Generalitat de Catalunya.

## Author Disclosure Statement

No competing financial interests exist.

## References

- Beerli RR, DJ Segal, B Dreier and CF Barbas, 3rd. (1998). Toward controlling gene expression at will: specific regulation of the *erbB-2/HER-2* promoter by using polydactyl zinc finger proteins constructed from modular building blocks. *Proc Natl Acad Sci U S A* 95:14628–14633.
- Christian M, T Cermak, EL Doyle, C Schmidt, F Zhang, A Hummel, AJ Bogdanove and DF Voytas. (2010). Targeting DNA double-strand breaks with TAL effector nucleases. *Genetics* 186:757–761.
- Mali P, L Yang, KM Esvelt, J Aach, M Guell, JE DiCarlo, JE Norville and GM Church. (2013). RNA-guided human genome engineering via Cas9. *Science* 339:823–826.
- Wiedenheft B, SH Sternberg and JA Doudna. (2012). RNA-guided genetic silencing systems in bacteria and archaea. *Nature* 482:331–338.
- Gaj T, CA Gersbach and CF Barbas, 3rd. (2013). ZFN, TALEN, and CRISPR/Cas-based methods for genome engineering. *Trends Biotechnol* 31:397–405.
- Villalobos X, L Rodriguez, J Prevot, C Oleaga, CJ Ciudad and V Noe. (2013). Stability and immunogenicity properties of the gene-silencing polypurine reverse Hoogsteen hairpins. *Mol Pharm* 11:254–264.
- de Almagro MC SC, V Noé and CJ Ciudad. (2009). Polypurine hairpins directed against the template strand of DNA knock down the expression of mammalian genes. *J Biol Chem* 284:11.
- de Almagro MC, N Mencia, V Noe and CJ Ciudad. (2011). Coding polypurine hairpins cause target-induced cell death in breast cancer cells. *Hum Gene Ther* 22:451–463.
- Rodriguez L, X Villalobos, S Dakhel, L Padilla, R Hervas, JL Hernandez, CJ Ciudad and V Noe. (2013). Polypurine reverse Hoogsteen hairpins as a gene therapy tool against survivin in human prostate cancer PC3 cells *in vitro* and *in vivo*. *Biochem Pharmacol* 86:1541–1554.
- Alitalo K, G Ramsay, JM Bishop, SO Pfeifer, WW Colby and AD Levinson. (1983). Identification of nuclear proteins encoded by viral and cellular myc oncogenes. *Nature* 306:274–277.
- Haines DS. (1997). The *mdm2* proto-oncogene. *Leuk Lymphoma* 26:227–238.
- Hall C, SM Troutman, DK Price, WD Figg and MH Kang. (2013). Bcl-2 family of proteins as therapeutic targets in genitourinary neoplasms. *Clin Genitourin Cancer* 11:10–19.
- Meyer N and LZ Penn. (2008). Reflecting on 25 years with MYC. *Nat Rev Cancer* 8:976–990.
- Oliner JD, KW Kinzler, PS Meltzer, DL George and B Vogelstein. (1992). Amplification of a gene encoding a p53-associated protein in human sarcomas. *Nature* 358:80–83.
- Samuels Y, Z Wang, A Bardelli, N Silliman, J Ptak, S Szabo, H Yan, A Gazdar, SM Powell, *et al.* (2004). High frequency of mutations of the PIK3CA gene in human cancers. *Science* 304:554.
- Tsujimoto Y, J Cossman, E Jaffe and CM Croce. (1985). Involvement of the *bcl-2* gene in human follicular lymphoma. *Science* 228:1440–1443.
- Azmi AS, Z Wang, PA Philip, RM Mohammad and FH Sarkar. (2011). Emerging Bcl-2 inhibitors for the treatment of cancer. *Expert Opin Emerg Drugs* 30:10.
- Bold RJ, J Chandra and DJ McConkey. (1999). Gemcitabine-induced programmed cell death (apoptosis) of human pancreatic carcinoma is determined by Bcl-2 content. *Ann Surg Oncol* 6:279–285.
- Zhang X, CG Koh, B Yu, S Liu, L Piao, G Marcucci, RJ Lee and LJ Lee. (2009). Transferrin receptor targeted lipopolyplexes for delivery of antisense oligonucleotide

- g3139 in a murine k562 xenograft model. *Pharm Res* 26:1516–1524.
20. Giovanella BC, JS Stehlin, ME Wall, MC Wani, AW Nicholas, LF Liu, R Silber and M Potmesil. (1989). DNA topoisomerase I—targeted chemotherapy of human colon cancer in xenografts. *Science* 246:1046–1048.
  21. Goldwasser F, T Shimizu, J Jackman, Y Hoki, PM O'Connor, KW Kohn and Y Pommier. (1996). Correlations between S and G2 arrest and the cytotoxicity of camptothecin in human colon carcinoma cells. *Cancer Res* 56:4430–4437.
  22. Mross K, H Richly, N Schleucher, S Korfee, M Tewes, ME Scheulen, S Seeber, T Beinert, M Schweigert, *et al.* (2004). A phase I clinical and pharmacokinetic study of the camptothecin glycoconjugate, BAY 38–3441, as a daily infusion in patients with advanced solid tumors. *Ann Oncol* 15:1284–1294.
  23. Mita MM, A Mita and EK Rowinsky. (2003). Mammalian target of rapamycin: a new molecular target for breast cancer. *Clin Breast Cancer* 4:126–137.
  24. Tokunaga E, E Oki, A Egashira, N Sadanaga, M Morita, Y Kakeji and Y Maehara. (2008). Deregulation of the Akt pathway in human cancer. *Curr Cancer Drug Targets* 8:27–36.
  25. Vogelstein B, D Lane and AJ Levine. (2000). Surfing the p53 network. *Nature* 408:307–310.
  26. Lane DP, CF Cheok and S Lain. (2010). p53-based cancer therapy. *Cold Spring Harb Perspect Biol* 2:a001222.
  27. Vassilev LT, BT Vu, B Graves, D Carvajal, F Podlaski, Z Filipovic, N Kong, U Kammlott, C Lukacs, *et al.* (2004). In vivo activation of the p53 pathway by small-molecule antagonists of MDM2. *Science* 303:844–848.
  28. Wang H, L Nan, D Yu, S Agrawal and R Zhang. (2001). Antisense anti-MDM2 oligonucleotides as a novel therapeutic approach to human breast cancer: in vitro and in vivo activities and mechanisms. *Clin Cancer Res* 7:3613–3624.
  29. Li Y, SC Casey and DW Felsher. (2014). Inactivation of MYC reverses tumorigenesis. *J Intern Med* 276:52–60.
  30. Kang J, CM Sergio, RL Sutherland and EA Musgrove. (2014). Targeting cyclin-dependent kinase 1 (CDK1) but not CDK4/6 or CDK2 is selectively lethal to MYC-dependent human breast cancer cells. *BMC Cancer* 14:32.
  31. Shachaf CM, AJ Gentles, S Elchuri, D Sahoo, Y Soen, O Sharpe, OD Perez, M Chang, D Mitchel, *et al.* (2008). Genomic and proteomic analysis reveals a threshold level of MYC required for tumor maintenance. *Cancer Res* 68:5132–5142.
  32. Rodriguez L, X Villalobos, A Sole, C Lliberos, CJ Ciudad and V Noe. (2015). Improved design of PPRHs for gene silencing. *Mol Pharm* 12:867–877.
  33. Matsuda H, N Fukuda, T Ueno, Y Tahira, H Ayame, W Zhang, T Bando, H Sugiyama, S Saito, *et al.* (2006). Development of gene silencing pyrrole-imidazole polyamide targeting the TGF-beta1 promoter for treatment of progressive renal diseases. *J Am Soc Nephrol* 17:422–432.
  34. Yang F, NG Nickols, BC Li, GK Marinov, JW Said and PB Dervan. (2013). Antitumor activity of a pyrrole-imidazole polyamide. *Proc Natl Acad Sci U S A* 110:1863–1868.
  35. Goni JR, JM Vaquerizas, J Dopazo and M Orozco. (2006). Exploring the reasons for the large density of triplex-forming oligonucleotide target sequences in the human regulatory regions. *BMC Genomics* 7:63.
  36. Lin Y, TJ Cradick, MT Brown, H Deshmukh, P Ranjan, N Sarode, BM Wile, PM Vertino, FJ Stewart and G Bao. (2014). CRISPR/Cas9 systems have off-target activity with insertions or deletions between target DNA and guide RNA sequences. *Nucleic Acids Res* 42:7473–7485.
  37. Fu Y, JA Foden, C Khayter, ML Maeder, D Reyon, JK Joung and JD Sander. (2013). High-frequency off-target mutagenesis induced by CRISPR-Cas nucleases in human cells. *Nat Biotechnol* 31:822–826.
  38. Mussolino C, R Morbitzer, F Lutge, N Dannemann, T Lahaye and T Cathomen. (2011). A novel TALE nuclease scaffold enables high genome editing activity in combination with low toxicity. *Nucleic Acids Res* 39:9283–9293.
  39. Wijshake T, DJ Baker and B van de Sluis. (2014). Endonucleases: new tools to edit the mouse genome. *Biochim Biophys Acta* 1842:1942–1950.
  40. Cox DB, RJ Platt and F Zhang. (2015). Therapeutic genome editing: prospects and challenges. *Nat Med* 21:121–131.

Address correspondence to:

Carlos J. Ciudad, PhD

Department of Biochemistry and Molecular Biology

School of Pharmacy

University of Barcelona

Av. Diagonal 643

Barcelona E-08028

Spain

E-mail: cciudad@ub.edu

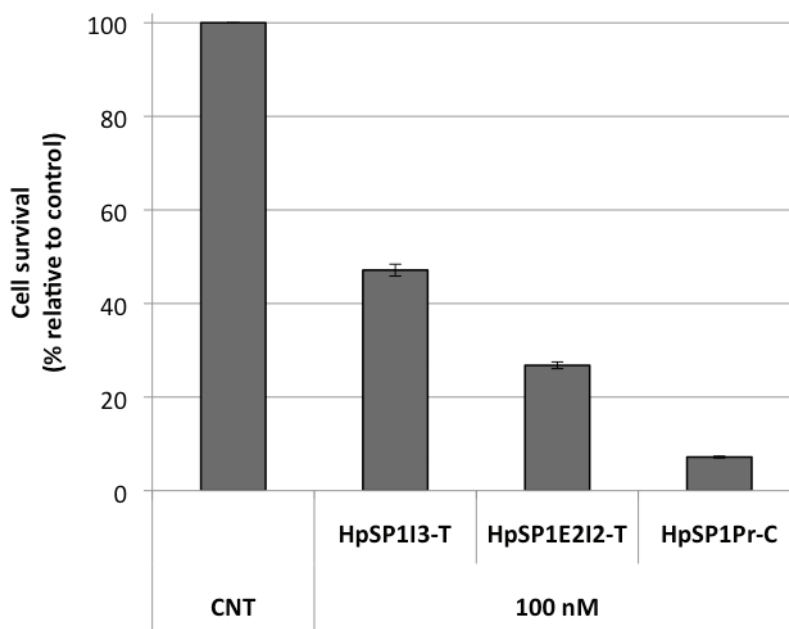
Received for publication January 2, 2015; accepted after revision May 1, 2015.



## 4.2.1 Additional results to article II

### 4.2.1.1 Effect of a PPRH designed against transcription factor Sp1

Once it was demonstrated that the PPRHs are useful against a collection of genes related to cancer, we decided to study the effect that PPRHs designed against the transcription factor Sp1 had on its transcriptional activity. Therefore we designed three PPRHs against the promoter region (HpSP1Pr-C), against exon 2 - intron 2 boundary (HpSP1E2I2-T), and against intron 3 (HpSP1I3-T). We performed cell survival experiments in SKBR3 cells to validate these PPRHs. All PPRHs were effective in decreasing cell survival, yet the best results were obtained with HpSP1Pr-C, which decreased it a 93%.

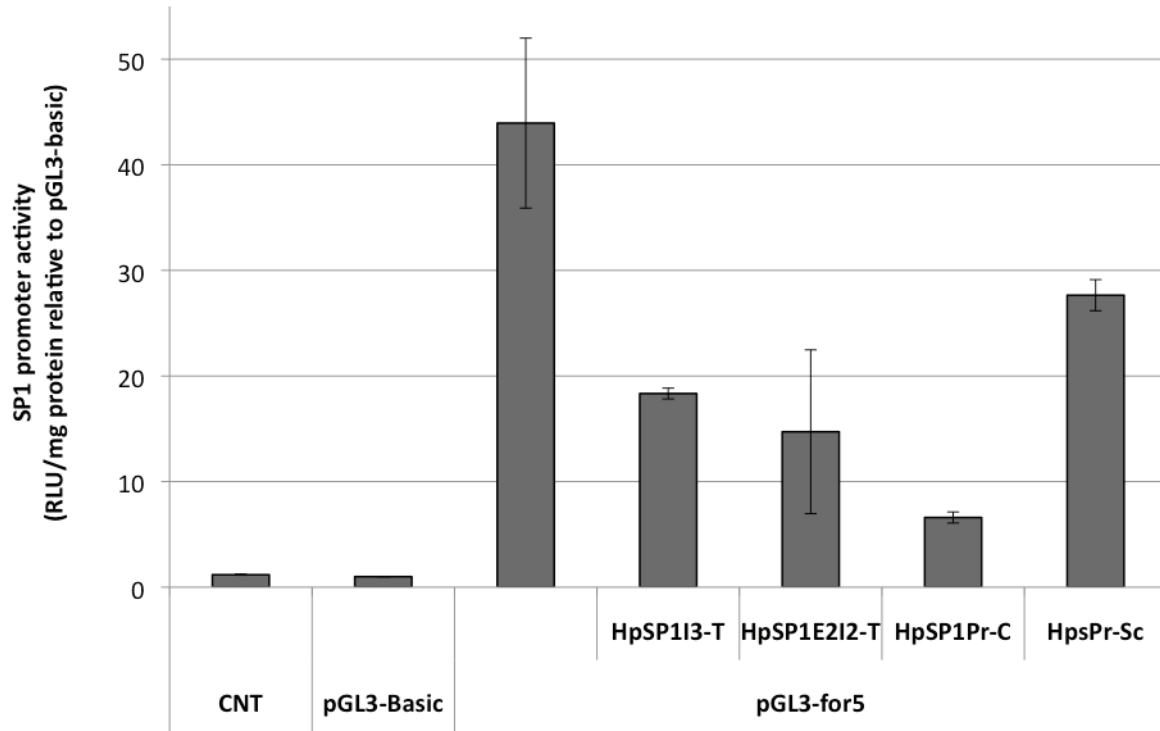


**Figure 16.** Effect of the PPRHs designed against Sp1 on cell viability, cells (30,000) were plated in six-well dishes and transfected with the different PPRHs at 100 nM. MTT assays to determine the cell survival were performed 6 days after transfection.

Sp1 is a gene that autoregulates its expression, therefore to study the effect that the Sp1-specific PPRHs had on the transcriptional activity of Sp1 we used a reporter vector (pGL3-for5) that contains the luciferase gene under the control of the *Sp1* promoter sequence.



We transfected SKBR3 cells with the specific PPRHs to decrease the endogenous Sp1 levels, after 48 h the transfection of the reporter vector was performed, and 30 h later the luciferase activity was determined.



**Figure 17.** Sp1 promoter activity in SKBR3 cells upon transfection of PPRHs directed against Sp1. SKBR3 cells (250 000) were plated in 35 mm well plates. PPRHs were transfected 24 h later, after 48 h of this the reporter gene was transfected. Luciferase activity was evaluated 30 h later.

Figure 15 shows that upon transfection of the reporter vector there was a 44-fold increase of luciferase activity relative to the pGL3-Basic vector. When 100 nM of HpSP1I3-T, HpSP1E2I2-T and HpSP1Pr-C were transfected the luciferase activity relative to the pGL3-Basic vector was considerably lower: 18-, 15- and 7-fold, respectively. The transfection of an unspecific PPRH had a slight effect on the promoter activity, which was 28-fold higher than pGL3-Basic vector. However, the HpSP1Pr-C was 4 times more effective than the negative control.

### 4.3 ARTICLE III:

#### Effect of a chimeric PPRH-aptamer in human breast cancer cells

Xenia Villalobos, Carlos J. Ciudad, and Véronique Noé

Submitted to *Nucleic Acid Therapeutics* (Impact factor: 2.929).

##### *Background:*

When administered systematically oligonucleotides present a poor cellular uptake. This remains a barrier for their use as therapeutic molecules. In 1990 a new type of nucleic acid-based molecules were described. Aptamers are DNA or RNA sequences that have been evolved *in vitro* to bind to a desired target –either protein or small molecules– after a reiterative process called SELEX. Because of their capacity to bind efficiently to specific targets, and following the idea of using antibodies as targeting agents, several aptamers have been developed for their use in cancer research taking advantage of the particularities of the cancer cells, such as the overexpression of several membrane proteins. The fusion of aODNs to antibodies has already been explored in our laboratory, as well as the use of aptamers as targeting agents for siRNAs.

##### *Objectives:*

Our aim was to potentiate the effect of a PPRH against the *DHFR* gene fusing it to an aptamer directed to the membrane protein HER2. Using this approach we assayed the specificity and effect of the chimeric oligonucleotide in breast cancer cell lines with different HER2 status: SKBR3 cells, which overexpress HER2, MCF7 cells, with a normal expression of HER2, and MDA-MB-231 cells, which are negative for this receptor.

##### *Results:*

We studied the effect of a chimera formed by the fusion of an aptamer recognizing the HER2 membrane protein (ApHER2(t)) to a PPRH designed to silence the *DHFR* gene (HpdI3-B). We determined that the fusion of both molecules (ApHER2(t)-5T-HpdI3-B) did not alter the structural prediction of the aptamer, or compromised the capacity of the PPRH to bind to its target sequence. We studied the

uptake of 100 nM of the fluorescent ApHER2(t)-F incubating the cells without any transfection reagent. We determined that, after 24 h of incubation, the percentage of FITC positive cells increased nonspecifically in the three cell lines. When DOTAP was used to transfect ApHER2(t)-F, there was a high degree of internalization since the mean fluorescence intensity increased 12-fold in SKBR3 cells, 20-fold in MCF7 cells, and 28-fold in MDA-MB-231 cells, relative to the values obtained in the absence of DOTAP. It is interesting to note that MCF7 and MDA-MB-231 cells were able to internalize more oligonucleotide than SKBR3 cells.

We determined the cytotoxic effect of 100 nM HpdI3-B, ApHER2(t) or ApHER2(t)-5T-HpdI3-B after their transfection into SKBR3, MCF7, and MDA-MB-231 cells with increasing concentrations of the cationic liposome DOTAP. In all cell lines the effect of all three molecules increased with DOTAP in a dose dependent manner. In the case of SKBR3 cells, survival upon transfection of ApHER2(t)-5T-HpdI3-B with 10 $\mu$ M DOTAP, was 35% and 20% lower than when transfected with HpdI3-B and ApHER2(t), respectively. This was not the case for MCF7 or MDA-MB-231 cells. We performed dose response experiments to calculate the IC<sub>50</sub> of HpdI3-B, ApHER2(t), ApHER2(t)-5T-HpdI3-B, and the control ApHER2(t)Sc-5T-HpdI3-B in the three cell lines. While the IC<sub>50</sub> of HpdI3-B was similar in the three cell lines, that of ApHER2(t) was slightly lower in SKBR3. The IC<sub>50</sub> of ApHER2(t)-5T-HpdI3-B in MCF7 and MDA-MB-231 cells was 2- and 4-fold higher, respectively, compared to that in SKBR3 cells. This indicates that the ApHER2(t)-5T-HpdI3-B was more effective in the cell line overexpressing HER2 than in the other cell lines studied. The control scrambled oligonucleotide ApHER2(t)Sc-5T-HpdI3-B did not cause a relevant effect in any cell line.

#### *Conclusions:*

To be internalized the oligonucleotides tested need to be transfected using the cationic liposome DOTAP. The internalization rate of the transfected oligonucleotides is lower in SKBR3 cells than in MCF7 or MDA-MB-231 cells. However, in SKBR3 cells transfection of ApHER2(t)-5T-HpdI3-B produces a higher cytotoxic effect compared to the two molecules separately. In the case of MCF7 and MDA-MB-231 cells, a higher transfection rate does not translate into a higher cytotoxic effect of ApHER2(t)-5T-HpdI3-B.

# Effect of a chimeric PPRH-aptamer in human breast cancer cells

Xenia Villalobos, Carlos J. Ciudad<sup>§</sup> and Véronique Noé

Department of Biochemistry and Molecular Biology, School of Pharmacy, University of Barcelona, Av. Diagonal 643, E-08028 Barcelona, Spain.

<sup>§</sup>Corresponding author

Running title: PPRH-aptamer in human breast cancer cells

Email addresses:

XV: [xvillalobos@ub.edu](mailto:xvillalobos@ub.edu)

VN: [vnoe@ub.edu](mailto:vnoe@ub.edu)

CJC: [cciudad@ub.edu](mailto:cciudad@ub.edu)

## **Abstract**

Research on nucleic acids as therapeutic agents has increased considerably since the description of several types of nucleic acid-based molecules such as Triplex Forming Oligonucleotides, antisense oligonucleotides, siRNAs, aptamers and more recently PPRHs. PPRHs are polypurine hairpins that produce specific gene silencing by binding to polypyrimidine targets in the DNA. In this work we studied the effect of a chimera formed by the fusion of an aptamer recognizing the HER2 membrane protein to a PPRH designed to silence the *DHFR* gene. We determined that the fusion of both molecules did not alter the structural prediction of the aptamer, nor compromised the capacity of the PPRH to bind to its target sequence. We tested the internalization and target-dependent cytotoxicity of the aptamer and the chimeric molecule in three breast cancer cell lines with different HER2 expression status: SKBR3 cells, overexpressing HER2, MCF7 cells, with a normal expression of this protein and MDA-MB-231 cells which do not express HER2. Survival of SKBR3 cells upon transfection of the chimeric molecule was much lower than that of MCF7 cells or MDA-MB-231, despite the lower internalization rate of the former. These determinations indicated that the fusion of both molecules was specific and more effective than the two molecules separately.

## Introduction

In the last years nucleic acids have emerged as promising therapeutic agents. Since the description of Triplex Forming Oligonucleotides (TFO) [1] and antisense oligonucleotides (aODN) [2] several advances have been made, which resulted in the approval of the first DNA-based drug (fomivirsen) in 1998. More recently, in 2013, the cholesterol-reducing antisense oligonucleotide mipomersen was approved and other antisense therapies are in preclinical or early clinical phases [3]. Still, systemic administration of nucleic acid drugs for gene silencing purposes faces several difficulties, especially in finding the balance to maintain their effect while decreasing nuclease degradation and immunotoxicity.

Recently, we developed a novel DNA-based silencing molecule, called Polypurine Reverse Hoogsteen hairpins (PPRHs), capable of specifically inhibiting the expression of target genes [4,5]. These molecules have the advantages of increased stability and low immunogenicity compared to siRNAs [6]. PPRHs are non-modified DNA molecules formed by two antiparallel polypurine strands linked by a pentathymidine loop that allows the formation of intramolecular reverse-Hoogsteen bonds between both strands, acquiring a hairpin structure. The hairpins bind by Watson-Crick bonds to a specific polypyrimidine sequence within the target gene forming a triplex structure that knocks down its expression. The target sequence can be located either in the template or the coding strand of the dsDNA. Template-PPRHs [7] bind to the template strand of the DNA whereas coding-PPRHs bind to the coding sequence of the DNA, and can also bind to transcribed RNA.

The mechanism of action of PPRHs depends on the location of their target within the gene: we demonstrated that a coding-PPRH directed against a

polypyrimidine region in intron 3 of DHFR pre-mRNA produced a splicing alteration [8]. Also, two PPRHs directed against the template or coding strand of the *survivin* promoter sequence decreased the binding of transcription factors Sp1 and GATA-3, respectively. The *in vivo* administration of the coding-PPRH against the promoter region of *survivin* was able to delay tumor growth in a prostate xenograft mouse model [9].

Aptamers are another class of nucleic acid-based molecules with therapeutic potential. Indeed, in 2004 the aptamer pegaptanib (Macugen), a selective vascular endothelial growth factor (VEGF) antagonist [10], was accepted for the treatment of age-related macular degeneration. Aptamers are DNA or RNA sequences that have been evolved *in vitro* to bind to a desired target –protein or small molecule– after a reiterative process called SELEX [11, 12]. Because of their capacity to bind efficiently to specific targets, and following the idea of using antibodies as targeting agents, several aptamers have been developed for their use in cancer research [13-16] taking advantage of the particularities of cancer cells, such as the overexpression of several membrane proteins.

Herein our objective was to potentiate the effect of a PPRH against the *DHFR* gene fusing it to an aptamer against the membrane protein HER2 [17]. Using this approach we assayed the specificity and effect of the chimeric oligonucleotide on the cytotoxicity caused in breast cancer cell lines with different HER2 status: SKBR3 cells, which overexpress HER2, MCF7 cells, with a normal expression of HER2 and MDA-MB-231 which do not express HER2.

## Materials and methods

### Oligonucleotides

Oligonucleotides were synthesized as non-modified oligodeoxynucleotides by Sigma-Aldrich (Madrid, Spain). They were dissolved in sterile RNase-free Tris-EDTA buffer (1 mM EDTA and 10 mM Tris, pH 8.0) and stored at -20°C until use. The Triplex-Forming Oligonucleotide Target Sequence Search tool (<http://spi.mdanderson.org/tfo/>) was used as starting point for the design of PPRHs. This software finds the polypurine tracks present in a gene and thus the polypyrimidine targets. The specificity of the chosen polypurine tracks is checked by BLAST analyses [18]. The template-PPRH against *DHFR* intron 3 was previously described [7]. The sequence of the DNA aptamer against HER2 was obtained from Mahlknecht et al, 2013 [17]. To design the chimeric oligonucleotide ApHER2(t)-5T-HpdI3-B we added a five thymidine linker between the sequences of ApHER2(t) and HpdI3-B. As a negative control for ApHER2(t)-5T-HpdI3-B we designed an oligonucleotide with a scrambled ApHER2(t) sequence. This molecule, named ApHER2(t)Sc-5T-HpdI3-B had the same length and DNA base content than ApHER2(t)-5T-HpdI3-B. Table 1 describes all oligonucleotides names and sequences used in this work.

### *In silico* studies

The secondary structures of the original aptamer ApHER2(t) and the chimeric oligonucleotide ApHER2(t)-5T-HpdI3-B were predicted using the mfold server (The RNA Institute. College of Arts and Sciences University of Albany; <http://mfold.rna.albany.edu/?q=mfold/DNA-Folding-Form>) [19] which predicts



minimum free energy structures and base pair probabilities from single RNA or DNA sequences. The DNA Folding Form was chosen and the parameters of the ionic conditions were changed to 140 mM Na<sup>+</sup> and 10 mM Mg<sup>2+</sup> for the structural prediction.

### **Binding experiments**

Preparation of Polypurine/Polypyrimidine Duplexes. The polypurine/polypyrimidine duplexes to be targeted by the PPRHs were formed by mixing 25 µg of each single-stranded oligodeoxynucleotide (Target seq fwd strand and Target seq rev strand) in 150mM NaCl. After incubation at 90 °C for 5 min, samples were allowed to cool down slowly to room temperature. Duplexes were purified in non-denaturing 20% polyacrylamide gels and quantified by their absorbance at 260 nm.

Oligodeoxynucleotide Labeling. One hundred ng of double-stranded oligodeoxynucleotide was 5'-end labeled with [ $\gamma$ -<sup>32</sup>P]ATP by T4 polynucleotide kinase (New England Bio-Labs) in a 10-µl reaction mixture, according to the manufacturer's protocol. After incubation at 37 °C for 1 h, 90 µl of TE buffer (1 mM EDTA, 10 mM Tris, pH 8.0) were added to the reaction mixture, which was filtered through a Sephadex G-25 spin column to eliminate the unincorporated [ $\gamma$ -<sup>32</sup>P]ATP.

Electrophoretic Mobility Shift Assay. Triplex formation was analyzed by incubating radiolabeled double-stranded DNA targets in the presence or absence of unlabeled HpdI3-B and ApHER2(t)-5T-HpdI3-B (10, 30, 100 and 300 nM) in a buffer containing 10 mM MgCl<sub>2</sub>, 100 mM NaCl and 50 mM HEPES, pH 7.2. Binding reactions (20 µl) were incubated 30 min at 37 °C before the electrophoresis, which was performed on non-denaturing 12% polyacrylamide gels containing 10 mM MgCl<sub>2</sub>, 5% glycerol, and

50 mM HEPES, pH 7.2. Gels were run for 3-4 h at 180 V at 4 °C, dried, and analyzed on a Storm 840 PhosphorImager (Molecular Dynamics).

### **Cell culture**

Human breast cancer SKBR3, MCF7 and MDA-MB-231 cell lines were used throughout the study. Cell lines were routinely grown in Ham's F12 medium supplemented with 7% Fetal Calf Serum (FCS, both from Gibco), at 37°C in a 5% CO<sub>2</sub> controlled humidified atmosphere. Cell survival experiments were performed in Ham's F12 medium lacking the final products of the DHFR activity: glycine, hypoxanthine and thymidine (-GHT medium), containing 7% of dialyzed FCS.

### **Western blot**

SKBR3, MCF7 and MDA-MB-231 cells were harvested from 100 mm culture dishes and centrifuged for 5 min at 800 x g at 4°C. Cell pellets were washed once in PBS 1X and resuspended in 40 µL of RIPA buffer (150mM NaCl, 5mM EDTA, 50mM Tris-HCl pH 7.4 (all from Applichem, Barcelona, Spain); 1% Igepal CA-630, 0.5mM PMSF, Protease inhibitor cocktail, 1 mM NaF (all from Sigma-Aldrich). Cell lysates were kept on ice for 30 min with vortexing every 10 min. Cell debris was removed by centrifugation at 15,000 × g at 4°C for 10 min. Five µl of the extracts was used to determine the protein concentration using the Bradford assay (Bio-Rad). Whole cell extracts (100 µg) were resolved in 7% SDS-polyacrylamide gels and transferred to PVDF membranes (Immobilon P, Millipore) using a semidry electroblotter. Membranes were blocked for one hour with Blotto 5% and probed overnight at 4°C with a primary antibody against HER2 (1:100 Calbiochem). Signals were detected by secondary horseradish peroxidase-conjugated anti-mouse (1:2000 dilution, sc-2005 Santa Cruz

Biotechnology Inc.) antibody, and enhanced chemiluminescence using the ECL method, as recommended by the manufacturer (GE Healthcare). Chemiluminescence was detected with ImageQuant LAS 4000 Mini technology (GE Healthcare).

### **Transfection of PPRHs**

Cells were plated the day before transfection which consisted in mixing the appropriate amount of oligonucleotide and N-[1-(2,3-dioleoyloxy)propyl]-N,N,N-trimethylammonium methylsulfate (DOTAP) (Biontex, München, Germany) for 20 minutes in a volume of 200 µl of medium at room temperature, followed by the addition of the mixture to the cells in a total volume of 1 mL.

### **Cellular uptake of oligonucleotides**

FITC-labelled ApHER2(t)-F and ApHER2(t)-5T-HpdI3-BF were transfected into SKBR3, MCF7 and MDA-MB-231 cells to determine their uptake. Cells (150,000) were plated in 55 mm dishes in a final volume of 1.8 mL of F12 medium and transfected with 100 nM of the oligonucleotides either with or without 10 µM DOTAP. After 24 h of the transfection, cells were collected and washed twice in PBS. The pellet was resuspended in 500µL PBS and stained with propidium iodide (5µg/mL) (Sigma-Aldrich, Madrid, Spain) to analyze them on a Beckman Coulter Epics XL cytometer.

### **Confocal microscopy**

Cells (300,000) were plated on cover-slips placed inside 35 mm dishes 24 h before the transfection with ApHER2(t)-F. After 24 h of the transfection cells were washed once with fresh F12 medium and incubated with Wheat Germ Agglutinin (WGA), Alexa Fluor® 555 Conjugate (Life Technologies, Madrid, Spain) at 4°C for 30 min. Cells

were washed twice with PBS for 5 min at RT and fixed with paraformaldehyde 4% for 10 min, two more washes with PBS were performed. Cover-slips were mounted on slides using mowiol (Calbiochem, Madrid, Spain) and were kept protected from light at RT overnight. Confocal laser scanning microscopy was performed using a Leica TCS-SP2.

### **Cell survival experiments (MTT)**

Cells were plated in 6-well dishes in Ham's F12 -GHT medium. Six days after transfection of the oligonucleotides, 0.63 mM of 3-(4,5-dimethylthiazol-2-yl)-2,5-diphenyltetrazolium bromide and 100  $\mu$ M of sodium succinate (both from Sigma-Aldrich) were added to the culture medium and allowed to react for 3 hours at 37°C before the addition of the solubilization reagent (0.57% acetic acid and 10% SDS in DMSO). Cell viability was measured at 570 nm in a WPA S2100 Diode Array Spectrophotometer. The results were expressed as the percentage of cell survival relative to the control (untreated cells).

## Results

### *In silico* studies

The mfold studies showed that the secondary structures generated for the aptamer ApHER2(t) (Fig. 1A) and the chimeric oligonucleotide ApHER2(t)-5T-HpdI3-B (Fig. 1B) have a negative  $\Delta G$  of -5.43, which indicates high stability. In both cases we observed the formation of a stem-loop near the 5' end of the molecules. Most importantly, the addition of the PPRH sequence to the 3' end of the aptamer did not alter the secondary structure of the latter. The PPRH apparently did not form any stable intramolecular secondary structure.

### **Binding of PPRHs and aptamer-PPRH to the target sequence**

To determine if the addition of the sequence corresponding to the aptamer compromised the binding affinity of the PPRH to its target duplex, we studied the binding capacity of HpdI3-B and that of the chimeric oligonucleotide ApHER2(t)-5T-HpdI3-B by EMSA. As shown in Fig. 2, the incubation of the radiolabelled target duplex with different concentrations of HpdI3-B or ApHER2(t)-5T-HpdI3-B gave rise to the appearance of different shifted bands, indicated by arrows. The band with the lowest mobility corresponded to the binding of the chimeric aptamer-PPRH. The intensity of the shifted band increased in a dose dependent manner for both molecules. This indicated that the PPRH was still able to bind to its target even in the presence of the aptamer. We calculated the  $K_d$  for both HpdI3-B and ApHER2(t)-5T-HpdI3-B obtaining values of 385 and 714 nM, respectively.

**HER2 expression and internalization of oligonucleotides in the absence or in the presence of DOTAP.**

As a control for the expression level of HER2 in the different cells lines, we performed WB analyses that showed that SKBR3 cells expressed high amounts of this protein whereas MCF cells had a basal expression and MDA-MB-231 cells were negative for this receptor (figure 3A)

The cellular uptake of HpdI3-BF and ApHER2(t)-F in SKBR3, MCF7 and MDA-MB-231 cells was determined using flow cytometry. Figures 3B show the overlay of the histograms obtained for the three cell lines. We measured the percentage of fluorescent cells and their mean fluorescence intensity 24 h after incubation with ApHER2(t)-F and HpdI3-BF, and also upon transfection of ApHER2(t)-F using DOTAP (Table 2). As shown in figure 3B, when cells were treated with 100 nM ApHER2(t)-F the percentage of FITC positive cells increased in the three cell lines. However, after treating the cells with fluorescent HpdI3-BF the percentage of FITC-positive cells also increased in all lines, indicating that the presence of a fluorescent molecule produced a slight increase in cell fluorescence. On the other hand, when DOTAP was used to transfect ApHER2(t)-F, there was a high degree of internalization since the mean intensity increased 12-fold in SKBR3 cells, 20-fold in MCF7 cells, and 28-fold in MDA-MB-231 cells, relative to the values obtained in the absence of DOTAP. It is interesting to note that MCF7 and MDA-MB-231 cells were able to internalize more oligonucleotide than SKBR3 cells.

Confocal microscopy in the two cell lines expressing HER2 also showed that the aptamer molecule was only internalized in the presence of DOTAP (figure 4A and B).

**Cell survival**

We determined the cytotoxic effect of 100 nM HpdI3-B, ApHER2(t) or ApHER2(t)-5T-HpdI3-B after their transfection into SKBR3, MCF7, and MDA-MB-231 cells with increasing concentrations of the cationic liposome DOTAP. In all cell lines the effect of all three molecules increased with DOTAP in a dose dependent manner. In the case of SKBR3 cells, survival upon transfection of ApHER2(t)-5T-HpdI3-B with 10 $\mu$ M DOTAP, was 35% and 20% lower than when transfected with HpdI3-B and ApHER2(t), respectively (Fig. 5A). This was not the case for MCF7 (Fig. 5B), in which cell viability after transfection with ApHER2(t)-5T-HpdI3-B was not decreased with respect to the transfection of either HpdI3-B or ApHER2(t). In the case of MDA-MB-231 cells ApHER2(t) and ApHER2(t)-5T-HpdI3-B did not have a notable effect on cell survival (Fig. 5C).

We compared the effect of the chimeric ApHER2(t)-5T-HpdI3-B with that of a control oligonucleotide, ApHER2(t)Sc-5T-HpdI3-B, which contained a scrambled sequence of the aptamer. Figure 6 shows that the survival of SKBR3 (6A) cells decreased abruptly as the concentration of ApHER2(t)-5T-HpdI3-B increased. This tendency was kept in MCF7 (6B) cells, but not in the MDA-MB-231 cell line (6C). These results are at variance with those obtained after transfecting the scrambled ApHER2(t)Sc-5T-HpdI3-B, since no specific effect was observed. In the three cell lines, transfecting 100 nM of this control molecule only caused a 20% decrease in cell survival.

We performed dose response experiments to calculate the IC<sub>50</sub> of HpdI3-B, ApHER2(t), ApHER2(t)-5T-HpdI3-B, and the control ApHER2(t)Sc-5T-HpdI3-B in the three cell lines (Fig. 7). While the IC<sub>50</sub> of HpdI3-B was similar in the three cell lines, that of ApHER2(t) was slightly lower in SKBR3. Interestingly enough, the IC<sub>50</sub> of ApHER2(t)-5T-HpdI3-B in MCF7 and MDA-MB-231 cells was 2- and 4-fold higher,

respectively, compared to that in SKBR3 cells. (Table inset in Fig. 7). This indicates that the ApHER2(t)-5T-HpdI3-B was more effective in the cell line overexpressing HER2 than in the other cell lines studied. The control scrambled oligonucleotide ApHER2(t)Sc-5T-HpdI3-B did not cause a relevant effect in any cell line.



## Discussion

The use of a DNA-based therapy can offer a wide span of combinatorial choices for the treatment of cancer. Not only could it be possible to silence a specific gene, but also to target specific cells, for instance with aptamers capable of recognizing membrane proteins. In this work we analyzed the effects of fusing a gene silencing PPRH, specifically designed against intron 3 of the *DHFR* gene, together with an aptamer recognizing the HER2 receptor [17], thus creating a bifunctional oligonucleotide that could be effective in a specific cell line, such as SKBR3. Through *in silico* studies we were able to determine that the aptamer maintained its secondary structure when fused to the HpdI3-B through a 5-thymidine linker. Apparently, the sequence corresponding to the PPRH did not acquire a hairpin structure, but one should take into account that the mfold server only considers the canonical Watson and Crick bonds, and the Wobble G-U bonds in the case of RNA. That means that the hairpin structure cannot be predicted, since Reverse-Hoogsteen bonds energy parameters are not included. However, the PPRH, in the context of the chimeric ApHER2(t)-5T-HpdI3-B molecule maintained its capability to bind to the dsDNA target sequence, as demonstrated by binding assays. The  $K_d$  of ApHER2(t)-5T-HpdI3-B was twice that of HpdI3-B demonstrating that even if the affinity of the PPRH for its target was decreased by the presence of the fused aptamer, it still can bind to the DNA target.

Regarding the internalization of the aptamer ApHER2(t), the fluorescence intensity upon incubation with the aptamer increased in a similar extent in all the cell lines. This effect was rather unspecific since incubation with the PPRH-F gave the same degree of fluorescence. However, when DOTAP was used to transfect the oligonucleotide, the internalized fluorescence increased considerably in the three cell

lines. It is interesting to point out that upon transfection with DOTAP, MDA-MB-231 and MCF7 cells internalized more fluorescent molecules than SKBR3 cells, thus indicating that MCF7 and MDA-MB-231 cells have a higher internalization rate. Confocal experiments confirmed that there was not internalization of the aptamer unless DOTAP was used.

Regarding the cytotoxicity produced by the oligonucleotides in all cell lines, the effect increased in a DOTAP concentration dependent manner, confirming the need of a transfection reagent to optimize the internalization of all molecules tested. Interestingly, when we performed the dose-response experiments with HpdI3-B, ApHER2(t) and ApHER2(t)-5T-HpdI3-B, the cytotoxicity in SKBR3 cells transfected with the chimeric aptamer-PPRH was higher than that of MCF7 and MDA-MB-231 cells, despite the higher internalization of the latter meaning that there was a specific effect of the PPRH fused to the aptamer directed against the HER2 epitope. It is noteworthy that in SKBR3 cells the IC<sub>50</sub> of the chimeric ApHER2(t)-5T-HpdI3-B was remarkably low compared to those of the PPRH or aptamer alone, whereas in MCF7 and MDA-MB-231 this effect was not observed.

It has been described that, upon binding, some antibodies are able to induce ubiquitination of HER2 and its subsequent degradation [20]. Aptamers can produce the same effect [21; 22]. In fact, the original article describing ApHER2(t) concludes that its biological activity relates to the ability to crosslink and sort HER2 to lysosomal degradation. Cytoplasmic overexpression of HER2 in breast cancer also occurs and there are molecules, such as lapatinib, which are used to target the intracellular domain of HER2. Therefore, upon transfection, ApHER2(t) and ApHER2(t)-5T-HpdI3-B might bind to cytoplasmic HER2, sort it to the mentioned degradation pathway and produce cell death. Our results show that the overexpression of HER2 in SKBR3 cells

does not promote the internalization of ApHER2(t) or ApHER2(t)-5T-HpdI3-B. Nevertheless, when DOTAP is used and the aptamer or chimera are internalized, a cytotoxic specific effect is observed in the HER2 overexpressing cell line, and the effect of the chimera is greater than those effected by the PPRH or the aptamer by themselves.

Aptamers offer promising opportunities to improve the current oligonucleotide-based therapies. The SELEX process allows selecting aptamers with high affinities for their targets. The affinities are often comparable to those observed for antibodies, with Kd values in the low nanomolar to picomolar range. Additionally, aptamers present several advantages over antibodies: their obtention is not dependent on animals, they have lower batch-to-batch variation, and more stability to temperature variations than antibodies, specially if they are DNA aptamers. [23,24].

## **Conclusion**

The results presented in this work confirm that the usage of an aptamer against HER2 fused to a PPRH molecule improve the cytotoxic effect compared to the two molecules separately in SKBR3 cells, while this behavior is not observed in MCF7 or MDA-MB-231 cells. This effect depends on the internalization facilitated by the cationic liposome DOTAP. Therefore, although a selective delivery of the PPRH was not achieved, a specific activity of the chimeric molecule ApHER2(t)-5T-HpdI3-B was observed in HER2-overexpressing cells. Methods enabling the internalization of the aptamer-PPRHs molecules upon binding to their membrane receptor should be further investigated to allow for specific targeting and delivery without the need of a transfecting reagent.

## Acknowledgements

Work supported by grants SAF2011-23582 and SAF2014-51825-R. Our group holds the Quality Mention from the Government of Catalonia, Spain (2014SGR96). XV is the recipient of an APIF fellowship of the University of Barcelona.

## References

1. Felsenfeld G, A Rich. (1957). Studies on the formation of two- and three-stranded polyribonucleotides. *Biochim Biophys Acta* 26: 457-68.
2. Zamecnik PC, ML Stephenson. (1978). Inhibition of Rous sarcoma virus replication and cell transformation by a specific oligodeoxynucleotide. *Proc Natl Acad Sci U S A* 75: 280-4.
3. Bennett CF, EE Swayze. (2010). RNA targeting therapeutics: molecular mechanisms of antisense oligonucleotides as a therapeutic platform. *Annu Rev Pharmacol Toxicol* 50: 259-93.
4. Villalobos X, L Rodriguez, A Sole, C Lliberos, N Mencia, CJ Ciudad, V Noe. (2015). Effect of Polypurine Reverse Hoogsteen Hairpins on Relevant Cancer Target Genes in Different Human Cell Lines. *Nucleic Acid Ther.*
5. Rodriguez L, X Villalobos, A Sole, C Lliberos, CJ Ciudad, V Noe. (2015). Improved design of PPRHs for gene silencing. *Mol Pharm* 12: 867-77.
6. Villalobos X, L Rodriguez, J Prevot, C Oleaga, CJ Ciudad, V Noe. Stability and immunogenicity properties of the gene-silencing polypurine reverse Hoogsteen hairpins. *Mol Pharm* 11: 254-64.
7. de Almagro MC, S Coma, V Noe, CJ Ciudad. (2009). Polypurine hairpins directed against the template strand of DNA knock down the expression of mammalian genes. *J Biol Chem* 284: 11579-89.
8. de Almagro MC, N Mencia, V Noe, CJ Ciudad. Coding polypurine hairpins cause target-induced cell death in breast cancer cells. *Hum Gene Ther* 22: 451-63.
9. Rodriguez L, X Villalobos, S Dakhel, L Padilla, R Hervas, JL Hernandez, CJ Ciudad, V Noe. Polypurine reverse Hoogsteen hairpins as a gene therapy tool against survivin in human prostate cancer PC3 cells in vitro and in vivo. *Biochem Pharmacol* 86: 1541-54.
10. Ruckman J, LS Green, J Beeson, S Waugh, WL Gillette, DD Henninger, L Claesson-Welsh, N Janjic. (1998). 2'-Fluoropyrimidine RNA-based aptamers to the 165-amino acid form of vascular endothelial growth factor (VEGF165). Inhibition of receptor binding and VEGF-induced vascular permeability through interactions requiring the exon 7-encoded domain. *J Biol Chem* 273: 20556-67.
11. Tuerk C, L Gold. (1990). Systematic evolution of ligands by exponential enrichment: RNA ligands to bacteriophage T4 DNA polymerase. *Science* 249: 505-10.
12. Ellington AD, JW Szostak. (1990). In vitro selection of RNA molecules that bind specific ligands. *Nature* 346: 818-22.
13. Ferreira CS, MC Cheung, S Missailidis, S Bisland, J Gariepy. (2009). Phototoxic aptamers selectively enter and kill epithelial cancer cells. *Nucleic Acids Res* 37: 866-76.
14. Ray P, MA Cheek, ML Sharaf, N Li, AD Ellington, BA Sullenger, BR Shaw, RR White. (2012). Aptamer-mediated delivery of chemotherapy to pancreatic cancer cells. *Nucleic Acid Ther* 22: 295-305.
15. Thiel KW, LI Hernandez, JP Dassie, WH Thiel, X Liu, KR Stockdale, AM Rothman, FJ Hernandez, JO McNamara, 2nd, PH Giangrande. (2012). Delivery of chemo-sensitizing siRNAs to HER2+-breast cancer cells using RNA aptamers. *Nucleic Acids Res* 40: 6319-37.

16. Zhou J, JJ Rossi. (2011). Cell-specific aptamer-mediated targeted drug delivery. *Oligonucleotides* 21: 1-10.
17. Mahlknecht G, R Maron, M Mancini, B Schechter, M Sela, Y Yarden. (2013). Aptamer to ErbB-2/HER2 enhances degradation of the target and inhibits tumorigenic growth. *Proc Natl Acad Sci U S A* 110: 8170-5.
18. Altschul SF, W Gish, W Miller, EW Myers, DJ Lipman. (1990). Basic local alignment search tool. *J Mol Biol* 215: 403-10.
19. Zuker M. (2003). Mfold web server for nucleic acid folding and hybridization prediction. *Nucleic Acids Res* 31: 3406-15.
20. Ren XR, J Wei, G Lei, J Wang, J Lu, W Xia, N Spector, LS Barak, TM Clay, T Osada and others. (2012). Polyclonal HER2-specific antibodies induced by vaccination mediate receptor internalization and degradation in tumor cells. *Breast Cancer Res* 14: R89.
21. McNamara JO, 2nd, ER Andrechek, Y Wang, KD Viles, RE Rempel, E Gilboa, BA Sullenger, PH Giangrande. (2006). Cell type-specific delivery of siRNAs with aptamer-siRNA chimeras. *Nat Biotechnol* 24: 1005-15.
22. Thiel WH, KW Thiel, KS Flenker, T Bair, AJ Dupuy, JO McNamara, 2nd, FJ Miller, PH Giangrande. (2015). Cell-internalization SELEX: method for identifying cell-internalizing RNA aptamers for delivering siRNAs to target cells. *Methods Mol Biol* 1218: 187-99.
23. Stoltenburg R, C Reinemann, B Strehlitz. (2007). SELEX--a (r)evolutionary method to generate high-affinity nucleic acid ligands. *Biomol Eng* 24: 381-403.
24. Kruspe S, F Mittelberger, K Szameit, U Hahn. (2014). Aptamers as drug delivery vehicles. *ChemMedChem* 9: 1998-2011.

**Table 1 - Oligonucleotides used in this study**

Name	Sequence (5' → 3')
Target seq fwd strand	CATTCTCTTGATT <u>GCCTCCTCCCTCTCCCTCCTC</u>
Target seq rev strand	GAGGAGGGAGAGGGAGGAGGCAATCAAGAGAATG
HpdI3-B	GGAGGAGGGAGAGGGAGGAGTTTTTGAGGAGGGA GAGGGAGGAGG
ApHER2(t)	GCAGCGGTGTGGGGGCAGCGGTGTGGGGGCAGCG GTGTGGGG
ApHER2(t)-5T-HpdI3-B	GCAGCGGTGTGGGGGCAGCGGTGTGGGGGCAGCG GTGTGGGG <b>TTTTT</b> GAGGAGGGAGAGGGAGGAGT TTTTGAGGAGGGAGAGGGAGGAGG
ApHER2(t)Sc-5T-HpdI3-B	GACGGCGGTTGGGGGCCGAGGTGTGGGGGCAGCG GTGTGGGG <b>TTTTT</b> GAGGAGGGAGAGGGAGGAGT TTTTGAGGAGGGAGAGGGAGGAGG

Name and sequence of the oligonucleotides used in this study. The underlined sequence represents the polypyrimidine target of HpdI3-B. Letters in bold indicate the thymidine linker between the aptamers and HpdI3-B.

**Table 2 - Uptake experiments in SKBR3, MCF7 and MDA-MB-231 cells**

		CNT	HpdI3-BF	ApHER2(t)-F	ApHER2(t)-F + DTP
SKBR3	% FITC +	9,0	44,6	56,7	99,2
	Mean	5,10	10,2	11,2	136,6
MCF7	% FITC +	5,4	82,4	78,7	99,0
	Mean	5,5	38,4	29,6	575,0
MDA-MB-231	% FITC +	6,3	80,0	87,9	99,4
	Mean	11,0	81,1	120,9	3365,6

The percentage of FITC positive (+) cells and the mean fluorescence intensity were calculated for the three cell lines SKBR3, MCF7 and MDA-MB-231 upon incubation with 100 nM HpdI3-BF and ApHER2(t)-F or transfection with 100 nM ApHER2(t)-F using 10 µM DOTAP.

## Figure legends

**Figure 1.** Structure predictions of Hpdl3-B (A) and ApHER2(t)-5T-Hpdl3-B (B) using the mfold software.

**Figure 2.** Binding between Hpdl3-B and ApHER2(t)-5T-Hpdl3-B to the target duplex. Lane 1 corresponds to the radiolabelled (\*) target alone, lanes 2 - 5 correspond to the incubation of the target with the indicated increasing concentrations of Hpdl3-B, and lanes 6 - 9 correspond to the incubation of the target with increasing concentrations of ApHER2(t)-5T-Hpdl3-B. Arrows indicate the shifted band corresponding to the binding between the Hpdl3-B and the chimera with the target DNA.

**Figure 3.** A) HER2 protein expression. Whole protein extracts from SKBR3, MCF7 and MDA-MB-231 cells were subjected to Western analyses using specific anti-HER2 antibody (Calbiochem). Tubulin was used as reference. B) Uptake analyses by flow cytometry. Cells were incubated with 100 nM fluorescent Hpdl3-BF (orange) or 100 nM fluorescent ApHER2(t)-F in the absence (bright green) or the presence (dark green) of 10  $\mu$ M DOTAP. The background autofluorescence of cells is shown in the black histogram. Histograms show the fluorescence detected using either SKBR3, MCF7 or MDA-MB-231 cells.

**Figure 4.** Uptake analyses by confocal microscopy. SKBR3 (A) and MCF7 (B) cells were incubated with 100 nM ApHER2(t)-F in the absence and in the presence of 10  $\mu$ M DOTAP. Confocal fluorescent scanning was performed after 24 hour of incubation and labelling with Wheat Germ Agglutinin (WGA), Alexa Fluor® 555 Conjugate. Results



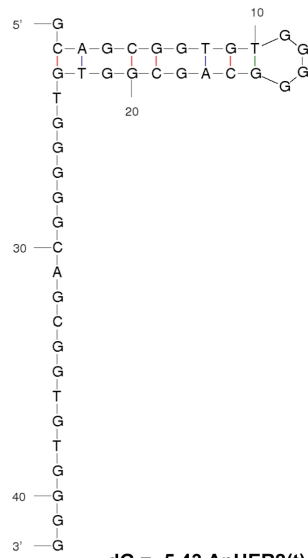
from control cells are shown in the upper panels. The uptake of the fluorescent aptamer ApHER2(t)-F without DOTAP and with 10  $\mu$ M DOTAP are shown in the center and lower panels, respectively.

**Figure 5.** Cell survival upon transfection of 100 nM of HpdI3-B (■, black bars), ApHER2(t) (■, grey) or ApHER2(t)-5T-HpdI3-B (□, white) in SKBR3 (A), MCF7 (B) and MDA-MB-231 cells (C) with the indicated increasing concentrations of DOTAP. MTT assays to determine cell survival were performed 6 days after transfection.

**Figure 6.** Cell viability of SKBR3 (A), MCF7 (B) and MDA-MB-231 (C) cells upon transfection of the indicated increasing concentrations of the ApHER2(t)-5T-HpdI3-B chimera (■) and the negative control ApHER2(t)Sc-5T-HpdI3-B (□). MTT assays to determine cell survival were performed 6 days after transfecting 30 and 50 nM of the oligonucleotides with 5  $\mu$ M DOTAP, and 100 nM of the oligonucleotides with 10  $\mu$ M DOTAP.

**Figure 7.** IC<sub>50</sub> of the oligonucleotides in the different cell lines. The effect on cell survival of the indicated increasing concentrations of HpdI3-B (black solid line), ApHER2(t) (grey solid line), ApHER2(t)-5T-HpdI3-B (black dashed line) and ApHER2(t)Sc-5T-HpdI3-B (grey dashed line) was used to calculate the corresponding IC<sub>50</sub> values. MTT assays to determine cell survival in SKBR3 (A), MCF7 (B) and MDA-MB-231 (C) cells were performed 6 days after transfecting 30 and 50 nM of the oligonucleotides with 5  $\mu$ M DOTAP and 100 nM of the oligonucleotides with 10  $\mu$ M DOTAP.

**A**



**B**

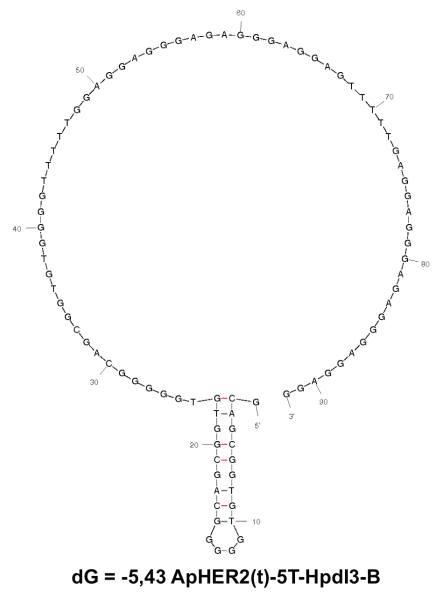


Figure 1

Results

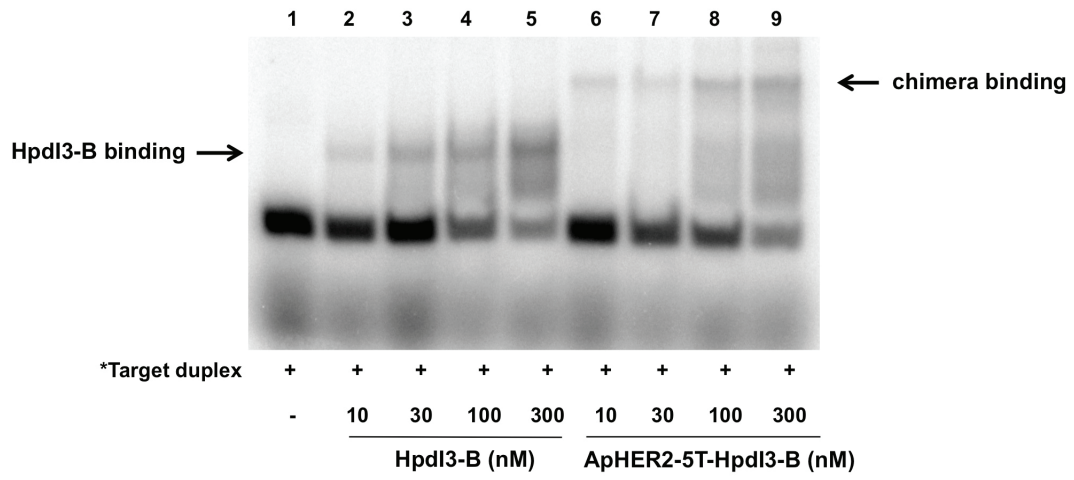
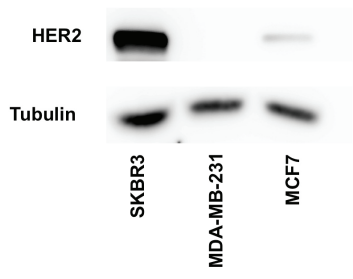


Figure 2

A



B

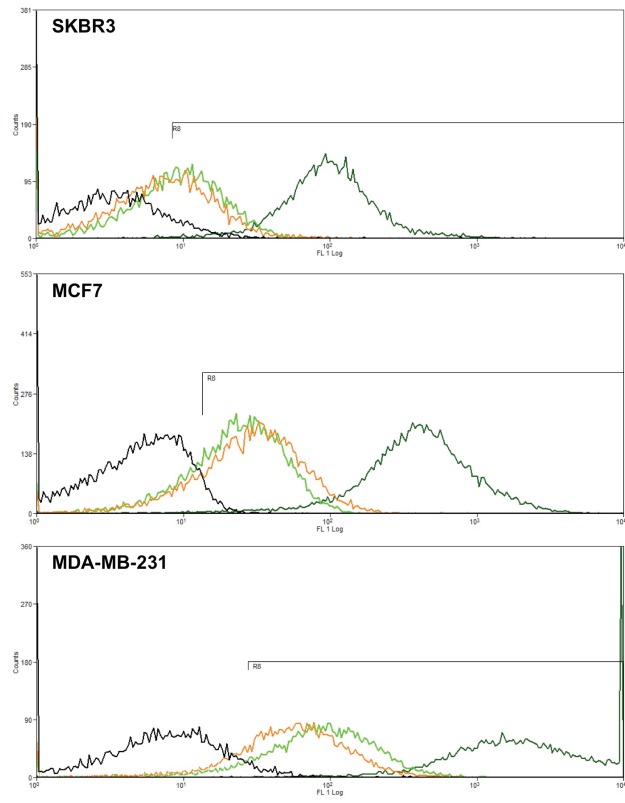
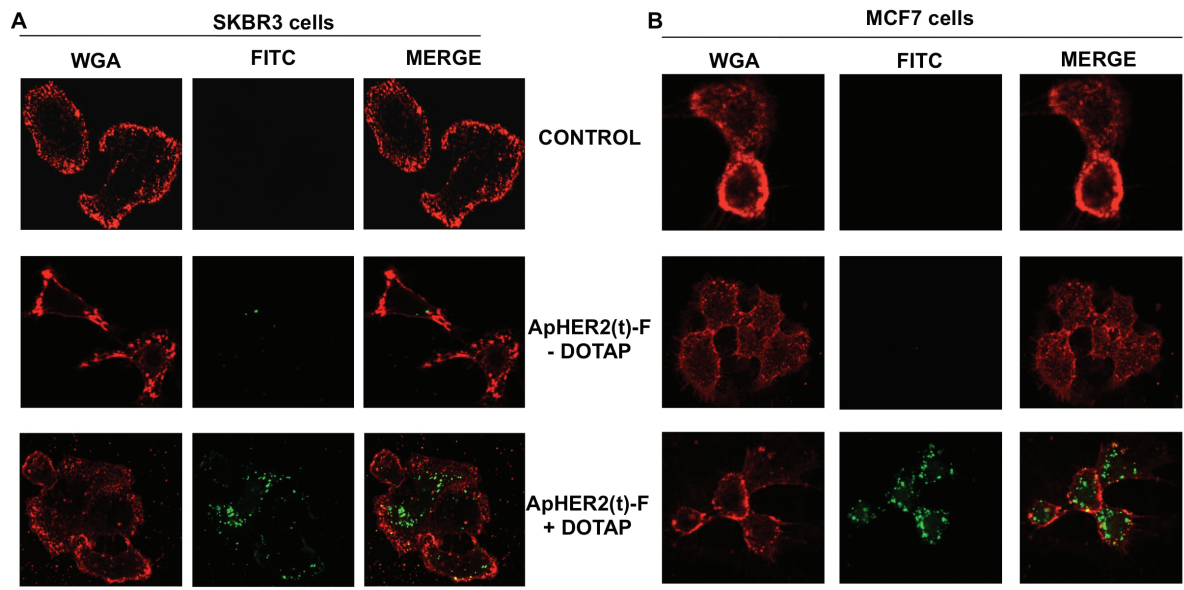


Figure 3



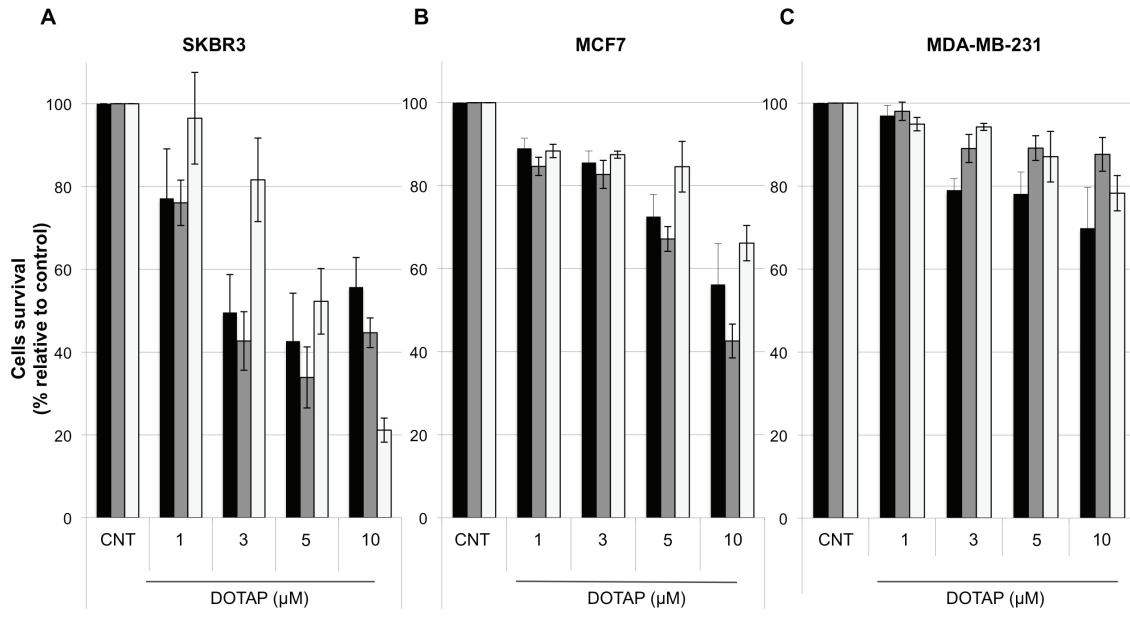


Figure 5

Results

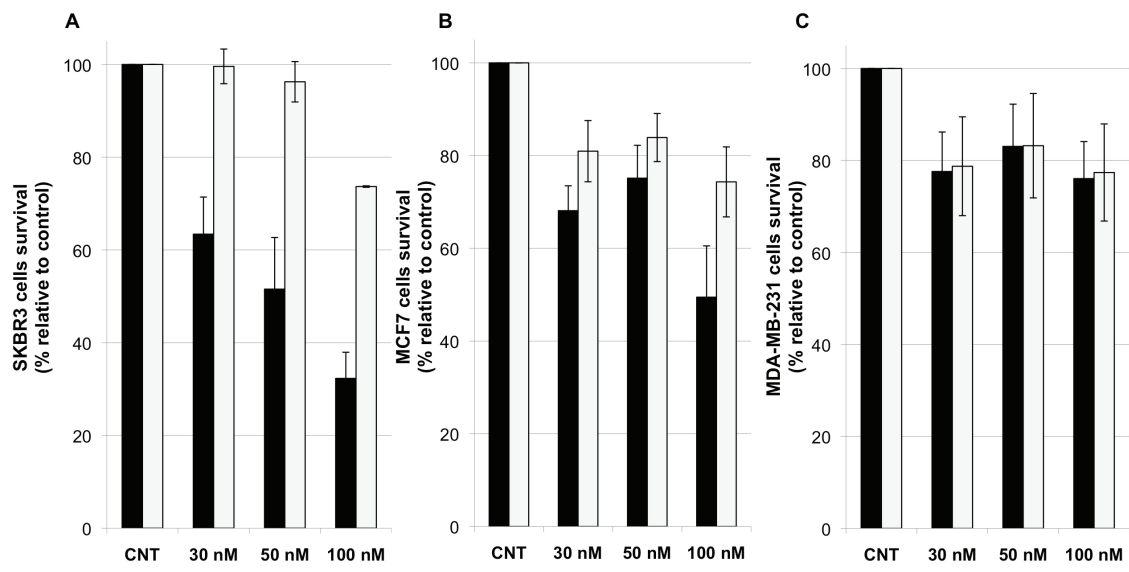


Figure 6

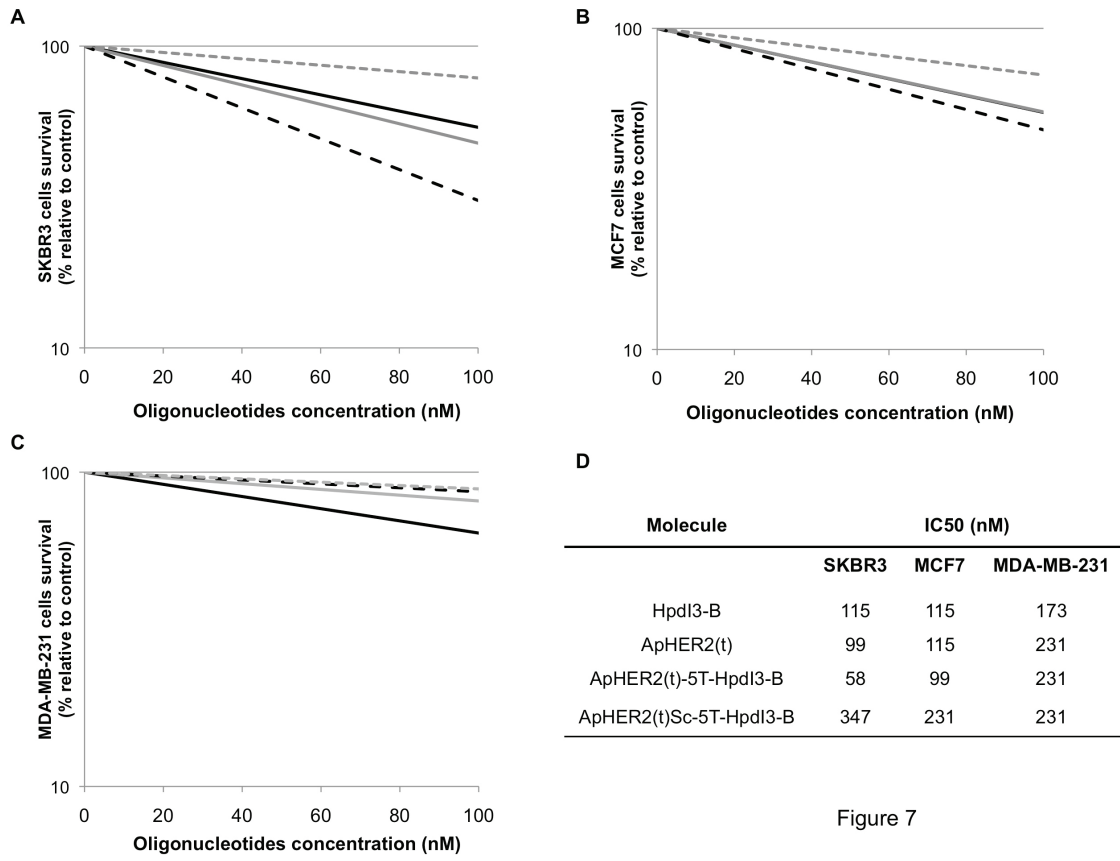


Figure 7





## FIVE | DISCUSSION



A long-term objective of our laboratory is to prove that PPRHs can be considered as an additional type of gene silencing molecule. To achieve this, several steps have to be taken; these started demonstrating that PPRHs can bind to dsDNA, displacing the polypyrimidine strand of the duplex, followed by the confirmation that PPRHs can bind to both strands in the DNA, and finishing by establishing the proof of principle that PPRHs can be used *in vivo*.

### 5.1 Delivery and stability

In this work we add new insight to the knowledge of PPRHs. We studied the properties of PPRHs in terms of stability and immunogenicity and compared them with those shown by siRNAs. The relevance of comparing the stability of these two silencing molecules is that regardless their different mechanisms of action, an increased stability of the PPRHs will extend their biological effects. We determined the stability of both types of molecules in three different types of serum, as well as intracellularly, using fluorescent oligonucleotides.

The primary routes of administration of oligonucleotides for systemic applications are either intravenous (IV) infusion or subcutaneous (SC) injection. After these, oligonucleotides are rapidly absorbed from the injection site into the circulation with peak plasma concentrations reached within 3 to 4 h (Geary *et al.* 2015). At this point, if no vehicle is used (gymnotic administration), the clearance of the oligonucleotides depends on their metabolism by blood nucleases, their renal filtration, and their accumulation in tissues. Therefore, the bioavailability of DNA-based molecules depends in great measure on their chemical properties. It has been clearly established that unmodified oligonucleotides, PNAs, morpholinos, and oligonucleotides that lack charge exhibit more rapid clearance from blood primarily due to either metabolism in blood (specially unmodified oligonucleotides) or excretion in urine (Dirin & Winkler 2013; Amantana & Iversen 2005). In contrast, oligonucleotides containing a phosphorothioate backbone are extensively bound to plasma proteins ( $\geq 85\%$ ), especially to albumin, with relatively low affinity ( $K_d$  approximately 150  $\mu\text{M}$ ). This prevents loss of the oligonucleotide to renal filtration and facilitates uptake in tissues (Geary *et al.* 2015). Thus, appropriate and balanced plasma protein binding is required for optimal delivery to tissues and cells systemically. Either too tightly bound or not bound enough result in inefficient distribution properties.

PPRHs are unmodified DNA molecules; therefore one could speculate that their PK would be similar to that of unmodified aODNs. In this case, DNase I and 3'-exonuclease are the primary enzymes to degrade circulating deoxyribonucleotides. DNase I recognizes the B form of dsDNA and degrades it by single-stranded nicking mechanisms in the presence of  $Mg^{2+}$ , or by double-stranded cutting, in the presence of  $Mn^{2+}$  or  $Mg^{2+}$  and  $Ca^{2+}$  (Pan *et al.* 1998; Blume *et al.* 1999). The rate of hydrolysis of this enzyme depends strongly on the oligonucleotide conformation and sequence: extended A-T or G-G sites are quite resistant to degradation (Fujihara *et al.* 2012), as seen in G-rich anti-HIV oligonucleotides (Bishop *et al.* 1996) and in aptamers against nucleolin (Bates *et al.* 2010).

In the case of siRNAs, ribonucleases belonging to the RNase A family (Haupenthal *et al.* 2006) are the predominant nucleases to degrade circulating ribonucleotides. The reported half-life for unmodified siRNAs in serum ranges from several minutes to 1 h (Bartlett & Davis 2007; Layzer *et al.* 2004; Dykxhoorn *et al.* 2006), depending on the experimental conditions. In *in vivo* rat experiments plasma half-life was estimated to be less than 8 minutes (Thompson *et al.* 2012). Notably, the siRNAs sequence can have an impact on their own stability: regions rich in UpA clusters, which have low thermal stability, are most susceptible toward RNase A degradation (Haupenthal *et al.* 2006) especially when they are located toward the end of the strands (Turner *et al.* 2007).

We studied two different PPRHs and determined that their half-lives were much longer compared to the siRNA. The half-life of the PPRHs was between 7 and 10 times longer than that of the siRNA, depending on the type of serum, and twice as longer when transfected to PC3 cells. This extended half-life of the PPRHs could be explained by the nature of their structure. PPRHs are double-stranded DNA molecules, protected by the pentathymidine loop on one side and intramolecularly linked by reverse Hoogsteen bonds. This means that PPRHs are not a standard double-stranded DNA.

Because this susceptibility to be degraded is a serious drawback to use oligonucleotides as therapeutic agents, the higher stability of the PPRHs, even without chemical modifications, is a remarkable advantage. Normally, nuclease-resistant oligonucleotides are necessary to enable their systemic distribution. Phosphate modifications at the 3'-end and the inclusion of 2'-protected nucleosides at internal sites

of the ribose are necessary to provide protection against exonucleases and endonucleases, respectively. Nevertheless, these modifications can have unintended consequences, such as the activation of the Complement system or the prolongation of clotting times (Henry *et al.* 2014). Also, they increase the complexity of synthesis and the cost of the oligonucleotides.

Despite the rapid plasma clearance, non-modified oligonucleotides distribute broadly into most tissues with the exception of the central nervous system, but they accumulate markedly in the kidneys and liver, followed by bone marrow, adipocytes and lymph nodes. This is attributable to the reticuloendothelial system (RES) absorbing a significant part of the administered oligonucleotide. Specifically, scavenger receptors in liver (Kupffer cells), bone marrow (fibroblasts) and kidney are suggested to be contributing to the elimination of oligonucleotides from blood by phagocytosis. In the case of the liver, this results from the abundant presence of phagocytic Kupffer cells, together with the high blood flow received and, importantly, the existence of a fenestrated vasculature with an average 70 – 150 nm pore diameter between endothelial cells (Moreno & Pêgo 2014).

If “naked” PPRHs were to be administered as anti-cancer therapy, it is probable that very high amounts should be used, because oligonucleotides tend to accumulate in organs rather than in tumor tissue. Additionally, there could be a large heterogeneity in the distribution of PPRHs, not only between tumors, but due to the tumors nature, also within the same tumor. Solid tumors possess specific microvasculature characteristics that promote the EPR (Jang *et al.* 2003), responsible for the accumulation of macromolecules or nanoparticles in them. Furthermore, tumors present a usually high interstitial fluid pressure (IFP), which makes drug accessibility even more difficult. All this, together with a dense structure of extracellular matrix, would ultimately lead to some cancer cells within the tumor to evade the anti-cancer action of the PPRHs (Netti *et al.* 2000).

Therefore, vehicles capable of bypassing these characteristics are necessary for optimal PPRHs delivery. In this sense, PPRHs have the advantage of being very stable molecules, even without a delivery vehicle. In order to be effective, a delivery vehicle needs to: i) protect the PPRH from extracellular and intracellular degradation, until it reaches its target, ii) achieve a prolonged circulation time in order to be accumulated in

the location of interest, iii) efficiently interact with the cellular membrane to promote uptake, iv) promote escape from endocytic vesicles, and v) dissociate from the active nucleic-acid in order for it to function. Cationic lipids generally used with nucleic acids comprise DOPE or DOTAP. Cationic polymers have been also used. These have a vast chemical diversity and are easy to functionalize. Some examples of polymeric systems that have been used are poly(L-Lysine) (Stewart *et al.* 1996) and poly(ethylene imine) (Seong *et al.* 2006). However, some issues regarding efficiency and toxicity have justified the development of other polymers based on natural and biodegradable compounds such as chitosan (Sadio *et al.* 2014) or protamine. It is also worth mentioning the delivery systems based on inorganic nanoparticles, an emerging field, of which gold nanoparticles and carbon nanotubes are very promising (Safari & Zarnegar 2014).

Regarding size, the smaller the particle (10 – 20 nm) the better the intratumoral diffusion (Goodman *et al.* 2007), however the EPR effect is more pronounced for bigger particles (10 – 200nm). Also, bigger sizes tend to be cleared by the RES, although modifying the surface of the NP with other polymers like poly(ethylene glycol) (van Vlerken *et al.* 2007) can prevent this drawback.

## 5.2 Immunogenicity

A major concern about the use of siRNAs, and of therapeutic oligonucleotides in general, is the unintended activation of the immune response. Immune activation by oligonucleotides has previously led to misinterpretation of data, especially when inhibition of tumor growth was not primarily due to the antisense mechanism but to the immunostimulatory properties of the oligonucleotides (Moreno & Pêgo 2014). Herein, the immune response to both, PPRHs and siRNAs, was evaluated in the monocytic cell line THP-1 by monitoring the TLR and the inflammasome pathways.

The innate immune system can sense microbial pathogens through the presence of their genomes. This recognition, mediated by the PRRs, is based in two key aspects: (i) recognition of patterns that are not naturally occurring in the human cell, such as dsRNA or unmethylated cytosine-phosphate-guanosine (CpG)-rich DNA and (ii) sensing of nucleic acids in cellular compartments that are normally free of these molecules (i.e., the cytoplasm). Several PRRs participate in the recognition of nucleic

acids patterns; from them the toll-like receptor family has been best characterized. TLR3, TLR7/TLR8, and TLR9 are located in the endolysosomes of dendritic cells and macrophages and are responsible for the recognition of dsRNA, ssRNA, and CpG-rich DNA, respectively. Upon detection and binding of non-self genetic material, these TLRs trigger the phosphorylation and nuclear translocation of transcription factors, such as IRF3, which controls the expression of type 1 interferons, and NF- $\kappa$ B, which controls the expression of the proinflammatory cytokines IL-6, TNF $\alpha$ , IL-1 $\beta$ , and IL-18, among others. Data suggest that siRNAs are recognized in a sequence-independent and sequence-dependent manner (Blume *et al.* 1999; Judge *et al.* 2005; Sioud 2005), with immunostimulatory sequences appearing very frequently in conventionally designed siRNAs (Judge *et al.* 2005). The size of RNAs is also important for activation of the immune system. Hornung *et al.* 2005 observed that 12-nt ssRNAs containing the immunostimulatory motif (GUCCUCAA) were poor inducers of IFN- $\alpha$  in pDCs but that increasing their size to 16 nt or 19 nt completely restored cytokine induction. Our results on the immunostimulatory effect of siRNAs are in agreement with previous results (Judge *et al.* 2005; Sioud 2005; Hornung *et al.* 2005), in which siRNAs activate the innate immune response through the TLR pathway, as shown by the increase of IL-6, TNF- $\alpha$ , and IFN $\beta$  expression levels.

PPRHs on the other hand did not have an immunostimulatory effect, probably because they are relatively short DNA molecules, less than 100 bases in length, and usually around 50 nucleotides. It is well established that TLR9 recognizes unmethylated CpG-rich DNA, which is characteristic of bacterial DNA and a potent inducer of innate immune response (Hanagata 2012). In fact, peripheral blood mononuclear cells (PBMCs) from human and nonhuman primates respond to at least two structurally distinct types of oligonucleotides: D-ODN and K-ODN. A critical feature of these is their expression of at least one unmethylated CpG motif. PPRHs are unmethylated oligonucleotides rich in adenines and guanines, and thus cannot possess the unmethylated CpG sequences. This may allow them to escape TLR9 recognition and avert the innate immune activation. Other families of receptors recognize nucleic acids in the cytoplasm: NLR-family proteins recognize many ligands, including nucleic acids. The dsRNA is sensed specifically by RIG-1 and PKR, while DAI and AIM2 recognize dsDNA. These receptors trigger a series of pathways that also culminate in the expression and activation of proinflammatory cytokines.



The inflammasome is a multiprotein complex that, upon binding of its ligand, mediates the proteolysis of procaspase-1 to the active caspase-1, which leads to the post-transcriptional activation of IL-1 $\beta$  and IL-18, and to pyroptosis, a form of programmed cell death in which immune cells die upon recognition of danger signals. Some of these receptors such as AIM2 do not discriminate between self and nonself DNA, so the fact that PPRHs do not induce the inflammasome response is an interesting finding. Moreover, pro-IL-1 $\beta$  and -IL-18 are limiting factors in this pathway (Davis *et al.* 2011), and their transcription depends on NF- $\kappa$ B. In this regard, PPRHs have a double advantage over siRNAs: (i) they do not induce the levels of NF- $\kappa$ B and hence the levels of pro-IL-1 $\beta$  nor -IL-18, and (ii) they most likely do not promote the assembly of the inflammasome since they do not activate the proteolytic activity of caspase-1.

The innate immune response limits the early spread of infectious organisms while promoting the development of adaptive immunity. Therefore, a thorough evaluation of the PPRHs effect on PBMCs obtained from human samples could provide further insight into the PPRHs effect on innate immunity in humans. The immune response is a very complex system that possesses several layers of defense. In this sense, acquired immunity, especially towards the delivery vehicle, and the activation of the complement system need to be evaluated to complete the immunotoxic profile of PPRHs.

In addition to the stability and immunogenic advantages of PPRHs over siRNAs, there are other aspects worth considering. For example PPRHs do not use the intracellular RNA-processing pathways, whereas high concentrations of siRNA can saturate the RNAi machinery, leading to a global perturbation of miRNA-mediated regulation (Khan *et al.* 2009). In mice, oversaturation of miRNA pathways with shRNA is fatal (Grimm *et al.* 2006).

### 5.3 Improving the structure of PPRHs

We also evaluated the properties of a novel design of PPRH: the nicked-circular-PPRHs, since it has been described that circular structures can offer advantages over their linear counterparts, such as tighter binding affinity, a greater specificity for binding a particular intended target and, in the case of oligonucleotides, resistance to

degradation by nucleases (Kool 1991; Prakash & Kool 1992), all of which are interesting properties for our purposes. By designing the nicked-circle-PPRHs, we aimed to pre-organize the PPRHs into their functional conformation to increase the binding affinity to their dsDNA target sequence and to protect the PPRHs against nucleases, specifically once the PPRHs were bound to their targets. It has to be noted that the binding between the PPRHs and the dsDNA target sequence requires  $Mg^{2+}$ , which increases DNase I activity. Therefore, the stability to degradation of the PPRHs in this condition is shorter than when no binding is required. As expected, the half-life of both ncPPRHs, when bound to their target, was longer than the regular PPRH, even when the stability to degradation of the regular PPRH and the ncPPRH-out by themselves was similar. Therefore, the higher stability of the ncPPRH takes place only when it is bound to the target due to their almost circular structure, as compared with the open structure of the regular PPRH. In this sense, it is known that TFOs bound to dsDNA by Hoogsteen bonds confer protection against DNase I (Blume *et al.* 1999). Interestingly, ncPPRH-in half-life when bound to the target is shorter than that of ncPPRH-out. It is worth noting that PPRHs bind to their target sequence through WC bonds; once the ncPPRH-in is bound to its target, the strand that is forming WC bonds has a nick, and this could render the ncPPRH-in more vulnerable to the attack of endonucleases present in the serum. On the other hand, ncPPRH-out is forming a perfectly matched triplex, which enhances its stability.

The fact that PPRHs are easily modifiable makes them very versatile molecules, and other modifications of these molecules have been tested. For example, a design called wedge-PPRH (Rodríguez *et al.* 2015) increased the cytotoxic effect of a PPRH directed against the *survivin* promoter. Wedge-PPRHs are able to lock the strand displacement produced by the PPRH. This is possible by extending the 5' end of the PPRH with the sequence complementary to the displaced polypurine strand. Therefore, wedge-PPRHs are able to bind to both strands of the target DNA at the same time. The idea of using oligonucleotides capable of binding to both strands of the DNA has also been explored by other groups. For example, Eman and collaborators have developed an LNA-based molecule, called Zorro-LNA that can target both strands of a target sequence (Zaghloul *et al.* 2011). However, as previously stated, the fact that PPRHs do not need to be modified surely adds to the interest of these molecules.

#### 5.4 RNA-PPRHs

Reverse Hoogsteen bonds can also be formed between RNA sequences. To expand the use of PPRHs as silencing tools we designed PPRHs made out of RNA, RNA-PPRH. We were able to determine that an RNA-PPRH was also capable of binding specifically to a dsDNA sequence *in vitro*, and of forming a triplex structure. Moreover, using a vector containing the sequence that encodes for an RNA-PPRH targeting the *DHFR* gene, we determined that this particular RNA-PPRH is active intracellularly. Further experiments to determine DHFR mRNA and protein levels after plasmid transfection should be performed to validate the activity of RNA-PPRHs. This approach could also be used in others targets, but also these results open up the possibility of developing RNA-PPRHs systems to silence target genes in a more regulated manner. This could be achieved, for instance, by cloning the sequence that encodes for a given PPRH into an inducible promoter, and controlling the expression of the functional RNA-PPRH, in a similar way to the inducible shRNA systems that are available commercially.

#### 5.5 Validation of PPRHs

One of the objectives of this work was to evaluate if PPRHs could be used as gene silencing agents against different targets in cell lines corresponding to several cancer types. In this way we could expand the usage of PPRHs in cancer therapy and prove their general applicability. For this purpose, we chose an array of therapeutically interesting genes to act as reporter genes for the silencing activity of the PPRHs. The chosen target genes encompass a variety of biological functions: antiapoptotic genes, topoisomerases, protein kinases, and transcription factors. Additionally, these targets are usually overexpressed either by gene amplification or by over-activation in tumors. We were able to design PPRHs directed against polypyrimidine stretches of every gene to be targeted; three of these stretches were located in introns (*c-myc*, *mdm2*, *top1*), one in a promoter region (*mtor*), and one in an exonic sequence (*bcl2*), which were tested in a variety of cell lines (HCT 116, PC-3, MIA PaCa-2, SKBR3, MCF7, and MDA-MB-468).

All PPRHs were effective, yet the most remarkable results in decreasing cell survival and mRNA levels and increasing apoptosis were obtained with those against

*bcl2* in PC3, MIA PaCa-2 and HCT 116 cell lines. Also, 3 out of 4 PPRHs designed against *mtor* were highly effective in HCT 116 cells. Additionally, when targeting *mtor* we performed time-course experiments, in which we observed that short incubations of 8 h after transfection already produced a 50% decrease in HCT 116 cells survival. In the case of TOP1, MDM2, and MYC, their corresponding PPRHs produced a strong effect in decreasing cell viability and mRNA levels and increasing apoptosis in the three breast cancer cell lines used.

We have determined that PPRHs produce a 40 - 70% decrease in the mRNA target levels, and that this decrease is enough to reduce cell survival significantly. We were interested in studying the effect of using PPRHs directed against a TF since it was possible to study if the function of the TF upon PPRH transfection was affected, even if a complete decrease of the mRNA levels was not achieved. Using three different PPRHs designed against Sp1 we were able to determine that the PPRH that targets the promoter sequence of Sp1 had a higher cytotoxic activity and that its transfection correlates with a decrease on Sp1 promoter activity, therefore affecting the expression of the genes under the control of this TF at the transcriptional level.

PPRHs, TFOs, aODNs, and siRNAs have in common the silencing of gene expression. It is important to note that although PPRHs share with TFOs the formation of triplex structures, there are differences in their binding properties; while the TFOs bind to the double-stranded DNA by Hoogsteen bonds, PPRHs bind intramolecularly by reverse Hoogsteen bonds and to the dsDNA by Watson-Crick bonds. Previously, we studied the differences of both PPRHs and TFOs (Rodríguez *et al.* 2015) and determined two important features: i) PPRHs have a higher binding affinity to the dsDNA target, and ii) PPRHs have a higher biological activity than TFOs. Therefore, for the purpose of inhibiting gene expression, we showed that PPRHs offer advantages over TFOs. Moreover, the results presented in this thesis indicate that PPRHs, while working at a similar range of concentrations (de Almagro *et al.* 2009) have advantages over siRNAs in terms of stability, lack of immunogenicity, and economy, while no off-target effects have been found (de Almagro *et al.* 2011; Rodríguez *et al.* 2013).

There are other gene silencing approaches being developed. One of them is based on pyrrole-imidazole polyamides, oligomers that bind to the minor groove of the DNA targeting short sequences of DNA of around 6 bp (Matsuda *et al.* 2006; Yang *et*

*al.* 2013). In comparison, PPRHs cover a 19–25 nucleotide region, which would confer a greater specificity. Regarding the potential target sites for PPRHs, TTS are generally found in regulatory regions, specifically in promoters, introns, and to a lesser extent in exons. It has been described that even if these regions are overrepresented in promoters, they are not necessarily the binding sites for transcription factors (Goñi *et al.* 2006). PPRHs not only bind to transcription factors binding sites but also to other regions in the promoter and to both intronic and exonic sequences. Moreover, PPRHs have the ability to bind to transcribed mRNA.

Recently, protein-based approaches with different degrees of complexity have come forward; these include ZFN, TALENs, and CRISPR-Cas9, and their initial goal was the editing of the genome. Their mechanism of action is based on the introduction of double-strand breaks and its subsequent repair through homology-directed repair or non-homologous end joining, where the latter can cause unwanted insertions or deletions (Lin *et al.* 2014). Even if these methods are considered very robust platforms for genome editing, they present several drawbacks, including potential off-target DNA cleavage and unwanted cytotoxic activity (Fu *et al.* 2013), they are labor- and time-consuming (Mussolino *et al.* 2011; Wijshake *et al.* 2014), and they face the additional complications linked to viral gene therapy (Cox *et al.* 2015). Another concern for these strategies could be the immune response triggered by the peptides from editing nucleases or by the large amounts of virus necessary for the *in vivo* delivery. In contrast, PPRHs are easy to design and to synthesize, since they are just like regular unmodified oligonucleotides of about 50 bases and can be directly used without further manipulation, avoiding engineering issues. PPRHs can be labeled in their primary synthesis with fluorophores or biotin and can also be fused to targeting or delivering agents, such as aptamers and antibodies. Moreover, several PPRH-binding sites can be found per targeted gene allowing for combination therapy. We have previously studied the *in vivo* efficiency of the PPRHs (Rodríguez *et al.* 2013) using a subcutaneous xenograft tumor model of prostate cancer. Using two different types of administration, intratumoral and intravenous, a PPRH against *survivin* promoter (HpsPr-C) was able to delay the tumor growth, without affecting mice weight. We determined the decrease in the levels of survivin and a lower degree of blood vessel formation.

## 5.6 Use of aptamers

Delivery of PPRHs is a relevant topic for their further development. We began addressing this issue by using aptamers as targeting molecules. In this work we analyzed the effects of fusing a gene silencing PPRH, specifically designed against intron 3 of the *DHFR* gene (HpdI3-B), to an aptamer recognizing the HER2 receptor (ApHER2(t)). It has been described that upon binding to its target protein, this aptamer is internalized and promotes the degradation of HER2, ultimately leading to cell death (Mahlknecht *et al.* 2013). By fusing both molecules with 5-thymidine linker, our aim was to create a bifunctional oligonucleotide (ApHER2(t)-5T-HpdI3-B) that could be effective in a specific cell line, such as SKBR3, which overexpresses HER2 protein.

We began by performing the structural prediction of the aptamer through *in silico* studies, and determined that the aptamer maintained its secondary structure even when it was fused to the PPRH by a 5-thymidine linker. It is worth mentioning that the expected hairpin structure of the PPRH could not be predicted because the server used, mfold, only considers the canonical Watson-Crick bonds, and the Wobble G-U bonds (in the case of RNA sequences) when performing the structural prediction. Therefore, the PPRH sequence is shown as a circle. However, we determined that upon fusing both molecules, the PPRH domain of the chimeric molecule maintained the capacity to bind to its dsDNA target sequence. This was proved performing EMSA, in which we compared the binding of both molecules, HpdI3-B and ApHER2(t)-5T-HpdI3-B, to the target duplex and calculated their K<sub>d</sub>: 385 nM for HpdI3-B, and 714 nM in the case of ApHER2(t)-5T-HpdI3-B.

To determine if the uptake of a fluorescent ApHER2(t) varied in the different cell lines, we performed flow cytometry analyses. We concluded that, when no transfection agent was used, the fluorescence intensity upon incubation with the aptamer increased in a similar extent in the three cell lines. We believe that this effect was unspecific since incubation with a fluorescent PPRH produced the same effect. However, when DOTAP was used to transfect ApHER2(t)-F, the internalized fluorescence increased considerably in the three cell lines. It is interesting to point out that upon transfection with DOTAP, MDA-MB-231 and MCF7 cells internalized more fluorescent molecules than SKBR3 cells, thus indicating that MCF7 and MDA-MB-231

cells have a higher internalization rate. Confocal experiments confirmed that there was not internalization of the aptamer unless DOTAP was used.

We performed cell survival experiments in the three cell lines and determined that the cationic liposome DOTAP is necessary for the molecules to produce an effect on cell survival. In fact, we observed that the cytotoxic effect of the oligonucleotides increased in a DOTAP-concentration dependent manner. Interestingly, when we performed the dose-response experiments with HpdI3-B, ApHER2(t) and ApHER2(t)-5T-HpdI3-B, the cytotoxicity in SKBR3 cells transfected with the chimeric aptamer-PPRH was higher than that of MCF7 and MDA-MB-231 cells, despite the higher internalization of the latter, meaning that there was a specific effect of the PPRH fused to the aptamer directed against the HER2 epitope. It is noteworthy that in SKBR3 cells the IC<sub>50</sub> of the chimeric ApHER2(t)-5T-HpdI3-B was remarkably low compared to those of the PPRH or aptamer alone, whereas in MCF7 and MDA-MB-231 this effect was not observed. Moreover, when a scrambled chimeric sequence was transfected to all cell lines, there was no cytotoxic effect, confirming the specificity of ApHER2(t)-5T-HpdI3-B. We believe that the overexpression of HER2 in SKBR3 cells, even if it does not facilitates the internalization of ApHER2(t)-5T-HpdI3-B, could be playing a role in the cytotoxic effect of this chimeric molecule. However, methods enabling the internalization of the chimeric molecules should be further investigated to allow for specific targeting and delivery without the need of a transfecting reagent.

Aptamers offer promising opportunities to improve current oligonucleotide-based therapies. The SELEX process allows selecting aptamers with high affinities for their targets, which are comparable to those shown by antibodies. But aptamers present some advantages over the latter: obtaining them is independent of animal use, they have lower batch-to-batch variation, and more stability to temperature changes, especially if they are DNA aptamers.

## **5.7 Concluding remarks**

In summary, PPRHs as DNA molecules present substantial advantages as a new silencing tool such as high stability, low immunogenicity, and versatility of design since they can be directed against different gene regions such as promoter, introns, and exons, providing various mechanisms to knock down gene expression. In fact, we have



incorporated the use of PPRHs as a silencing tool on a regular basis (Oleaga *et al.* 2012; Mencia *et al.* 2011; Barros *et al.* 2013). In addition, it is not necessary to introduce chemical modifications in the DNA synthesis, making PPRHs 10 times less expensive than siRNAs. Moreover, the results presented in this work confirm that the PPRH technology is broadly useful to silence the expression of genes, and we made a special emphasis in genes related to cancer. Regardless of the gene or cell line tested, PPRHs were able to decrease cell survival and mRNA expression levels, and to increase apoptosis. Thus, we have extended the number of PPRHs used in cancer therapy, now spanning metabolism (DHFR), proliferation (mTOR), DNA-topology (TOP1), lifespan and senescence (Telomerase), apoptosis (Survivin, BCL2), transcription factors (Sp1, MYC), and proto-oncogenes (MDM2). Additionally, PPRHs can be functionalized with targeting molecules to increase the specificity of their action. Therefore, we wish to put forward the use of PPRHs as a new silencing tool. We believe that developing new approaches, and not only modifying the existent molecules, could broaden the therapeutic scope of gene silencing.

Clearly oligonucleotide therapeutics has come a long way. Since the first report of a DNA sequence being used as disruptor of genetic flow, many landmarks have been set. Although some limitations are still present, chief among them an inefficient delivery to tumors, the development of therapeutic oligonucleotides is likely to continue, supported in part by the improvement in nucleotides chemistry and nanomaterials.





## SIX | CONCLUSIONS



1. PPRHs can be designed in a straightforward way, they work at the nanomolar range, and do not need to be modified in their synthesis, offering economical advantages over siRNAs.
2. The stability of PPRHs is higher than that of siRNAs, as evidenced by the longer half-life of the former in different types of serum and in PC3 cells.
3. PPRHs do not induce the levels of NF- $\kappa$ B and IRF3, or the phosphorylation of the latter, when transfected to THP-1 cells. Also, PPRHs do not increase the expression levels of the proinflammatory cytokines IL-6, INF- $\alpha$ , INF- $\beta$ , TNF- $\alpha$ , IL-1 $\beta$  or IL-18, all of which are involved in the Toll-like Receptor pathway.
4. PPRHs do not trigger the formation of the inflammasome complex, as confirmed by the lack of caspase-1 cleavage activity in THP-1 iGLuc cells transfected with different PPRHs.
5. Nicked-circle-PPRHs have a better binding capacity *in vitro* than regular PPRHs. They maintain the cytotoxic effect and when bound to their target they are more stable than regular PPRHs.
6. RNA-PPRHs are able to bind to a dsDNA target and form a triplex structure. The transfection of a vector containing the sequence that encodes for an RNA-PPRH targeting the *DHFR* gene allows for the intracellular transcription and activity of the RNA-PPRH.
7. PPRHs have the capacity to decrease the mRNA expression levels of several target genes (*BCL2*, *TOP1*, *MTOR*, *MDM2*, and *MYC*) in a variety of cancer cell lines.
8. PPRHs are able to decrease the survival of several tumor cell lines (HCT 116, MCF7, MDA-MB-468, MIA PaCa2, PC3 and SKBR3) and to increase apoptosis when genes involved in cancer are targeted.

9. PPRHs targeting TFs, such as Sp1, can exert their action by decreasing the transcriptional activity on their target genes.
10. PPRHs can be used as *in vitro* tools to validate genes involved in cancer. Additionally, because of their gene silencing capacity, in the future PPRHs could be considered as therapeutic oligonucleotides if they target genes related to cancer progression or resistance to drugs.
11. The fusion of the aptamer ApHER2(t), directed against HER2, to the HpdI3-B PPRH, directed against *DHFR*, in a single chimeric oligonucleotide does not prevent the binding of HpdI3-B to its target sequence.
12. In SKBR3 cells, the cytotoxic effect of the chimeric ApHER2(t)-5T-HpdI3-B molecule is greater than that of the two molecules (HpdI3-B and ApHER2(t)) separately. The effect of the evaluated oligonucleotides is facilitated with the presence of DOTAP.
13. The effect of the chimeric ApHER2(t)-5T-HpdI3-B oligonucleotide is higher in SKBR3 cells, which overexpress HER2 protein; moderate in MCF7 cells which have a normal expression of HER2; and negligible in the HER2 negative cell line MDA-MB-231.

## BIBLIOGRAPHY



**A**

- Adisheshaiah, P.P., Hall, J.B. & McNeil, S.E., 2009. Nanomaterial standards for efficacy and toxicity assessment. *Wiley interdisciplinary reviews. Nanomedicine and nanobiotechnology*, 2(1), pp.99–112.
- Ahn, J.D. et al., 2003. E2F decoy oligodeoxynucleotides effectively inhibit growth of human tumor cells. *Biochemical and biophysical research communications*, 310(4), pp.1048–53.
- De Almagro, M.C. et al., 2011. Coding polypurine hairpins cause target-induced cell death in breast cancer cells. *Human gene therapy*, 22(4), pp.451–463.
- De Almagro, M.C. et al., 2009. Polypurine hairpins directed against the template strand of DNA knock down the expression of mammalian genes. *Journal of Biological Chemistry*, 284(17), pp.11579–11589.
- Amantana, A. & Iversen, P.L., 2005. Pharmacokinetics and biodistribution of phosphorodiamidate morpholino antisense oligomers. *Current Opinion in Pharmacology*, 5(5 SPEC.ISS.), pp.550–555.
- Assaraf, Y.G., 2007. Molecular basis of antifolate resistance. *Cancer and Metastasis Reviews*, 26(1), pp.153–181.
- Atianand, M.K. & Fitzgerald, K. a, 2013. Molecular basis of DNA recognition in the immune system. *Journal of immunology (Baltimore, Md. : 1950)*, 190(5), pp.1911–8.
- Avery, O.T., Macleod, C.M. & McCarty, M., 1944. Studies on the chemical nature of the substance inducing transformation of pneumococcal types: induction of transformation by a desoxyribonucleic acid fraction isolated from pneumococcus type III. *The Journal of experimental medicine*, 79(2), pp.137–58.
- Azmi, A.S. et al., 2011. Emerging Bcl-2 inhibitors for the treatment of cancer. *Expert opinion on emerging drugs*, 16(1), pp.59–70.

**B**

- Barlan, A.U. et al., 2011. Adenovirus membrane penetration activates the NLRP3 inflammasome. *Journal of virology*, 85(1), pp.146–55.
- Barros, S. et al., 2013. The redox state of cytochrome c modulates resistance to methotrexate in human MCF7 breast cancer cells. *PloS one*, 8(5), p.e63276.
- Bartlett, D.W. & Davis, M.E., 2007. Effect of siRNA nuclease stability on the in vitro and in vivo kinetics of siRNA-mediated gene silencing. *Biotechnology and Bioengineering*, 97(4), pp.909–921.
- Bartok, E. et al., 2013. iGLuc: a luciferase-based inflammasome and protease activity reporter. *Nature methods*, 10(2), pp.147–54.
- Bates, P.J. et al., 2010. Discovery and Development of the G-rich Oligonucleotide AS1411 as a Novel Treatment for Cancer. *Exp Mol Pathol.*, 86(3), pp.151–164.
- Belotserkovskii, B.P. et al., 2007. A triplex-forming sequence from the human c-MYC promoter interferes with DNA transcription. *The Journal of biological chemistry*, 282(44), pp.32433–41.
- Bishop, J.S. et al., 1996. Intramolecular G-quartet motifs confer nuclease resistance to a potent anti-HIV oligonucleotide. *The Journal of biological chemistry*, 271(10), pp.5698–703.
- Blume, S.W. et al., 1999. The integral divalent cation within the intermolecular purine\*purine. pyrimidine structure: a variable determinant of the potential for and



characteristics of the triple helical association. *Nucleic acids research*, 27(2), pp.695–702.

Bold, R.J., Chandra, J. & McConkey, D.J., 1999. Gemcitabine-induced programmed cell death (apoptosis) of human pancreatic carcinoma is determined by Bcl-2 content. *Annals of surgical oncology*, 6(3), pp.279–85.

Breaker, R.R., 2004. Natural and engineered nucleic acids as tools to explore biology. *Nature*, 432(7019), pp.838–845.

Brown, J. et al., 2011. TLR-signaling networks: an integration of adaptor molecules, kinases, and cross-talk. *Journal of dental research*, 90(4), pp.417–27.

## C

Coma, S. et al., 2005. Strand Displacement of Double-Stranded DNA by Triplex-Forming Antiparallel Purine-Hairpins. , 283, pp.269–283.

Coma, S. et al., 2004. Use of siRNAs and antisense oligonucleotides against survivin RNA to inhibit steps leading to tumor angiogenesis. *Oligonucleotides*, 14(2), pp.100–13.

Conradt, L. et al., 2013. Mdm2 inhibitors synergize with topoisomerase II inhibitors to induce p53-independent pancreatic cancer cell death. *International journal of cancer. Journal international du cancer*, 132(10), pp.2248–57.

Cox, D.B.T., Platt, R.J. & Zhang, F., 2015. Therapeutic genome editing: prospects and challenges. *Nature Medicine*, 21(2), pp.121–131.

Culver, K.W. et al., 1999. Correction of chromosomal point mutations in human cells with bifunctional oligonucleotides. *Nature biotechnology*, 17(10), pp.989–93.

## D

Davis, B.K., Wen, H. & Ting, J.P.-Y., 2011. The inflammasome NLRs in immunity, inflammation, and associated diseases. *Annual review of immunology*, 29, pp.707–35.

Deng, C. et al., 2013. Suppression of cell proliferation and collagen production in cultured human hypertrophic scar fibroblasts by Sp1 decoy oligodeoxynucleotide. *Molecular medicine reports*, 7(3), pp.785–90.

Dirin, M. & Winkler, J., 2013. Influence of diverse chemical modifications on the ADME characteristics and toxicology of antisense oligonucleotides. *Expert opinion on biological therapy*, 13(6), pp.875–88.

Duca, M. et al., 2008. The triple helix: 50 years later, the outcome. *Nucleic acids research*, 36(16), pp.5123–38.

Dupont Jensen, J. et al., 2011. PIK3CA mutations may be discordant between primary and corresponding metastatic disease in breast cancer. *Clinical cancer research : an official journal of the American Association for Cancer Research*, 17(4), pp.667–77.

Dyxhoorn, D.M., Palliser, D. & Lieberman, J., 2006. The silent treatment: siRNAs as small molecule drugs. *Gene therapy*, 13(6), pp.541–52.

## E

Ellington, A.D. & Szostak, J.W., 1990. In vitro selection of RNA molecules that bind specific ligands. *Nature*, 346(6287), pp.818–22.

## F

- Faruqi, a F. et al., 2000. Triple-helix formation induces recombination in mammalian cells via a nucleotide excision repair-dependent pathway. *Molecular and cellular biology*, 20(3), pp.990–1000.
- Felsenfeld, G., Davies, D.R. & Rich, A., 1957. FORMATION OF A THREE-STRANDED POLYNUCLEOTIDE MOLECULE. *Journal of the American Chemical Society*, 79(8), pp.2023–2024.
- Ferreira, C.S.M. et al., 2008. DNA aptamers against the MUC1 tumour marker: Design of aptamer-antibody sandwich ELISA for the early diagnosis of epithelial tumours. *Analytical and Bioanalytical Chemistry*, 390(4), pp.1039–1050.
- Fire, A. et al., 1998. Potent and specific genetic interference by double-stranded RNA in *Caenorhabditis elegans*. *Nature*, 391(6669), pp.806–11.
- Fitzgerald, K. a et al., 2003. IKKepsilon and TBK1 are essential components of the IRF3 signaling pathway. *Nature immunology*, 4(5), pp.491–496.
- Fu, Y. et al., 2013. High-frequency off-target mutagenesis induced by CRISPR-Cas nucleases in human cells. *Nature biotechnology*, 31(9), pp.822–6.
- Fujihara, J. et al., 2012. Comparative biochemical properties of vertebrate deoxyribonuclease I. *Comparative Biochemistry and Physiology Part B: Biochemistry and Molecular Biology*, 163(3-4), pp.263–273.

## G

- Geary, R.S. et al., 2015. Pharmacokinetics, biodistribution and cell uptake of antisense oligonucleotides. *Advanced Drug Delivery Reviews*, 87, pp.46–51.
- Giovanella, B.C. et al., 1989. DNA topoisomerase I--targeted chemotherapy of human colon cancer in xenografts. *Science (New York, N.Y.)*, 246(4933), pp.1046–8.
- Goldwasser, F. et al., 1996. Correlations between S and G2 arrest and the cytotoxicity of camptothecin in human colon carcinoma cells. *Cancer research*, 56(19), pp.4430–7.
- Goni, J.R., 2004. Triplex-forming oligonucleotide target sequences in the human genome. *Nucleic Acids Research*, 32(1), pp.354–360.
- Goñi, J.R. et al., 2006. Exploring the reasons for the large density of triplex-forming oligonucleotide target sequences in the human regulatory regions. *BMC genomics*, 7, p.63.
- Goodchild, J.M., *Therapeutic oligonucleotides*,
- Goodman, T.T., Olive, P.L. & Pun, S.H., 2007. Increased nanoparticle penetration in collagenase-treated multicellular spheroids. *International journal of nanomedicine*, 2(2), pp.265–74.
- Grimm, D. et al., 2006. Fatality in mice due to oversaturation of cellular microRNA/short hairpin RNA pathways. *Nature*, 441(7092), pp.537–41.
- Gu, L. et al., 2008. MDM2 antagonist nutlin-3 is a potent inducer of apoptosis in pediatric acute lymphoblastic leukemia cells with wild-type p53 and overexpression of MDM2. *Leukemia*, 22(4), pp.730–9.
- Guglielmi, A. et al., 2004. Phase II study of a triplet regimen in advanced colorectal cancer using methotrexate, oxaliplatin and 5-fluorouracil. *British journal of cancer*, 91(8), pp.1428–33.

**H**

- Hall, C. et al., 2013. Bcl-2 family of proteins as therapeutic targets in genitourinary neoplasms. *Clinical genitourinary cancer*, 11(1), pp.10–9.
- Hanagata, N., 2012. Structure-dependent immunostimulatory effect of CpG oligodeoxynucleotides and their delivery system. *International Journal of Nanomedicine*, 7, p.2181.
- Hanahan, D. & Weinberg, R. a., 2011. Hallmarks of cancer: the next generation. *Cell*, 144(5), pp.646–74.
- Hanahan, D. & Weinberg, R.A., 2000. The hallmarks of cancer. *Cell*, 100(1), pp.57–70.
- Hartman, D.A. et al., 1992. Intermolecular triplex formation distorts the DNA duplex in the regulatory region of human papillomavirus type-11. *The Journal of biological chemistry*, 267(8), pp.5488–94.
- Hauptenthal, J. et al., 2006. Inhibition of RNAse A family enzymes prevents degradation and loss of silencing activity of siRNAs in serum. *Biochemical Pharmacology*, 71(5), pp.702–710.
- Henry, S.P. et al., 2014. Mechanism of Alternative Complement Pathway Dysregulation by a Phosphorothioate Oligonucleotide in Monkey and Human Serum. *Nucleic acid therapeutics*, 00(0), pp.1–10.
- Herdewijn, P., 2000. Heterocyclic Modifications of Oligonucleotides and Antisense Technology. *Antisense and Nucleic Acid Drug Development*, 10(4), pp.297–310.
- Hobbs, S.K. et al., 1998. Regulation of transport pathways in tumor vessels: role of tumor type and microenvironment. *Proceedings of the National Academy of Sciences of the United States of America*, 95(8), pp.4607–12.
- Hoogsteen, K., 1963. The crystal and molecular structure of a hydrogen-bonded complex between 1-methylthymine and 9-methyladenine. *Acta Crystallographica*, 16(9), pp.907–916.
- Hornung, V. et al., 2005. Sequence-specific potent induction of IFN-alpha by short interfering RNA in plasmacytoid dendritic cells through TLR7. *Nature medicine*, 11(3), pp.263–70.
- Hosoya, T., 1999. Sequence-specific inhibition of a transcription factor by circular dumbbell DNA oligonucleotides.

**I**

- Ishii, K.J. et al., 2006. A Toll-like receptor-independent antiviral response induced by double-stranded B-form DNA. *Nature immunology*, 7(1), pp.40–48.

**J**

- Jang, S.H. et al., 2003. Drug delivery and transport to solid tumors. *Pharmaceutical research*, 20(9), pp.1337–50.
- Judge, A.D. et al., 2005. Sequence-dependent stimulation of the mammalian innate immune response by synthetic siRNA. *Nature biotechnology*, 23(4), pp.457–62.

**K**

- Kalish, J.M. et al., 2005. Triplex-induced recombination and repair in the pyrimidine motif. *Nucleic acids research*, 33(11), pp.3492–502.

- Khan, A. a et al., 2009. Transfection of small RNAs globally perturbs gene regulation by endogenous microRNAs. *Nature biotechnology*, 27(6), pp.549–555.
- Kole, R., Krainer, A.R. & Altman, S., 2012. RNA therapeutics: beyond RNA interference and antisense oligonucleotides. *Nature reviews. Drug discovery*, 11(2), pp.125–40.
- Kool, E.T., 1991. Molecular recognition by circular oligonucleotides: increasing the selectivity of DNA binding. *Journal of the American Chemical Society*, 113(16), pp.6265–6266.

## L

- Lander, E.S. et al., 2001. Initial sequencing and analysis of the human genome. *Nature*, 409(6822), pp.860–921.
- Lane, D.P., Cheok, C.F. & Lain, S., 2010. p53-based cancer therapy. *Cold Spring Harbor perspectives in biology*, 2(9), p.a001222.
- Layzer, J.M. et al., 2004. In vivo activity of nuclease-resistant siRNAs. *RNA (New York, N.Y.)*, 10(5), pp.766–71.
- Li, Y. et al., 2012. Delivery of nanomedicines to extracellular and intracellular compartments of a solid tumor. *Advanced drug delivery reviews*, 64(1), pp.29–39.
- Li, Y., Casey, S.C. & Felsher, D.W., 2014. Inactivation of MYC reverses tumorigenesis. *Journal of internal medicine*, 276(1), pp.52–60.
- Lin, S. et al., 2014. Enhanced homology-directed human genome engineering by controlled timing of CRISPR/Cas9 delivery. *eLife*, 3, p.e04766.
- Lundin, K.E., Gissberg, O. & Smith, C.I.E., 2015. Oligonucleotide Therapies: The Past and the Present. *Human gene therapy*, 26(8), pp.475–85.

## M

- Mahlknecht, G. et al., 2013. Aptamer to ErbB-2 / HER2 enhances degradation of the target and inhibits tumorigenic growth. , 2013.
- Matsuda, H. et al., 2006. Development of gene silencing pyrrole-imidazole polyamide targeting the TGF-beta1 promoter for treatment of progressive renal diseases. *Journal of the American Society of Nephrology : JASN*, 17(2), pp.422–432.
- McWhirter, S.M. et al., 2004. IFN-regulatory factor 3-dependent gene expression is defective in Tbk1-deficient mouse embryonic fibroblasts. *Proceedings of the National Academy of Sciences of the United States of America*, 101(1), pp.233–8.
- Mencia, N. et al., 2011. Underexpression of miR-224 in methotrexate resistant human colon cancer cells. *Biochemical pharmacology*, 82(11), pp.1572–82.
- Mencía, N. et al., 2010. Overexpression of S100A4 in human cancer cell lines resistant to methotrexate. *BMC cancer*, 10, p.250.
- Mita, M.M., Mita, A. & Rowinsky, E.K., 2003. The molecular target of rapamycin (mTOR) as a therapeutic target against cancer. *Cancer biology & therapy*, 2(4 Suppl 1), pp.S169–77.
- Miyashita, T. & Reed, J.C., 1993. Bcl-2 oncoprotein blocks chemotherapy-induced apoptosis in a human leukemia cell line. *Blood*, 81(1), pp.151–7.
- Moreno, P.M.D. & Pêgo, A.P., 2014. Therapeutic antisense oligonucleotides against cancer: hurdling to the clinic. *Frontiers in Chemistry*, 2(October), pp.1–7.
- Mross, K. et al., 2004. A phase I clinical and pharmacokinetic study of the camptothecin glycoconjugate, BAY 38-3441, as a daily infusion in patients with advanced solid

tumors. *Annals of oncology : official journal of the European Society for Medical Oncology / ESMO*, 15(8), pp.1284–94.

Müller, S., 2015. Engineering of ribozymes with useful activities in the ancient RNA world. *Annals of the New York Academy of Sciences*, 1341, pp.54–60.

Mussolino, C. et al., 2011. A novel TALE nuclease scaffold enables high genome editing activity in combination with low toxicity. *Nucleic acids research*, 39(21), pp.9283–93.

## N

Nakaya, T. et al., 1997. Decoy approach using RNA-DNA chimera oligonucleotides to inhibit the regulatory function of human immunodeficiency virus type 1 Rev protein. *Antimicrobial agents and chemotherapy*, 41(2), pp.319–25.

Netti, P.A. et al., 2000. Role of extracellular matrix assembly in interstitial transport in solid tumors. *Cancer research*, 60(9), pp.2497–503.

Nicolas, M. et al., 2001. Cloning and Characterization of the 5'-Flanking Region of the Human Transcription Factor Sp1 Gene. *Journal of Biological Chemistry*, 276(25), pp.22126–22132.

## O

Oleaga, C. et al., 2012. Identification of novel Sp1 targets involved in proliferation and cancer by functional genomics. *Biochemical pharmacology*, 84(12), pp.1581–91.

Omidi, Y., Barar, J. & Coukos, G., 2013. Cancer Gene Therapy : Targeted Genomedicines, Novel Gene Therapy Approaches, Prof. Ming Wei (Ed.), ISBN: 978-953-51-0966-2, InTech, DOI: 10.5772/54739. Available from: <http://www.intechopen.com/books/novel-gene-therapy-approaches/cancer-gene-therapy-targeted-genomedicines>

## P

Pan, C.Q. et al., 1998. Mutational analysis of human DNase I at the DNA binding interface: implications for DNA recognition, catalysis, and metal ion dependence. *Protein science : a publication of the Protein Society*, 7(3), pp.628–36.

Peñuelas, S., Noé, V. & Ciudad, C.J., 2005. Modulation of IMPDH2, survivin, topoisomerase I and vimentin increases sensitivity to methotrexate in HT29 human colon cancer cells. *The FEBS journal*, 272(3), pp.696–710.

Powell, A.A. et al., 2012. Single cell profiling of circulating tumor cells: transcriptional heterogeneity and diversity from breast cancer cell lines. *PloS one*, 7(5), p.e33788.

Prakash, G. & Kool, E.T., 1992. Structural effects in the recognition of DNA by circular oligonucleotides. *Journal of the American Chemical Society*, 114(9), pp.3523–3527.

Praseuth, D., Guieysse, A.L. & He, C., 1999. Triple helix formation and the antigene strategy for sequence-specific control of gene expression. *Biochimica et Biophysica Acta*, 1489, pp. 181-206.

## R



- Ray, P. et al., 2012. Aptamer-mediated delivery of chemotherapy to pancreatic cancer cells. *Nucleic acid therapeutics*, 22(5), pp.295–305.
- Rodríguez, L. et al., 2015. Improved design of PPRHs for gene silencing. *Molecular pharmaceutics*, 12(3), pp.867–77.
- Rodríguez, L. et al., 2013. Polypurine reverse Hoogsteen hairpins as a gene therapy tool against survivin in human prostate cancer PC3 cells in vitro and in vivo. *Biochemical Pharmacology*, 86(11), pp.1541–1554.
- Rodríguez, M. et al., 2002. Development and effects of immunoliposomes carrying an antisense oligonucleotide against DHFR RNA and directed toward human breast cancer cells overexpressing HER2. *Antisense & nucleic acid drug development*, 12(5), pp.311–325.

## S

- Sadio, A. et al., 2014. Modified-Chitosan/siRNA Nanoparticles Downregulate Cellular CDX2 Expression and Cross the Gastric Mucus Barrier F. X. Real, ed. *PLoS ONE*, 9(6), p.e99449.
- Safari, J. & Zarnegar, Z., 2014. Advanced drug delivery systems: Nanotechnology of health design A review. *Journal of Saudi Chemical Society*, 18(2), pp.85–99.
- Selga, E. et al., 2009. Networking of differentially expressed genes in human cancer cells resistant to methotrexate. *Genome medicine*, 1(9), p.83.
- Selga, E. et al., 2008. Role of caveolin 1, E-cadherin, Enolase 2 and PKCalpha on resistance to methotrexate in human HT29 colon cancer cells. *BMC medical genomics*, 1, p.35.
- Seong, J.-H. et al., 2006. Polyethylenimine-based antisense oligodeoxynucleotides of IL-4 suppress the production of IL-4 in a murine model of airway inflammation. *The Journal of Gene Medicine*, 8(3), pp.314–323.
- Seymour, L.W., 1992. Passive tumor targeting of soluble macromolecules and drug conjugates. *Critical reviews in therapeutic drug carrier systems*, 9(2), pp.135–87.
- Shigdar, S. et al., 2013. The Use of Sensitive Chemical Antibodies for Diagnosis: Detection of Low Levels of Epcam in Breast Cancer. *PLoS ONE*, 8(2).
- Sioud, M., 2005. Induction of inflammatory cytokines and interferon responses by double-stranded and single-stranded siRNAs is sequence-dependent and requires endosomal localization. *Journal of molecular biology*, 348(5), pp.1079–90.
- Song, X. et al., 2015. Targeted delivery of doxorubicin to breast cancer cells by aptamer functionalized DOTAP/DOPE liposomes. *Oncology Reports*, 34(4), pp.1953–1960.
- Stetson, D.B. & Medzhitov, R., 2006. Recognition of cytosolic DNA activates an IRF3-dependent innate immune response. *Immunity*, 24(1), pp.93–103.
- Stewart, A.J. et al., 1996. Enhanced biological activity of antisense oligonucleotides complexed with glycosylated poly-L-lysine. *Molecular pharmacology*, 50(6), pp.1487–94.
- Suzuki, J.-I. et al., 2012. Applications of nucleic acid drugs for organ transplantation. *Current topics in medicinal chemistry*, 12(15), pp.1608–12.

## T

- Thiel, K.W. et al., 2012. Delivery of chemo-sensitizing siRNAs to HER2+-breast cancer cells using RNA aptamers. *Nucleic Acids Research*, 40(13), pp.6319–6337.

- Thompson, J.D. et al., 2012. Toxicological and pharmacokinetic properties of chemically modified siRNAs targeting p53 RNA following intravenous administration. *Nucleic acid therapeutics*, 22(4), pp.255–64.
- Tokunaga, E. et al., 2008. Deregulation of the Akt pathway in human cancer. *Curr Cancer Drug Targets*, 8(1), pp.27–36.
- Tuerk, C. & Gold, L., 1990. Systematic evolution of ligands by exponential enrichment: RNA ligands to bacteriophage T4 DNA polymerase. *Science (New York, N.Y.)*, 249(4968), pp.505–10.
- Turner, J.J. et al., 2007. MALDI-TOF mass spectral analysis of siRNA degradation in serum confirms an RNase A-like activity. *Mol. Biosyst.*, 3(1), pp.43–50.

## V

- Vassilev, L.T. et al., 2004. In vivo activation of the p53 pathway by small-molecule antagonists of MDM2. *Science (New York, N.Y.)*, 303(5659), pp.844–8.
- Vassilev, L.T., 2004. Small-molecule antagonists of p53-MDM2 binding: research tools and potential therapeutics. *Cell cycle (Georgetown, Tex.)*, 3(4), pp.419–21.
- Van Vlerken, L.E., Vyas, T.K. & Amiji, M.M., 2007. Poly(ethylene glycol)-modified nanocarriers for tumor-targeted and intracellular delivery. *Pharmaceutical research*, 24(8), pp.1405–14.
- Vogelstein, B., Lane, D. & Levine, A.J., 2000. Surfing the p53 network. *Nature*, 408(6810), pp.307–10.

## W

- Watson, James D; Crick, F.H., 1953. Molecular structure of nucleic acids; a structure for deoxyribose nucleic acid. - PubMed - NCBI. *Nature*, pp.737–8.
- Wijshake, T., Baker, D.J. & van de Sluis, B., 2014. Endonucleases: new tools to edit the mouse genome. *Biochimica et biophysica acta*, 1842(10), pp.1942–1950.
- Wullschleger, S., Loewith, R. & Hall, M.N., 2006. TOR Signaling in Growth and Metabolism. *Cell*, 124(3), pp.471–484.

## Y

- Yachida, S. et al., 2010. Distant metastasis occurs late during the genetic evolution of pancreatic cancer. *Nature*, 467(7319), pp.1114–7.
- Yang, F. et al., 2013. Animal toxicity of hairpin pyrrole-imidazole polyamides varies with the turn unit. *Journal of Medicinal Chemistry*, 56(18), pp.7449–7457.
- Yoneyama, M. & Fujita, T., 2010. Recognition of viral nucleic acids in innate immunity. *Reviews in medical virology*, 20(1), pp.4–22.

## Z

- Zaghloul, E.M. et al., 2011. Optimizing anti-gene oligonucleotide “Zorro-LNA” for improved strand invasion into duplex DNA. *Nucleic Acids Research*, 39(3), pp.1142–1154.
- Zamecnik, P.C. & Stephenson, M.L., 1978. Inhibition of Rous sarcoma virus replication and cell transformation by a specific oligodeoxynucleotide. *Proceedings of the National Academy of Sciences of the United States of America*, 75(1), pp.280–4.

- Zampino, M.G. et al., 2006. Oxaliplatin combined with 5-fluorouracil and methotrexate in advanced colorectal cancer. *Anticancer research*, 26(3B), pp.2425–8.
- Zuker, M., 2003. Mfold web server for nucleic acid folding and hybridization prediction. *Nucleic acids research*, 31(13), pp.3406–15.





## APPENDIX



I have collaborated in the performance of experiments related to PPRHs development that led to the following publications:

**ARTICLE IV:**

**Polypurine Reverse Hoogsteen hairpins as a gene therapy tool against *surviving* in human prostate cancer PC3 cells *in vitro* and *in vivo*.**

Laura Rodríguez, Xenia Villalobos, Sheila Dakhel, Laura Padilla, Rosa Hervas, José Luis Hernández, Carlos J. Ciudad, Véronique Noé

Biochemical Pharmacology, 2013, 86, 1541-1554 (Impact factor: 4,650)





Contents lists available at ScienceDirect

## Biochemical Pharmacology

journal homepage: [www.elsevier.com/locate/biochempharm](http://www.elsevier.com/locate/biochempharm)

## Polypurine reverse Hoogsteen hairpins as a gene therapy tool against *survivin* in human prostate cancer PC3 cells *in vitro* and *in vivo*



Laura Rodríguez<sup>a</sup>, Xenia Villalobos<sup>a</sup>, Sheila Dakhel<sup>b</sup>, Laura Padilla<sup>b</sup>, Rosa Hervas<sup>b</sup>, Jose Luis Hernández<sup>b</sup>, Carlos J. Ciudad<sup>a,\*</sup>, Véronique Noé<sup>a</sup>

<sup>a</sup> Department of Biochemistry and Molecular Biology, School of Pharmacy, University of Barcelona, 08028 Barcelona, Spain

<sup>b</sup> Biomed Division of LEITAT Technological Center, 08028 Barcelona, Spain

## ARTICLE INFO

## Article history:

Received 24 July 2013

Accepted 12 September 2013

Available online 23 September 2013

## Keywords:

PPRH

*Survivin*

Gene silencing

Xenograft

Prostate cancer

## ABSTRACT

As a new approach for gene therapy, we recently developed a new type of molecule called polypurine reverse Hoogsteen hairpins (PPRHs). We decided to explore the *in vitro* and *in vivo* effect of PPRHs in cancer choosing *survivin* as a target since it is involved in apoptosis, mitosis and angiogenesis, and overexpressed in different tumors. We designed four PPRHs against the *survivin* gene, one of them directed against the template strand and three against different regions of the coding strand. These PPRHs were tested in PC3 prostate cancer cells in an *in vitro* screening of cell viability and apoptosis. PPRHs against the promoter sequence were the most effective and caused a decrease in *survivin* mRNA and protein levels. We confirmed the binding between the selected PPRHs and their target sequences in the *survivin* gene. In addition we determined that both the template- and the coding-PPRH targeting the *survivin* promoter were interfering with the binding of transcription factors Sp1 and GATA-3, respectively. Finally, we conducted two *in vivo* efficacy assays using the Coding-PPRH against the *survivin* promoter and performing two routes of administration, namely intratumoral and intravenous, in a subcutaneous xenograft tumor model of PC3 prostate cancer cells. The results showed that the chosen Coding-PPRH proved to be effective in decreasing tumor volume, and reduced the levels of *survivin* protein and the formation of blood vessels. These findings represent the preclinical proof of principle of PPRHs as a new silencing tool for cancer gene therapy.

© 2013 Elsevier Inc. All rights reserved.

### 1. Introduction

Nowadays, modulation of gene expression by nucleic acids has become a routine tool for laboratory research. Different molecules are used as gene modulating tools, such as antisense oligonucleotides (aODNs) or small-interference RNAs (siRNAs). In addition, we have recently described the development of a new type of molecules named polypurine reverse Hoogsteen hairpins (PPRHs), capable of decreasing gene expression.

PPRHs are non-modified DNA molecules formed by two antiparallel polypurine stretches linked by a five-thymidine loop

[1,2]. The intramolecular linkage consists of reverse Hoogsteen bonds between adenines and guanines. Then, PPRHs bind to their polypyrimidine target sequence by Watson–Crick bonds forming a triplex structure and displacing the fourth strand of the dsDNA [2].

To design a PPRH, it is essential to find polypyrimidine/polypurine stretches within the gene sequence. These sequences are more common in the genome than it was predicted by random models [3]; they are mostly located in non-coding sequences, including promoters and introns, although they can also be found in coding regions at low frequency. The target sequences do not have to be pure stretches of polypyrimidines and may contain a small number of purine interruptions, since the usage of adenines as a wild card in the PPRH overcomes the instability caused by the interruptions, thus maintaining a functional binding to the target [4].

In previous studies, we described two types of PPRHs with the ability to bind to a target sequence located either in the template DNA strand, Template-PPRHs [4] or in the coding DNA strand, Coding-PPRHs [5]. Each of these molecules is able, through different mechanisms, to decrease gene expression. On the one hand, Template-PPRHs interfere with the transcription

**Abbreviations:** aODN, antisense oligonucleotide; CRPC, castration-resistant prostatic cancer; DOTAP, *N*-[1-(2,3-dioleoyloxy)propyl]-*N,N,N*-trimethylammonium methylsulfate; EMSA, electrophoretic mobility shift assay; MTT, (3-(4,5-dimethylthiazol-2-yl)-2,5-diphenyltetrazolium bromide; NE, nuclear extract; PPRHs, Polypurine Reverse Hoogsteen hairpins.

\* Corresponding author. Tel.: +34 93 403 4455; fax: +34 93 402 4520.

E-mail addresses: [laura.rodriguez@ub.edu](mailto:laura.rodriguez@ub.edu) (L. Rodríguez), [xvillalobos@ub.edu](mailto:xvillalobos@ub.edu) (X. Villalobos), [sdakhel@leitat.org](mailto:sdakhel@leitat.org) (S. Dakhel), [lpadilla@leitat.org](mailto:lpadilla@leitat.org) (L. Padilla), [rhervas@leitat.org](mailto:rhervas@leitat.org) (R. Hervas), [jlhernandez@leitat.org](mailto:jlhernandez@leitat.org) (J.L. Hernández), [ciudad@ub.edu](mailto:ciudad@ub.edu), [cjciudad@gmail.com](mailto:cjciudad@gmail.com) (C.J. Ciudad), [vnoe@ub.edu](mailto:vnoe@ub.edu) (V. Noé).

process, thus decreasing the mRNA and protein levels of the target gene. On the other hand, Coding-PPRHs are able to bind, not only to the coding strand of the DNA but also to the mRNA, because both have the same sequence and orientation. A Coding-PPRH against an intron sequence of the *dhfr* gene caused a splicing alteration by preventing the binding of U2AF65, a pre-mRNA splicing factor, ultimately decreasing gene expression [5]. We proved the efficacy of different Template-PPRHs against genes related to proliferation in breast cancer: *dhfr*, *telomerase* and *survivin* [4].

We decided to further explore the *in vitro* and *in vivo* effects of PPRHs against *survivin*, since it is an anti-apoptotic protein, also involved in mitosis and angiogenesis [6]. *Survivin* is overexpressed in different tumors, such as prostate [7], lung [8], breast [9], colon [10,11] stomach [12], esophagus [13], pancreas [14], bladder [15], uterus [16], ovary [17], large-cell non-Hodgkin's lymphoma [18], leukemias [19], neuroblastoma [20], melanoma [21] and non-melanoma skin cancers [22]. However, *survivin* levels are undetectable in most differentiated normal tissues, with the exception of thymus [7], CD34+ bone-marrow-derived stem cells at low levels [23], and the basal colonic epithelium [24]. Moreover, *survivin* expression correlates to shorter survival [8–10,13,17,18], resistance to chemotherapy [13,25], worse disease progression [18,20], and higher rates of recurrence [15]. All of the above reasons make *survivin* a good anticancer target and prognosis marker [26].

We focused on prostate cancer, the second cause of death related to cancer in men in the Western world. Given that the treatment options for this disease are limited and barely effective, targeted-therapy has been under development [27]. Examples of this type of therapy are either small molecules or antibodies against tyrosine kinase receptors, such as IGF-1R, EGFR and FGFR or against genes involved in important hallmarks for cancer, such as anti-apoptotic (*survivin*) or proangiogenic proteins (VEGFR) [27].

*Survivin* is considered a good target to inhibit in prostate cancer for its association with androgen resistance and with aggressive phenotypes. In fact, several Phase-II clinical trials using either small-molecule inhibitors – YM155 – or antisense therapy – LY2181308 – have been conducted for castration-resistant prostatic cancer (CRPC), after showing apoptosis in prostate cancer cell lines and in xenografts [11,28]. However, these two molecules showed modest or lack of activity in Phase II clinical trials, and are currently under investigation in combination with docetaxel [29,30].

Therefore, the aim of this work was to assess the efficacy of PPRHs as a preclinical proof of principle for its application as a new gene therapy approach using a subcutaneous xenograft tumor model of PC3 prostate cancer cells.

## 2. Materials and methods

### 2.1. Design and usage of PPRHs

Both Template and Coding-PPRHs were used in these experiments. To find polypyrimidine sequences in the target gene, we used the Triplex-Forming Oligonucleotide Target Sequence Search software ([spi.mdanderson.org/tfo/](http://spi.mdanderson.org/tfo/)), M.D. Anderson Cancer Center, Houston, TX). Once we had selected proper candidates, BLAST analyses were performed to confirm specificity of the designed PPRHs and the ones with less unintended targets were chosen. PPRHs were synthesized as non-modified oligodeoxynucleotides by Sigma-Aldrich (Madrid, Spain) (0.05 mmol scale). Lyophilized PPRHs were resuspended in sterile Tris-EDTA buffer (1 mM EDTA and 10 mM Tris, pH 8.0; AppliChem, Barcelona, Spain) and stored at  $-20^{\circ}\text{C}$ .

### 2.2. Preparation of polypurine/polypyrimidine duplexes

The duplexes to be targeted by the hairpins were formed by mixing 25  $\mu\text{g}$  of each single-stranded (ss) polypurine and polypyrimidine oligodeoxynucleotides with 150 mM NaCl (AppliChem, Barcelona, Spain) and incubated at  $90^{\circ}\text{C}$  for 5 min as described in de Almagro et al. [4].

### 2.3. Oligodeoxynucleotide labeling

One hundred nanograms of PPRHs or double stranded (ds) oligodeoxynucleotides was 5'-end-labeled with T4 polynucleotide kinase (New England Biolabs, Beverly, MA) and  $[\gamma\text{-}^{32}\text{P}]\text{ATP}$  (3000 Ci/mmol, Perkin Elmer, Madrid, Spain) as described in de Almagro et al. [4].

### 2.4. DNA-PPRH binding analysis

Binding of PPRHs to their target sequence was analyzed using two approaches: (a) by incubation of the radiolabeled PPRHs (20,000 cpm) in the presence or absence of unlabelled ds target sequence, or (b) by incubation of the radiolabeled ds target sequence with the unlabelled PPRH. In both cases, a buffer containing 10 mM  $\text{MgCl}_2$ , 100 mM NaCl, and 50 mM HEPES, pH 7.2 was used (AppliChem, Barcelona, Spain). Binding reactions (20  $\mu\text{l}$ ) were incubated for 30 min at  $37^{\circ}\text{C}$  before electrophoresis, which was performed on non denaturing 12% polyacrylamide gels (PAGE) containing 10 mM  $\text{MgCl}_2$ , 5% glycerol, and 50 mM HEPES, pH 7.2 (AppliChem, Barcelona, Spain). Gels were electrophoresed for 3–4 h at 10 V/cm at  $4^{\circ}\text{C}$ , dried, exposed to Europium plates OVN and analyzed using a Storm 840 Phosphorimager (Molecular Dynamics, Sunnyvale, CA). Binding specificity was tested by addition of 1  $\mu\text{g}$  of poly-dI-dC (Sigma-Aldrich, Madrid, Spain) to the binding reaction.

### 2.5. Electrophoretic mobility shift assay (EMSA)

To analyze the binding of transcription factors to the target sequences of the chosen PPRHs within the *survivin* promoter, EMSA was performed using HeLa nuclear extracts. HeLa cells were harvested by trypsinization, centrifuged at  $800 \times g$  for 5 min and resuspended in hypotonic buffer (15 mM NaCl, 60 mM KCl, 0.5 mM EDTA, 1 mM PMSF, 1 mM  $\beta$ -mercaptoethanol and 15 mM Tris-HCl, pH 8.0; AppliChem, Barcelona, Spain) for 5 min. Then, cells were centrifuged again at  $800 \times g$  for 5 min and washed with hypotonic buffer containing 0.05% Triton (Sigma-Aldrich, Madrid, Spain) to lyse the cells. After centrifugation for 5 min at  $1200 \times g$ , nuclei were washed with hypotonic buffer once more without triton, and resuspended in hypotonic buffer containing a final concentration of 360 mM KCl (AppliChem, Barcelona, Spain). Sample tubes were rotated (12 rpm) with a  $45^{\circ}$  inclination at  $4^{\circ}\text{C}$  for 45 min. Finally, nuclear extracts were separated from chromatin after centrifugation at  $100,000 \times g$  for 30 min.

The radiolabeled ds target sequences (20,000 cpm) were incubated in 20  $\mu\text{l}$  reaction mixtures also containing 1  $\mu\text{g}$  Herring Sperm DNA (Invitrogen, Barcelona, Spain) as unspecific competitor, 2  $\mu\text{g}$  nuclear extract protein, 5% glycerol, 4 mM  $\text{MgCl}_2$ , 60 mM KCl and 25 mM Tris-HCl, pH 8.0 (AppliChem, Barcelona, Spain). After a pre-incubation of 15 min, the probe was added for 15 more minutes. Then samples were resolved by gel electrophoresis (5% polyacrylamide/bisacrylamide, 5% glycerol, 1 mM EDTA and 45 mM Tris-borate, pH 8.0; AppliChem, Barcelona, Spain). In competition experiments, ds DNA consensus sequences (Sp1: 5'-ATTGATCGGGGCGGGCGAGC-3'; GATA: 5'-CACTTGATAACA-GAAAGTGATAACTCT-3'; non-related: 5'-AGGAAGTTCGGTCC-CAGCCA-3') for the putative transcription factors determined by

the MATCH™ software, as well as the different PPRHs, were added in excess (ranging between 10- and 200-fold relative to the radiolabeled probe) to the reaction mixture. In the supershift assays, 2 µg of rabbit polyclonal antibodies against either Sp1 (PEP-2X) or Sp3 (D-20X), GATA-2 (H-116X) or GATA-3 (H-48X) (Santa Cruz Biotechnology, Heidelberg, Germany), was added to the reaction mixture 15 min before the electrophoresis. The dried gel was exposed to Europium plates OVN and analyzed using a Storm 840 Phosphorimager (Molecular Dynamics, GE Healthcare Life Sciences, Barcelona, Spain).

## 2.6. Cell culture

PC3 prostate adenocarcinoma cells (ECACC) and HeLa cervical cancer cells (ATCC) were grown in Ham's F-12 medium supplemented with 7% fetal bovine serum (FBS, GIBCO, Invitrogen, Barcelona, Spain) and incubated at 37 °C in a humidified 5% CO<sub>2</sub> atmosphere. Human Umbilical Vein Endothelial Cells (HUVECs, Lonza, Barcelona, Spain) were cultured in Endothelial cell Basal Medium EBM (Lonza, Barcelona, Spain), supplemented with hEGF, hydrocortisone, brain bovine extract and gentamicine (EGM, Lonza, Barcelona, Spain), and 10% FCS (Invitrogen, Barcelona, Spain). 4T1 breast cancer and CT26 colon cancer cell lines (ECACC), both from mouse, used as negative controls, were also cultured in F-12 medium and 7% FBS.

## 2.7. Transfection

Cells were plated in 35-mm-diameter dishes. The transfection procedure consisted in mixing the appropriate amount of PPRH and *N*-[1-(2,3-dioleoyloxy)propyl]-*N,N,N*-trimethylammonium methylsulfate (DOTAP) (Roche, Barcelona, Spain) for 15 min at room temperature, followed by the addition of the mixture to the cells.

## 2.8. MTT assay

Cells (10,000) were plated in 35-mm-diameter dishes in F12 medium. After 6 days, 0.63 mM of 3-(4,5-dimethylthiazol-2-yl)-2,5-diphenyltetrazolium bromide and 18.4 mM of sodium succinate (both from Sigma-Aldrich, Madrid, Spain) were added to the culture medium and incubated for 3 h at 37 °C. After incubation, the medium was removed and the solubilization reagent (0.57% acetic acid and 10% sodium dodecyl sulfate in dimethyl sulfoxide) (Sigma-Aldrich, Madrid, Spain) was added. Cell viability was measured at 570 nm in a WPA S2100 Diode Array spectrophotometer (Biochrom Ltd., Cambridge, UK).

## 2.9. mRNA analysis

Total RNA from 60,000 PC3 cells was extracted using Trizol (Life Technologies, Madrid, Spain) following the manufacturer's specifications. Quantification of RNA was conducted measuring its absorbance (260 nm) at 25 °C using a Nanodrop ND-1000 spectrophotometer (Thermo Scientific, Wilmington, DE).

## 2.10. Reverse transcription

cDNA was synthesized in a 20 µl reaction mixture containing 500 ng of total RNA, 12.5 ng of random hexamers (Roche, Barcelona, Spain), 10 mM dithiothreitol, 20 units of RNasin (Promega, Madrid, Spain), 0.5 mM each dNTP (AppliChem, Barcelona, Spain), 4 µl of buffer (5×), and 200 units of Moloney murine leukemia virus reverse transcriptase (RT) (Invitrogen, Barcelona, Spain). The reaction was incubated at 37 °C for 1 h.

3 µl of the cDNA mixture was used for Real-Time PCR amplification.

## 2.11. Real-time PCR

The StepOnePlus™ Real-Time PCR Systems (Applied Biosystems, Barcelona, Spain) was used to perform these experiments. Survivin (BIRC5) (HS04194392\_S1), adenine phosphoribosyltransferase (APRT) (HS00975725\_M1) and 18S rRNA (HS99999901\_S1) mRNA Taqman probes were used (Applied Biosystems). The final volume of the reaction was 20 µl, containing 1× TaqMan Universal PCR Mastermix (Applied Biosystems, Barcelona, Spain), 1× TaqMan probe (Applied Biosystems, Barcelona, Spain) and 3 µl of cDNA and H<sub>2</sub>O mQ. PCR cycling conditions were 10 min denaturation at 95 °C, followed by 40 cycles of 15 s at 95 °C and 1 min at 60 °C. The mRNA amount of the target gene was calculated using the  $\Delta\Delta C_T$  method, where  $C_T$  is the threshold cycle that corresponds to the cycle where the amount of amplified mRNA reaches the threshold of fluorescence. APRT and 18S mRNA levels were used as endogenous controls. To analyze the off-target effects of PPRHs we used TaqMan probes for the following unrelated genes: APOA1 (HS00163641\_M1), Bcl2 (HS00608023\_M1), DHFR (HS00758822\_S1), S100A4 (HS00243202\_M1) and PDK1 (HS01561850\_M1).

## 2.12. Western analysis

Cells (60,000) were plated in 35-mm-diameter dishes and treated with PPRHs at 100 nM. At different times after transfection (3, 6, 9 h) total protein extracts were obtained and Western blot analyses were performed to detect the levels of survivin protein.

Cells were collected by trypsinization and after a PBS wash, RIPA buffer (50 Tris-HCl pH 7.4, 1% Igepal CA630, 1 mM EDTA, 150 mM NaCl, supplemented with 100 µg/ml of PMSF and Protease Inhibitor Mixture by Sigma-Aldrich, Madrid, Spain) was added to lyse the cells. The extracts were maintained at 4 °C for 30 min, vortexing every 10 min. Cell debris was removed by centrifugation (13,500g for 10 min). The Bio-Rad protein assay (Bio-Rad, Barcelona, Spain), based on the Bradford method, was used to determine the protein concentrations using bovine serum albumin as a standard (Sigma-Aldrich, Madrid, Spain).

Total protein cell extracts (100 µg) were electrophoresed on SDS-polyacrylamide gels (15%/7%), and transferred to a polyvinylidene fluoride membrane (Immobilon P, Millipore, Madrid, Spain) using a semidry electroblotter. The membranes were probed with antibodies against survivin (1/250 dilution; 614701, Biolegends, San Diego, CA and AF886, R&D systems, Minneapolis, MN) and tubulin (1/800 dilution; CP06, Calbiochem, Merck, Darmstadt, Germany). Signals were detected by secondary HRP-conjugated antibodies: anti-rabbit (1:2500 dilution; P0399, Dako, Denmark) for survivin, anti-mouse (1/5000 dilution; sc-2005, Santa Cruz Biotechnology, Heidelberg, Germany) for tubulin and enhanced chemiluminescence using ECL™ Prime Western Blotting Detection Reagent, as recommended by the manufacturer (GE Healthcare, Barcelona, Spain). Tubulin and total protein loading were both used to normalize the results. Quantification was performed using ImageQuant LAS 4000 Mini (GE Healthcare, Barcelona, Spain).

## 2.13. Cellular uptake of PPRHs

200,000 cells were plated in 55-mm dishes with 2 ml complete F-12 medium and treated with different concentrations of FITC PPRH (Hpd13-F). 24 h after transfection, cells were collected,



centrifuged at  $800 \times g$  at  $4^\circ\text{C}$  for 5 min, and washed once in PBS. The pellet was resuspended in  $500 \mu\text{l}$  PBS plus Propidium iodide (PI) (final concentration  $5 \mu\text{g}/\text{ml}$ ) (Sigma-Aldrich, Madrid, Spain). Cells were kept on ice for no longer than 30 min before flow cytometry analysis performed in a Coulter XL cytometer. Different ratios of PPRH:DOTAP were tested to determine the most appropriate to ensure internalization of the molecule.

#### 2.14. Apoptosis

Apoptosis was determined by two different methodologies: Rhodamine method and Caspase 3/7 assay.

**Rhodamine method:** PC3 cells (120,000) were plated in 55-mm dishes with 2 ml complete F-12 medium and treated with 100 nM of each PPRH. 24 h after treatment, Rhodamine (final concentration  $5 \text{ ng}/\mu\text{l}$ ) (Sigma-Aldrich, Madrid, Spain) was added for 30 min and the cells were collected as previously described for the cellular uptake experiments. Flow-cytometry data were analyzed using the software Summit v4.3. The percentage of Rho-negative, IP-negative cells, corresponded to the apoptotic population.

**Caspase-Glo 3/7 assay:** 5,000 cells (PC3, HUVEC, 4T1 and CT26) were plated in a 96-well plate in  $50 \mu\text{l}$  F12-complete medium. After 24 h, 100 nM of each PPRH was transfected, and 24 h after transfection,  $50 \mu\text{l}$  of Caspase-Glo 3/7 reagent (Promega, Madrid, Spain) was added. After 1 h of incubation, luminescence was measured using a Modulus<sup>TM</sup> Microplate luminometer (Turner Biosystems, Promega, Madrid, Spain). F12-complete medium and the reagent were considered the blank control and untreated cells as background.

#### 2.15. In vivo studies

Tumor growth studies were performed on female athymic mice of 5 weeks old (Hsd:ATHYMIC Nude-Foxn1<sup>nu</sup>). Mice were purchased from Harlan Interfauna Iberica S.L. (Barcelona, Spain) and maintained in the facilities of the PCB-UB. *In vivo* procedures were approved by the institutional ethical committee and by the local authorities according to the Catalanian and Spanish guidelines governing experimental animal care.

Human PC3 cell line growing in exponential phase was used to implant xenografts in mice.  $2 \times 10^6$  cells were subcutaneously injected in the right dorso-lateral side of these mice. Tumor growth was measured using calipers twice a week and its volume was calculated using the formula:  $\text{volume} = (D \times d^2)/2$ , in which  $D$  is the longest axis of the tumor and  $d$  is the shortest.

Those animals with a tumor of approximately  $100 \text{ mm}^3$  were selected to conduct the experiments, using a minimum of 10 animals for the intratumoral administration and 6 for the intravenous one.

Mice were administered with either a scramble PPRH (Hps-Sc) or with the anti-survivin PPRH (HpsPr-C) using as a vehicle in vivo-jetPEI<sup>®</sup> (Polyplus transfection, France) at a  $N/P$  ratio of 8 in a buffer containing 5% glucose. Two types of administration were used: Intratumoral administration of  $10 \mu\text{g}$  of PPRH (volume of administration  $20 \mu\text{l}$ ) and intravenous administration (via tail vein) of  $50 \mu\text{g}$  of PPRH (volume of administration  $200 \mu\text{l}$ ). In both cases, the administration of PPRHs and the measurement of body weight and tumor volume were performed twice a week. Treatments were continued for 3 weeks, after which animals were killed.

#### 2.16. Immunodetection of survivin in tumor samples

At the end of the *in vivo* intratumoral experiment, subcutaneous tumors from PC3 cells were processed for survivin detection, both by Western Blot and Immunofluorescence in histological sections. For protein extraction from tumor samples, frozen tissue was disrupted

in ice cold Cell Lysis Buffer ( $150 \text{ mM NaCl}$ , 1% IGEPAL CA630, 5 mM EDTA,  $100 \mu\text{g}/\text{ml}$  PMSF, 1 mM  $\text{Na}_2\text{VO}_4$ , 1 mM NaF and 50 mM Tris-HCL, pH 7.4) (AppliChem, Barcelona, Spain) with the aid of a mixer. After centrifugation, protein concentration was determined with the Bradford Reagent. Total extracts ( $60 \mu\text{g}$ ) were solved in SDS-polyacrylamide gels using the same conditions as described in section 2.12. The following antibodies were used: rabbit polyclonal antibody anti-survivin (1:2000 dilution, AF886, R&D systems, Minneapolis, MN); monoclonal anti-beta actin peroxidase conjugate (1:25,000 dilution, A3854, Sigma-Aldrich, Madrid, Spain); goat anti-rabbit (1:25,000 dilution, A0545, Sigma-Aldrich, Madrid, Spain) was used as secondary antibodies. For immunofluorescence detection, five micrometer-thick sections from the tumor blocks were deparaffinised, rehydrated in grade alcohols and processed. Briefly, antigen retrieval was performed in a microwave oven for 15 min in 10 mM sodium citrate pH 6.0 with 0.05% Tween-20 (AppliChem, Barcelona, Spain). The slides were incubated in 5% normal goat serum for 60 min to prevent nonspecific staining. Then, they were incubated OVN at  $4^\circ\text{C}$  with rabbit polyclonal anti-human survivin ( $5 \mu\text{g}/\text{ml}$ , AF886, R&D systems, Minneapolis, MN). Thereafter the sections were incubated with Alexa Fluor 488 goat anti-rabbit IgG (H + L) (Invitrogen, Barcelona, Spain) at  $2 \mu\text{g}/\text{ml}$  in PBS  $1 \times$  for 60 min. The slides were kept in a dark environment, washed three times with PBS  $1 \times$  for 5 min each and mounted with mounting solution (Mowiol, Sigma-Aldrich, Madrid, Spain). Five pictures per tumor were taken using a Leica DM IRBE microscope.

#### 2.17. Immunohistochemical CD31 staining

At the end of the *in vivo* intratumoral experiment, subcutaneous tumors from PC3 cells were OCT (Tissue-Tek<sup>®</sup>, Sakura, Barcelona, Spain) embedded and frozen. One cryosection ( $5 \mu\text{m}$ ) corresponding to 3 tumors of each group were analyzed. Sections were fixed in acetone/chloroform (1:1) at  $-20^\circ\text{C}$  for 5 min, dried overnight at room temperature, washed with PBS and treated for 10 min at  $4^\circ\text{C}$  in a dark chamber with  $\text{H}_2\text{O}_2$  (0.03%) in PBS. Then, sections were washed with PBS and blocked for 20 min using PBS-BSA (2%) plus rabbit serum (5%) (Vector, Burlingame, CA) and with Avidin-biotin blocking solution (Dako, Denmark) for 10 min at  $4^\circ\text{C}$ . Samples were incubated for 1 h at room temperature with the monoclonal rat anti-mouse primary antibody directed against CD31 (dil 1:200, BD PharMingen, Belgium) diluted in blocking buffer. Afterwards, sections were incubated with a polyclonal biotinylated anti-rat antibody as secondary antibody (dil 1:500, Vector, Burlingame, CA) for 30 min at room temperature and then the ABC reagent (Pierce, Rockford, IL) was added for 30 min at room temperature. Finally, sections were incubated with NovaRed (Vector, Burlingame, CA) for 20 min at  $4^\circ\text{C}$  and mounted using DPX non-aqueous mounting medium (Sigma-Aldrich, Madrid, Spain). Angiogenesis quantification was measured using two criteria:

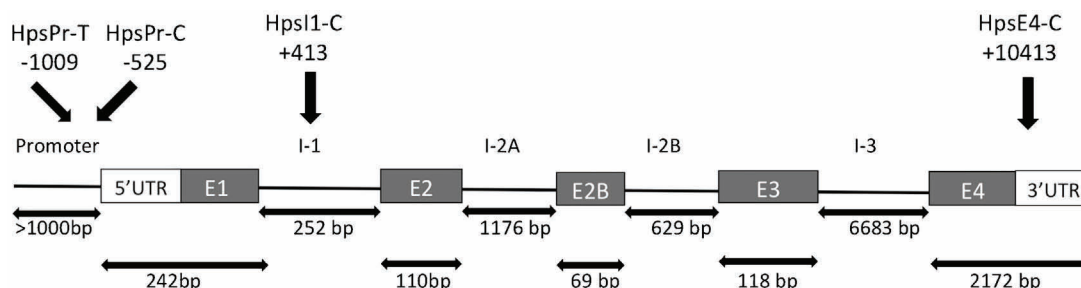
$$M.V.D (v.p./mm^2) = 10^6 \times (\text{sum of vessels of each tumor (image A + image B + \dots + image N)}) / (\text{area of one tumor in } \mu\text{m}^2 (\text{area A} + \text{area B} + \dots + \text{area N}))$$

$$A.A. (\text{fractional area of vessels}) = (\text{area of vessels of each tumor (image A + image B + \dots + image N)}) / (\text{area of one tumor in } \mu\text{m}^2 (\text{area A} + \text{area B} + \dots + \text{area N}))$$

More than 10 pictures per slice, depending on the size of tumors, were taken and analyzed using the NIH ImageJ imaging software.

#### 2.18. Statistical analysis

The *in vitro* data are presented as the mean  $\pm$  SE values. Statistical analysis was performed using Student's *t* test using SPSS



**Fig. 1.** Scheme representing the target sequences of the PPRHs used against the *survivin* gene. Four PPRHs were designed against the *survivin* gene. Two were directed toward the promoter, one template (HpsPr-B) and one Coding (HpsPr-C), and two other coding-PPRHs against intron 1 (HpsI1-C) and the 3'UTR within exon 4 (HpsE4-C). Nomenclature used was Hp (Hairpin), s (*survivin*), Pr (promoter), I (intron), E (exon). The numbering below the PPRHs corresponds to the start of the target sequence location in the gene referred to the transcriptional start site. The arrows indicate the length of each gene element.

(Chicago, IL) version 20 software for Mac OS X (Apple Computer, Cupertino, CA). In the *in vivo* experiments comparison between groups were performed using the two-tailed nonparametric Mann Whitney *U* test. Results were considered significant if  $p < 0.05$  (\*),  $p < 0.01$  (\*\*), or  $p < 0.005$  (\*\*\*)

### 3. Results

#### 3.1. Design of PPRHs

We designed four PPRHs against the *survivin* gene, one of them directed against the template strand and three against different regions of the coding strand. We selected polypyrimidine stretches in the promoter, intron 1 and 3'UTR of the gene (Fig. 1). All the sequences have 2 or 3 purine interruptions and therefore adenines were included in the PPRHs at those positions to maintain the binding to the target sequence [4]. The PPRH sequences are listed in Table 1. As negative controls we used a PPRH with a scrambled sequence (Hps-Sc) and a PPRH with intramolecular Watson–Crick bonds instead of Hoogsteen bonds (Hps-WC), which is not able to form triplexes.

#### 3.2. Cellular uptake of PPRHs in PC3 cells

The demonstration of the cellular uptake of PPRHs in PC3 cells was carried out using flow cytometry. Specifically, we measured the percentage of fluorescent cells and their mean fluorescence intensity 24 h after transfection with a fluorescent PPRH (Fig. 2). Given the intrinsic apoptotic effect of the PPRHs against *survivin*, we decided to use a fluorescent PPRH designed against the *dihydrofolate reductase* (*dhfr*) gene (HpdI3-F) for the uptake experiments, previously tested in SKBR3 cells [4]. This model is useful for this purpose because the incubation of the cells in F12-complete medium -containing the final products of the DHFR enzyme-avoids PPRHs cytotoxicity.

As shown in Fig. 2, 90–95% of cells were FITC-positive at the concentrations tested (100 nM and 1  $\mu$ M). Surprisingly, the mean fluorescence was 5-times higher at 100 nM than at 1  $\mu$ M. This can be explained because the best PPRH:DOTAP ratio was 1:100 [4],

achieved by mixing 100 nM of PPRH and a fixed concentration of 10  $\mu$ M of DOTAP which is the maximum concentration of vehicle with no toxicity; when using 1  $\mu$ M PPRHs this ratio was not longer maintained. Therefore, the chosen concentration to conduct further experiments was 100 nM.

#### 3.3. Effects of PPRHs on cell viability

To compare the effects of PPRHs against different regions of the *survivin* gene in PC3 cells, dose response studies were performed. The resulting cell viabilities are shown in Fig. 3A. The two PPRHs designed against the promoter – HpsPr-T and HpsPr-C – caused the greatest effect at 100 nM with more than 90% decrease in viability. HpsI1-C was highly cytotoxic at 30 nM although its effect was partially reversed at 100 nM; and HpsE4-C showed the lowest effect. We also determined the cytotoxicity caused by the negative controls –Hps-WC and Hps-Sc- observing 101.9% and 83.3% survival, respectively, at the maximum concentration assayed. PPRHs were also tested in HeLa cells, to demonstrate that they are effective in other cancer cell lines and to validate the usage of HeLa nuclear extracts to conduct further mechanism analyses (Fig. 3B). Furthermore, the two most cytotoxic PPRHs against *survivin* were assayed in normal, non-tumoral cells (HUVEC), which do not express the *survivin* protein (Fig. 3C). We did not observe a decrease in survival in this cell line at 100 nM, indicating that these PPRHs are harmless to cells whose proliferation is not related with *survivin* expression. We also tested both PPRHs in murine cell lines, namely, CT26 (colorectal cancer) and 4T1 (breast cancer) which express murine *survivin* and have been used as a model to test the antitumor effect of dominant-negative mutants of *survivin* [31,32]. These cell lines were not sensitive to PPRHs designed against the human *survivin* promoter (Fig. 3C).

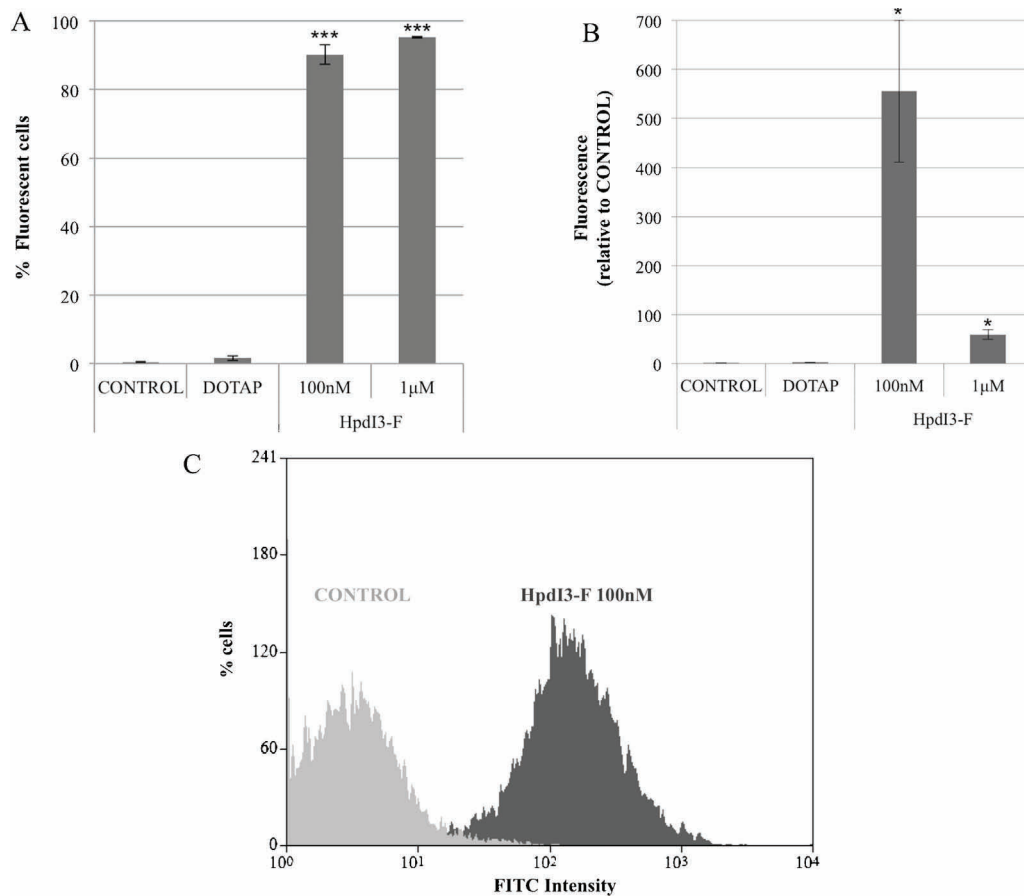
#### 3.4. Effects of PPRHs on apoptosis

To associate the effect of PPRHs with *survivin* gene function, we measured the apoptotic effect of the PPRHs at 100 nM after 24 h of incubation using two different methodologies, the rhodamine

**Table 1**  
PPRH sequences.

Name	Sequence (5'–3')	Location
HpsPr-T	GGGGAGGGAGGGGAGGGGGAAGAATTTTTAAAGAAAAGGGGAGGGGAGGGGAGGGG	Promoter –1009
HpsPr-C	AGGGGAGGGAAGGAGAGAAGTTTTTGAAGAGAGGAAGGGAGGGGA	Promoter –525
HpsI1-C	GGGGAAAAGAAGGGAGGGGAGGTTTTTGGAGGGGAGGGAAGAAAAGGGG	Intron 1 +413
HpsE4-C	AAGAAAGGGAGGAGGAGAATTTTTAAGAGGGAGGAGGGAAGAA	3'UTR +10413
Hps-WC	CCCCTCCCTCCCTCCCTTTCTTTTTTTAAAGAAAAGGGGAGGGGAGGGAGGGG	
Hps-Sc	AAGAGAAAAGAGAAAAGAAGAGAGGGTTTTTGGGAGAGAAGAAAGAGAAAAGAGAA	
HpdI3-F	[F]GGGAGGAGGAGAGGGAGGAGTTTTTGAGGAGGGAGAGGGAGGAGG	

List of the PPRHs sequences used in this study, including their target location in the *survivin* gene. T, template; C, coding; WC and Sc, negative controls; F, fluorescent.



**Fig. 2.** Uptake of PPRHs in PC3 cells. Cells were incubated with 100 nM and 1  $\mu$ M of fluorescent-PPRH with DOTAP for 24 h and uptake was measured by flow cytometry. (A) Percentage of fluorescent cells determined as FITC-positive and IP-negative cells. Data represent the mean  $\pm$  SE of four experiments. \*\*\* $p < 0.005$ . (B) Mean intensity of fluorescence of FITC-positive cells. Data represent the mean  $\pm$  SE of three experiments. \* $p < 0.05$ . (C) Representative image showing an overlay of control cells and cells treated with 100 nM of fluorescent-PPRH. DOTAP was used at the maximum concentration of 10  $\mu$ M, resulting in a PPRH:DOTAP ratio of 1:100 and 1:10 for the concentrations of 100 nM and 1  $\mu$ M of PPRH, respectively.

method (Fig. 4A) and the caspase-3 activity assay (Fig. 4B). The concentration chosen caused the greatest effect on cell viability. HpsPr-C produced the highest apoptotic effect, provoking apoptosis in 50% of the cell population as determined by flow cytometry and inducing a 1.65-fold increase in caspase-3 activity. Surprisingly, HpsPr-T caused a smaller but significant effect than HpsPr-C in apoptosis, even though the decrease in viability was almost as high as that provoked by HpsPr-C (Fig. 4C). The apoptosis produced by HpsE4-C and HpsI1-C was lower than that of HpsPr-C in accordance to the lower decrease in cell viability. The apoptotic levels produced by the most effective PPRHs (HpsPr-T and HpsPr-C) were determined by a caspase-3 assay in control cells (HUVEC, 4T1 and CT26) and no significant changes relative to untreated cells were observed.

### 3.5. Effects of PPRHs on survivin mRNA levels

Given that both PPRHs against the *survivin* promoter sequence were the most effective in decreasing cell viability, we further explored the ability of those PPRHs to decrease *survivin* expression. Both, HpsPr-T and HpsPr-C were able to decrease *survivin* mRNA levels up to 2-fold (Fig. 5A). The different controls (Hps-Sc and Hps-WC) did not affect *survivin* mRNA levels.

We checked for off-target effects of HpsPr-T and HpsPr-C at a 100 nM, by determining mRNA levels of a set of 5 non-related genes. As shown in Table 2, there was no decrease in the mRNA levels of these genes. We further confirmed the lack of expression

of survivin at the mRNA and protein levels in HUVEC cells (Fig. 5B and C), in which no cytotoxicity was observed when using these PPRHs (Fig. 3C).

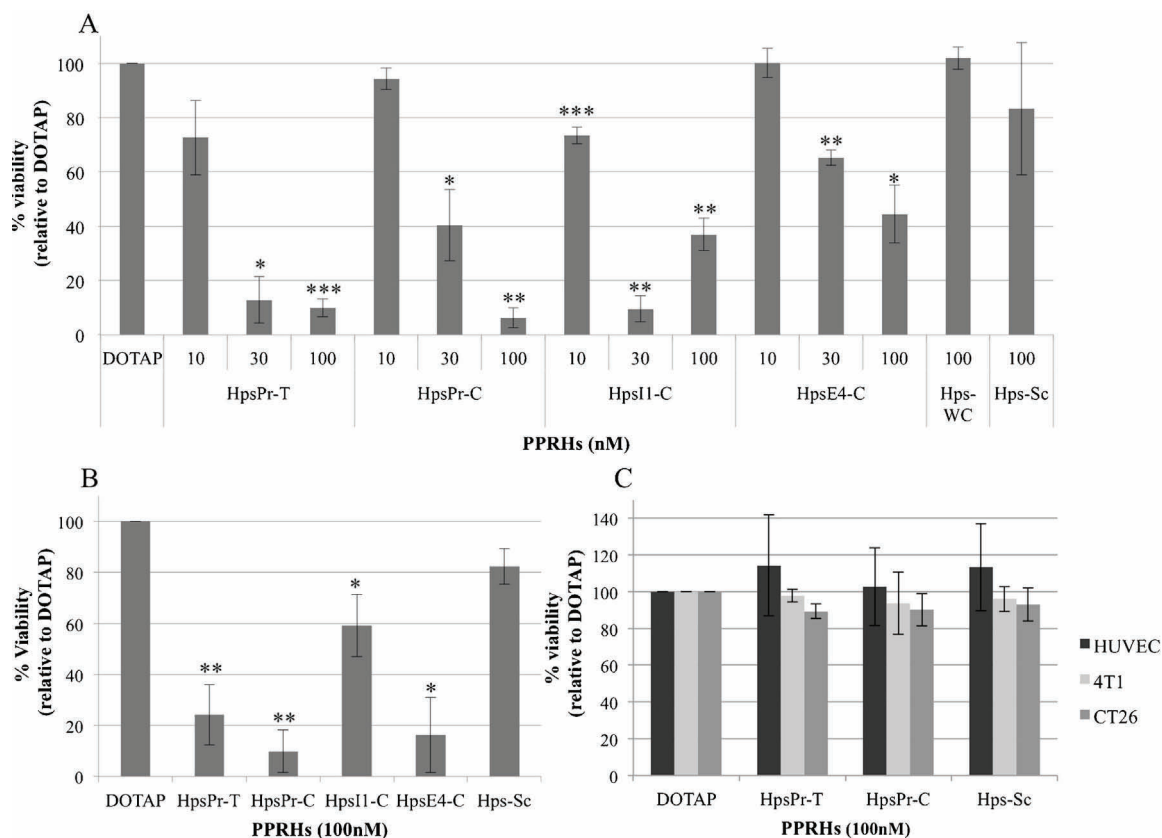
### 3.6. Effects of PPRHs on survivin protein levels

Survivin protein levels were also determined in PC3 cells following incubation with 100 nM of either HpsPr-T or HpsPr-C during different periods of time. The Template-PPRH induced a 5-fold decrease in survivin protein levels at 9 h (Fig. 6A), whereas the Coding-PPRH reached only a 2-fold decrease 6 h after transfection (Fig. 6B).

### 3.7. Binding of PPRHs to their target sequences

The binding between the selected PPRHs and their target sequences was analyzed either by labelling the double-stranded target sequence or the PPRH themselves.

When labelling the target sequences, we observed a maximum binding of 48% of HpsPr-T and 6% of HpsPr-C at the highest concentration of PPRH used (Fig. 7A). When labelling the PPRHs, we also observed their binding to the target sequences, 50% for the HpsPr-T and 18% for the HpsPr-C, respectively, when using 1  $\mu$ M of the target sequences (Fig. 7B). As seen in Fig. 7B, HpsPr-C presented different electrophoretic structures and to ensure that those conformations belonged to a unique molecular species, the samples were run in a denaturing PAGE obtaining a single band in each case (data not shown).



**Fig. 3.** Effect of PPRHs against survivin on cell viability. MTT assays to determine cell survival were performed 6 days after transfection. (A) Dose response of the four designed PPRHs against the *survivin* gene in PC3 cells. DOTAP was used at 5  $\mu$ M to transfect the PPRHs at 10 and 30 nM, and at 10  $\mu$ M when transfecting 100 nM PPRH. (B) Cell viability upon transfection of 100 nM PPRHs in HeLa cells. (C) Cell viability upon transfection of 100 nM of PPRHs against the promoter sequence in HUVEC, 4T1 and CT26. Data are mean  $\pm$  SE values of at least three experiments. \* $p$  < 0.05, \*\* $p$  < 0.01, \*\*\* $p$  < 0.005.

### 3.8. EMSA analyses

The targets of the two PPRHs that worked more efficiently are located within the *survivin* promoter; the target sequence for HpsPr-T is located at  $-1009$  and the one for HpsPr-C at  $-525$ , both relative to the transcriptional initiation site. To study the mechanism of action of these PPRHs, we started analyzing the putative transcription factors that might bind to the target sequences of the PPRHs. We performed an *in silico* search using the MATCH<sup>TM</sup> software applying a cut-off of 0.95 for both, matrix similarity and core similarity. After literature mining of the found transcription factors, we decided to further explore the role of Sp1 when using HpsPr-T [33] and GATA when using HpsPr-C [34], because of their well-characterized implication in cancer. Moreover, these two transcription factors had the highest core similarity and matrix similarity for the target sequence of the corresponding PPRH (1.0 and 1.0 for Sp1 and 1.0 and 0.979 for GATA). Next, we performed EMSA analyses using HeLa nuclear extracts and radiolabeled probes for the double-stranded target sequences of the two PPRHs. The binding pattern for each target sequence is shown in the corresponding lane 2 of Fig. 8A and B.

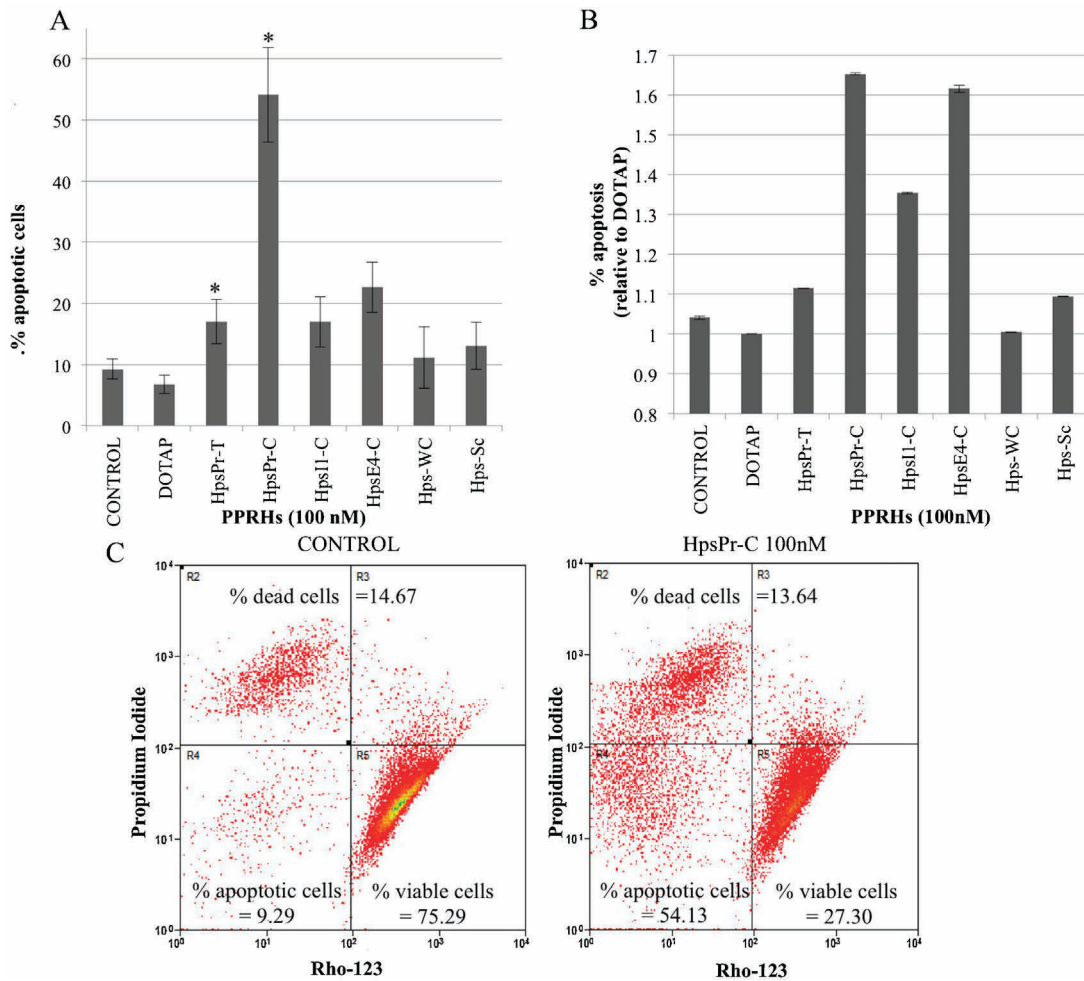
In both cases, incubation of the radiolabeled target sequence with an excess (100 $\times$ ) of the respective PPRH induced a decrease in the intensity of the binding pattern of nuclear proteins. Incubation with HpsPr-T produced a 52% decrease in the binding (Fig. 8A, lane 3). Incubation with HpsPr-C produced a decrease of 15% that induced a visible release of the free probe (Fig. 8B, lane 3). These results indicated that the specific PPRHs and proteins present in the nuclear extract were competing for the binding to

the probe. To identify these proteins, we performed competition assays using the consensus binding sequences for either Sp1 [33] or GATA [35].

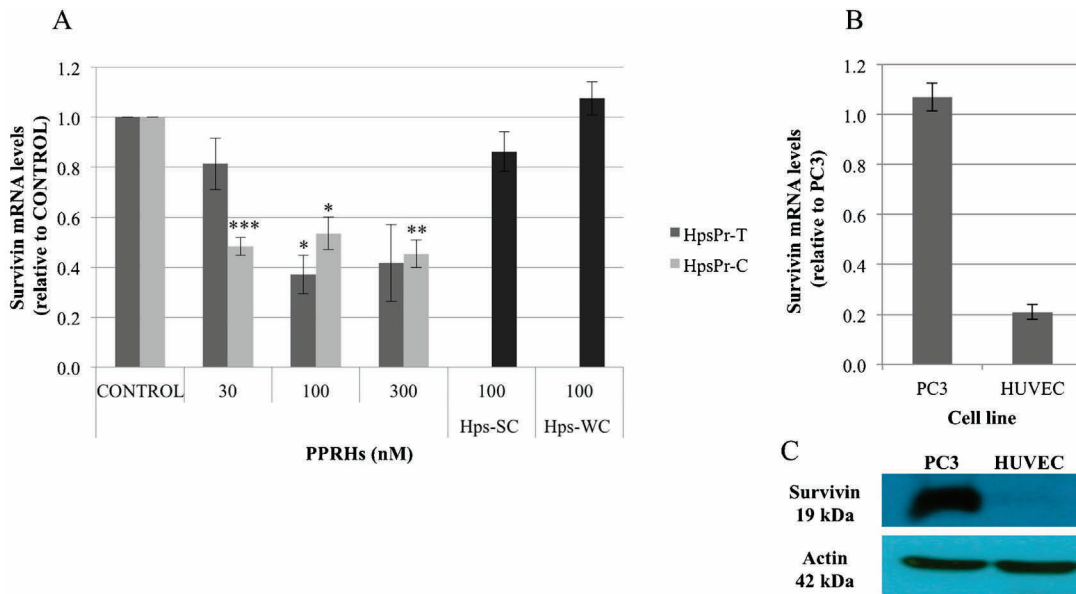
In the case of the template-PPRH (HpsPr-T), three bands were identified using competition (Fig. 8A, lanes 4 and 5) and supershift assays (Fig. 8A, lanes 6 and 7). We observed a decrease in the intensity of three bands in the EMSA in the presence of the Sp1/3-consensus binding sequence as a competitor. When using a 5-fold excess of the Sp1/3-consensus sequence, the band corresponding to Sp1 decreased by 98%, and those corresponding to Sp3 by 85% and 72% (Fig. 8A, lane 4). Using specific antibodies against Sp1 and Sp3 we determined that the upper band corresponded to the binding of Sp1 (Fig. 8A, lane 6), and that two lower bands corresponded to the binding of Sp3 (Fig. 8A, lane 7). Interestingly, the band in-between the two Sp3 bands increased its intensity after the incubation with the antibodies against Sp1 or Sp3, but was decreased in the presence of the Sp1/3 consensus binding sequence. This band might correspond to a factor whose binding sequence overlaps with that for Sp1/3; then, when these two factors are sequestered by antibodies, that other factor – probably Pax4 according to the *in silico* analysis – has a better access to the probe.

In the case of the coding-PPRH (HpsPr-C), a prominent band was observed when incubating the target sequence with the nuclear extract. Competition assays using the GATA consensus sequence were performed confirming the *in silico* prediction (Fig. 8B, lanes 4 and 5). While the GATA consensus sequence at 5 and 50-fold excess produced a decrease in the intensity of the band of 74% and 92%, respectively (Fig. 8B, lanes 4 and 5), the non-related sequence did not cause a significant change in intensity (Fig. 8B, lane 6).





**Fig. 4.** Effect of PPRHs on apoptosis. PC3 cells were transfected with 100 nM of HpsPr-T, HpsPr-C, HpsE4-C and HpsI1-C against the *survivin* gene and two negative controls –Hps-Sc and Hps-WC. 24 h after transfection, apoptosis was measured by two methods. (A) Rhodamine method: Cells Rho123-negative and IP-negative were considered as apoptotic cells. Data represent the mean  $\pm$  SE of at least three experiments. \* $p < 0.05$ . (B) Caspase-3/7 assay: Fold change in RLU relative to DOTAP. (C) Representative flow cytometer histograms displaying the cell population treated with 100 nM HpsPr-C and the control sample.

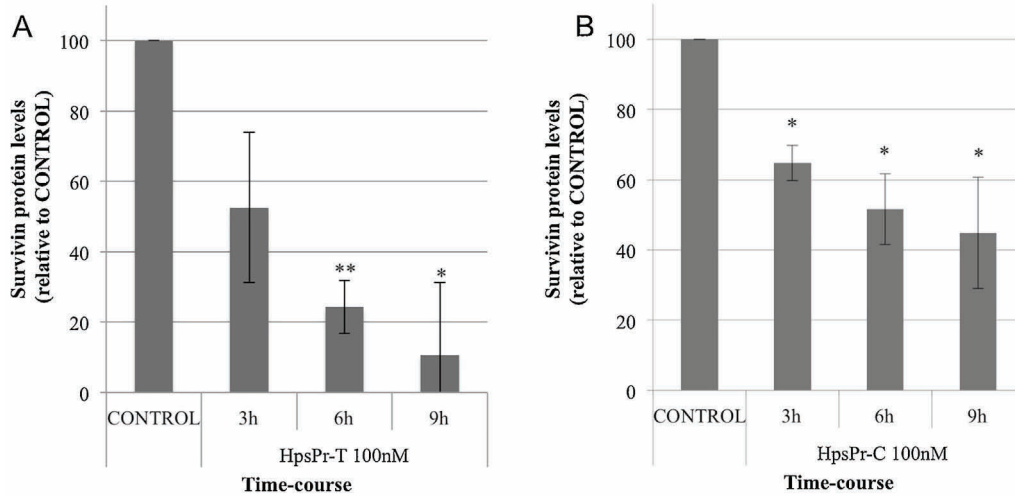


**Fig. 5.** *Survivin* mRNA levels. (A) RNA was extracted from PC3 cells treated with increasing concentrations of either HpsPr-T for 72 h or HpsPr-C for 24 h. mRNA levels were determined using qRT-PCR and referred to the levels of endogenous controls. Data represent the mean  $\pm$  SE of at least three experiments. \* $p < 0.05$ , \*\* $p < 0.01$ , \*\*\* $p < 0.005$ . (B) *Survivin* mRNA levels were analyzed in HUVEC cells and referred to the mRNA levels in PC3 cells. (C) Representative image of a Western blot showing comparatively *survivin* protein levels in PC3 and HUVEC cell lines.

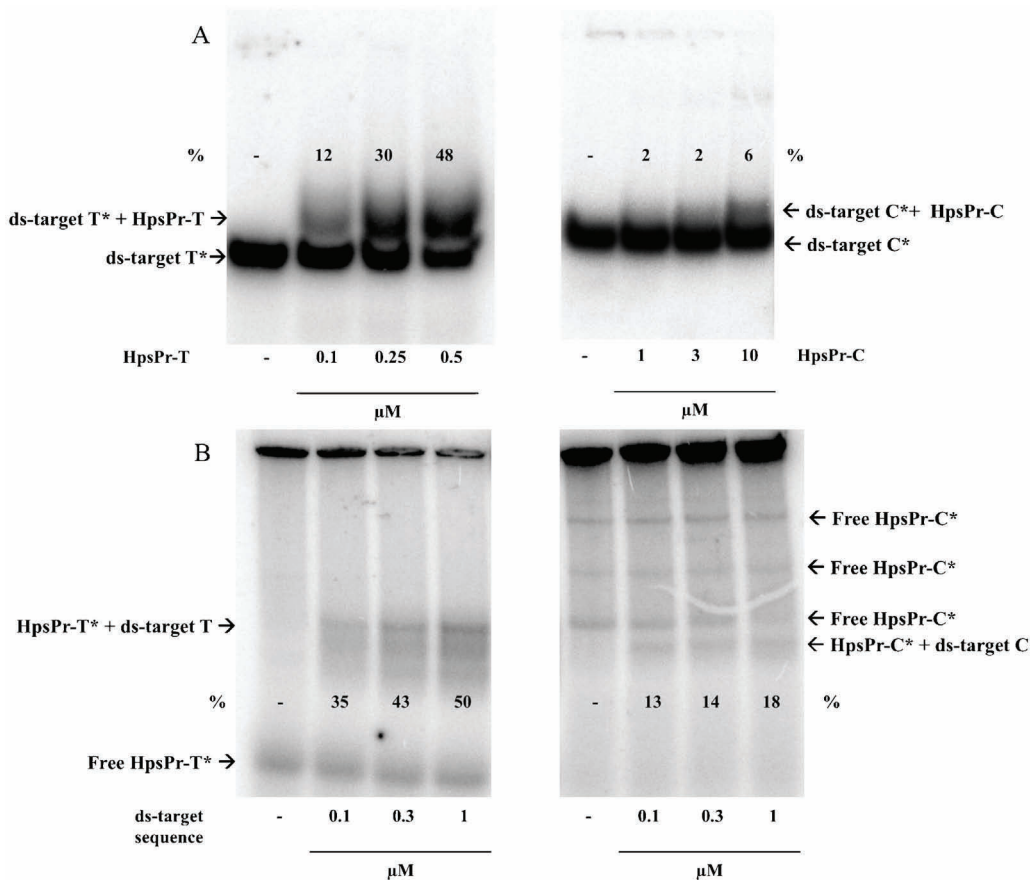
**Table 2**  
Off-target effects.

	Survivin	APOA1	Bcl2	DHFR	PDK1	S100A4
CONTROL	1	1	1	1	1	1
HpsPr-T	0.37 ± 0.08	1.39 ± 0.16	1.27 ± 0.22	0.93 ± 0.06	1.38 ± 0.25	1.26 ± 0.62
HpsPr-C	0.54 ± 0.07	1.06 ± 0.13	1.05 ± 0.15	0.90 ± 0.04	0.89 ± 0.11	0.93 ± 0.13

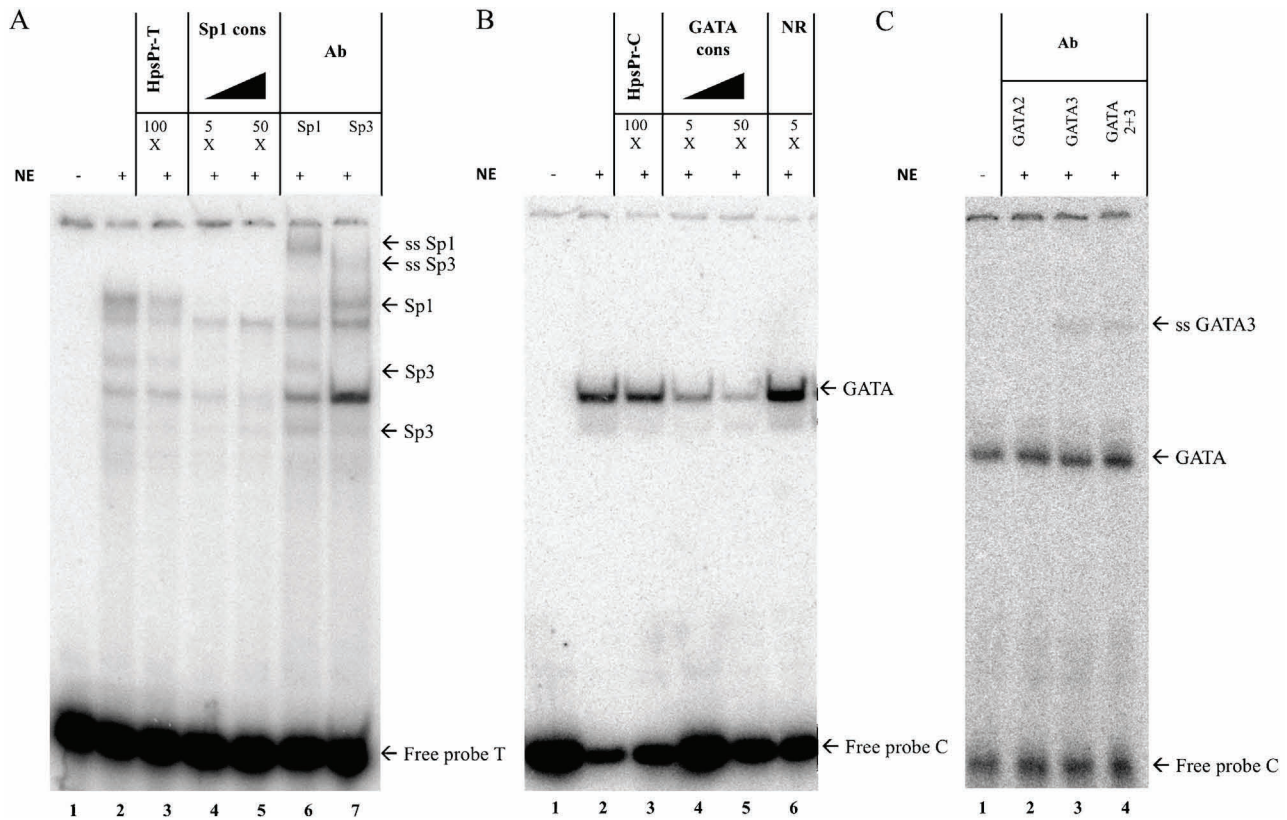
mRNA levels of unrelated genes were determined by qRT-PCR after incubation with 100 nM of PPRHs (HpsPr-T and HpsPr-C) against the *survivin* gene.



**Fig. 6.** Survivin protein levels. 60,000 PC3 cells were incubated with 100 nM of either HpsPr-T (A) or HpsPr-C (B) for different periods of time. Total protein extracts were obtained and analyzed by Western Blot. Protein levels were normalized using tubulin. Data represent the mean ± SE of at least three experiments. \*  $p < 0.05$ , \*\*  $p < 0.01$ .



**Fig. 7.** PPRHs binding to their target sequence. (A) Binding of increasing concentrations of the Template-PPRH (HpsPr-T) or the Coding-PPRH (HpsPr-C) after incubation with their radiolabelled ds-target sequences (20,000 cpm). (B) Binding of the radiolabelled Template-PPRH (HpsPr-T) or the radiolabelled Coding-PPRH (HpsPr-C) after incubation with increasing concentrations of their ds-target sequences. 1 μg of poly-dI-dC as non-specific DNA was added to all the binding reactions. \* indicates the radiolabelled probes. Binding experiments were performed at least three times. Quantification was performed by phosphorimaging and referred to the total radioactivity. The numbers over (A) or underneath (B) the bands represent the percentage of binding referred to the control (NE).



**Fig. 8.** Binding of transcription factors to PPRH target sequences. EMSA assays were conducted using radiolabelled target sequence (20,000 cpm), Herring Sperm DNA as non-specific competitor and HeLa nuclear extracts as the protein source. (A) Bindings obtained using radiolabelled ds-target sequence for HpsPr-T. The binding pattern using HeLa nuclear extracts is shown in lane 2. Competition assays were performed using a 100-fold excess of HpsPr-T (lane 3) or a 5 to 50-fold excess of Sp1/3 consensus sequence (lanes 4 and 5). Supershift assays were performed four times in the presence of antibodies against Sp1 (lane 6) or Sp3 (lane 7). Shifted and supershifted (ss) bands are indicated by arrows. (B) Bindings obtained using radiolabelled ds-target sequence for HpsPr-C. The binding pattern using HeLa nuclear extracts is shown in lane 2. Competition assays were performed using a 100-fold excess of HpsPr-C (lane 3), a 5 to 50-fold excess of GATA consensus sequence (lanes 4 and 5) and a 50-fold excess of a non-related sequence (lane 6). Shifted bands are indicated by arrows. (C) Supershift assays were performed four times in the presence of antibodies against GATA-2 (lane 2), GATA-3 (lane 3) and both antibodies (lane 4). The supershifted (ss) band is indicated by an arrow.

Supershift assays were performed using GATA-2 and GATA-3 antibodies, the GATA family members most abundant in prostate tissue [34]. As shown in Fig. 8C, incubation with GATA-3 antibody produced a supershifted band indicating that this specific factor is binding to the target sequence of HpsPr-C.

### 3.9. Effects of PPRHs in vivo

Two types of administration, intratumoral and intravenous, were performed using PC3 subcutaneous xenograft tumor model in athymic mice. Two groups were compared, one mock-injected with a scrambled PPRH-Hps-Sc-, and the other injected with the most effective PPRH tested *in vitro*, HpsPr-C (Figs. 2 and 3). Depending upon the route of administration, the dosage of the PPRH varied from 10  $\mu$ g/injection in the case of intratumoral, and 50  $\mu$ g/injection for the intravenous. Administration was performed twice a week during 3 weeks and results are presented as tumor volume.

#### 3.9.1. Intratumoral

In the case of intratumoral administration (Fig. 9A), we observed that the PPRH targeting *survivin* (HpsPr-C) produced a delay in tumor growth compared with the scrambled PPRH. At the end of the experiment, the mean relative tumor volume (RTV) of the control group (scrambled-PPRH) was 663.1% with respect to the initial volume, whereas the treated group (HpsPr-C) showed a mean RTV of 396.6%. Taking into account all this data, we calculated the Treatment/Control (T/C) ratio, which compares the

difference in the mean RTV or tumor weight between treated and control groups. These values showed a statistically significant reduction of 40% in tumor volume and almost 30% in tumor weight. The doubling time of the control group was 7.45 days, whereas tumors of the treated group had a doubling time of 9.43, which translates into an absolute growth delay of almost 2 days caused by the administration of the PPRH against *survivin*.

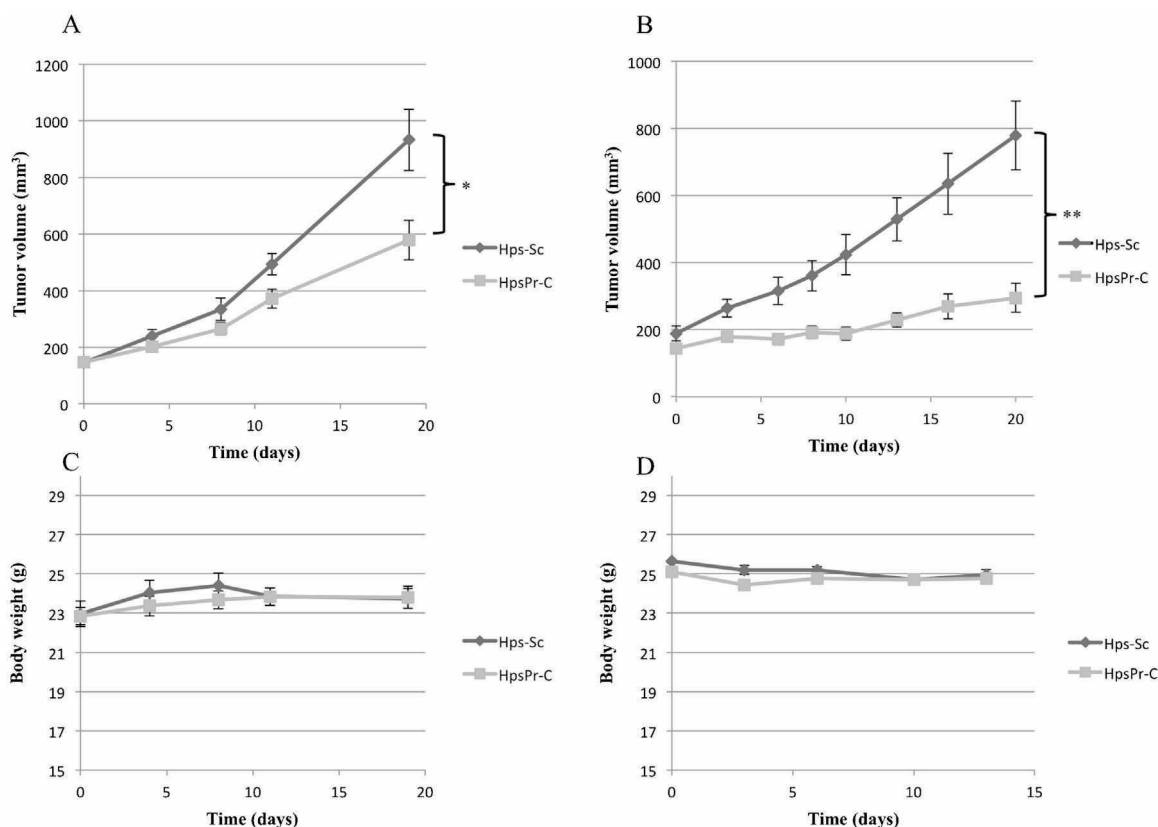
#### 3.9.2. Intravenous

When injecting the PPRHs through the tail vein, the dosage was increased five times to diminish problems associated with whole body distribution or degradation in the bloodstream. As it is shown in Fig. 9B, the PPRH against *survivin* was able to decrease tumor growth *in vivo*, thus producing a delay in tumor growth. In fact, the delay in tumor growth administering HpsPr-C intravenously was higher than intratumorally. This was reflected in the RTV mean which in the treated group was 200% inferior to the control group, meaning a T/C ratio of 49.6%. Accordingly, the doubling time of the tumor treated with the specific PPRH was almost 2 times higher (19.3 vs 10.6) than that of the control group (scramble-PPRH), which means that the cells treated with HpsPr-C took twice the time to double.

In both types of administration, the body weight loss was approximately 2%, indicating lack of toxicity (Fig. 9C and D).

#### 3.9.3. Survivin protein levels and blood vessel formation

To explore the potential correlation between the inhibition of tumor growth and the silencing of *survivin*, we selected tumors



**Fig. 9.** PPRH effect on tumor growth and body weight in a PC3 subcutaneous xenograft tumor model. (A) Progression of tumor volume throughout time when Hps-Sc (negative control) or HpsPr-C were administered by i.t. route twice a week (1001000). Tumor volume is represented as the mean  $\pm$  SE; \* $p < 0.05$ . (B) Progression of tumor volume throughout time when Hps-Sc (negative control) or HpsPr-C were administered by i.v. route twice a week (1001000). Tumor volume is represented as the mean  $\pm$  SE; \*\* $p < 0.01$ . (C) and (D) Evolution of body weight of the animals throughout time corresponding to the intratumoral and intravenous administrations, respectively. Data represent the mean  $\pm$  SE.

from the intratumoral study to perform Western blot and immunofluorescence analyses. We measured the protein levels of survivin in a minimum of 4 tumors from both the control and the treated groups, from samples of the center part and in the tip of the tumor. In both cases, we observed a decrease in survivin protein levels, 52% in the center part and 71% in the tip of the tumor, respectively (Fig. 10A). In addition, we determined survivin expression by immunofluorescence analysis in histological sections, observing a decrease in expression in tumors treated with HpsPr-C, as shown in Fig. 10B.

We also investigated the role of *survivin* in angiogenesis by performing histological analyses of murine CD31 staining for three tumor samples from each group to evaluate blood vessel formation. A representative image is shown in Fig. 11A. Quantification of microvessel density and the fraction area of the vessels revealed a decrease in the vasculature, with a T/C ratio of 25%, for both microvessel density (Fig. 11B) and fractional area of vessels (Fig. 11C).

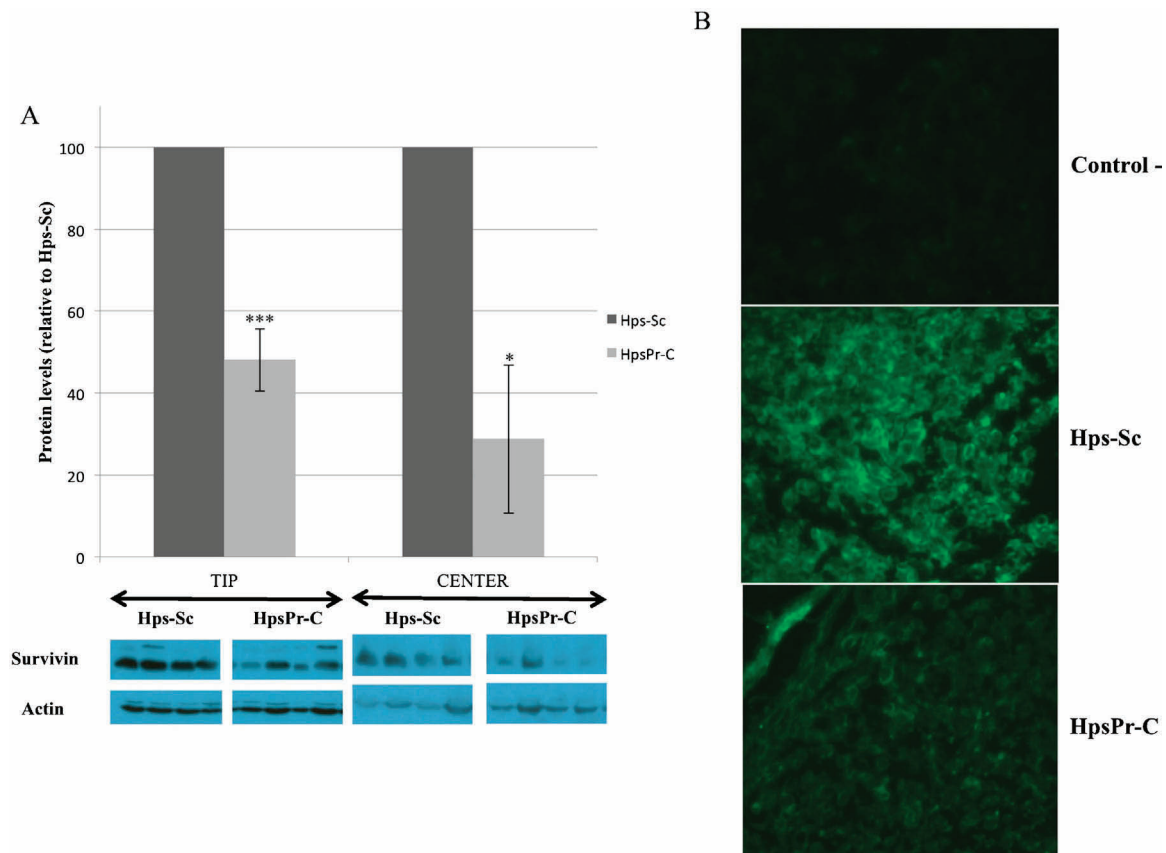
#### 4. Discussion

The objectives of this work were to get further knowledge of the effects of PPRHs as new silencing tools and their possibilities to be used as therapeutic agents in *in vivo* approaches. As a model we inhibited the *survivin* gene, since its overexpression in cells promotes the evasion of apoptosis, one of the six hallmarks of cancer [36]. *Survivin* has been used as a suitable target in several experimental settings to decrease cell proliferation using antisense oligonucleotides [37], siRNAs [6,38] or small molecules [29,39,40]. Since we had previously described PPRHs as an alternative gene

silencing tool in breast cancer cells (SKBR3, MCF7) [4,5], we decided to design a set of four PPRHs, three Coding- and one Template-PPRH against *survivin* to test the efficacy of PPRHs in prostate cancer cells (PC3) *in vitro* and *in vivo*.

A conclusion of this work is that after comparing the PPRHs against different regions of the *survivin* gene, those against its promoter sequence (HpsPr-T and HpsPr-C) were the most effective in decreasing cell viability in PC3 cells. We previously described the ability of a template-PPRH against the *dhfr* gene to decrease mRNA and protein levels. In this work, we corroborate the action of a template-PPRH against another target, *survivin*. In addition, we observed that the coding-PPRH, HpsPr-C, was also able to decrease mRNA and protein levels of the targeted protein. This was unforeseen since a coding-PPRH against intron 3 of the *dhfr* gene was able to decrease viability without showing a great decrease in mRNA levels [5]. The difference between those two coding-PPRHs is the location of their target sequences, one in an intron (Hpd13-A-TA) and the other within the promoter (HpsPr-C). The effect of the PPRH against *dhfr* intron 3 was due to its interference with the binding of the splicing factor U2AF65, thus altering the splicing process [5]. PPRHs against the *survivin* promoter worked through a different mechanism by inhibiting transcription, thus decreasing gene expression. Specifically, we demonstrated that these PPRHs decreased the binding of transcription factors, such as Sp1 (using HpsPr-T) and GATA (using HpsPr-C), which have binding sites within the PPRHs target sequences. Other authors have proved that both Sp1 and Sp3 regulate the *survivin* promoter via several Sp1-boxes [33,41] and that degradation of Sp1 is related to a decrease in *survivin* expression [42]. Regarding GATA transcription factors, although





**Fig. 10.** Survivin protein levels after intratumoral administration of PPRHs. (A) Quantification of survivin protein levels in the tip and the center of tumors after administration of either Hps-Sc or HpsPr-C. Total protein extracts were obtained and analyzed by Western Blot. Protein levels were normalized using actin. Data represent the mean  $\pm$  SE of at least four tumors. \*  $p < 0.05$ , \*\*\*  $p < 0.005$ . (B) Representative image of the immunofluorescent analysis of tumors after the administration of either Hps-Sc or HpsPr-C. The negative control corresponds to the fluorescence background given by Alexa Fluor 488. Original magnification: 40 $\times$ .

they are mainly expressed in hematopoietic cells, GATA-2 and -3 are the predominant family members expressed in the prostate tissue [34] that might be playing a role in *survivin* expression in this tissue. From our work, we can conclude that prevention of the binding of GATA-3 to the *survivin* promoter by HpsPr-C might cause a decrease in *survivin* expression.

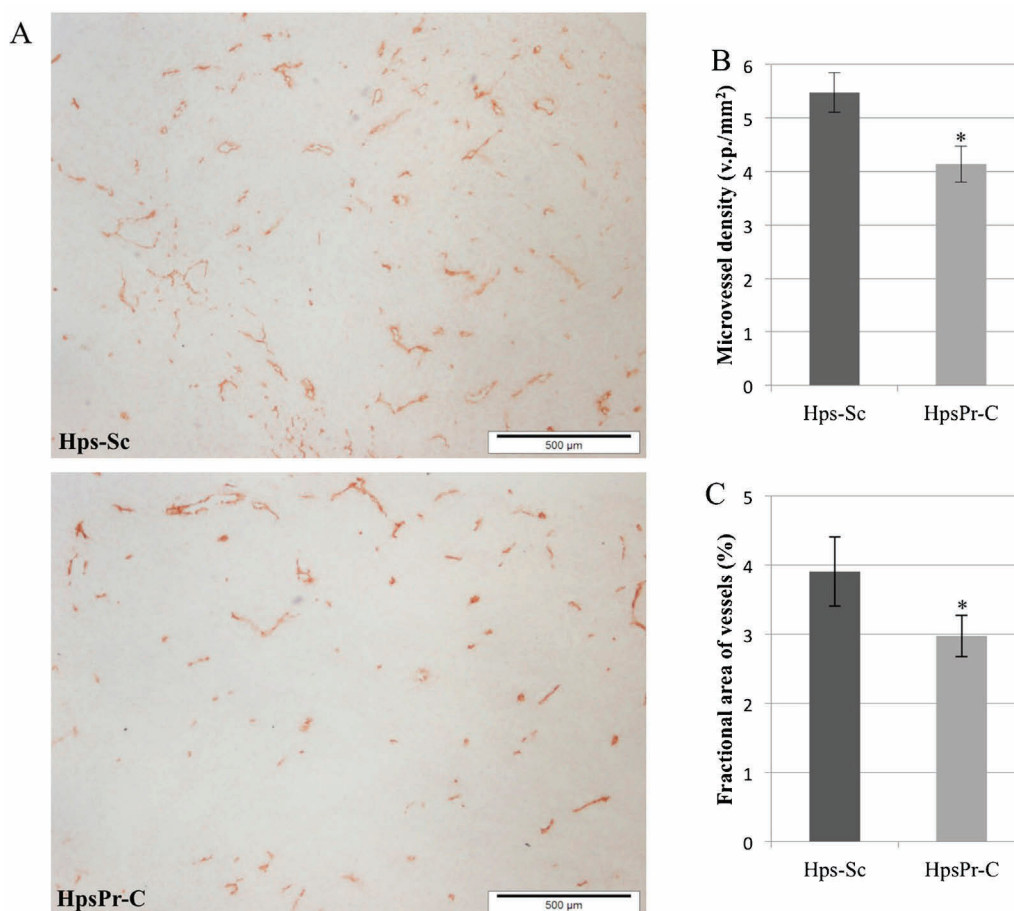
There are different Sp1- and GATA-binding sites within the *survivin* promoter. However, upon comparison by multiple alignment analysis of those binding sites, only the core of the binding site is conserved, while the flanking sequences are different enough so that the PPRH will be specific only for its target sequence. In fact, the promoters of the genes selected to study off-target effects all presented binding sites for both GATA and Sp1 and none of those genes were downregulated by the treatment (Table 2).

Regarding the *in vitro* effects, our observations corroborate the extensively reported involvement of *survivin* in the mitochondrial apoptotic pathway and how the decrease in its levels produces an increase in apoptosis [11,37,39]. To decrease mRNA and protein levels of survivin as a therapeutic approach, several molecules have been used such as aODNs [6,37], locked nucleic acids (LNAs) [43], siRNAs [6] and small molecules like the Ras inhibitor farnesylthiosalicylic acid (FTS) [39], YM155 [29] or FL118 [40]. However, the LNA SPC3042 and FL118 presented lack of specificity, by down-regulating or modulating other genes in the IAP or Bcl-2 family [40,43], while others required higher dosages to induce a proper effect, ranging from 200 nM to 1  $\mu$ M [6,37,38] or even higher (75  $\mu$ M) when using FTS [39].

As an alternative, we present PPRHs, a new gene silencing tool that work at nanomolar concentrations, a lower range compared to

aODNs, and similar to the concentrations of siRNAs used in *in vitro* experiments [6]. We observed a maximum decrease in viability at 100 nM for each one of the PPRHs against the *survivin* promoter sequence. This concentration assured the optimal PPRH uptake in PC3 cells when transfected with DOTAP. Other advantages of PPRHs are their high stability, without the need of modifying residues, and their low cost [4]. To prove their specificity and possible toxicities, we tested our best PPRHs (HpsPr-T and HpsPr-C) in human normal cells. Other authors have used HUVEC cells as normal cells [44,45]. In our case, this cell line was an ideal negative control because it does not express *survivin* and, in consequence, treatment with the selected PPRHs at 100 nM is innocuous. In addition, the species selectivity of these PPRHs against human *survivin* was tested in murine cancer cell lines, where no decrease in viability was observed due to the difference in the *survivin* sequences. To further discard off-target effects, we studied the expression of several genes after treatment with either HpsPr-T or HpsPr-C, not observing decreases in their mRNA levels. It is worth noting that Bcl-2 was one of those genes, thus proving that *survivin* silencing produced apoptosis by itself and not by changing the expression levels of another gene with a similar antiapoptotic function. However, we cannot dismiss other off-target effects due to the binding of the PPRH to unintended targets.

We aimed to explore the usage of PPRHs *in vivo* using a subcutaneous xenograft tumor model of prostate cancer. Using two different types of administration, intratumoral and intravenous, the coding-PPRH against *survivin* promoter was able to decrease the volume of the tumor, demonstrating the efficacy of this PPRH in this model. The delay in tumor growth caused by the administration of HpsPr-C may be related to the decrease in



**Fig. 11.** Blood vessel formation after intratumoral administration of PPRHs. (A) Representative image of the immunohistochemical analysis in tumors after administration of either Hps-Sc or HpsPr-C, using anti-CD31 antibody that recognises endothelial cells. (B) Microvessel density and (C) fractional area of vessels of the tumors after administration of either Hps-Sc or HpsPr-C. Data represent the mean  $\pm$  SE of three tumors. \* $p < 0.05$ .

the levels of survivin and to a lower degree of blood vessel formation.

The reason for including the intravenous injection as a second route of administration was to overcome the possible drawbacks of the intratumoral administration such as aggressiveness – thus causing loss of tumor structure and alterations in the measurement- and poor-distribution within the tumor – because of the high interstitial fluid pressure and the stiffness of the extracellular matrix [46].

In an aging society with growing life expectancy, diseases such as prostate cancer are going to increase its incidence and effective therapeutic approaches are needed. Up until now, treatment options are limited to surveillance in early stage, surgery or radiotherapy when a radical treatment is needed, hormone therapy in HRPC and chemotherapy in case of metastasis [27]. Currently, different targeted-directed therapies against *survivin* are undergoing clinical trials, such as small molecules – YM155 – and antisense oligonucleotide LY2181308, proving that inhibition of *survivin* is a cutting-edge target for anticancer treatments. However, YM155 have showed modest activity and therefore combination therapies have been suggested for new trials [29]. LY2181308 inhibited growth in subcutaneous xenografted tumors [11], but showed no significant increase in toxicity in Phase II clinical trials in combination with docetaxel in castrate-resistant prostate cancer [30]. Our results are encouraging, but it is important to note that pre-clinical models, such as xenografts, are far from useful to extrapolate results to humans, so there is need to improve the models and test in other organisms.

In summary, this work represents the preclinical proof of principle for the *in vivo* application of PPRHs, opening the possibility to use this technology as a new therapeutic approach.

#### Acknowledgements

The work was supported by Grant SAF2011-23582 from “Plan Nacional de Investigación Científica” (Spain). Our group holds the Quality Mention from the “Generalitat de Catalunya” SGR2009-118. LR is the recipient of a fellowship (FI) from the “Generalitat de Catalunya”.

#### References

- [1] Avino A, Frieden M, Morales JC, Garcia de la Torre B, Guimil Garcia R, Azorin F, et al. Properties of triple helices formed by parallel-stranded hairpins containing 8-aminopurines. *Nucleic Acids Res* 2002;30:2609–19.
- [2] Coma S, Noe V, Eritja R, Ciudad CJ. Strand displacement of double-stranded DNA by triplex-forming antiparallel purine-hairpins. *Oligonucleotides* 2005;15:269–83.
- [3] Goni JR, de la Cruz X, Orozco M. Triplex-forming oligonucleotide target sequences in the human genome. *Nucleic Acids Res* 2004;32:354–60.
- [4] de Almagro MC, Coma S, Noe V, Ciudad CJ. Polypurine hairpins directed against the template strand of DNA knock down the expression of mammalian genes. *J Biol Chem* 2009;284:11579–89.
- [5] de Almagro MC, Mencía N, Noe V, Ciudad CJ. Coding polypurine hairpins cause target-induced cell death in breast cancer cells. *Hum Gene Ther* 2011;22:451–63.
- [6] Coma S, Noe V, Lavarino C, Adan J, Rivas M, Lopez-Matas M, et al. Use of siRNAs and antisense oligonucleotides against *survivin* RNA to inhibit steps leading to tumor angiogenesis. *Oligonucleotides* 2004;14:100–13.
- [7] Ambrosini G, Adida C, Altieri DC. A novel anti-apoptosis gene, *survivin*, expressed in cancer and lymphoma. *Nat Med* 1997;3:917–21.

- [8] Monzo M, Rosell R, Felip E, Astudillo J, Sanchez JJ, Maestre J, et al. A novel anti-apoptosis gene: Re-expression of survivin messenger RNA as a prognosis marker in non-small-cell lung cancers. *J Clin Oncol* 1999;17:2100–4.
- [9] Tanaka K, Iwamoto S, Gon G, Nohara T, Iwamoto M, Tanigawa N. Expression of survivin and its relationship to loss of apoptosis in breast carcinomas. *Clin Cancer Res* 2000;6:127–34.
- [10] Kawasaki H, Altieri DC, Lu CD, Toyoda M, Tenjo T, Tanigawa N. Inhibition of apoptosis by survivin predicts shorter survival rates in colorectal cancer. *Cancer Res* 1998;58:5071–4.
- [11] Carrasco RA, Stamm NB, Marcussen E, Sandusky G, Iversen P, Patel BK. Antisense inhibition of survivin expression as a cancer therapeutic. *Mol Cancer Ther* 2011;10:221–32.
- [12] Lu CD, Altieri DC, Tanigawa N. Expression of a novel antiapoptosis gene, survivin, correlated with tumor cell apoptosis and p53 accumulation in gastric carcinomas. *Cancer Res* 1998;58:1808–12.
- [13] Kato J, Kuwabara Y, Mitani M, Shinoda N, Sato A, Toyama T, et al. Expression of survivin in esophageal cancer: correlation with the prognosis and response to chemotherapy. *Int J Cancer* 2001;95:92–5.
- [14] Satoh K, Kaneko K, Hirota M, Masamune A, Satoh A, Shimosegawa T. Expression of survivin is correlated with cancer cell apoptosis and is involved in the development of human pancreatic duct cell tumors. *Cancer* 2001;92:271–8.
- [15] Swana HS, Grossman D, Anthony JN, Weiss RM, Altieri DC. Tumor content of the antiapoptosis molecule survivin and recurrence of bladder cancer. *N Engl J Med* 1999;341:452–3.
- [16] Saitoh Y, Yaginuma Y, Ishikawa M. Analysis of Bcl-2, Bax and Survivin genes in uterine cancer. *Int J Oncol* 1999;15:137–41.
- [17] Yoshida H, Ishiko O, Sumi T, Matsumoto Y, Ogita S. Survivin, bcl-2 and matrix metalloproteinase-2 enhance progression of clear cell- and serous-type ovarian carcinomas. *Int J Oncol* 2001;19:537–42.
- [18] Adida C, Haioun C, Gaulard P, Lepage E, Morel P, Briere J, et al. Prognostic significance of survivin expression in diffuse large B-cell lymphomas. *Blood* 2000;96:1921–5.
- [19] Adida C, Recher C, Raffoux E, Daniel MT, Taksin AL, Rousselot P, et al. Expression and prognostic significance of survivin in de novo acute myeloid leukaemia. *Br J Haematol* 2000;111:196–203.
- [20] Adida C, Berrebi D, Peuchmaur M, Reyes-Mugica M, Altieri DC. Anti-apoptosis gene, survivin, and prognosis of neuroblastoma. *Lancet* 1998;351:882–3.
- [21] Grossman D, McNiff JM, Li F, Altieri DC. Expression and targeting of the apoptosis inhibitor, survivin, in human melanoma. *J Invest Dermatol* 1999;113:1076–81.
- [22] Grossman D, McNiff JM, Li F, Altieri DC. Expression of the apoptosis inhibitor, survivin, in nonmelanoma skin cancer and gene targeting in a keratinocyte cell line. *Lab Invest* 1999;79:1121–6.
- [23] Carter BZ, Milella M, Altieri DC, Andreeff M. Cytokine-regulated expression of survivin in myeloid leukemia. *Blood* 2001;97:2784–90.
- [24] Gianani R, Jarboe E, Orlicky D, Frost M, Bobak J, Lehner R, et al. Expression of survivin in normal, hyperplastic, and neoplastic colonic mucosa. *Hum Pathol* 2001;32:119–25.
- [25] Sarella AI, Guthrie JA, Seymour MT, Ride E, Guillou PJ, O'Riordain DS. Non-operative management of the primary tumour in patients with incurable stage IV colorectal cancer. *Br J Surg* 2001;88:1352–6.
- [26] Altieri DC. The molecular basis and potential role of survivin in cancer diagnosis and therapy. *Trends Mol Med* 2001;7:542–7.
- [27] Ramsay AK, Leung HY. Signalling pathways in prostate carcinogenesis: potentials for molecular-targeted therapy. *Clin Sci (Lond)* 2009;117:209–28.
- [28] Nakahara T, Takeuchi M, Kinoyama I, Minematsu T, Shirasuna K, Matsuhsu A, et al. YM155, a novel small-molecule survivin suppressant, induces regression of established human hormone-refractory prostate tumor xenografts. *Cancer Res* 2007;67:8014–21.
- [29] Tolcher AW, Quinn DI, Ferrari A, Ahmann F, Giaccone G, Drake T, et al. A phase II study of YM155, a novel small-molecule suppressor of survivin, in castration-resistant taxane-pretreated prostate cancer. *Ann Oncol* 2012;23:968–73.
- [30] Wiechno PJCP, Smok-Kalwat J, Pikilel J, Henry DH, Christianson DF, et al. Interim results of a randomized phase II study with window-design to evaluate antitumor activity of the survivin antisense oligonucleotide (ASO) LY2181308 in combination with docetaxel for first-line treatment of castrate-resistant prostate cancer (CRPC). *J Clin Oncol* 2011;29:abstr 4592.
- [31] Li HX, Zhao XY, Wang L, Wang YS, Kan B, Xu JR, et al. Antitumor effect of mSurvivinThr34->Ala in murine colon carcinoma when administered intravenously. *Med Oncol* 2010;27:1156–63.
- [32] Peng XC, Yang L, Yang LP, Mao YQ, Yang HS, Liu JY, et al. Efficient inhibition of murine breast cancer growth and metastasis by gene transferred mouse survivin Thr34->Ala mutant. *J Exp Clin Cancer Res* 2008;27:46.
- [33] Li F, Altieri DC. Transcriptional analysis of human survivin gene expression. *Biochem J* 1999;344(Pt 2):305–11.
- [34] Perez-Stable CM, Pozas A, Roos BA. A role for GATA transcription factors in the androgen regulation of the prostate-specific antigen gene enhancer. *Mol Cell Endocrinol* 2000;167:43–53.
- [35] Boidot R, Vegran F, Jacob D, Chevrier S, Cadouet M, Feron O, et al. The transcription factor GATA-1 is overexpressed in breast carcinomas and contributes to survivin upregulation via a promoter polymorphism. *Oncogene* 2010;29:2577–84.
- [36] Hanahan D, Weinberg RA. The hallmarks of cancer. *Cell* 2000;100:57–70.
- [37] Olie RA, Simoes-Wust AP, Baumann B, Leech SH, Fabbro D, Stahel RA, et al. A novel antisense oligonucleotide targeting survivin expression induces apoptosis and sensitizes lung cancer cells to chemotherapy. *Cancer Res* 2000;60:2805–9.
- [38] Kappler M, Bache M, Bartel F, Kotszsch M, Paniam M, Wurl P, et al. Knockdown of survivin expression by small interfering RNA reduces the clonogenic survival of human sarcoma cell lines independently of p53. *Cancer Gene Ther* 2004;11:186–93.
- [39] Blum R, Jacob-Hirsch J, Rechavi G, Kloog Y. Suppression of survivin expression in glioblastoma cells by the Ras inhibitor farnesylthiosalicylic acid promotes caspase-dependent apoptosis. *Mol Cancer Ther* 2006;5:2337–47.
- [40] Ling X, Cao S, Cheng Q, Keefe JT, Rustom YM, Li F. A novel small molecule FL118 that selectively inhibits survivin, Mcl-1, XIAP and cIAP2 in a p53-independent manner, shows superior antitumor activity. *PLoS One* 2012;7:e45571.
- [41] Xu R, Zhang P, Huang J, Ge S, Lu J, Qian G. Sp1 and Sp3 regulate basal transcription of the survivin gene. *Biochem Biophys Res Commun* 2007;356:286–92.
- [42] Sankpal UT, Abdelrahim M, Connelly SF, Lee CM, Madero-Visbal R, Colon J, et al. Small molecule tolfenamic acid inhibits PC-3 cell proliferation and invasion in vitro, and tumor growth in orthotopic mouse model for prostate cancer. *Prostate* 2012;72:1648–4858.
- [43] Hansen JB, Fisker N, Westergaard M, Kjaerulff LS, Hansen HF, Thru CA, et al. SPC3042: a proapoptotic survivin inhibitor. *Mol Cancer Ther* 2008;7:2736–45.
- [44] Kitano T, Yoda H, Tabata K, Miura M, Toriyama M, Motohashi S, et al. Vitamin K3 analogs induce selective tumor cytotoxicity in neuroblastoma. *Biol Pharm Bull* 2012;35:617–6123.
- [45] Mukherjee A, Huber K, Evans H, Lakhani N, Martin S. A cellular and molecular investigation of the action of PMX464, a putative thioredoxin inhibitor, in normal and colorectal cancer cell lines. *Br J Pharmacol* 2007;151:1167–75.
- [46] Holback H, Yeo Y. Intratumoral drug delivery with nanoparticulate carriers. *Pharm Res* 2011;28:1819–30.

**ARTICLE V:**

**Improved Design of PPRHs for Gene Silencing**

Laura Rodríguez, Xenia Villalobos, Anna Solé, Carolina Lliberós,  
Carlos J. Ciudad, and Véronique Noé.

Molecular Pharmaceutics, 2015 Mar 2;12(3):867-877 (Impact factor 4,787)





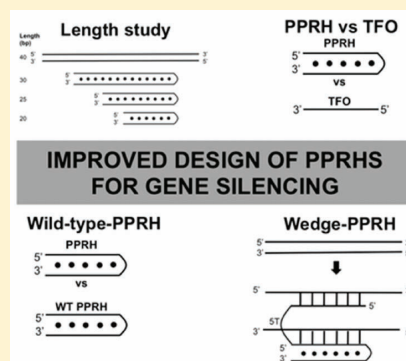
## Improved Design of PPRHs for Gene Silencing

Laura Rodríguez, Xenia Villalobos, Anna Solé, Carolina Lliberós, Carlos J. Ciudad, and Véronique Noé\*

Department of Biochemistry and Molecular Biology, School of Pharmacy, University of Barcelona, 08028 Barcelona, Spain

**ABSTRACT:** Nowadays, the modulation of gene expression by nucleic acids has become a routine tool in biomedical research for target validation and it is also used to develop new therapeutic approaches. Recently, we developed the so-called polypurine reverse Hoogsteen hairpins (PPRHs) that show high stability and a low immunogenic profile and we demonstrated their efficacy both in vitro and in vivo. In this work, we explored different characteristics of PPRHs to improve their usage as a tool for gene silencing. We studied the role of PPRH length in the range from 20 to 30 nucleotides. We also proved their higher affinity of binding and efficacy on cell viability compared to nonmodified TFOs. To overcome possible off-target effects, we tested wild-type PPRHs, which proved to be capable of binding to their target sequence with more affinity, displaying a higher stability of binding and a higher effect in terms of cell viability. Moreover, we developed a brand new molecule called Wedge-PPRH with the ability to lock the ds-DNA into the displaced structure and proved its efficacy in prostate and breast cancer cell lines.

**KEYWORDS:** gene silencing, PPRH, wild-type, Wedge-PPRH, nucleic acid



### INTRODUCTION

In 1957, Felsenfeld described the existence of triple-stranded nucleic acids<sup>1</sup> and K. Hoogsteen justified triplex formation with the finding of Hoogsteen bonds.<sup>2</sup> These discoveries prompted the development of a gene-silencing tool called triplex forming oligonucleotides (TFOs), capable of binding to the purine strand in the major groove of the double helix by hydrogen bonds. The study of their mechanism of action concluded that TFOs interfered with the transcription process.<sup>3–5</sup> Purine TFOs have several advantages over pyrimidine TFOs because they bind to their target sequence in a pH-independent manner, with higher affinity and faster kinetics.<sup>6</sup> Kool and colleagues found out that purine sequences in a hairpin or a circular structure could form triplexes with their single-stranded pyrimidine target sequence with a higher binding affinity.<sup>7</sup>

All these studies led us to develop the polypurine reverse Hoogsteen hairpins (PPRHs), which are composed of two antiparallel polypurine domains, which form intramolecular reverse-Hoogsteen bonds linked by a five-thymidine loop, therefore forming a hairpin structure. PPRHs are capable of binding to polypyrimidine stretches in the DNA, causing strand displacement.<sup>8</sup> Template-PPRHs are directed against the template strand and cause inhibition of transcription.<sup>9</sup> Coding PPRHs are directed against the coding strand and can also bind to the mRNA. Depending on the location of the target sequence, either in introns or promoters, PPRHs act through different mechanisms. A coding-PPRH against an intronic sequence in the *dhfr* gene caused a splicing alteration by preventing the binding of the splicing factor U2AF65 to its target sequence.<sup>10</sup> PPRHs against promoter sequences, both a template-PPRH (HpsPr-T) and a coding-PPRH (HpsPr-C) directed against two different regions of the *survivin* promoter, prevented the binding of transcription factors specific for the corresponding target

sequences -Sp1, Sp3 and GATA-3-, causing a decrease in *survivin* expression.<sup>11</sup>

The main limitation for the design of either TFOs or PPRHs would be the presence of polypurine/polypyrimidine stretches. However, their rate of occurrence in the genome has been proved to be higher than predicted by random models,<sup>12,13</sup> which opens the possibility to design sequence-specific molecules against genes that play important roles in cancer, such as *survivin* or *TERT*.

We have previously studied the role of *survivin* in cancer using siRNAs and ODNs,<sup>14</sup> and more recently, we used PPRHs against *survivin* to validate this new technology both in vitro and in vivo. This approach allowed us to confirm their efficacy in terms of decrease in mRNA and protein levels, resulting in a decrease in cell viability and increase in apoptosis in vitro. Using a xenografted model of prostate cancer we proved that the administration of a PPRH against a promoter sequence in the *survivin* gene caused a reduction in tumor growth, through the decrease in survivin levels and in blood vessel formation, thus establishing the proof of principle for PPRHs usage in vivo.<sup>11</sup>

We have also studied important properties of PPRHs and concluded that they are less immunogenic and much more stable than siRNAs.<sup>15</sup> Even though these advantages make PPRHs an attractive tool for gene silencing, there is room for improvement.

The aim of this work was to further improve PPRHs in terms of affinity and specificity and to compare them with nonmodified TFOs. To do so, we studied the influence of length and

**Received:** October 17, 2014

**Revised:** December 16, 2014

**Accepted:** January 15, 2015

**Published:** January 15, 2015

pyrimidine interruptions within the PPRHs and developed the Wedge-PPRH, a brand new molecule based on PPRHs.

## MATERIALS AND METHODS

**Design and Usage of PPRHs.** PPRHs of different length against an intronic sequence of the *telomerase* gene (Table 1) and

**Table 1. DNA Oligonucleotides Sequences and PPRHs of Different Lengths against the *Telomerase* Gene**

Name*	Sequence (5'-3')
TERT target sequence	5' CAGGCAGGACAAGGAAGCGGAGGAAGGCAGGAGCTCTT 3' 3' GTCCGTCCTGTTCTTTCGCCCTCCTCCGTCCTCCGAGAA 5'
Hpt110-T	5' AGGAAAAGGAAGAGGGAGGAAGGAAGGAGG 5T 3' AGGAAAAGGAAGAGGGAGGAAGGAAGGAGG
Hpt110-T2	5' AAGGAAGAGGGAGGAAGGAAGGAGG 5T 3' AAGGAAGAGGGAGGAAGGAAGGAGG
Hpt110-T3	5' GAAGAGGGAGGAAGGAAGGA 5T 3' GAAGAGGGAGGAAGGAAGGA

PPRH hairpins against the template strand of intron 10 of the *telomerase* gene (TERT target): Hpt110-T, 30 nt carrying three A-substitutions in place of the pyrimidine interruptions in each domain. Hpt110-T2, 25 nt carrying two A-substitutions and Hpt110-T3, 20 nt carrying two A-substitutions. Interruptions are marked in bold. Bullets represent reverse-Hoogsteen bonds and lines Watson–Crick bonds.

PPRHs and nonmodified TFOs against promoter sequences of the *survivin* gene (Table 2) were used in these experiments. The Triplex-Forming Oligonucleotide Target Sequence Search software (M.D. Anderson Cancer Center, Houston, TX) ([www.spi.mdanderson.org/tfo/](http://www.spi.mdanderson.org/tfo/)) was used to find polypurine sequences and BLAST software was carried out to confirm the specificity of the designed molecules. The nomenclature used in this study was: Hp for PPRH hairpin; s for survivin; t for TERT; Pr for promoter; I10 for intron 10; T for template-PPRH; C for coding-PPRH; and WT for wild type. Wedge-PPRHs were designed by extending the 5' end of HpsPr-T WT, with a pyrimidine sequence complementary to the upper strand that is displaced by the PPRH (Table 3). PPRHs were synthesized as nonmodified oligodeoxynucleotides by Sigma-Aldrich (Madrid, Spain) (0.05  $\mu$ mol scale; DESALT-unmodified and desalted). Lyophilized PPRHs were resuspended in sterile Tris-EDTA buffer (1 mM EDTA and 10 mM Tris, pH 8.0) and stored at  $-20$  °C.

### Preparation of Polypurine/Polypyrimidine Duplexes.

The duplexes to be targeted by the hairpins corresponded to the intronic sequence within the *TERT* gene (Table 1) and two promoter sequences of the *survivin* gene (Table 2). The single-stranded molecules were purchased from Sigma and resuspended in Tris-EDTA buffer. To make the duplexes, 25  $\mu$ g of each single-stranded (ss) polypurine and polypyrimidine oligodeoxynucleotides were incubated with 150 mM NaCl at 90 °C for 5 min as described by de Almagro et al.<sup>9</sup>

**Oligodeoxynucleotide Labeling.** One hundred nanograms of PPRHs or double stranded (ds) oligodeoxynucleotides were 5'-end-labeled with T4 polynucleotide kinase (New England Biolabs, Beverly, MA) and [ $\gamma$ -<sup>32</sup>P]ATP as described by de Almagro et al.<sup>9</sup>

**Table 2. DNA Oligonucleotides Sequences, PPRHs, and TFOs Directed against the *Survivin* Gene**

Name*	Sequence (5'-3')
Template-PPRHs and Coding-TFO against the <i>survivin</i> promoter sequence at -1009	
Target sequence	5' ATTAAGAATGGGGCGGGGTGGGAGGGGTGG 3' 3' TAATTCCTACCCCGCCGCCACCTCCGCCACC 5'
HpsPr-T	5T (AAAGAAAAGGGGAGGGGAGGGGAGGGG 3' AAAGAAAAGGGGAGGGGAGGGGAGGGG 5')
HpsPr-T WT	5T (AAAGAATGGGGCGGGGTGGGAGGGG 3' AAAGAATGGGGCGGGGTGGGAGGGG 5')
TFO-sPr-C	5' GGGGAGGGAGGGGAGGGGAAAGAAA 3'
Coding-PPRHs and Template-TFO against the <i>survivin</i> promoter sequence at -525	
Target sequence	5' CTGCTGCACTCCATCCCTCCCTGTT 3' 3' GACGACGTGAGGTAGGGAGGGGACAA 5'
HpsPr-C	5T (GAAGAGAGGAAGGGAGGGGA 3' GAAGAGAGGAAGGGAGGGGA 5')
HpsPr-C WT	5T (GACGTGAGGTAGGGAGGGGA 3' GACGTGAGGTAGGGAGGGGA 5')
TFO-sPr-T	5' GAAGAGAGGAAGGGAGGGGA 3'
Negative controls	
Hps-WC	5' CCCTCCCTCCCTCCCTCCCTTTCTTT 5T 3' GGGGAGGGAGGGGAGGGGAAAGAAA
Hps-Sc	5' AAGAGAAAAGAGAAAAGAGAGAGGG 5T 3' AAGAGAAAAGAGAAAAGAGAGAGGG
TFO-Sc	5' GGAAAAAGGAGGA 3'

\* PPRH hairpins and TFO against the *survivin* promoter at  $-1009$ : HpsPr-T, 26 nt carrying three A-substitutions in place of the pyrimidine interruptions in each domain; HpsPr-T WT 26 nt carrying the corresponding three pyrimidine interruptions in each domain; TFO-sPr-C carrying three A-substitutions in place of the pyrimidine interruptions. PPRH hairpins and TFO against the *survivin* promoter at  $-525$ : HpsPr-C, 20 nt carrying three A-substitutions in place of the pyrimidine interruptions in each domain; HpsPr-T WT 20 nt carrying the corresponding three pyrimidine interruptions in each domain; TFO-sPr-T carrying three A-substitutions in place of the pyrimidine interruptions. Negative controls: Hps-WC is a hairpin with intramolecular Watson–Crick bonds; Hps-Sc is a hairpin with intramolecular reverse-Hoogsteen bond and no target in the genome; TFO-Sc is a polypurine sequence and no target in the human genome. Interruptions are marked in bold. Bullets represent reverse-Hoogsteen bonds and lines Watson–Crick bonds.

**PPRH and TFO DNA Binding Analyses.** Binding studies for PPRHs and TFOs were performed using radiolabeled ds-target sequences (20 000 cpm). The radiolabeled sequences were incubated with increasing concentrations (0.1  $\mu$ M, 1  $\mu$ M, and 10  $\mu$ M) of each PPRH or TFO in a buffer containing 10 mM MgCl<sub>2</sub>, 100 mM NaCl, and 50 mM HEPES, pH 7.2 and 0.5  $\mu$ g of poly dI-dC (Sigma-Aldrich) as a nonspecific competitor. Binding reactions (20  $\mu$ L) were preincubated for 5 min at 65 °C, followed by 30 min at 37 °C and then, loaded in nondenaturing 12% polyacrylamide gels (PAGE) containing 10 mM MgCl<sub>2</sub>, 5% glycerol and 50 mM HEPES, pH 7.2. Electrophoresis was carried

**Table 3. Sequence of Wedge-PPRHs against the *Survivin* Gene\***

Name	Sequence (5'-3')
Target sequence	<pre> 5' ATTAAGAATGGGGGCGGGGTGGGAGGGGTGG 3' 3' TAATTTCTTACCCCGCCCGCCACCTCCACC 5' </pre>
Wedge-PPRH-23	<pre> 5' TTTCTTACCCCGCCCGCCACCTC 5' 5T ( AAAGAATGGGGGCGGGGTGGGAGGGG ) 5T 3' AAAGAATGGGGGCGGGGTGGGAGGGG </pre>
Wedge-PPRH-17	<pre> 5' TTTCTTACCCCGCCCGCC 5' 5T ( AAAGAATGGGGGCGGGGTGGGAGGGG ) 5T 3' AAAGAATGGGGGCGGGGTGGGAGGGG </pre>
Wedge-PPRH WC	<pre> 5' TTTCTTACCCCGCCCGCC 5' 5T ( AAAGAATGGGGGCGGGGTGGGAGGGG ) 5T 3' TTTCTTACCCCGCCCGCCACCTCCACC </pre>

\*Wedge-PPRH-23 is constituted of HpsPr-T WT with a 23-nt 5' extension corresponding to the polypyrimidine sequence complementary to the coding strand of the target sequence. Wedge-PPRH-17 is constituted of HpsPr-T WT with a shorter 5' extension of 17-nt. Wedge-PPRH WC is constituted of Hps-WC with the same 17-nt 5' extension as Wedge-PPRH-17. Interruptions are marked in bold. Bullets represent reverse-Hoogsteen bonds and lines Watson-Crick bonds.

out for approximately 4 h at 10 V/cm at 4 °C. After drying the gel, it was exposed to Europium plates OVN and analyzed using a Storm 840 Phosphorimager (Molecular Dynamics, Sunnyvale, CA).

**UV Absorption Studies.** Previous to the analyses, the PPRHs in combination with their single-stranded target sequence (0.5 μM of each strand) were incubated in a buffer containing 100 mM NaCl and 50 mM HEPES, pH 7.2, heated to 90 °C during 5 min, cooled slowly to room temperature, and stored at 4 °C.

Melting experiments were performed using a V-650 Spectrophotometer (Jasco, Madrid, Spain) connected to a temperature controller that increased temperature at a rate of 1 °C/min from 10 to 90 °C. Absorbance of the samples was measured in a 1 cm path length quartz cells.

The MeltWin 3.5 software was used to perform a thermodynamic analysis to calculate melting temperatures ( $T_m$ ) and free energy values ( $\Delta G$ ) as the mean of two independent melting experiments.

**Cell Culture.** PC3 prostate adenocarcinoma cells (ECACC), SKBR3 breast adenocarcinoma cells (ATCC) and MiaPaCa-2 pancreas carcinoma cells (ATCC) were cultivated in Ham's F-12 medium supplemented with 7% fetal bovine serum (GIBCO, Invitrogen, Barcelona, Spain) and incubated at 37 °C in a humidified 5% CO<sub>2</sub> atmosphere.

**Transfection.** The transfection procedure consisted in mixing the appropriate amount of either PPRH or TFO and the transfection reagent DOTAP (Roche, Mannheim, Germany or Biontex, Germany) for 20 min in a volume of 200 μL of medium at room temperature, followed by the addition of the mixture to the cells plated in 35 mm-diameter dishes in a total volume of 1 mL.

**MTT Assay.** MiaPaCa 2 (5000), PC3 (10 000), or SKBR3 (10 000) cells were plated in 35 mm-diameter dishes in F12 medium and treated with the appropriate concentration of each molecule. After 6 days, MTT assay was performed as described by Rodríguez et al.<sup>11</sup>

**mRNA Analyses.** A total of 60 000 PC3 or MiaPaCa 2 cells were plated in 35 mm-diameter dishes in F12 medium and total RNA was extracted 48 or 72 h after transfection, using Ultraspec (Biontex) or Trizol (Life Technologies, Madrid, Spain), following the manufacturer's specifications. Quantification of RNA was performed measuring its absorbance (260 nm) at 25 °C using a Nanodrop ND-1000 spectrophotometer.

**Reverse Transcription.** cDNA was synthesized using 1 μg of total RNA, as described by Rodríguez et al.<sup>11</sup> for *TERT* mRNA levels determination.

For *survivin* mRNA levels, 500 ng were used in a total volume of 20 μL of reaction containing 2 μL of Buffer 10x (500 mM Tris-HCl pH 8.3, 750 mM KCl, 30 mM MgCl<sub>2</sub>, 100 mM DTT) (Lucigen, Middleton, Wisconsin), 12.5 ng of random hexamers (Roche), 0.5 mM each dNTP (AppliChem, Barcelona, Spain), 20 units of NxGen RNase inhibitor (Lucigen) and 200 units of NxGen M-MuLV reverse transcriptase (Lucigen). The reaction was incubated at 37 °C for 1 h and 3 μL of the cDNA per sample were used for qRT-PCR.

**Real Time-PCR.** The StepOnePlus Real-Time PCR Systems (Applied Biosystems, Barcelona, Spain) was used to perform these experiments.

SYBR was used to determine *TERT* mRNA levels. Primer sequences were: *TERT*-Fw, 5'-GCGGAAGACAGTGGT-GAACT-3'; *TERT*-Rv, 5'-AGCTGGAGTAGTCGCTCTGC-3'; and the endogenous control, *APRT*-Fw, 5'-AAGGCT-GAGCTGGAGATTCA-3'; *APRT*-Rv, 5'-GGTACAGGTGC-CAGCTTCTC-3'.

The final volume of the reaction was 20 μL, containing 10 μL of Biotools Mastermix (2X) (Biotools, Madrid, Spain), 1 μL of SYBR (dilution 1/1000, Life technologies), 0.25 μM of each primer, 3 μL of cDNA and H<sub>2</sub>O mQ. PCR cycling conditions were 2 min at 50 °C, 10 min denaturation at 95 °C, followed by 35 cycles of 15 s at 95 °C and 1 min at 60 °C.

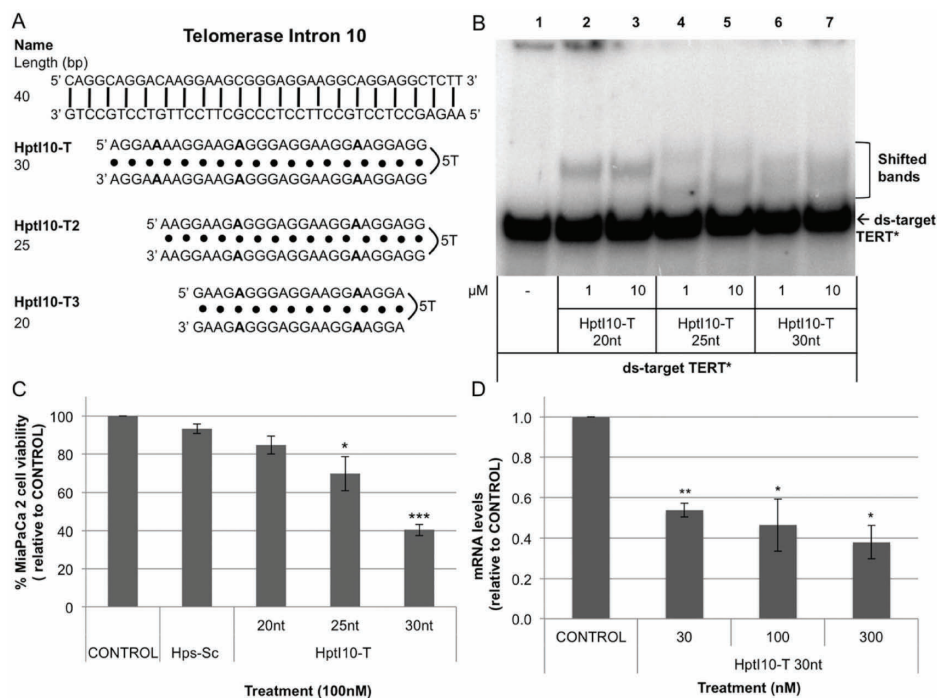
To determine *survivin* mRNA levels, the following TaqMan probes were used: *Survivin* (BIRC5) (HS04194392\_S1), and adenine phosphoribosyl-transferase (*APRT*) (HS00975725\_M1) and 18S rRNA (HS99999901\_S1), as endogenous controls. The reaction contained 1x TaqMan Universal PCR Mastermix (Applied Biosystems), 1x TaqMan probe (Applied Biosystems), 3 μL of cDNA and H<sub>2</sub>O mQ to a final volume of 20 μL. PCR cycling conditions were 10 min denaturation at 95 °C, followed by 40 cycles of 15 s at 95 °C and 1 min at 60 °C.

The mRNA quantification was calculated using the  $\Delta\Delta C_T$  method, where  $C_T$  is the threshold cycle that corresponds to the cycle where the amount of amplified mRNA reaches the threshold of fluorescence.

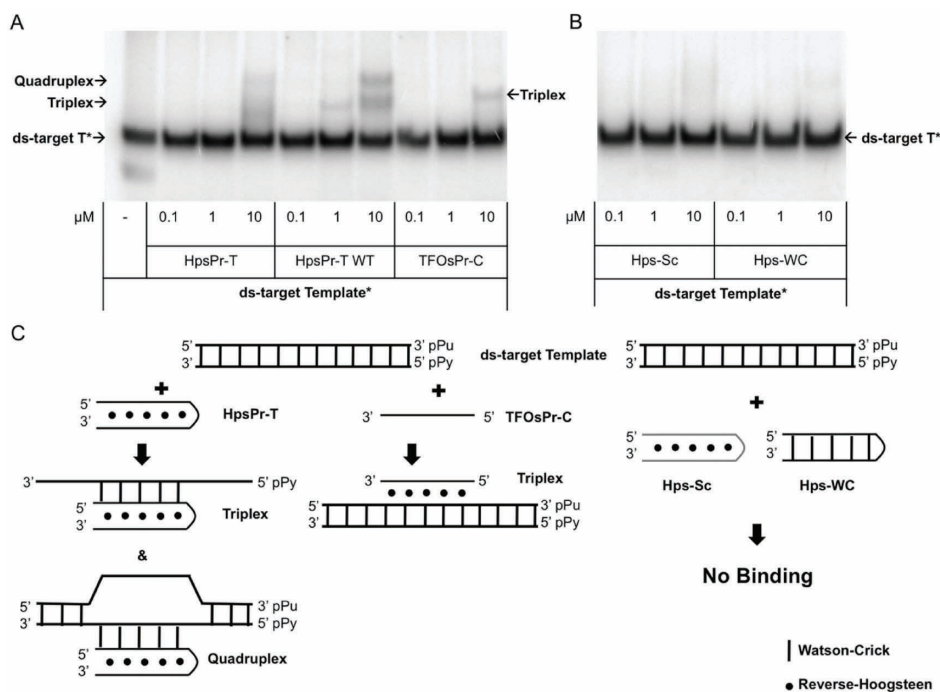
## RESULTS

**Design of PPRHs.** Different PPRHs were designed to assess the effect of length, their efficacy compared with TFOs, and how to cope with the presence of purine interruptions in the polypyrimidine target sequence. Furthermore, we tested new designs for improving the effectiveness of the PPRHs. The specific design in each case is described below. To test for specificity, we performed BLAST analyses with all PPRHs using as a database the reference genomic sequence of *Homo sapiens*. In

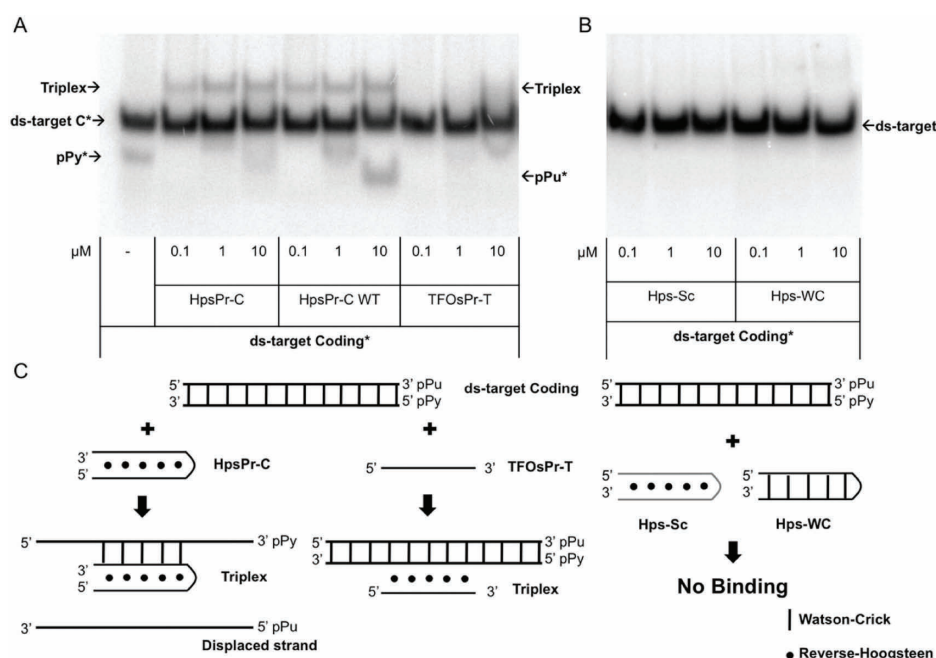




**Figure 1.** PPRHs of different length: diagram, binding to their target sequence, effect on cell viability, and *TERT* mRNA levels. (A) Representative diagram of the three PPRHs designed against the same intronic sequence of the *TERT* gene, but with different lengths. Bullets represent reverse-Hoogsteen bonds. Interruptions, substituted by adenines, are marked in bold. (B) Hpt110-T of different lengths (lane 2 and 3, 20 nucleotides; lane 4 and 5, 25 nucleotides; and lane 6 and 7, 30 nucleotides) was incubated with the radiolabeled ds-target sequence (20 000 cpm) within intron 10 of the *TERT* gene (40 nucleotides). (C) CONTROL cells are untreated MiaPaCa 2 cells. A total of 100 nM of PPRHs against the *TERT* gene were transfected in MiaPaCa 2 cells. DOTAP was used at 10  $\mu$ M. MTT assays to determine cell survival were performed 6 days after transfection. Data are mean  $\pm$  SEM values of at least three experiments. \* $p < 0.05$ , \*\* $p < 0.01$ , \*\*\* $p < 0.005$ . (D) RNA was extracted from MiaPaCa 2 cells treated with increasing concentrations of Hpt110-T for 72h. mRNA levels were determined using qRT-PCR and referred to the levels of endogenous controls. Data are mean  $\pm$  SEM values of at least three experiments. \* $p < 0.05$ , \*\* $p < 0.01$ , \*\*\* $p < 0.005$ .



**Figure 2.** Binding of template-PPRHs and TFO to their target sequence. (A) Binding of the template-PPRH either with adenines in the pyrimidine interruptions (HpsPr-T) or the wild-type version (HpsPr-T WT) and the TFOsPr-C after incubation with increasing concentrations of their radiolabeled ds-target sequence (20 000 cpm). Shifted bands are indicated by arrows. (B) Binding of the negative controls, either Hps-Sc or Hps-WC to the radiolabeled ds-target sequence (20 000 cpm) for the specific PPRHs. (C) Schematic representation of the binding of the different molecules used in this study, including HpsPr-T, HpsPr-T WT, TFOsPr-C, Hps-Sc, Hps-WC.



**Figure 3.** Binding of coding-PPRHs and TFO to their target sequence. (A) Binding of the coding-PPRH either with adenines in the pyrimidine interruptions (HpsPr-C) or the wild-type version (HpsPr-C WT) and the TFOsPr-T after incubation with increasing concentrations of their radiolabeled ds-target sequence (20 000 cpm). Shifted bands are indicated by arrows. (B) Binding of the negative controls, either Hps-Sc or Hps-WC to the radiolabeled ds-target sequence (20 000 cpm) for the specific PPRHs. (C) Schematic representation of the binding of the different molecules used in this study, including HpsPr-C, HpsPr-C WT, TFOsPr-T, Hps-Sc, Hps-WC.

all experiments, we used as negative controls either a PPRH with a scrambled sequence (Hps-Sc) or a PPRH with intramolecular Watson–Crick bonds instead of Hoogsteen bonds (Hps-WC), which is not able to form triplexes with the DNA. We also used as negative control a TFO with a scrambled sequence without target in the human genome (TFO-Sc).

**Effect of PPRHs Length on Binding to the Target, Cell Viability and mRNA.** To compare the effects of PPRHs with different lengths, we needed to start with a gene containing a polypurine/polypyrimidine stretch long enough to allow the design of PPRHs with different number of nucleotides. We found a 30 nucleotides polypyrimidine sequence within intron 10 of the *TERT* gene that opened the possibility to test PPRHs lengthening 20, 25, or 30 nucleotides against the same target sequence (Table 1, Figure 1A). HptI10-T had 3 three pyrimidine interruptions, whereas HptI10-T2 and HptI10-T3 had two interruptions. For these experiments, we used PPRHs where the pyrimidine interruptions were substituted by adenines in both strands of the PPRH. As shown in Figure 1B the three PPRHs tested were capable of binding to their target sequence at a concentration as low as 1  $\mu\text{M}$ . However, in terms of cell viability, we observed that the longer the sequence, the higher the effect. Specifically, the 20-, 25-, and 30-nucleotide PPRHs decreased cell viability by 15%, 30%, and 60%, respectively (Figure 1C). In the case of TERT inhibitors, reaching 60% decrease in cell viability can be considered a notable effect because a long time is needed for the cell to shorten the telomeres enough to enter senescence. For that reason, inhibitors of TERT are commonly used in combination with other drugs.<sup>16</sup> We also determined the mRNA levels of TERT using the longest PPRH that caused a dose-dependent decrease, reaching 60% at 300 nM (Figure 1D).

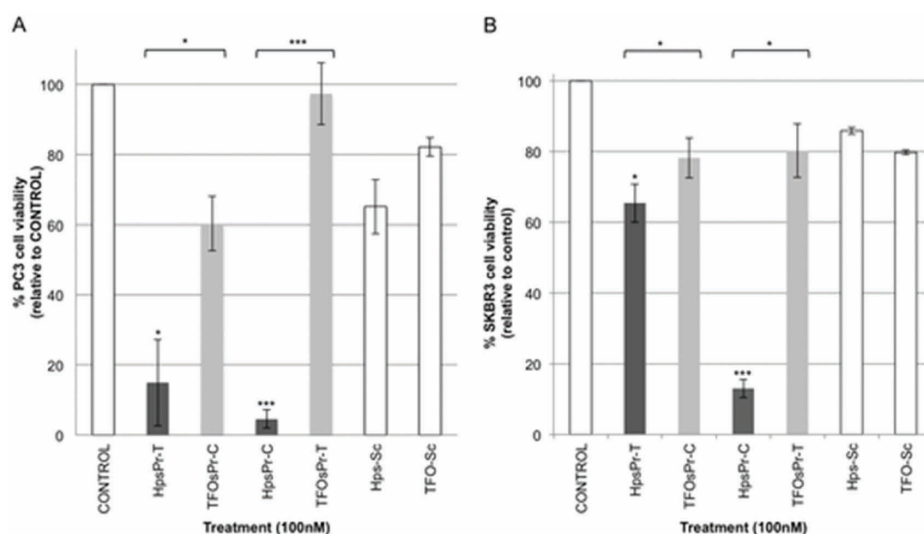
**Comparison between PPRHs and Nonmodified TFOs. Binding to Target Sequences.** For the comparative analyses, we used PPRHs against the promoter sequence of *survivin*, which

have been previously validated in terms of efficacy in prostate cancer cells and in a xenografted tumor model.<sup>11</sup> Those PPRHs were designed against two different sequences within the promoter, one against a distal region, at-1009, in the template strand of the DNA (Template-PPRH), and another against a more proximal region, at -525, in the coding strand (Coding-PPRH). Thus, the corresponding TFOs that would bind to the same sequence as PPRHs were designed. PPRHs are double-stranded molecules formed by two polypurine strands that bind to the pyrimidine target in the DNA sequence by Watson–Crick bonds, whereas TFOs are single-stranded polypurine molecules that will bind to the purine strand in the DNA by reverse-Hoogsteen bonds forming a triplex structure. Therefore, the TFO that binds to the same region as the template-PPRH will bind to the coding strand, and the TFO that binds to the same region as the coding-PPRH will bind to the template strand. PPRHs and TFOs sequences are listed in Table 2.

The binding was analyzed using the corresponding radiolabeled ds-target sequence for each PPRH either template or coding, shown in Figures 2 and 3.

We observed that both the Template-PPRH (HpsPr-T) and the corresponding TFO (TFOsPr-C) were specific for their target sequence, as indicated by the shifted bands (Figure 2A), whereas the two negative controls, Hps-Sc and Hps-WC, did not bind to the target sequences (Figure 2B). The template-PPRH against the promoter sequence (HpsPr-T) was bound to the target sequence forming a triplex structure-binding of the PPRH to the pyrimidine target sequence- and quadruplex structure-binding of the PPRH to the duplex, whereas the TFO formed a single triplex structure-binding of the TFO to the duplex (Figure 2A and 2C).

Regarding the coding-PPRH, we also observed specificity of both HpsPr-C and TFOsPr-T, as indicated by the shifted band (Figure 3), in contrast to the two negative controls, Hps-Sc and



**Figure 4.** Effect of PPRHs and TFOs against *survivin* on cell viability. (A) Cell viability in PC3 cells upon incubation with 100 nM of the two PPRHs (dark gray) or the two TFOs (light gray) against the *survivin* gene. Negative controls -Hps-Sc and TFO-Sc (blank bars)- were tested at the same conditions. CONTROL cells are untreated PC3 cells. (B) Cell viability in SKBR3 cells upon incubation with 100 nM of the two PPRHs (dark gray) or the two TFOs (light gray) against the *survivin* gene. Negative controls -Hps-Sc and TFO-Sc (blank bars)- were tested at the same conditions. CONTROL cells are untreated SKBR3 cells. MTT assays to determine cell survival were performed 6 days after transfection. DOTAP was used at 10  $\mu$ M. Data are mean  $\pm$  SEM values of at least three experiments. \* $p < 0.05$ , \*\* $p < 0.01$ , \*\*\* $p < 0.005$ .

Hps-WC, which did not bind to the target sequence (Figure 3B). HpsPr-C was capable of binding to its target sequence from 100 nM to 10  $\mu$ M, causing strand displacement at 10  $\mu$ M. On the other hand, the TFO against the same sequence only showed some binding at 10  $\mu$ M (Figure 3A), proving that it had less affinity to the target sequence than the coding-PPRH. In Figure 3C there is a representation of the different structures observed in the binding assays. In this case, we only observed the triplex structure because the PPRH was capable of displacing the purine strand completely. The different length of their target sequences might cause the difference of binding between the template- and coding-PPRH. In the case of the coding-PPRH, the target sequence is shorter, and in consequence, easier to displace.

**Cell Viability.** We compared the effect of PPRHs and TFOs in two cell lines, PC3 from prostate cancer and SKBR3 from breast cancer, upon incubation with 100 nM of the DNA molecules (PPRH or TFO) plus 10  $\mu$ M of the liposomal reagent DOTAP (Roche). In both cell lines, there was a significant difference between the use of PPRHs vs TFOs; both template- and coding-PPRHs exerted a higher decrease in cell viability than the corresponding TFOs at 100 nM, as shown in Figure 4. Negative controls for each type of molecule -Hps-Sc and TFO-Sc- were used at the same conditions and a rather small effect was observed upon incubation in both cell lines, probably due to the transfection reagent.

It was also observed that PPRHs and TFOs caused a higher decrease in viability in PC3 than in SKBR3 cells. This could be caused by the different transfection efficiency of DOTAP in each cell line. PC3 cells internalize almost four times more PPRH than SKBR3 using the same conditions of transfection, as determined in uptake experiments using flow cytometry and fluorescently labeled PPRHs. Using this methodology, we also compared the uptake of fluorescently labeled PPRH and TFO, observing that 24 h after transfection, more than 90% of PC3 cells showed a similar mean intensity of fluorescence with either molecule (data not shown). This result indicated that the difference in effect of

PPRHs and TFOs was due to a different intrinsic efficacy rather than a different uptake.

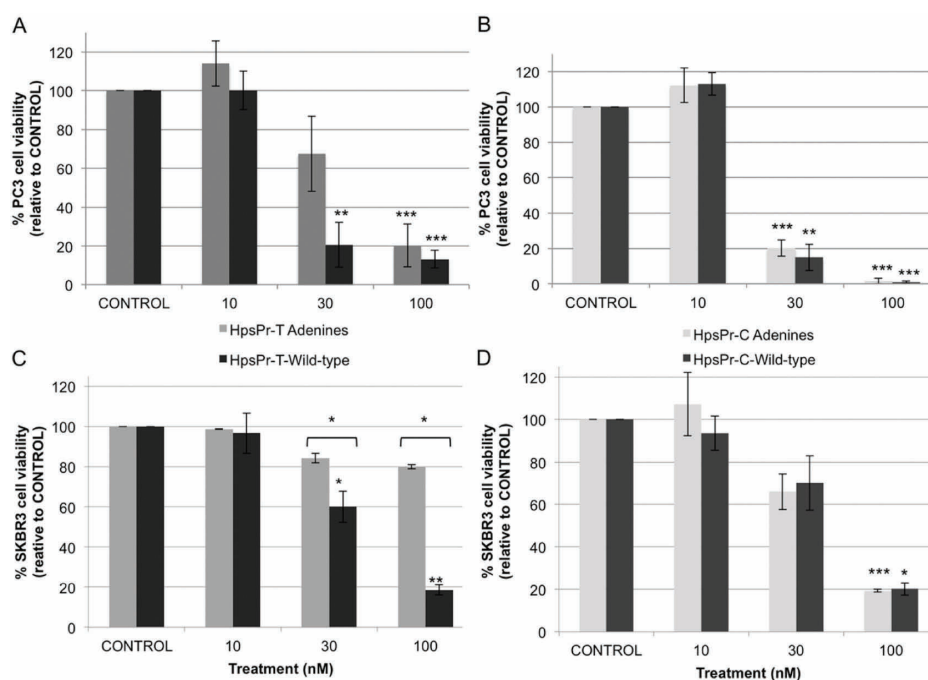
#### Comparison between PPRHs Carrying Adenines and Wild-Type Sequences. Binding to Their Target Sequence.

Once we had compared PPRHs and nonmodified TFOs, we wanted to improve our PPRHs in terms of efficacy and specificity. To do so, we decided to explore the usage of wild-type PPRHs including pyrimidine interruptions in their sequences instead of substituting the interruptions by adenines. We had previously stated that the best base—in terms of binding and cytotoxicity—to substitute a single interruption was adenine;<sup>9</sup> however, it is usual to find polypurine stretches with several interruptions that could compromise the specificity of the molecule. We studied HpsPr-T and HpsPr-C against *survivin*, both of which contained three interruptions substituted by adenines, and their counterparts, HpsPr-T WT and HpsPr-C WT, in which the wild-type sequence was used. PPRHs sequences are listed in Table 2, including a scheme of the molecules. It is important to mention the difference between the two approaches: The A-substitution involved using two adenines in each interruption, one in the Watson–Crick strand (that will bind to the pyrimidine target sequence) and one in the reverse-Hoogsteen strand (that forms the hairpin structure). In the wild-type version, the same pyrimidine (C or T) of the interruption was used in both strands of the PPRH.

When performing BLAST analyses using the wild-type sequences, the first match with the lowest e-value and maximum identity was always the target sequence within the *survivin* gene. However, when using the sequences where the pyrimidines were substituted by adenines, several sequences were found with the same identity but higher e-value, indicating possible off-target effects.

In the binding assays with the *survivin* promoter shown in Figure 2 and 3, there was the general tendency that the wild-type PPRHs were capable of binding to the polypyrimidine target sequences with more affinity and at lower concentrations than the PPRHs with adenines in front of the purine interruptions. In





**Figure 5.** Effect of PPRHs against *survivin* on cell viability. (A) Dose response of template-PPRHs against *survivin* in PC3 cells. (B) Dose response of coding-PPRHs against *survivin* in PC3 cells. (C) Dose response of template-PPRHs against *survivin* in SKBR3 cells. (D) Dose response of coding-PPRHs against *survivin* in SKBR3 cells. DOTAP was used at 5  $\mu\text{M}$  to transfect 10 nM and 30 nM and at 10  $\mu\text{M}$  to transfect 100 nM PPRH. CONTROL cells are untreated cells. MTT assays to determine cell survival were performed 6 days after transfection. Data are mean  $\pm$  SEM values of at least three experiments. \* $p < 0.05$ , \*\* $p < 0.01$ , \*\*\* $p < 0.005$ . Light gray corresponds to the adenine version and dark gray to the wild-type version.

the case of the template-PPRH, there was a clear difference in the binding affinity between HpsPr-T and HpsPr-T WT, only the wild-type version bound to its target at concentrations as low as at 1  $\mu\text{M}$ , whereas the other PPRH did not generate a shifted band up until 10  $\mu\text{M}$  (Figure 2A). In the case of the coding-PPRH, both PPRHs originated a band corresponding to the triplex at all concentrations tested (from 0.1 to 10  $\mu\text{M}$ ), but the wild-type showed five times more strand displacement upon binding (Figure 3A).

**Cell Viability Assays.** To compare the effect of PPRHs with or without pyrimidine interruptions, dose response studies in PC3 and SKBR3 were performed and the  $\text{IC}_{50}$  for each molecule was calculated. The resulting cell viabilities are shown in Figure 5 and the  $\text{IC}_{50}$ 's in Table 4. Template and coding-PPRHs decreased cell viability in a dose-dependent manner in both cell lines, and in all cases, the wild-type counterpart presented a lower  $\text{IC}_{50}$ .

**Melting Experiments.** Melting temperatures and  $-\Delta G$  were obtained using the MeltWin 3.5 software<sup>17</sup> and are displayed in Table 5. We measured the changes in absorbance at 260 nm when increasing temperature from 10 to 90  $^{\circ}\text{C}$ ; in all cases, sigmoidal curves with a single transition corresponding to the

**Table 4.**  $\text{IC}_{50}$  Calculated for PPRHs and Wedge-PPRH in PC3 and SKBR3

PPRH*	PC3	SKBR3
	$\text{IC}_{50}$ (nM)	$\text{IC}_{50}$ (nM)
HpsPr-T A	46.21	346.57
HpsPr-T WT	30.14	40.77
HpsPr-C A	16.50	43.32
HpsPr-C WT	14.44	43.32
Wedge-PPRH-17	21.62	41.17

\*A indicates adenines and WT wild-type.

**Table 5.** Melting Transition Temperatures,  $T_m$ , and Free Energies,  $\Delta G$ , at pH 7.2

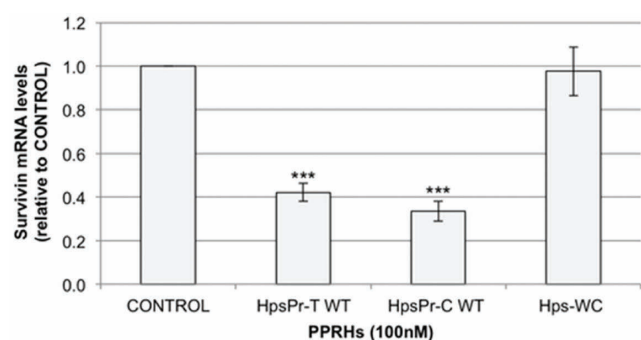
complex*	$T_m \pm \text{std error}$ ( $^{\circ}\text{C}$ )	$\Delta G \pm \text{std error}$ (kcal/mol, at 37 $^{\circ}\text{C}$ )
HpsPr-T A + Ppy	54.05 $\pm$ 0.23	-12.60 $\pm$ 0.13
HpsPr-T WT + Ppy	73.47 $\pm$ 0.30	-19.81 $\pm$ 0.70
HpsPr-C A + Ppy	37.24 $\pm$ 2.42	-9.29 $\pm$ 0.53
HpsPr-C WT + Ppy	66.45 $\pm$ 0.07	-25.96 $\pm$ 2.29

\*A indicates adenines and WT wild-type.

switch from bound complex to random coil were observed, which corresponds to a bimolecular melting curve, previously described in ref 18. Comparison between the PPRH containing interruptions substituted by adenines and the wild-type counterpart showed a clear difference of around 20  $^{\circ}\text{C}$ , the wild-type presenting the higher temperature and the lower  $\Delta G$ , meaning these PPRHs had a higher affinity for the target sequence. It was also clear that the longer the PPRH, the higher the melting temperature; therefore, the template-PPRH, which is 26 nucleotides long, had a higher temperature than the coding-PPRH that was 20 nucleotides long.

***Survivin mRNA Levels.*** Treatment for 48 h of wild-type PPRHs against *survivin* caused a decrease in its expression. Specifically, HpsPr-T WT caused a 2.4-fold decrease and HpsPr-C WT caused a 3-fold decrease in mRNA levels, whereas no effect was observed with the negative control HpsPr-WC (Figure 6).

**Wedge-PPRH.** *Design.* Concurrently to the study of wild-type PPRHs, we decided to further improve PPRHs by designing a structure that would lock the strand displacement, which may stabilize the PPRH-DNA complex and cause a higher effect. The design consisted in extending the 5' with the sequence of polypyrimidines complementary to the polypurine strand. The



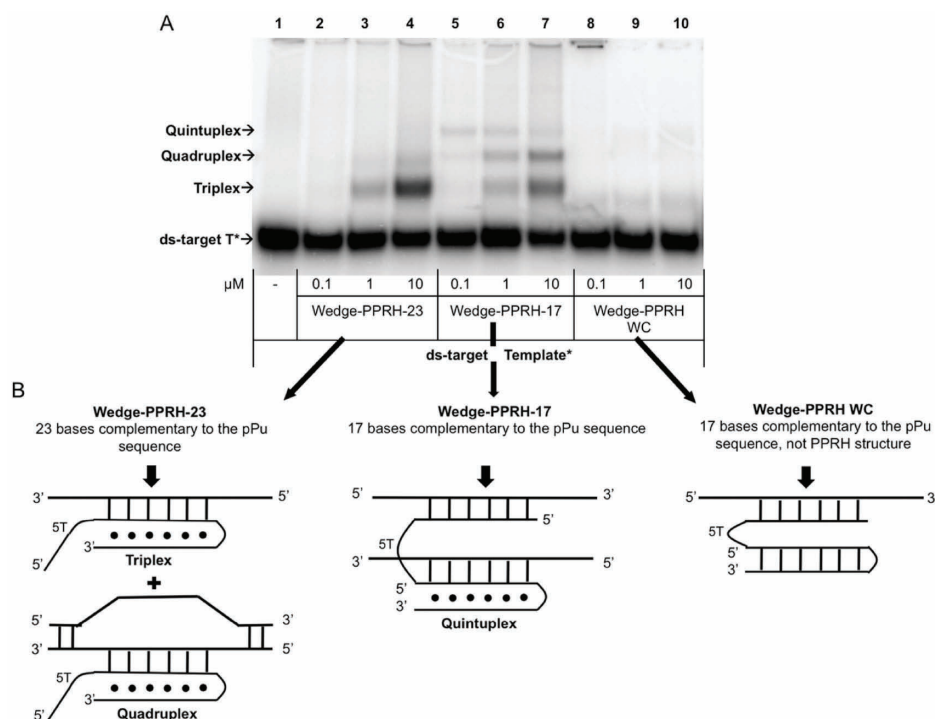
**Figure 6.** Effect of wild-type PPRHs on *survivin* mRNA levels. RNA was extracted from PC3 cells treated with 100 nM of HpsPr-T WT, HpsPr-C WT and the negative control Hps-WC for 48 h. mRNA levels were determined using qRT-PCR and referred to the levels of *APRT* as an endogenous control. DOTAP was used at 8  $\mu$ M. Data are mean  $\pm$  SEM values of at least three experiments. \* $p < 0.05$ , \*\* $p < 0.01$ , \*\*\* $p < 0.005$ .

rationale was that such PPRH could open the double strand and the extension could bind to the coding strand, as detailed in Figure 7B.

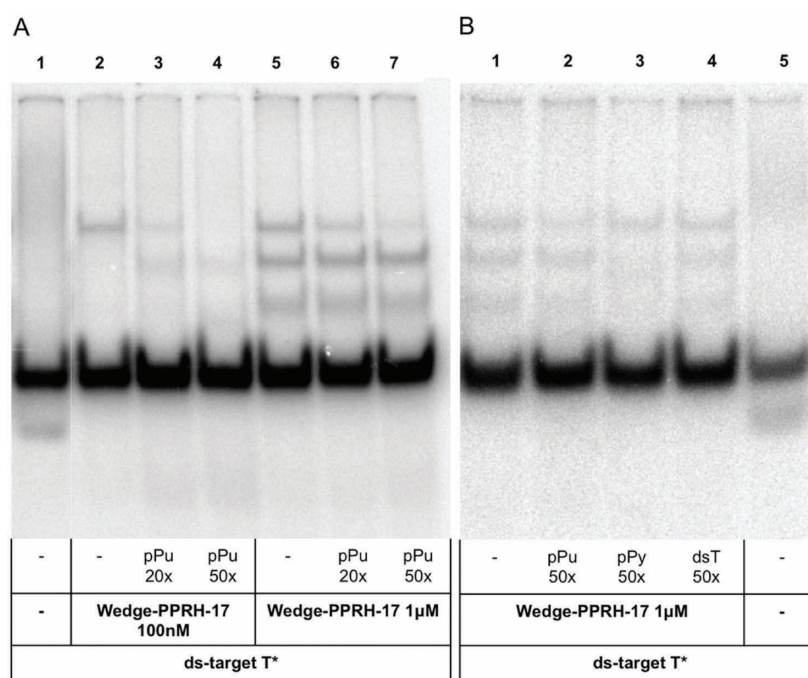
The Template-PPRH was selected to perform this study. We designed two Wedge-PPRHs; one had a 5' extension of 23 bases complementary to the purine sequence, linked by a 5T loop to give flexibility for the turn, and another with a shorter extension of 17 nucleotides. As a negative control we used Wedge-PPRH WC, which presented the 17-nucleotide complementary sequence followed by a hairpin that formed Watson–Crick bonds instead of reverse-Hoogsteen bonds, a useful control to determine the importance of the PPRH in this structure. All the sequences are listed in Table 3.

**Binding to the Target Sequence.** We performed binding analyses for the three wedge structures. We observed a similar pattern of binding between the Wedge-PPRH-23 and the HpsPr-T WT (Figure 7A compared to Figure 2A), indicating that the presence of the 5' extension did not prevent the binding of the PPRH to its target sequence. Wedge-PPRH-23 formed two bands corresponding to a triplex and a quadruplex structure (Figure 7B). We expected to observe an additional band (quintuplex) if the 5' extension could bind to the displaced polypurine strand which was not seen with the Wedge-PPRH-23. Therefore, we tested a shorter version of the Wedge-PPRH with an extension of only 17 nucleotides, so it could hybridize to the polypurine displaced strand. Using Wedge-PPRH-17 we observed an additional shifted band corresponding to the quintuplex structure (Figure 7B). Moreover, Wedge-PPRH-17 bound to the target sequence at a lower concentration (100 nM) than when using PPRHs and Wedge-PPRH-23. It is important to note that binding with the Wedge-PPRH WC showed a low intensity band that might correspond to the binding of the 17-nucleotide extension to its complementary sequence, no additional bands were observed because of the lack of PPRH structure, indicating the importance of this structure for the opening of the dsDNA.

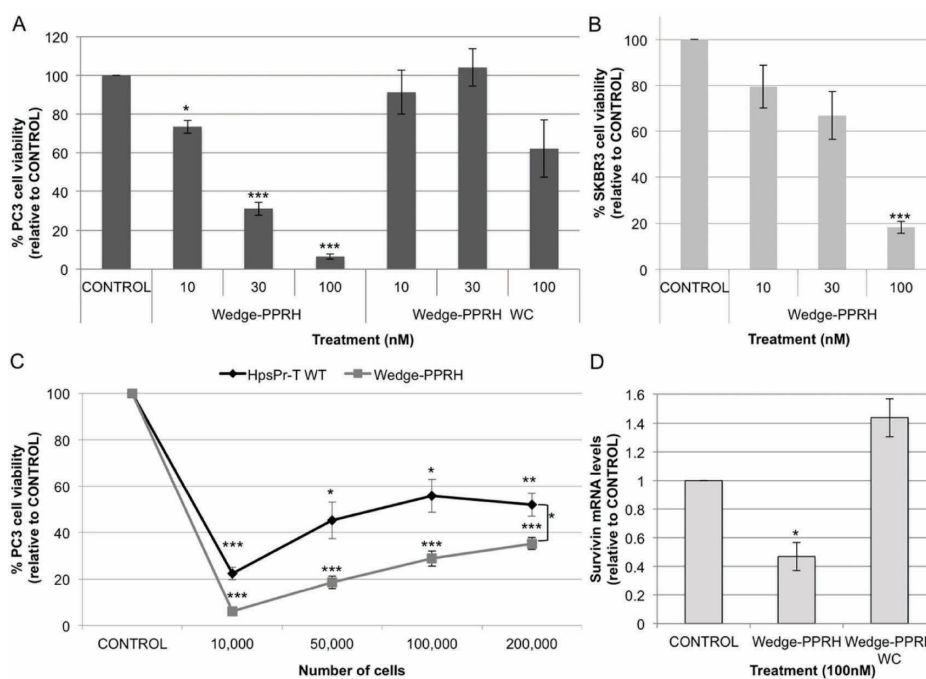
To really demonstrate the identity of the quintuplex, we performed binding experiments with both the Wedge-PPRH-17 and the duplex and competing with either the coding strand (pPu) (Figure 8A and B), the pyrimidine strand (pPy), or the duplex (dsT) (Figure 8B). In Figure 8A, we observed the competition between the polypurine sequence (at 20 $\times$ , lanes 3 and 6; or 50 $\times$ , lanes 4 and 7) and the radiolabeled duplex (20 000 cpm) at different concentrations of Wedge-PPRH-17 (100 nM, lanes 2–4; and 1  $\mu$ M, lanes 5–7). The disappearance of the



**Figure 7.** Binding of Wedge-PPRH to its target sequence. (A) Binding of Wedge-PPRH to its radiolabeled ds-target sequence (20 000 cpm). The mobility of the ds-target sequence is shown in lane 1. Binding of Wedge-PPRH-23 is shown in lane 2, 3, and 4. Binding of Wedge-PPRH-17 is shown in lane 5, 6, and 7. The negative control, Wedge-PPRH WC is shown in lane 8, 9, and 10. Shifted bands are indicated by arrows. (B) Schematic representation of the structures corresponding to the different bands observed in the electrophoresis.



**Figure 8.** Identification of the shifted bands in the binding assays with Wedge-PPRH-17. (A) Binding of Wedge-PPRH-17 to its radiolabeled ds-target sequence (20 000 cpm). The mobility of the ds-target sequence is shown in lane 1. The binding pattern of the Wedge-PPRH-17 is shown at two different concentrations of Wedge-PPRH: 100 nM (lane 2–4) and 1  $\mu$ M (lane 5–7); competition assays were performed using 20-fold (lane 3 and 6) and 50-fold (lane 4 and 7) excess of the coding strand of the target sequence. (B) Binding of Wedge-PPRH-17 at 1  $\mu$ M to its radiolabeled ds-target sequence (20 000 cpm). The mobility of the ds-target sequence is shown in lane 5. The binding pattern of the Wedge-PPRH is shown in lane 1 and competition assays were performed using 50-fold excess of either the coding (lane 2) or the template strand (lane 3) or the ds-target sequence (lane 4).



**Figure 9.** Effect of Wedge-PPRH-17 on cell viability and *survivin* mRNA levels. (A) Effect in PC3 cells. (B) Effect in SKBR3 cells. In both cases, DOTAP was used at 5  $\mu$ M to transfect 10 nM and 30 nM, and at 10  $\mu$ M to transfect 100 nM of Wedge-PPRH. CONTROL cells are untreated cells. MTT assays to determine cell survival were performed 6 days after transfection. Data are mean  $\pm$  SEM values of at least three experiments. \* $p$  < 0.05, \*\* $p$  < 0.01, \*\*\* $p$  < 0.005. (C) Effect of HpsPr-T WT and Wedge-PPRH-17 on cell viability when scaling-up the number of PC3 cells. (D) RNA was extracted from PC3 cells treated with 100 nM of Wedge-PPRH-17 or Wedge-PPRH WC for 48 h. DOTAP was used at 8  $\mu$ M. mRNA levels were determined using qRT-PCR and referred to the levels of the endogenous control *18S*. Data are mean  $\pm$  SEM values of at least three experiments. \* $p$  < 0.05.

upper band, corresponding to the quintuplex, indicates its high affinity to the polypurine sequence and that the 5' pyrimidine

extension was binding to the displaced polypurine sequence. In fact, when using the lowest concentration of Wedge-PPRH-17



(100 nM), the competition by pPu (20× or 50×) produced the disappearance of the quintuplex while the quadruplex appeared. When the Wedge-PPRH-17 was increased at 1  $\mu$ M, the competition with pPu also decreased the intensity of the band corresponding to the quintuplex.

In Figure 8B, aside from competing the duplex with pPu (lane 2), we competed with pPy (lane 3) and the duplex (lane 4). Competition with pPy caused a decrease in the intensity of the bands corresponding to the triplex and quadruplex structures, but not the quintuplex, reaffirming the quintuplex was the band most difficult to displace because it had the highest affinity. In lane 4, we observed the decrease of the three shifted bands because the competition was performed with the duplex.

**Cell Viability Assays and Survivin mRNA Levels.** We decided to further explore the effect of the Wedge-PPRH with the extension of 17-nucleotides in terms of cell viability and mRNA levels because we had shown that it was capable of forming the locked structure.

In PC3 cells, we observed a similar effect on cell viability of the Wedge-PPRH-17 compared to the original or wild-type-PPRHs (Figure 9A compared to Figure 5A). However, when analyzing the data, the Wedge-PPRH-17 presented a lower  $IC_{50}$  than HpsPr-T WT (Table 4), indicating that the Wedge-PPRH-17 had a higher efficacy. Wedge-PPRH WC was innocuous at 10 and 30 nM and caused only a slight decrease at 100 nM (Figure 9A). In SKBR3, Wedge-PPRH-17 had a dose-dependent effect (Figure 9B) similar to HpsPr-T WT (Figure 5D) and, as a result, a similar  $IC_{50}$  was obtained (Table 4).

We performed a scale-up experiment to figure out the effect of PPRHs when increasing the number of cells. Keeping the concentration of either the PPRH or the Wedge-PPRH (100 nM) unchanged, we observed that there was a slight loss of effect when increasing the number of cells, but both molecules maintained its efficacy up to 200 000 cells. As shown in Figure 9C, Wedge-PPRH-17 maintained its efficacy significantly in a more stable way.

Regarding mRNA levels, Wedge-PPRH-17 caused a 2-fold decrease at 100 nM, whereas Wedge-PPRH WC did not cause a decrease in *survivin* mRNA level. (Figure 9D).

## DISCUSSION

The purpose of this study was to improve the suitability of the polypurine reverse Hoogsteen hairpins as gene targeting tools by exploring several characteristics. Specifically, we focused on the following properties of PPRHs: (i) nucleotide length to define the optimal range in their design, (ii) affinity and effect compared with nonmodified TFOs, (iii) specificity toward the target sequence by using wild-type-PPRHs, and (iv) development of a new structure termed Wedge-PPRH.

**PPRH Nucleotide Length.** The possibility to design PPRHs depends on the presence of polypurine/polypyrimidine sequences in the target genes. Goñi et al.<sup>13</sup> reported that triplex target sequences were overrepresented in the human genome, finding them commonly in regulatory regions. This abundance allows the design of PPRHs against almost any gene although each one will present different options of length for targeting. From our study, we can conclude that whenever possible, the longer the PPRH, the greater the effect, starting with a minimum of 20 nucleotides. In the case of the *TERT* gene used in this study, we observed binding of the PPRHs to their target from 20 to 30 nucleotides but the higher effect was obtained with the longest one.

## Comparison between PPRHs and Nonmodified TFOs.

One difference between PPRHs and TFOs is that PPRHs are double-stranded DNA molecules whereas TFOs are single-stranded. Because of this, their binding differs: PPRHs form intramolecular reverse Hoogsteen bonds and bind by Watson–Crick bonds to their polypyrimidine target sequence, TFOs form Hoogsteen bonds with the purine strand in the double helix. Using the same binding conditions of pH and salt composition, and taking into account that the PPRH and the corresponding TFO have the same sequence, we observed that PPRHs bind at lower concentrations than TFOs to the target sequence, indicating a higher affinity. Moreover, in terms of cell viability, both PPRHs exerted a higher effect in PC3 and SKBR3 cells than TFOs, indicating that PPRHs were more effective.

Kool and colleagues<sup>18</sup> had previously shown that hairpin structures formed by two purine domains could bind to the pyrimidine target sequence in a cooperative fashion and with higher affinity than the two separate strands. Thus, the existence of the hairpin structure represents a clear advantage over single-stranded molecules and proves that the strand that does not interact directly with the DNA contributes to the binding. In our work, we corroborated that the strand that allows the formation of the intramolecular Hoogsteen bonds within the PPRH favors its binding to the target sequence with higher affinity than TFOs. In addition, we prove that the increase in affinity displayed by PPRHs is reflected in a stronger effect in terms of cell viability.

**Specificity of PPRHs.** In the mismatches study,  $T_m$  experiments showed that the presence of mismatches caused a decrease in  $T_m$ , indicating less affinity for the target sequence, in accordance with previous results from Kool.<sup>18</sup> In the case of HpsPr-T, 3 mismatches caused a decrease of around 17 °C in the  $T_m$  relative to the wild-type, whereas HpsPr-C, which also contained three mismatches, had a melting temperature of 25 °C below its wild-type counterpart. Therefore,  $T_m$  is affected not only by the length of the oligonucleotide but also by the presence of mismatches, proving the wild-type version is a better choice. Wang et al.<sup>7</sup> also reported that the presence of a hairpin structure stabilized the binding, then allowing for the presence of mismatches, even though with a lower  $T_m$ .

Currently, one of the main problems of gene-silencing technologies is the off-target effects caused by lack of specificity. siRNAs are known to activate TLRs, leading to inflammation and other off-target effects.<sup>19</sup> In this regard, PPRHs avoid off-target effects caused by activation of the immune system as opposed to siRNAs.<sup>15</sup>

Another problem intrinsic to the siRNA pathway is that siRNAs could bind to nontarget genes by acting as miRNAs.<sup>19</sup> Other authors have reported that as few as 11 nucleotides are sufficient to silence nontargeted genes, so although degradation of siRNA is occurring, they can cause off-target effects.<sup>20</sup> Degradation of siRNAs is meant to occur earlier than in the case of PPRHs because their half-life is much shorter.<sup>15</sup>

In this work, we prove that wild-type PPRHs have a higher affinity to their target sequence, and therefore, they are meant to have less off-target effects caused by their binding to nontargeted sequences. That is, the more interruptions substituted by adenines, the lower the  $T_m$  and affinity, increasing the possible off-target effects. However, up to 3 mismatches in a sequence of 20 nucleotides has proved to be effective both in vitro and in vivo without known off-target effects.<sup>11</sup> Avoidance of off-target effects using the wild-type version and prevention of activation of the immune response are appreciable advantages of PPRHs over siRNAs.

**Wedge-PPRH.** As previously stated, PPRHs are highly stable and resistant without the need of chemical modifications, which is another advantage over aODNs, TFOs, or siRNAs. However, there is room for improvement in terms of binding or effect. For this reason, we developed a new molecule called Wedge-PPRH, which binds simultaneously to both strands of the target sequence. Other authors have tested similar strategies based on triplexes capable of binding to adjacent polypyrimidine and polypurine sequences in both strands, using what they called alternate-strand triplex formation.<sup>21,22</sup> A Wedge-PPRH of the adequate length had a slightly better effect than PPRHs in decreasing cell viability and its effect was more constant as the number of incubated cells increases. Considering that the only difference between the Wedge-PPRH and the HpsPr-T WT is the 5' extension, we can conclude that the formation of the quintuplex structure, which locks the displaced strand of the dsDNA, contributes to the higher effect observed with the Wedge-PPRH.

As a summary, in this work, we investigated characteristics to improve the performance of PPRHs as a gene silencing tool and suggest a number of criteria to take into account when designing these molecules.

## AUTHOR INFORMATION

### Corresponding Author

\*E-mail: vnoue@ub.edu. Phone: +34 93 403 4455. Fax: +34 93 402 4520. Address: Department of Biochemistry and Molecular Biology, School of Pharmacy, Av. Diagonal 643, E-08028 Barcelona, Spain.

### Notes

The authors declare no competing financial interest.

## ACKNOWLEDGMENTS

The work was supported by Grant SAF2014-51825-R from "Plan Nacional de Investigación Científica" (Spain). Our group holds the Quality Mention from the "Generalitat de Catalunya" 2014-SGR96. L.R. and A.S. are recipients of FI fellowships from the "Generalitat de Catalunya". X.V. is recipient of APIF fellowship from University of Barcelona. We thank Maria Tintoré and Sonia Pérez from CSIC for their help with  $T_m$  experiments and the use of MeltWin 3.5 software.

## ABBREVIATIONS:

PPRH, polypurine reverse Hoogsteen hairpin; TFO, triplex-forming oligonucleotide; WT, wild-type; DOTAP, *N*-[1-(2,3-dioleoyloxy)propyl]-*N,N,N*-trimethylammonium methylsulfate; MTT, (3-(4,5-dimethylthiazol-2-yl)-2,5-diphenyltetrazolium bromide

## REFERENCES

- (1) Felsenfeld, G.; Rich, A. Studies on the formation of two- and three-stranded polyribonucleotides. *Biochim. Biophys. Acta* **1957**, *26* (3), 457–68.
- (2) Hoogsteen, K. The crystal and molecular structure of a hydrogen-bonded complex between 1-methylthymine and 9-methyladenine. *Acta Crystallogr.* **1963**, *16*, 907–916.
- (3) Hewett, P. W.; Daft, E. L.; Laughton, C. A.; Ahmad, S.; Ahmed, A.; Murray, J. C. Selective inhibition of the human tie-1 promoter with triplex-forming oligonucleotides targeted to Ets binding sites. *Mol. Med.* **2006**, *12* (1–3), 8–16.
- (4) Postel, E. H.; Flint, S. J.; Kessler, D. J.; Hogan, M. E. Evidence that a triplex-forming oligodeoxyribonucleotide binds to the c-myc promoter

in HeLa cells, thereby reducing c-myc mRNA levels. *Proc. Natl. Acad. Sci. U.S.A.* **1991**, *88* (18), 8227–31.

(5) Praseuth, D.; Guieysse, A. L.; Helene, C. Triple helix formation and the antigene strategy for sequence-specific control of gene expression. *Biochim. Biophys. Acta* **1999**, *1489* (1), 181–206.

(6) Faucon, B.; Mergny, J. L.; Helene, C. Effect of third strand composition on the triple helix formation: purine versus pyrimidine oligodeoxynucleotides. *Nucleic Acids Res.* **1996**, *24* (16), 3181–8.

(7) Wang, S.; Kool, E. T. Recognition of Single-Stranded Nucleic Acids by Triplex Formation: The Binding of Pyrimidine-Rich Sequences. *J. Am. Chem. Soc.* **1994**, *116* (19), 8857–8858.

(8) Coma, S.; Noe, V.; Eritja, R.; Ciudad, C. J. Strand displacement of double-stranded DNA by triplex-forming antiparallel purine-hairpins. *Oligonucleotides* **2005**, *15* (4), 269–83.

(9) de Almagro, M. C.; Coma, S.; Noe, V.; Ciudad, C. J. Polypurine hairpins directed against the template strand of DNA knock down the expression of mammalian genes. *J. Biol. Chem.* **2009**, *284* (17), 11579–89.

(10) de Almagro, M. C.; Mencia, N.; Noe, V.; Ciudad, C. J. Coding polypurine hairpins cause target-induced cell death in breast cancer cells. *Human Gene Therapy* **2011**, *22* (4), 451–63.

(11) Rodriguez, L.; Villalobos, X.; Dakhel, S.; Padilla, L.; Hervas, R.; Hernandez, J. L.; Ciudad, C. J.; Noe, V. Polypurine reverse Hoogsteen hairpins as a gene therapy tool against survivin in human prostate cancer PC3 cells in vitro and in vivo. *Biochem. Pharmacol.* **2013**, *86* (11), 1541–54.

(12) Goni, J. R.; de la Cruz, X.; Orozco, M. Triplex-forming oligonucleotide target sequences in the human genome. *Nucleic Acids Res.* **2004**, *32* (1), 354–60.

(13) Goni, J. R.; Vaquerizas, J. M.; Dopazo, J.; Orozco, M. Exploring the reasons for the large density of triplex-forming oligonucleotide target sequences in the human regulatory regions. *BMC Genomics* **2006**, *7*, 63.

(14) Coma, S.; Noe, V.; Lavarino, C.; Adan, J.; Rivas, M.; Lopez-Matas, M.; Pagan, R.; Mitjans, F.; Vilaro, S.; Piulats, J.; Ciudad, C. J. Use of siRNAs and antisense oligonucleotides against survivin RNA to inhibit steps leading to tumor angiogenesis. *Oligonucleotides* **2004**, *14* (2), 100–13.

(15) Villalobos, X.; Rodriguez, L.; Prevot, J.; Oleaga, C.; Ciudad, C. J.; Noe, V. Stability and immunogenicity properties of the gene-silencing polypurine reverse Hoogsteen hairpins. *Mol. Pharmaceutics* **2014**, *11* (1), 254–64.

(16) Philippi, C.; Loretz, B.; Schaefer, U. F.; Lehr, C. M. Telomerase as an emerging target to fight cancer-opportunities and challenges for nanomedicine. *J. Controlled Release* **2010**, *146* (2), 228–40.

(17) McDowell, J. A.; Turner, D. H. Investigation of the structural basis for thermodynamic stabilities of tandem GU mismatches: solution structure of (rGAGGUCUC)<sub>2</sub> by two-dimensional NMR and simulated annealing. *Biochemistry* **1996**, *35* (45), 14077–89.

(18) Vo, T.; Wang, S.; Kool, E. T. Targeting pyrimidine single strands by triplex formation: structural optimization of binding. *Nucleic Acids Res.* **1995**, *23* (15), 2937–44.

(19) Burnett, J. C.; Rossi, J. J.; Tiemann, K. Current progress of siRNA/shRNA therapeutics in clinical trials. *Biotechnol. J.* **2011**, *6* (9), 1130–46.

(20) Jackson, A. L.; Bartz, S. R.; Schelter, J.; Kobayashi, S. V.; Burchard, J.; Mao, M.; Li, B.; Cavet, G.; Linsley, P. S. Expression profiling reveals off-target gene regulation by RNAi. *Natu. Biotechnol.* **2003**, *21* (6), 635–7.

(21) Balatskaya, S. V.; Belotserkovskii, B. P.; Johnston, B. H. Alternate-strand triplex formation: modulation of binding to matched and mismatched duplexes by sequence choice in the Pu-Pu-Py block. *Biochemistry* **1996**, *35* (41), 13328–37.

(22) Jayasena, S. D.; Johnston, B. H. Oligonucleotide-directed triple helix formation at adjacent oligopurine and oligopyrimidine DNA tracts by alternate strand recognition. *Nucleic Acids Res.* **1992**, *20* (20), 5279–88.